Oligomérisation sélective de l'éthylène avec des complexes de chrome : étude théorique et expérimentale combinée - et extensions à d'autres métaux

Christian Klemps

Palaiseau

THÈSE

Spécialité CHIMIE

Par Christian Klemps

Oligomérisation sélective de l'éthylène avec des complexes de chrome : étude théorique et expérimentale combinée – et extensions à d'autres métaux

Jury
Pierre Braunstein
Christophe Coperet
Marc Visseaux
Lionel Magna
Pascal Le Floch

Thèse soutenue le 28 octobre 2009 à l'Ecole Polytechnique, Palaiseau, France.

Acknowledgements

This work would not have been possible without the contribution and the dedication of a number of persons who I would like to thank warmly:

Prof. Pascal Le Floch for the the possibility to complete this PhD thesis in his lab, his constant support, his constant availability for discussion, and the ability to transfer his enthusiasm in science to his students.

I would equally like to thank Lionel Magna from IFP-Lyon for his tutoring work, fruitful discussions, and directions all along the three years of this thesis. Thanks go equally to the other members of the Catalysis and Separation team in Solaize.

X-ray crystal structures play an important role in this part of paramagnetic transition metal chemistry: I am thus grateful to both Louis Ricard and Xavier Le Goff for the crystal structure solution and refinement work presented in this thesis.

Further thanks goes to the master students with whom I had the pleasure to work with during the three years in the lab: Romaric Houdard and Thi Phuong-Anh Cao, who have both an important share in this thesis work.

I am equally indebted towards all other past and present permanent members, PhD and master students in the Hétéroéléments et Coordination lab for the scientifically inspiring atmosphere, their fruitful collaboration, and the help with all kinds of matters.

Pierre Braunstein, Christophe Coperet and Marc Visseaux are thanked for accepting to be part of the jury for this thesis.

My warmest and most loving gratitude is reserved to Thi-Loan, my wife and beacon wherever I go, for her constant support and encouragement during these three years we spent together in Paris.

Remarks

The present work has been realized in the « Laboratoire Hétéroéléments et Coordination », Ecole Polytechnique in collaboration with the « Institut Français du Pétrole (IFP-Lyon) ».

The bibliographic references are given per chapter, and a corresponding list can be found at the end of each chapter.

All cited, prepared, and calculated compounds are equally numbered independently and consecutively within each chapter.

Synthesized compounds are numbered with Arabian numbers: **1**, **2**, **3**…

Calculated structures are numbered with Latin numbers: **I**, **II**, **III**…

Compounds cited from the literature are given letters, in some cases with added Arabian numbers: **A1**, **A2**, **B**, **C1**…

Schemes, figures, and tables are equally numbered per chapter.

Abbreviations

MAO	methylaluminoxane
MMAO	modified methylaluminoxane
KHMDS	potassium hexamethyldisilazane
cod	cyclooctadiene
TMS	trimethylsilyl
THF	tetrahydrofurane
NMR	nuclear magnetic resonance
ESR	electronic spin resonance
DFT	density functional theory
Me	methyl
Et	ethyl
i-Pr	isopropyl
n-Bu	*n*-butyl
t-Bu	tertbutyl
Ph	phenyl
DME	dimethoxyethane
equiv.	equivalents

Index

Introduction. Selective Tri- and Tetramerization of Ethylene		**5**
1.	Ethylene	6
2.	Linear Alpha Olefins (LAOs)	6
3.	Chromium-Based Catalytic Systems for Selective LAO Production	8
3.1	Phillips Petroleum Trimerization Process	8
3.2	Systems with Cyclopentadienyl Ligands	10
3.3	Systems with Maleimidyl Ligands	11
3.4	Systems with Phenoxide Ligands	12
3.5	Systems with Carbene Ligands	13
3.6	Systems With Multidentate Heteroatomic Ligands	14
3.6.1	Systems With Oxygen Donor Ligands	15
3.6.2	Systems with Nitrogen Donor Ligands	15
3.6.2.1	Triazacycloalkane Ligands	15
3.6.2.2	Tris(pyrazolyl)methane Ligands	16
3.6.2.3	Diazabutadiene Ligands	18
3.6.3	Systems with Mixed Nitrogen-Sulfur Donor Ligands	18
3.6.3.1	Bis(pyrazolyl)methane Ligands With Pendant Sulfur and Oxygen Donor Groups	18
3.6.3.2	Bis(sulphanylethyl)amine Ligands	19
3.6.4	Systems with Phosphine Donors	20
3.6.4.1	Tridentate Phosphine Ligands	20
3.6.4.2	Bis(phosphinoethyl)amine Ligands	21
3.6.4.3	Diphosphinoamine Ligands	22
3.6.4.3.1	The British Petroleum PNP Trimerization System	22
3.6.4.3.2	The Sasol PNP Tri- and Tetramerization System	24
3.6.4.3.2.1.	Ligand Variations	25
3.6.4.3.2.1.1	Variation of the N and P Substituents	26
3.6.4.3.2.1.2	Carbon Substitution of the Central Nitrogen Bridge	28
3.6.4.3.2.2	Other Transformations with the BP and the Sasol PNP System	30
4.	Objectives of This Thesis	32
5.	Bibliography	34
Chapter 1. On the Mechanism of Selective Ethylene Tri- and Tetramerization		**37**
1.	Introduction	38
1.1	The Cossee-Arlman Metal Hydride Mechanism	38
1.2	Metallacyclic Mechanism in Ethylene Oligomerization	40
2.	The British Petroleum and the Sasol PNP Tri- and Tetramerization System	41
2.1	Establishment of a Metallacyclic Mechanism	41
2.2	Kinetic Studies on the Chromium-Catalyzed Selective Oligomerization Reaction	43
2.3	Oxidation State of the Chromium Metal Center	44
2.4	C_6 Cyclic Byproducts in the Sasol Tetramerization Reaction	49
3.	Theoretical Study on the Mechanism of Ethylene Tri- and Tetramerization with the Sasol PNP System	50
3.1	Objectives and Methods	50
3.2	Ethylene Coordination to the Catalytically Active Species	51
3.3	Formation of the Chromacyclopentane	51
3.4	The 1-Hexene Pathway	54
3.5	The 1-Octene Pathway – Formation of a Chromacyclononane	56
3.6	Formation of C_6 Cyclic Byproducts	58
4.	The PCNCP Catalytic System – Tri- versus Tetramerization	60
4.1	PCNCP Ligand Synthesis	61

4.2	Synthesis of [(**3**)$CrCl_3$(THF)] Complexes	61
4.3	Evaluation of Complexes **4a-g** in Ethylene Oligomerization	63
4.4	Tri- versus Tetramerization – Theoretical Study	64
5.	Conclusion	73
6.	Bibliography	75
Chapter 2. Variations on the PNP Ligand		**77**
1.	Introduction	78
2.	PNP Derivatives	78
2.1	Bis(phosphole)amine Ligands	79
2.2	Bis(dialkynylphosphino)amine Ligand	80
2.3.	A PCP Ligand	82
3.	Bidentate Ligands with Sulfur Donors	83
3.1	Dithioacetals	83
3.2	Thiocarboxylates	84
4.	A Manganese-PNP Complex and its Evaluation in Ethylene Oligomerization	85
5.	Conclusion and Perspectives	87
6.	Bibliography	88
Chapter 3. (Bisiminophosphoranyl)-methanide Ligands in the Ethylene Oligomerization and Polymerization Reaction		**89**
1.	Introduction	90
2.	Synthesis Starting from Bis(diphenylphophino)methane via Bromination	94
3.	Deprotonation and Coordination to $CrCl_3(THF)_3$	95
4.	Coordination to [$NiBr_2$(DME)]	98
5.	Ethylene Oligomerization and Polymerization with Complexes **3a-d**	100
6.	Conclusion and Perspectives	104
7.	Bibliography	105
Chapter 4. Mixed (N,E) (E = O,P,S) Iminophosphorane Ligands in the Ethylene Oligomerization and Polymerization Reaction		**107**
1.	Introduction to the Chemistry of Iminophosphoranes	108
1.1	Synthesis of Iminophosphoranes	108
1.1.1	The Staudinger Reaction	108
1.1.2	The Kirsanov Reaction	109
1.1.3	The Aza-Mitsunobu Reaction	110
1.2	Electronic Structure of the P=N function	110
1.3	Iminophosphorane Ligands in the Ethylene Oligomerization and Polymerization Reaction	111
2.	Nickel Catalyzed Selective Ethylene Dimerization with N,E (E = O, S, P) mixed Iminophosphorane Ligands	113
2.1	N,O-Iminophosphorane Ligands	114
2.2.1	Synthesis of Phenolato-Iminophosphoranes **1**	115
2.2.2	Coordination to Rh(I) and Pd(II)	116
2.2.3	Coordination to Ni(II)	118
2.2.4	Application in the Selective Dimerization of Ethylene	119
2.2.5	Synthesis of Ether-Iminophosphoranes **2**	120
2.3	(N,P)-Iminophosphorane Ligands	121
2.3.1	Synthesis of Mixed Phosphine-Iminophosphorane Ligands	123
2.3.2	Coordination to [$CrX_3(THF)_3$] (X = Cl, Br)	125
2.3.3	Evaluation of **21** and **22** in Ethylene Oligomerization/Polymerization	127
2.3.4	Coordination to [$NiBr_2$(DME)]	127
2.3.5	Evaluation of Complexes **23-25** in the Selective Dimerization of Ethylene	129
2.4	(N,S)-Iminophosphorane Ligands	131
2.4.1	Synthesis of Thioether-Iminophosphoranes **26**	132

2.4.2	Synthesis of Thiophenolato-Iminophosphoranes **27**	134
2.4.3	Coordination of **29a**,**b** to Pd(II) and Rh(I)	137
2.4.4	Coordination of **29a**,**b** to Ni(II) and Evaluation in the Oligomerization of Ethylene	139
3.	Conclusion and Perspectives	140
4.	Bibliography	143

Chapter 5. Phosphatitanocenes – Application in the Catalyzed Polymerization of Ethylene 147

1.	Introduction	148
2.	Synthesis of Phospholyl Ligands with Pendant Hemilabile Groups	151
3.	Coordination to $TiCl_4$	153
4.	Evaluation of Complexes **1** and **2** in the Polymerization of Ethylene	154
5.	Conclusion	157
5.	Bibliography	157

Conclusions and Perspectives 159

Experimental Part 163

Crystallographic Appendix 189

Introduction. Selective Tri- and Tetramerization of Ethylene

Introduction. Selective Tri- and Tetramerization of Ethylene

1. Ethylene

Ethylene (C_2H_4) constitutes a key intermediate in today's chemical industry. Originally obtained by either partial hydrogenation of acetylene, or the dehydration of ethanol, thermal cracking of saturated hydrocarbons has become the dominant process for the production of ethylene.[1]

Roughly 80% of all the ethylene produced is used for the manufacturing of thermoplastic polymers,[2] as it constitutes the starting material for low-density polyethylene (LDPE), high-density polyethylene (HDPE), linear low-density polyethylene (LLDPE), and ethylene oligomers. Polyethylenes are the largest volume polymers worldwide. In the U.S., the 2002 consumption of polyethylenes amounted to approximately 12.7×10^6 tons, with 46% of HDPE, and 54% of both LDPE and LLDPE.[2] Both HDPE and LLDPE are manufactured using linear alpha olefins (LAOs), notably 1-butene, 1-hexene and 1-octene as comonomer feedstock in quantities of up to 8%.

Copolymerization represents thus the most important field of application for LAOs, which constitute, apart from this, important building blocks in the production of detergents, synthetic lubricants, alkyl amines, and plasticizer alcohols, depending on the chain length of the LAO. Figure 1 presents the various uses of LAOs in bulk chemical production with respect to their market volume.[3]

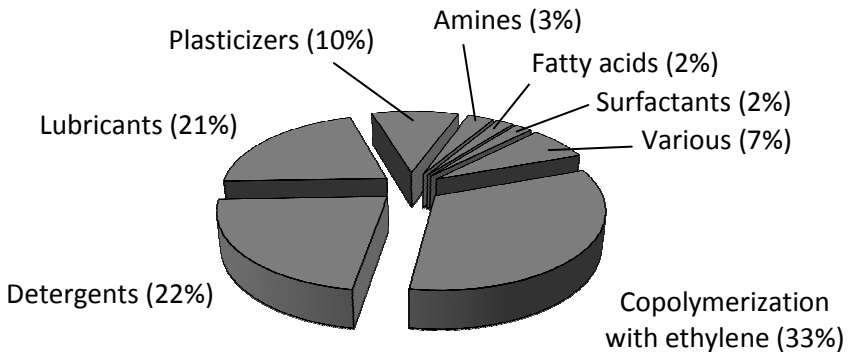

Figure 1. Market volume of products from LAOs.[3]

2. Linear Alpha Olefins (LAOs)

Today, the bulk of LAOs is produced by metal catalyzed ethylene oligomerization processes;[4] the only significant exception constitutes the extraction of 1-hexene and 1-octene byproducts from the Fischer-Tropsch conversion of coal to petroleum-like liquids by the South-African company Sasol. Currently, five different processes have been commercialized (table 1).

Table 1. Processes for ethylene oligomerization.

Company/Process	Catalytic System	Product distribution
Ethyl Corporation/ Ineos Process (stoichiometric Ziegler process)	Et_3Al	Pseudo-Poisson[5]
Gulf (Chevron-Phillips)/ (catalytic Ziegler process)	Et_3Al	Schulz-Flory[5]
Shell Oil Company/(SHOP process)	Ni-phosphine-enolato complexes	Schulz-Flory[5]
IFP/Alphabutol process	$Ti(IV)/AlEt_3$	Selectively 1-butene
Phillips Petroleum/Trimerization process	$Cr(III)$-alkanoate/2,5-dimethylpyrrole/$AlEt_3$	Selectively 1-hexene

A common inherent drawback of most of these so-called "full-range" processes constitutes the production of mathematical product distributions of Schultz-Flory or Poisson type, which makes subsequent separation of the product stream contents necessary. This implies an increase in plant complexity and thus capital expenditure. In the light of these problems, there has been a growing interest in both academic and industrial research in "on-purpose" routes towards the selective production of particular LAOs. Yet, only a limited number of systems with at the same time interesting productivies and selectivities towards either ethylene tri- or tetramerization have been disclosed up to date.

Catalyst systems based on titanium, nickel and chromium seem to be the most interesting candidates for selective ethylene oligomerization, even though a limited number of examples employing vanadium and tantalum have been reported and are included in this introduction. Otherwise, this introduction will comprehensively focus on homogeneous chromium-based tri- and tetramerization systems, while relevant literature on ethylene oligomerization with nickel and titanium catalyst is reviewed in the introductions of the relevant chapters 4 (Ni) and 5 (Ti). Furthermore, the present review is limited only to the presentation of productive catalytic systems, while the literature related to mechanistic aspects of the ethylene oligomerization reaction is treated in the introduction to chapter 1.

A last remark to the reader concerns the comparison of the performances of the catalytic systems presented in the following sections and throughout this manuscript. When reported catalyst productivities, selectivities, etc. are cited, it should be borne in mind that these results have often been obtained by different research groups, working with different experimental setups, activators from different sources, and the methods used for quantitative analysis of the catalysis product mixtures vary. Simple and immediate comparison of results from different sources, especially in the case of catalyst productivities, should thus be avoided.

3. Chromium-Based Catalytic Systems for Selective LAO Production

3.1 Phillips Petroleum Trimerization Process

The Union Carbide researchers Manyik, Walker and Wilson were the first to discover the potential of chromium based catalysts in ethylene oligomerization.[6] They observed that during ethylene polymerization with chromium-tris(2-ethylhexanoate), activated with partially hydrolyzed triisobutylaluminium, 1-hexene was formed in the reaction mixture, which subsequently incorporated into the polymer formed. Detailed analysis of the liquid fraction revealed that 1-butene, 1-hexene, 1-octene and 1-decene as well as some branched C_{10} isomers were equally formed, with 1-hexene being the most abundant oligomer in the liquid fraction of the product mixture. Upon variation of ethylene pressure and temperature, divergent dependences of the rate of polymerization and oligomerization were observed, indicating two distinct mechanisms for polymerization and olefin formation. Upon addition of 1,2-dimethoxyethane (DME) to the catalytic mixture, a significant increase in 1-hexene formation was observed, indicating the beneficial effect of donor ligands for the direction of the catalytic activity towards oligomerization.

The first example of a highly productive and selective oligomerization system is the Phillips Petroleum trimerization process, which was discovered when the catalytic properties of chromium pyrrolyl compounds were evaluated.[7] The idea behind this was the similarity of the cyclopentadienyl ligand, which is an abundant ligand for many polymerization catalysts, and the pyrrolyl ligand, the latter being the closest heterocyclic analogue to the cyclopentadienyl ligand from electronic and steric viewpoints. Given the extensive use of chromium cyclopentadienyl catalysts for ethylene polymerization, it was a logical approach. Reagan attempted the preparation of a couple of chromium pyrrolyl complexes starting from equimolar amounts of either $CrCl_2$ or $CrCl_3$ and sodium pyrrolide in THF, which yielded almost exclusively inorganic polymers, and only a few cluster compound such as $[Cr_5(C_4H_4N)_{10}(THF)_4]$ (from $[CrCl_2]$) could be structurally identified. Reaction of excess quantities of sodium pyrrolide with $[CrCl_2]$ yielded the dianionic square-planar complex $[(Na)_2Cr(C_4H_4N)_4]$ as the major product. These complexes were found to be highly active in ethylene oligomerization upon activation with 25 equiv. of Et_3Al. Jabri *et al.*[8] have recently reported on the isolation of Cr(I) and Cr(II) complexes from the reaction of either $[CrCl_3(THF)_3]$ or chromium(III)-octanoate with 2,3,4,5-tetrahydro-1*H*-carbazole and in the presence of Et_3Al or Et_2AlCl, respectively (Scheme 1).

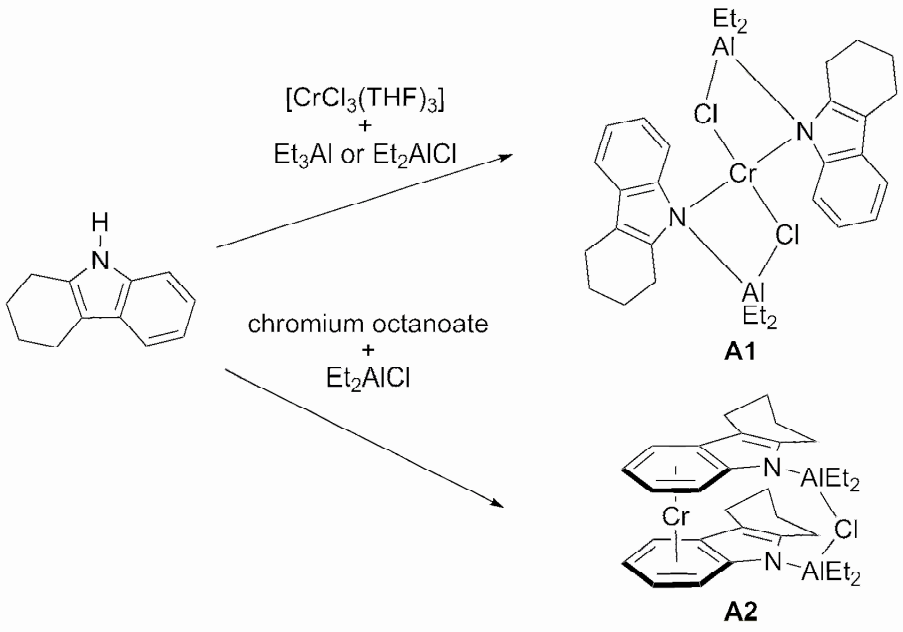

Scheme 1.

Whereas the Cr(II) complex **A1** was found to be active exclusively in polymerization upon contact with ethylene (41 bar, 115°C) , the Cr(I) complex **A2** yielded 1-hexene in 93% selectivity under the same reaction condition with only trace amounts of polymeric material.

A number of developments and improvements were disclosed by Phillips Petroleum Company patents and other follow-up patents following the initial discovery. Importantly, Reagan *et al.* found that an active trimerization catalyst system could be generated by simply mixing a chromium(III) alkanoate (such as chromium tris(2-ethylhexanoate)), pyrrole and Et_3Al, which represents a major simplification for industrial application of the process.[9] 2,5-dimethylpyrrole (**A3**) was found to be the ligand yielding the best results in the trimerization process, and the addition of Et_2AlCl was found to be beneficial towards both catalyst activity and selectivity. Activities of up to 156666 g × g $(Cr)^{-1}$ × h^{-1} and overall 1-hexene selectivities in excess of 93% were obtained using a catalytic mixture comprising chromium-tris(2-ethylhexanoate), **A3**, Et_2AlCl and Et_3Al in toluene in a molar ratio of 1/3.3/7.8/10.8 and carrying out the reaction at 115°C and 100 bar of ethylene pressure. Besides hexenes, mainly decenes (5.38%) stemming from the co-trimerization of 1-hexene and ethylene were observed (Scheme 2).[10]

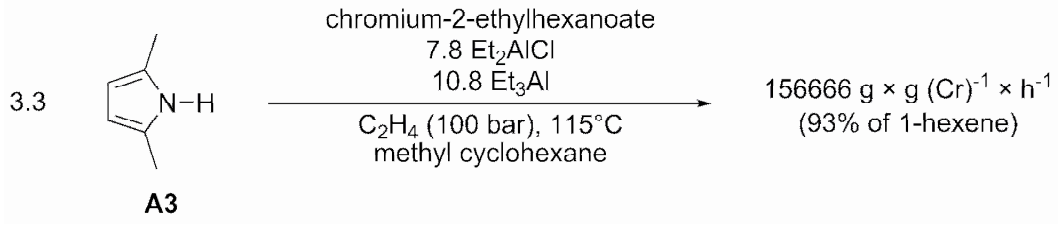

Scheme 2.

Mitsubishi Chemical Company disclosed the use of $B(C_6F_5)_3$ alongside with chromium tris(2-ethylhexanoate), Et_3Al, and pyrrole in the catalytic mixture, which led to significantly higher activities than catalytic mixtures without the borane Lewis acid.[11]

The Phillips Petroleum trimerization system has equally been applied to higher olefin substrates (1-pentene, 1-decene). While 1-decene oligomerization in a homogeneous catalytic system was found to be rather low in activity, conversions of up to 46% of the 1-decene were obtained when the catalytic reaction was carried out in ionic liquids, e.g. [1-butyl-2-methylimidazolium][$Et_{3n}Al_nCl$]. Other extensions include the tandem trimerization-copolymerization reaction of the Phillips Petroleum catalytic system together with supported chromium and titanium polymerization catalysts.[12]

The success of the Phillips Petroleum trimerization process technology has been headlined in 2003, when it was employed for the first time on a commercial scale in a 47000 tons/year plant in Quatar, operated by Quatar Chemical Company Ltd.[13, 14]

Following the exceptional success of the Phillips Petroleum trimerization system, a number of catalytic systems employing ligands with steric and electronic similarities to the pyrrolide ligand have been developed and evaluated in the ethylene trimerization reaction. These include cyclopentadienyl, maleimidyl, and boratabenzyl ligands.

3.2 Systems with Cyclopentadienyl Ligands

The inherent similarity of pyrrolyl and cyclopentadienyl ligands invoked the idea of returning the attention to cyclopentadienyl-chromium species, which are primarily known for their activity in the polymerization of ethylene.[15-18] Consequently, upon introduction of bulky π accepting substituents on the cyclopentadienyl ring system, a catalyst system for selective ethylene trimerization could be generated, as disclosed by Mahomed *et al.*[19, 20] The researchers at Sasol devised a four-component system including chromium-tris(2-ethylhexanoate), 5-(4'-*t*-butylphenyl)-1,2,3,4-tetraphenyl-1,3-cyclopentadiene (**B**), hexachloroethane, and Et_3Al, which, in their best example, when the four components were employed in a molar ratio of 1/3/2.5/45, yielded a productivity of 93500 g × g $(Cr)^{-1}$ × h^{-1} and an overall 1-hexene selectivity of 74.2%, the catalytic reaction being conducted at 50 bar of ethylene pressure, at 70°C, and in cyclohexane as solvent (Scheme 3).

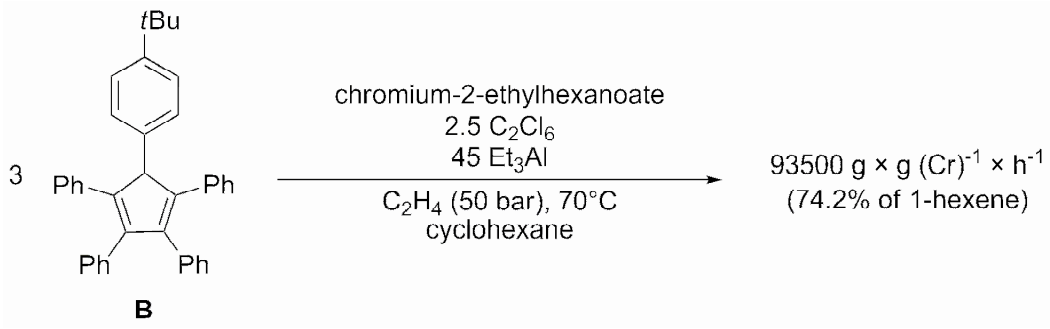

Scheme 3.

Approximately 15% of internal hexene isomers, alongside with small quantities of C_{10} alkenes and polymeric material were also produced. The beneficial effect of chloro compounds with germinal chloro groups, which has first been observed and investigated on the Phillips Petroleum trimerization system,[21] was confirmed.

Compared to the Phillips Petroleum system, the overall lower activity and selectivity toward 1-hexene, combined with the high cost associated with the synthesis of bulky cyclopentadienyl ligands such as **B**, are a major drawback of this catalytic system with regard to its industrial application.

3.3 Systems with Maleimidyl Ligands

Following the same philosophy of employing ligands with similar electronic and steric properties as the prominent pyrrolyl ligand, Tosoh Chemical Corporation disclosed an ethylene trimerization system based on maleimide (1*H*-pyrrole-2,5-dione, **C**).[22] Using an in situ formed catalytic system comprising chromium tris(2-ethylhexanoate), maleimide, Et_3Al, and Et_2AlCl, in a molar ratio of 1/60/430/160, a productivity of 278000 g × g $(Cr)^{-1}$ × h^{-1} and an overall 1-hexene selectivity of 79.6% was reported, when conduction the catalytic reaction at 120°C and at 40 bar of ethylene pressure (Scheme 4). A polymeric fraction of 1.5% was produced alongside with the liquid products.

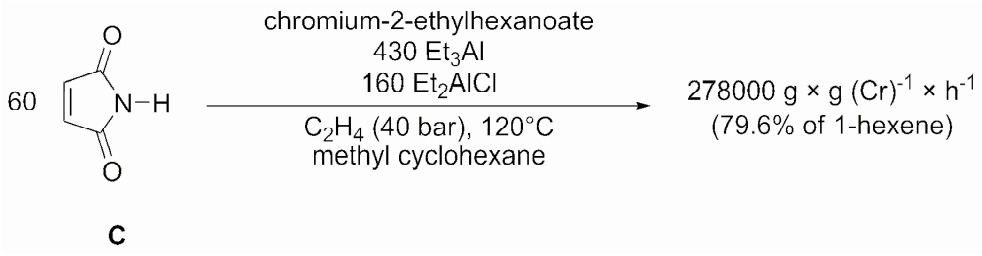

Scheme 4.

From a purely commercial viewpoint, the generally lower selectivity towards 1-hexene compared to the Phillips Petroleum system, renders the maleimidyl system less viable for commercial exploitation.

3.3 Systems with Boratabenzyl Ligands

The anionic boratabenzyl fragment $[C_5H_5B]^-$ is isoelectronic to the cyclopentadienyl ligand,[23] however, the catalytic activities of complexes with boratabenzyl ligands generally differ greatly from those of their cyclopentadienyl counterparts. Cr(III) boratabenzyl complexes such as $[(\eta^5\text{-}C_5H_5B)Cr(Me)_2(PMe_3)]$ were initially reported to yield highly active ethylene polymerization catalysts after activation with MAO.[24] The concept of increasing the steric bulk on the boratabenzyl ligand, as described for the cyclopentadienyl ligands, might thus turn the selectivity towards a trimerization system. Mitsubishi Chemical Industries disclosed in 1999 a catalytic system, based on an uncharacterized boratabenzyl chromium compound **D**, which had been formed previously from trimethylphosphine-boracyclohexa-2,4-diene, lithium diisopropylamide and $[CrCl_3(THF)_3]$, as outlined in scheme 5. Upon activation of **D** with 15 equiv. of Et_3Al, and conducting the reaction at 80°C and under 35 bars of ethylene pressure, a very modest productivity of 1072 g × g $(Cr)^{-1}$ × h^{-1} was reported, 62.5% of which was 1-hexene.[25]

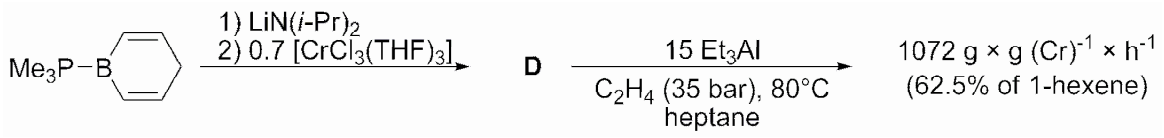

Scheme 5.

3.4 Systems with Phenoxide Ligands

In 1998, the IFP filed a patent describing a catalytic system for ethylene trimerization consisting of a chromium precursor, a phenoxyaluminium compound and a trialkylaluminium activator.[26] At 120°C and 50 bar of ethylene pressure, an activity of 3654 g × g $(Cr)^{-1}$ × h^{-1} and an overall selectivity of 77.4% towards 1-hexene was achieved, when an eight-fold excess (with respect to chromium tris(2-ethylhexanoate)) of both bis(2,6-diphenylphonoxy)isobutyl aluminium (**E1**) and Et_3Al is used. However, 18% of polymeric material was also obtained (Scheme 6 upper).

An improvement of this catalytic system was subsequently disclosed, which consisted in the use of earth alkaline phenoxides $[M(OR)_{2-n}X_n]$ (with M = earth alkaline metal, X = halogen, OR = phenoxide).[27] The best result reported was achieved using magnesium bis(2,6-diphenylphenoxide) (**E2**), chromium tris(2-ethylhexanoate), and Et_3Al in a molar ratio of 1/1/3, carrying out the reaction at 140°C in *o*-xylene and at 30 bar of ethylene pressure. A productivity of 7308 g × g $(Cr)^{-1}$ × h^{-1} was reported, alongside with an overall 1-hexene selectivity of 83.5% and a polymeric fraction accounting for 11% of the total productivity. (Scheme 6 lower)

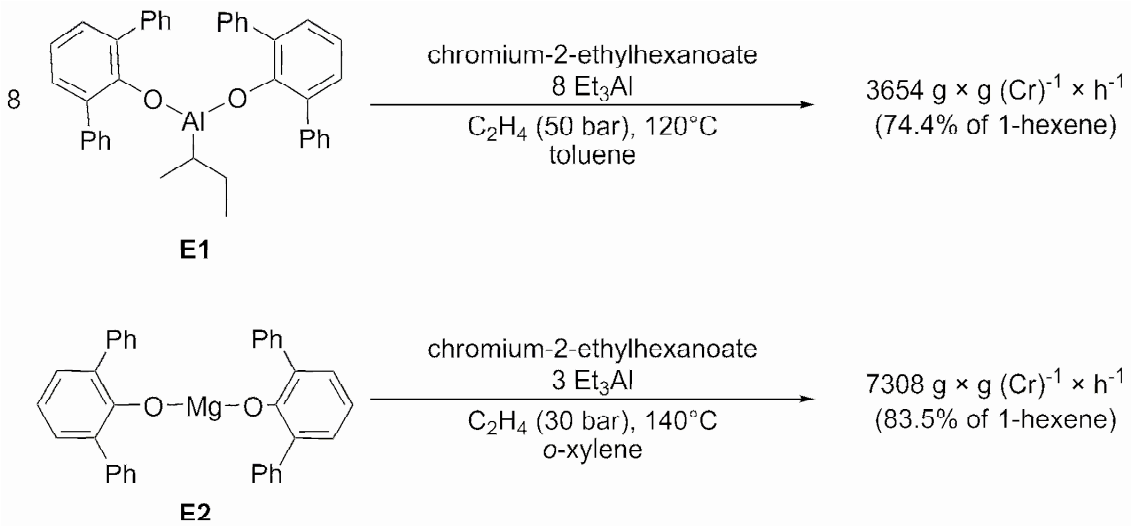

Scheme 6. The IFP Alphahexol® process.

Morgan *et al.*[28] of Sasol Technology found that the corresponding phenols could equally be employed in this process without the need for prior preparation of the corresponding aluminium or magnesium phenoxide. Furthermore, they reported on the beneficial effect of using anisole as solvent medium in this reaction. It was shown that the methyl phenyl ether plays also the role of a stabilizing ligand in the catalytic cycle, as deducted from magnetic susceptibility measurement on catalytic mixtures. The presence of anisole was found to be of pivotal importance for good productivity and selectivity towards 1-hexene. The best result was obtained using chromium tris(2-ethylhexanoate), bis(2,6-diphenylphenol) (**E3**), Et_3Al, in a molar ratio of 1/14.5/20, and anisole as solvent. A total productivity of 22769 g × g $(Cr)^{-1}$ × h^{-1} and 77.5% 1-hexene selectivity and 13.6% of polymeric material was obtained (Scheme 7).

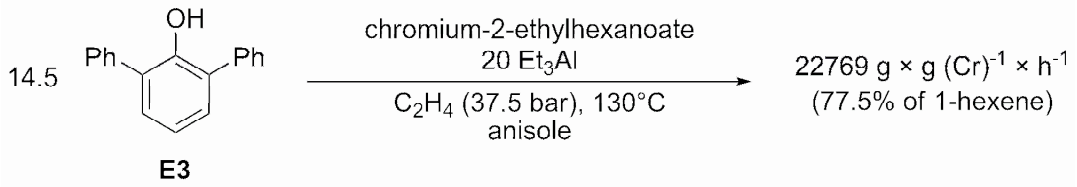

Scheme 7.

3.5 Systems with Carbene Ligands

Heterocyclic carbene ligands play a paramount role in a great variety of catalytic processes. Important developments include Pd-based catalysts for C-C coupling reactions,[29] and highly active Ru catalysts in ring opening metathesis polymerization.[30, 31] Surprisingly, the use of these ligands in olefin oligomerization and polymerization reactions is rather limited. Döhring *et al.*[32] reported on a number of η^5-C_5Me_5-Cr(III) complexes bearing NHC carbene ligands, which were found to be active in ethylene polymerization after activation with MAO. Mixed imine-carbene ligands and their complexes

with a broad range of transition metals and their application in olefin oligomerization and polymerization have been disclosed by Borealis Technology OY, however, only very modest activities were reported.[33] Zirconium-carbene adducts $[(NHC)_2ZrCl_4]$ proved to be moderately active in ethylene polymerization upon activation with 1650 to 2200 equiv. of MAO; square-planar $[(NHC)_2NiX_2]$ (X = halogen) complexes were very active in selective ethylene dimerization, when stabilized in a ionic liquid medium.[34]

In 2003, McGuinness *et al.*[35] reported on ethylene oligomerization employing Cr(III) complexes with the (C,N,C) pincer ligands **F1**. These octahedral complexes were found to be highly active in ethylene oligomerization upon activation with MAO, yielding olefin distributions with *K* values between 0.48 and 0.80. The complex **F2** with the bulky ligand **F1** (R = 2,6-(*i*-Pr)$_2$C$_6$H$_3$) yielded the highest productivity (388875 g × g (Cr)$^{-1}$ × h^{-1}), and 86% of the products were found to be α-olefins (Scheme 8).

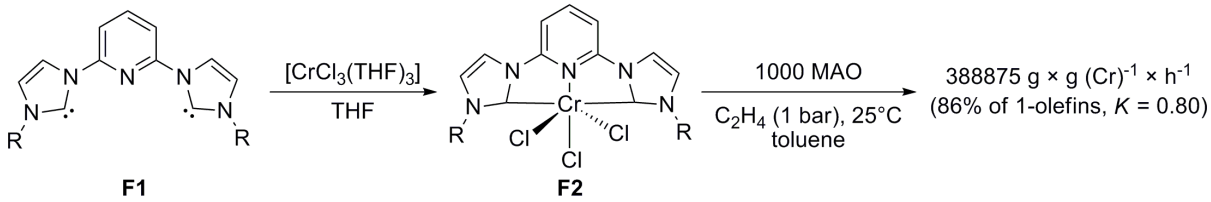

Scheme 8. R = *i*-Pr, 2,6-(*i*-Pr)$_2$C$_6$H$_3$, Ad.

Cr(III) complexes bearing structurally similar tridentate thiophene-bis(carbene) ligands,unsymmetric bidentate pyridine-carbene, or thiophene-carbene complexes were found to exhibit only modest activities, the majority of the products being polymers.[36]

Very recently, the application of **F2** in the homopolymerization of 1-hexene and 1-octene was reported, yielding predominantly head-to-tail dimers with vinylidene unsaturation, while the head-head coupling, leading to internal alkenes, was found to be less favored.[37]

3.6 Systems With Multidentate Heteroatomic Ligands

Multidentate heteroatomic ligands have experienced a continuously increased interest in chromium-based selective oligomerization over the last two decades. Most of the ligands employed coordinate either in bidentate or tridentate fashion to the chromium center, and this via nitrogen, phosphorus, oxygen, and sulfur donors, or combinations of these donors. Catalytic systems employing mixed heteroatomic donor ligands, are today the most active and most selective systems available, and one of these systems is even capable of selective ethylene tetramerization to form 1-octene in high yields.

3.6.1 Systems With Oxygen Donor Ligands

As mentioned above, Manyik was the first to notice the effect of DME in turning the selectivity of chromium-based catalytic systems for ethylene polymerization and oligomerization towards the formation of 1-hexene. Some ten years later, Briggs from UCC disclosed a catalytic system comprising a chromium precursor, a partially hydrolyzed organoaluminium compound as activator, and a donor ligand.[38] 74% of overall 1-hexene selectivity and an overall productivity of 2086 g × g $(Cr)^{-1}$ × h^{-1} was obtained with a catalytic mixture consisting of chromium tris(2-ethylhexanoate), partially hydrolyzed triisobutyl aluminium, and DME (in a ratio of 1/2/10), the remainder of the productivity being polymeric material, which featured no 1-hexene incorporation (Scheme 9).[39]

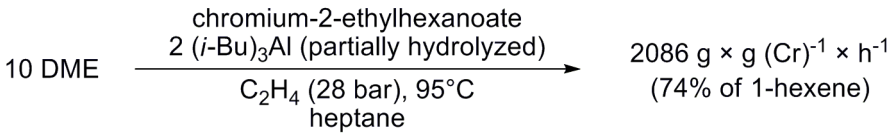

Scheme 9.

Various variations and improvements, concerning activators[40, 41] and process parameters[42] have subsequently been disclosed both by UCC and others. However, none of these systems were able to yield more than 84% overall 1-hexene.

3.6.2 Systems with Nitrogen Donor Ligands

3.6.2.1 Triazacycloalkane Ligands

Ethyl Corporation disclosed a chromium-based system for ethylene oligomerization employing a bulky 1,4,7-trialkyl-1,4,7-triazacyclononane ligand.[43] The system yielded, upon activation with various alkylaluminoxanes, Schultz-Flory distributions of α-olefins, selectively enriched with 1-hexene, with concomitant formation of only minor amounts of waxes and polymeric material. Steric bulk was considered responsible for the observed selectivity towards oligomerization over polymerization, as the unsubstituted 1,4,7-triazacyclononane ligand yielded exclusively polymerization.

Köhn *et al.* later reported on similar [(1,3,5-triazacyclohexane)$CrCl_3$] complexes **G**, whose x-ray crystal structure analysis revealed the η^3 facial coordination mode of these compounds.[44, 45] Upon activation with either MAO or [$(PhNMe_2H)(B(C_6F_5)_4)$] and $(i\text{-}Bu)_3Al$, these complexes were found to polymerize ethylene with high activities. Analysis of the liquid fraction of the polymerization experiments revealed, besides 1-hexene, decene isomers, resulting from a co-trimerization of 1-hexene

and ethylene. Equally, 1-hexene incorporation into the polymer was observed. Complexes **G** were thus considered as the first homogeneous model for the Phillips CrO_3/SiO_2 polymerization catalyst. [(1,3,5-triazacyclohexane)$CrCl_3$] complexes **G** with long N-alkyl chains were equally evaluated in the oligomerization of higher linear α-olefins (1-hexene, propene, and styrene). With 1-hexene as substrate, C_{18} products were selectively obtained in up to 80% conversion upon activation with 100 equiv. of MAO. Scheme 10 presents the obtained alkenes with their respective quantities.

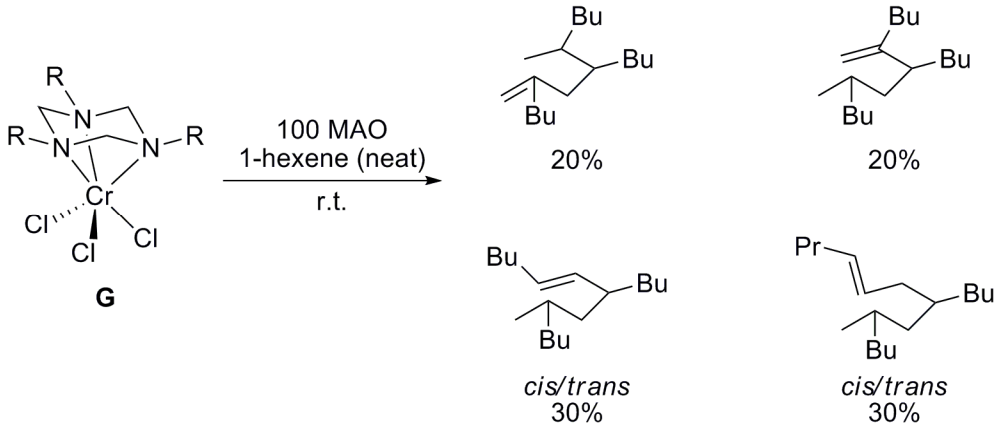

Scheme 10. R = *n*-octyl, *n*-dodecyl.

Up to today, complexes **G** are the only catalytic system capable of this transformation. They were equally shown to be capable to selectively trimerize 1-decene and 1-dodecene; the resulting C_{30} and C_{36} fractions, respectively, had, after hydrogenation, the physical properties required for lubricants.[46] Nenu and Weckhuysen reported on the successful grafting of complex **G** (with R = CH_2Ph) on a silanol functionalized silica surface, and the successful selective trimerization of ethylene after activation with [($PhNMe_2H$)($B(C_6F_5)_4$)] and (*i*-Bu)$_3$Al.[47] A productivity of 0.168 g × g $(Cr)^{-1}$ was obtained at 25°C, and an overall 1-hexene selectivity of 91.3% was reported. The selectivity dropped to 52.2% when the reaction was carried out at 90°C.

3.6.2.2 Tris(pyrazolyl)methane Ligands

In 2002, Tosoh Corporation disclosed a catalytic system for the selective ethylene trimerization employing tris(pyrazolyl)methane-$CrCl_3$ complexes, prepared from the tris(pyrazolyl)methane ligand and [$CrCl_3(THF)_3$] in THF. Upon activation either with MAO or with mixtures of MAO and a trialkylaluminium compound such as *i*-Bu_3Al. The best example included the use of tris(3,5-dimethylpyrazolyl)methane-$CrCl_3$ (**H1**), activated with 360 equiv. of MAO, at 80°C and 40 bar of ethylene pressure. An unprecedented overall selectivity towards 1-hexene of 99.1% in the liquid fraction was obtained, alongside with a polymeric fraction of 1.5%; and an overall productivity of 40100 g × g $(Cr)^{-1}$ × h^{-1} was reported (Scheme 11).

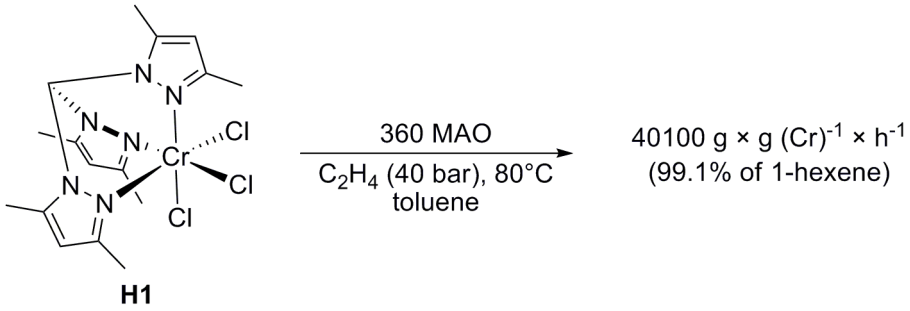

Scheme 11.

Tris(pyrazolyl)methane-$CrCl_3$ complexes were also reported to be moderately active in the formation of high-melting polyethylene upon activation with 1000 equiv. of MAO and comparatively low ethylene pressure (4 bar).[48]

Zhang *et al.*[49] recently studied the effect of Me_3Al and residual Me_3Al in commercial MAO solutions on these complexes. Me_3Al was found to abstract chloride anions from the monomeric complex **H1**, reducing it to a dicationic, dimeric pentacoordinated complex **H2**, which, however, exhibited only a very modest productivity upon activation with 50 equiv. of Et_3Al (630 g × g $(Cr)^{-1}$ × h^{-1}, 96.9% overall 1-hexene selectivity), whereas upon activation with 200 equiv. of MAO, an overall productivity of 36300 g × g $(Cr)^{-1}$ × h^{-1} and a 96.9% overall 1-hexene selectivity were found. This confirms the importance of MAO for catalyst activity (Scheme 12).

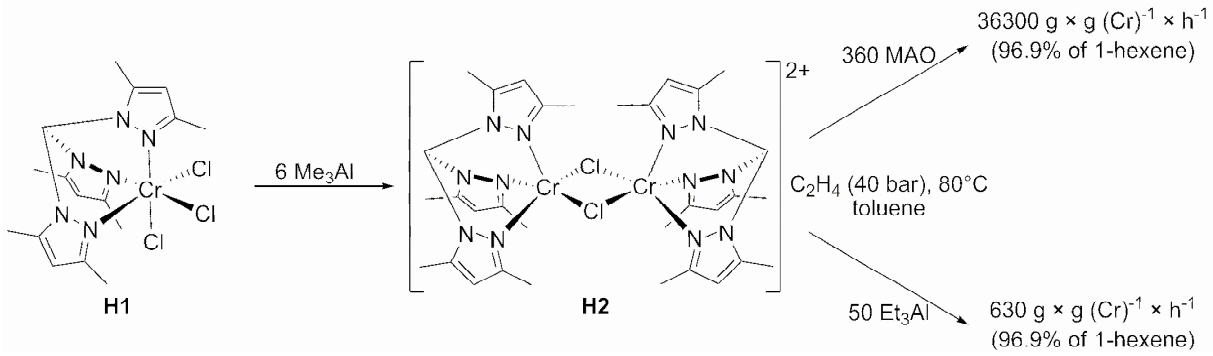

Scheme 12. The two chloro-methyl-aluminate counteranions of **H2** have been omitted for clarity reasons. They do not participate in the coordination to the chromium centers.

Tosoh Corporation equally disclosed catalytic systems for selective ethylene trimerization employing tris(pyrazolyl)methane-$Cr(CO)_3$ complexes. The best example involved the use of tris(3,5-dimethylpyrazolyl)methane-$Cr(CO)_3$, N,N-dimethylaniline, and *i*-Bu_3Al in a respective molar ratio of 1/10/20. The *i*-Bu_3Al acting probably as a CO scavenger, a 96% overall selectivity towards 1-hexene was obtained, virtually no polymeric material was formed, and a productivity of 15600 g × g $(Cr)^{-1}$ × h^{-1} was reported.

Due to its excellent selectivity towards ethylene trimerization and the competitive productivities reported, tris(pyrazolyl)methanes are possibly viable candidates for industrial application.

3.6.2.3 Diazabutadiene Ligands

Diazabutadiene ligands play a prominent role in late transition metal catalyzed ethylene polymerization. More detail on this aspect can be found in the introduction to chapter 3. Sumitomo Chemical Corporation disclosed the use of this ligand class in chromium catalyzed ethylene oligomerization. As an example, a catalytic system consisting of chromium tris(2-ethylhexanoate), the the sterically bulky diazabutadiene **I**, and Et_3Al in a molar ratio of 1/15/79, was reported to yield 22995 g × g $(Cr)^{-1}$ × h^{-1} at 120°C and at 40 bar of ethylene pressure (Scheme 13). An overall selectivity of 58.3% towards 1-hexene was achieved, and 3% of polymeric material was obtained.[50] Given this rather low 1-hexene yield, diazabutadiene ligands do not seem to be promising candidates for further development.

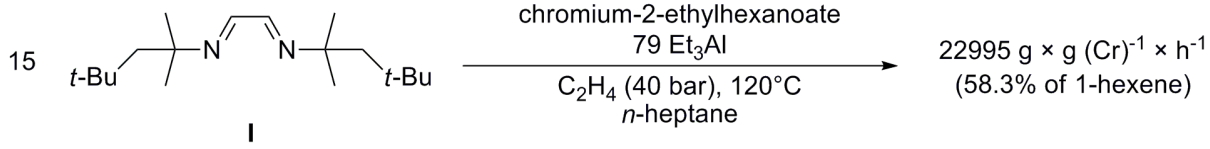

I

Scheme 13.

3.6.3 Systems with Mixed Nitrogen-Sulfur Donor Ligands

3.6.3.1 Bis(pyrazolyl)methane Ligands With Pendant Sulfur and Oxygen Donor Groups

Recently, Hor and collegues reported on so-called "heteroscorpionate" bis(pyrazolyl)methane ligands with pendant ether and thioether groups, which, upon coordination to $[CrCl_3(THF)_3]$ in THF yielded octahedral complexes **J**, where the tridentate "heteroscorpionate" ligand adopts a facial coordination mode.[51] These complexes, which present an undeniable similarity to Tosoh Corporation's tris(pyrazolyl)methane-$CrCl_3$ complexes **H**, match those in the observed 1-hexene selectivities. Upon activation with 200 equiv. of MAO, at 80°C, and at 25 bar of ethylene pressure, these complexes proved to be highly selective towards ethylene trimerization to 1-hexene (Scheme 14). The thioether complexes **J1**-**J3** presented productivities between 1050 g × g $(Cr)^{-1}$ × h^{-1} (**J1**) and 3900 g × g $(Cr)^{-1}$ × h^{-1} (**J3**) and overall 1-hexene selectivities of up to 95.5%, while less than 0.1% of polymeric material was formed.

Even better results were obtained with the analogous ether derivatives **J4**-**J7**, the slightly harder oxygen donor being apparently beneficial towards catalyst productivity. **J6** exhibited a productivity of 21000 g × g $(Cr)^{-1}$ g × h^{-1} and an overall selectivity towards 1-hexene of 98.5%. Substitution of the ether or thioether donor with long alkyl chains, which led to increased catalyst productivity, was ascribed to the increased solubility of the complexes. Methyl substitution in 3- and 5- positions of the

two pyrazole heterocycles was found to be essential for oligomerization activity, as the complex **J8** bearing the unsubstituted derivative yielded 51.7% of polymeric material.

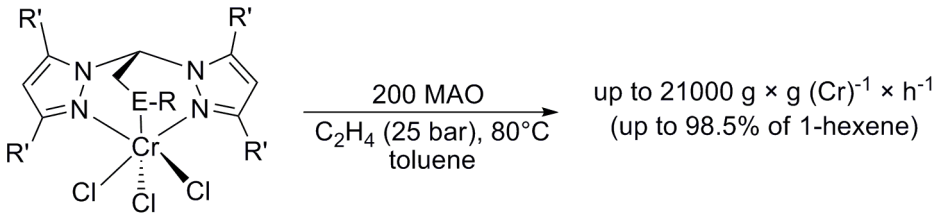

J1-J8

Scheme 14: J1: E = S, R = Me, R' = Me, **J2**: E = S, R = CH_2Ph, R' = Me, **J3**: E = S, R = *n*-decyl, R' = Me, **J4**: E = O, R = Et, R' = Me, **J5**: E = O, R = *i*-Pr, R' = Me, **J6**: E = O, R = Me, R' = *n*-hexyl, **J7**: E = O, R = Ph, R' = Me, **J8**: E = O, R = *n*-hexyl, R' = H.

3.6.3.2 Bis(sulphanylethyl)amine Ligands

In 2003, researchers from Sasol Technology reported[52, 53] Cr(III) complexes **K** bearing tridentate $(RS(CH_2)_2)_2N(H)$ (R = *n*-alkyl) ligands. The ligands were found to coordinate in a η^3-meridional fashion around the metal center, yielding complexes with a octahedral coordination geometry, as confirmed by x-ray crystal structure analysis. Upon activation with MAO, highly productive catalytic systems with excellent trimerization selectivities were obtained. In their best example (Scheme 15), the authors reported a productivity of 160840 g × g $(Cr)^{-1}$ × h^{-1} with the R = *n*-Bu derivative, of which 98.1% was 1-hexene, alongside with a polymeric fraction, which accounted for only 0.16%.

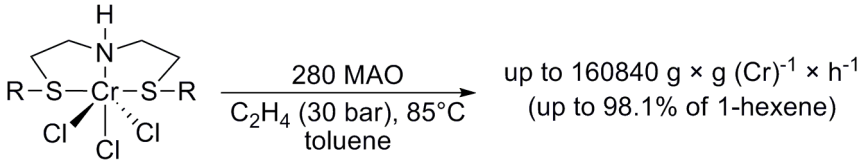

K

Scheme 15. R = Me, Et, *n*-Bu, *n*-Decyl.

This catalytic system, which now is referred to as the Sasol SNS trimerization system, has subsequently been subject of extensive investigation, to shed light on the ligand properties necessary for effective trimerization activity.

H-substitution of the central nitrogen was one of the factors found to be of determining importance, as N-methyl and N-benzyl substituted derivatives led to low catalyst activities and of a polymer fraction, which amounted to 30.6 and 66.7%, respectively.[54] Deprotonation by either MAO or residual $AlMe_3$ in MAO was suggested to occur during catalyst activation.[55]

A Cr(III) complex bearing an asymmetric SNS ligand $EtS(CH_2)_3N(H)(CH_2)_2SEt$ with a propyl spacer was equally evaluated. Even though this complex gave rise to an active trimerization catalyst, a

comparatively low overall selectivity of only 79.3% towards 1-hexene and a productivity of 14770 g × g $(Cr)^{-1}$ × h^{-1} was reported.[54] The unprecedented performance of the Sasol SNS trimerization system called for further derivatization. In line with this, SPS,[54] PSP,[54] SSS,[56] SOS,[56] and $MeC((CH_2)_2SR)_2$[56] (R = *n*-decyl) ligands were evaluated. SPS and PSP ligands, which present some similarity to the Amoco PPP ligand discussed in section 3.6.4.1 below, exhibited good productivities and 1-hexene selectivities, albeit lower than those of the parent SNS ligands.

The Cr(III) complex bearing the SSS trithioether ligand $S((CH_2)_2S(CH_2)_9CH_3)_2$ showed an overall 1-hexene selectivity of 71.4% alongside with an important C_8-C_{22} fraction, which amounted to 27.1%, but all other derivatives gave rise to catalyst active exclusively in polymerization.

The scope of the SNS trimerization system has been enlarged to tandem oligomerization/polymerization by combination with various metallocene catalysts. For example, when combined with polymerization catalyst $[((Me)_2Si(2\text{-Me-Ind})ZrCl_2]$ (Ind = indenyl), and upon activation with MAO, a polyethylene featuring 5.81% of 1-hexene incorporation could be obtained.[57]

Somewhat similar to the Sasol SNS trimerization system are the Cr(III) complexes bearing the 2,6-bis(CH_2SR)-pyridine ligands **L** (with R = Ph, Cy), which have been devised by Temple *et al.*[58] X-ray crystal structure analysis equally revealed a meridional coordination mode (Scheme 16). The complexes $[CrCl_3(\mathbf{L})]$ were found to be moderately active in ethylene oligomerization, however, selectivities towards the interesting α-olefins were not reported.

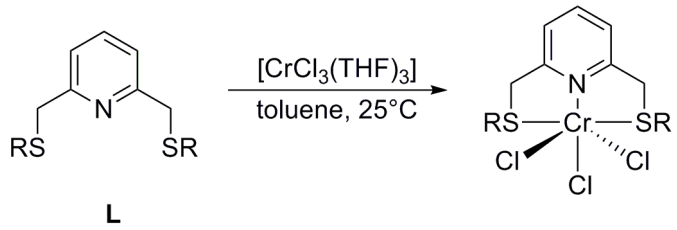

Scheme 16. R = Ph, Cy.

3.6.4 Systems with Phosphine Donors

3.6.4.1 Tridentate Phosphine Ligands

Chromium complexes **M** with tridentate phosphine ligands $R^1{}_2P(CH_2)_aP(R^2)(CH_2)_bPR^1{}_2$ (with a, b = 1 to 3), which, upon activation with aluminoxanes, gave catalysts with extremely high selectivity towards ethylene trimerization (Scheme 17), were disclosed by Amoco Corporation.[59] An x-ray crystal structure of the $[n\text{-}PrP((CH_2)_2PEt_2)_2CrCl_3]$ complex revealed the octahedral coordination geometry around the chromium center and the tridentate meridional coordination mode of the ligand similar to the coordination of the bis(sulphanylethyl)amine and 2,6-bis(CH_2SR)-pyridine ligands discussed above.

Contrary to what was found with the bis(sulphanylethyl)amine ligands, where an asymmetric ligand gave rise to an oligomerization catalyst with significantly lower activity and selectivity than its symmetric counterpart, the best results were obtained with a Cr(III) complex bearing the asymmetric $Me_2P(CH_2)_aP(Ph)(CH_2)_bPMe_2$ (a = 3, b = 2) ligand. Activated with 222 equiv. of butylaluminoxane, and at 35 bar of ethylene pressure, at 60°C, a productivity of 48700 g × g $(Cr)^{-1}$ × h^{-1} was reported. Only 0.33% of polymeric material was formed, while the liquid fraction contained 0.92% of butenes, 0.45% of C_{10} products, and 98.3% of hexenes (99.0% of 1-hexene, thus 97.3% overall 1-hexene selectivity).

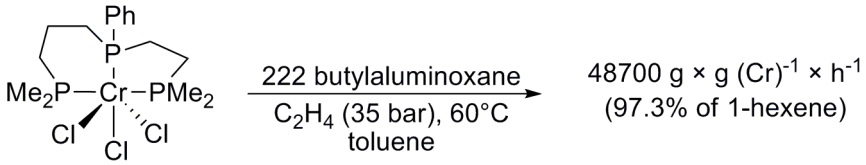

M

Scheme 17.

The unprecedented purity of the C_6 fraction in the catalyst product stream let the inventor suggest direct use of this product stream for further processing (e.g. co-polymerization), which would be an outstanding improvement for greater process plant simplicity. However, the required triphosphine ligands are not easily accessible and thus expensive, which somewhat hampers their industrial application.

3.6.4.2 Bis(phosphinoethyl)amine Ligands

Researcher from Sasol Technology developed a highly active and selective chromium-based trimerization system involving the use of tridentate bis(phosphinoethyl)amine ligands with the general formula $(R_2P(CH_2)_2)_2N(H)$, and MAO as activator.[60, 61] Upon coordination to $[CrCl_3(THF)_3]$, the resulting complexes **N** with octahedral geometry feature a tridentate meridional coordination mode of the ligand similar to the coordination found in bis(sulphanylethyl)amine-$CrCl_3$ complexes **K** and the triphosphino-$CrCl_3$ complexes **M**. The best results in terms of 1-hexene selectivity and overall catalyst activity were obtained with the R = Et ligand derivative. The best result reported gave thus an overall productivity of 58570 g × g $(Cr)^{-1}$ × h^{-1}, alongside with an overall 1-hexene selectivity of 96.9% and a polymer fraction which accounted for only 0.7% (Scheme 18). Catalytic runs employing the highly basic, but sterically bulky dicyclohexylphosphino-substituted ligand led predominantly to polymer formation (85.7%) and comparatively low overall activity (580 g × g $(Cr)^{-1}$ × h^{-1}). Acceptor substitution of the phosphino moieties (R = Ph) of the ligand gave rise to a catalyst with moderate overall productivity (8670 g × g $(Cr)^{-1}$ × h^{-1}) and a high 1-hexene selectivity (97.2%, only 0.1% of polymeric material), when catalyst activation was carried out with a low MAO/Cr ratio of 120/1.

Increase of this ratio to 680/1 resulted in a significant productivity increase to 17300 g × g $(Cr)^{-1}$ × h^{-1}, however, this was accompanied by a rise in the production of polymeric material to 10.2% of the total productivity.

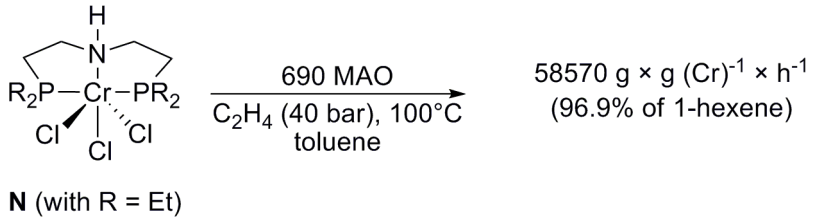

N (with R = Et)

Scheme 18.

In the same manner as the Sasol SNS trimerization system, the bis(phosphinoethyl)amine catalytic system has equally been subject of further investigations.[54, 55] Accordingly, H-substitution on the central amine moiety was found to be essential to avoid increased polymer formation during catalysis, and a possible deprotonation of the ligand by the activator was evoked. Deprotonation of the Cr(II) complex $[(Ph_2P(CH_2)_2)_2N(H)CrCl_2]$ with DABCO led to the μ_2-Cl dimeric complex $[((Ph_2P(CH_2)_2)_2NCr(\mu_2\text{-}Cl))_2]$, whose x-ray crystal structure analysis revealed anionic amide coordination to the Cr(II) metal center. This complex proved to be equally active towards ethylene trimerization upon activation with 300 equiv. of MAO, albeit with lower overall productivity, and a somewhat increased polymer formation compared to its monomeric Cr(III) congener **N** (R = Ph).

3.6.4.3 Diphosphinoamine Ligands[62]

3.6.4.3.1 The British Petroleum PNP Trimerization System

In 2002, British Petroleum both patented[63] and published[64] a catalytic system for the selective trimerization of ethylene to 1-hexene, based on the use of a Cr(III) precursor, bis(diarylphosphino)amine ligands **O** $Ar_2PN(R)PAr_2$, and an aluminoxane activator. Ligands **O** (Figure 2) whose utility in the nickel catalyzed olefin polymerization[65] and palladium catalyzed ethylene/CO copolymerization[66] had been previously demonstrated, are characterized in that at least one of the Ar groups bears an *ortho*-methoxy group.

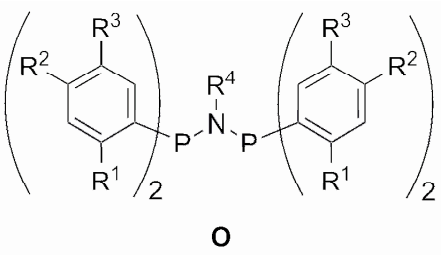

Figure 2. Bis(diarylphosphino)amine ligands **O**.

With ligand **O1** (R^1 = OMe, R^2, R^3 = H, R^4 = Me), [$CrCl_3(THF)_3$] as chromium source, and 300 equiv. of MAO as activator, an impressive productivity of 1033200 g × g $(Cr)^{-1}$ × h^{-1} was achieved, when running the reaction at 80°C and 20 bar of ethylene pressure (Scheme 19). Alongside with a C_6 fraction, which accounted for 90% of the total productivity, and of which 99.9% was 1-hexene, 1.8% of C_8 isomers and 8.5% of C_{10} isomers were detected in this run. A catalytic experiment conducted at 2 bar of ethylene pressure gave a somewhat increased C_6 fraction (91.5%, of which 99.7% was 1-hexene), however, the catalyst productivity dropped to only 4610 g × g $(Cr)^{-1}$ × h^{-1}.

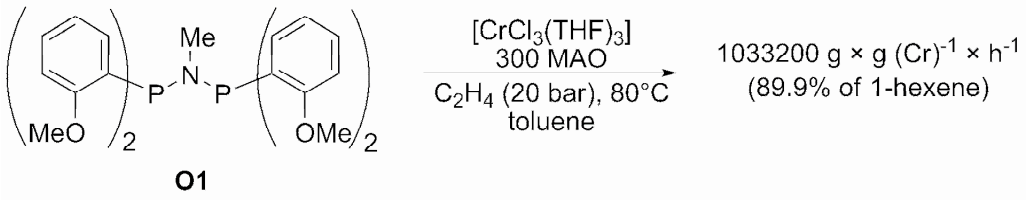

Scheme 19.

A couple of derivatives of ligand **O** with different substitution patterns on R^1, R^2, and R^3 were equally evaluated. While substitution on R^2 and R^3 was found to have less influence on catalyst selectivity, methoxy substitution on R^1 was found to be essential to catalyst activity. The R^1 = Et derivative was reported to be completely inactive in the oligomerization reaction, however, Blann *et al.* later reported an excellent activity towards ethylene trimerization with this ligand.[67]

Substitution of the nitrogen bridge between the phosphine moieties in ligands **O** with either CH_2 or CH_2CH_2 bridging groups yielded bis(diphenylphosphino)-methane and bis(diphenylphosphino)-ethane ligands, respectively, which did not yield active trimerization catalysts with chromium.

Bercaw and colleagues subsequently prepared well-defined Cr(III) complexes bearing ligand **O1** by coordination to [$Cr(CO)_6$] and subsequent oxidation with bromine or iodine (Scheme 20).[68] Crystal structure analysis confirmed the octahedral structure of these complexes and the η^3-P,P,O facial coordination mode of the ligand **O1** to the metal center. The resulting complexes were found to be active in ethylene trimerization after activation with MAO, however, no detailed productivity and selectivity numbers were reported.

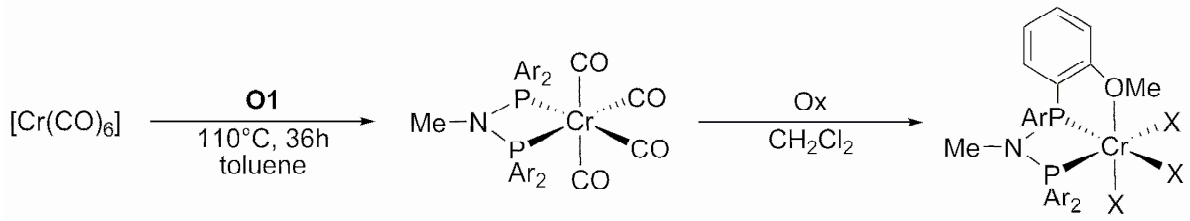

Scheme 20. Ar = *o*-MeO-C_6H_4, Ox = Br_2, thus X = Br, and Ox = I_2, thus X = I.

Complexe [$CrPh_3$(**O1**)] was equally prepared by the Bercaw group by coordination to [$CrPh_3(THF)_3$] and proved to be similar in terms of ethylene trimerization activity, when activated with one equivalent of [$H(OEt_2)_2(B((C_6H_3)$-$(CF_3)_2)_4)$]. A $CrPh_3$ complex bearing the *ortho*-thiomethoxy

derivative of ligand **O1** was also synthesized, however, crystal structure analysis showed an η^3-S,P,S coordination mode of the ligand different from the one observed with **O1** (Scheme 21). Accordingly, evaluation of this complex in the trimerization revealed inactivity in this reaction.[68]

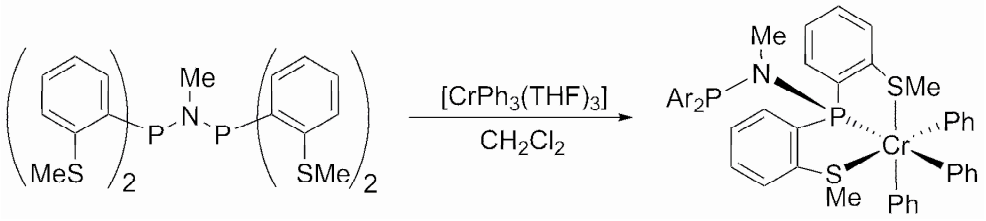

Scheme 21. Ar = *o*-MeS-C_6H_4.

3.6.4.3.2 The Sasol PNP Tri- and Tetramerization System

Shortly after the disclosure of the BP PNP trimerization system, Sasol Technology reported on[69] and patented[70] the first catalytic system for the tetramerization of ethylene to 1-octene with unprecedented selectivities. This system is based on the use of a Cr(III) precursor such as [Cr(acac)$_3$] or [$CrCl_3(THF)_3$], and a bis(phosphino)amine ligand **P**, with the difference, that the substituents on the phosphine moieties do not contain supplemental donor sites in their *ortho* position, as the ligands **O** used in the before mentioned BP PNP trimerization system. Upon activation with MAO, selectivities of up to approximately 70% towards 1-octene could be achieved (Scheme 22).

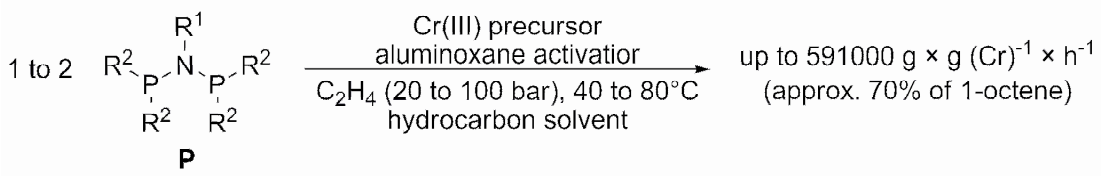

Scheme 22. The Sasol PNP tetramerization system.

Alongside with 1-octene, varying amounts of C_6 isomers, within which 1-hexene is the main product, account for approximately 15 to 30% of the productivity. The formation of polymeric material was reported to be <1% in most cases. In their initial report, the researchers from Sasol obtained the best results with $(Ph_2P)_2N(i\text{-Pr})$ (**P1**), [Cr(acac)$_3$], in a ligand/metal ratio of 1.35/1, 300 equiv. of modified methylaluminoxane (MMAO-3A), carrying out the reaction in toluene at 45°C and at 45 bar of ethylene pressure (Scheme 23).

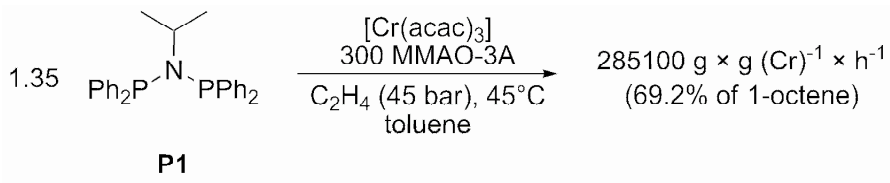

Scheme 23.

An overall productivity of 285100 g × g $(Cr)^{-1}$ × h^{-1} was reported, of which 70.7% were C_8 products (of which 97.9% was 1-octene), 16.0% of C_6 products (of which 66.4% was 1-hexene) and only 0.1% of polymeric material. Other minor products were reported to consist primarily of C_{10} to C_{14} products. An even higher productivity of 591000 g × g $(Cr)^{-1}$ × h^{-1} was obtained when the reaction was carried out in cyclohexane, in the presence of 200 equiv. of MAO. However, the quantity of polymeric material raised to 1.0% in this case, while the overall 1-octene selectivity (66.5%) was slightly lower than in the run carried out with toluene as solvent.

A complex **Q** as an example of a well defined catalyst precursor was equally prepared by addition of $(Ph_2P)_2N(Ph)$ (**P2**) to $[CrCl_3(THF)_3]$ and characterized through x-ray crystal structure analysis. As can be seen from scheme 24, a μ_2-Cl bridged dimeric structure with an octahedral coordination geometry around each Cr(III) center was obtained. Under the same catalytic conditions as presented in scheme 23, complex **Q** exhibited a productivity of 8800 g × g $(Cr)^{-1}$ × h^{-1} and an overall 1-octene selectivity of 59.4%, The relatively low productivity and an important polymeric fraction, which amounted to 6.7%, are most probably ascribed to the very low solubility of dimeric complex **Q** in hydrocarbon solvents.

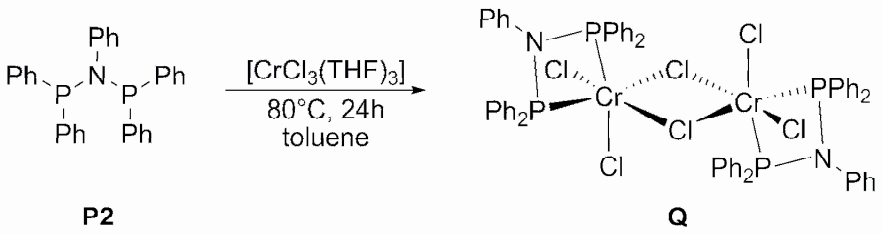

Scheme 24. Synthesis of complex **Q**.

The unprecedented selectivity towards the formation of 1-octene has raised the interest in this system and thus its systematic investigation has been undertaken by a variety of both academic and industrial research groups. In the following sections, investigations relating to variations of the bis(phosphine)amine ligand and other olefin transformations, which have proven to be feasible with the Sasol PNP system, are reviewed. On the other hand, studies and reports concerning the kinetics, the oxidation state of the catalytic species, the catalytic mechanism, and cocatalyst influence, have been omitted. These aspects are treated in the introduction to chapter 1.

3.6.4.3.2.1. Ligand Variations

The facile synthesis of bis(phosphine)amine ligands by simple reaction of 2 equiv. of a chlorophosphine $R^2R^{2'}PCl$ (with $R^2 = R^{2'}$ or $R^2 \neq R^{2'}$) with one equivalent of a primary amine R^1NH_2 in the presence of two equivalents of base to trap the formed HCl simplifies the task of systematic derivatization of this ligand. Accordingly, a number of studies dealing with the effect of varying either nitrogen substituent R^1 or, to a lesser extent, the phosphine substituents R^2 and $R^{2'}$ have appeared over

the last years. Care has to be taken when comparing catalytic results from different sources for the reasons already named before.

3.6.4.3.2.1.1 Variation of the N and P Substituents

The original Sasol patent application[70] and the corresponding follow-up publication[69] presented some results obtained under approximately comparable conditions, while the substitution pattern on the phosphine moieties was varied. Table 2 presents these catalytic results, which were obtained using chromium tris(2-ethylhexanoate), a metal/ligand ratio of 1/1 and an activation with 300 equiv. of MAO, at 45 to 65°C and 30 to 45 bar of ethylene pressure.

Table 2. Catalytic results with different ligands **P** (R^1 = Me) with different phosphine substituents R^2 and $R^{2'}$.

R^2	$R^{2'}$	Productivity[a]	$\%C_6$	$\%C_8$ ($\%1\text{-}C_8$)
m-Me-C_6H_4	*m*-Me-C_6H_4	30500	20.0	57.0(95.3)
p-Me-C_6H_4	*p*-Me-C_6H_4	47000	20.7	56.7(95.0)
2-napthyl	2-napthyl	26300	26.0	54.2(93.4)
p-biphenyl	p-biphenyl	15400	22.9	56.1(95.3)
Ph	Ph	27400	23.9	56.5(93.9)
Et	Ph	580	13.3	42.1(97.1)
Et	Et	2200	16.8	45.2(97.4)

Conditions: [Cr] = 8 µmol, [Cr]/ligand ratio = 1, 30 mL of toluene, 45°C-60°C, P(C2H4) = 30-45 bar, [a] in g × g $(Cr)^{-1}$

From these results, it may easily be deduced that aryl acceptor substituents on phosphorous are a prerequisite for good catalyst productivity and selectivity towards tetramerization products. Within the class of ligands **P** with aryl substitution on the phosphine moieties, no clear relationship between steric bulk and catalyst activity can be established.

More systematic studies have been undertaken on the effect of varying the central nitrogen substituent R^1 on the performance of the catalytic system. Kuhlmann *et al*. recently reported on a series of bis(diphenylphosphino)amine ligands with N-cycloalkyl substituents (Figure 3).[71]

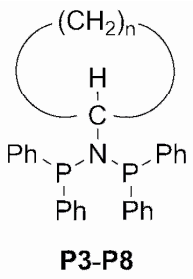

Figure 3. P3: n = 2, **P4**: n = 3, **P5**: n = 4, **P6**: n = 5, **P7**: n = 6, **P8**: n = 11.

It was found that ligands with small ring size substiuents on nitrogen (e.g. **P3**, **P4**) gave comparatively unselective catalyst systems, with notably high amounts of cyclic C_6 byproducts (their formation will be mechanistically explained in chapter 1). Increasing the N-cycloalkyl ring size from 3 (**P3**) to 12 (**P8**) yielded catalyst systems whose 1-hexene selectivity (within the C_6 fraction) improved from 44.3% (with **P3**) to 84.6% (with **P8**). This evolution was less striking in the 1-octene selectivity (within the C_8 fraction), where a concomitant improvement from 96.5% of 1-octene selectivity to 99.4% was observed. Thus an overall 16% improvement in α-selectivity was obtained by increasing the N-cycloalkyl ring size. A parallel increase in catalyst productivity was ascribed to better solubility of the ligands with large cycles.

Hor and colleagues prepared bis(phosphino)amine ligands with pendant ether and thioether substituents $R^1 = (CH_2)_nEMe$ (n = 2, 3; E= O, S).[72] One of these ligands, $(Ph_2P)_2N((CH_2)_3)SMe$ (**P9**) could be coordinated to $[CrCl_3(THF)_3]$. Through addition of acetonitrile, a monomeric octahedral complex could be obtained and structurally characterized by x-ray crystal structure analysis (Scheme 25).

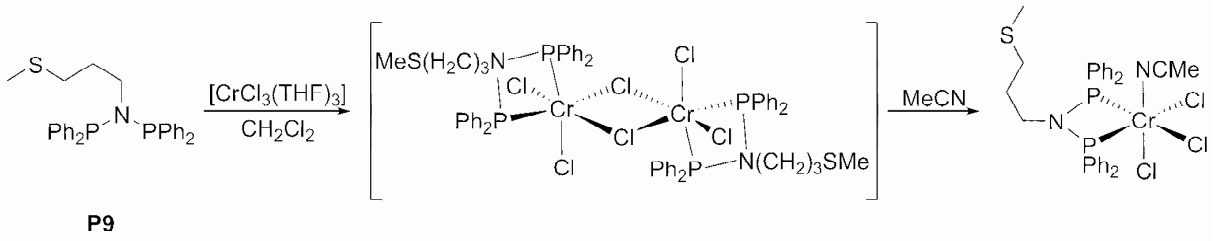

Scheme 25.

The ligand **P9** was found to coordinate in a η^2-P,P fashion to the Cr(III) center, while the pendant thioether did not participate in the coordination to the metal. Catalytic runs employing this ligand in an in situ manner, together with $[Cr(acac)_3]$ (metal/ligand ratio = 1/2), and upon activation with 440 equiv. of MAO (80°C, 30 bar of ethylene pressure), revealed productivities in the range of 10180 to 17866 g × g $(Cr)^{-1}$ × h^{-1}. In all cases, important quantities of polymeric material, accounting for between 4.9 (with the $R^1 = (CH_2)_3SMe$, R^2 = Et ligand) and 62.4% (**P9**) of the total productivity, were obtained. Apart from this, no clear conclusion on the effect of the pendant ether or thioether group could be draw, as admitted by the authors. Interestingly, however, the productivity of the catalyst

system with the $R^1 = (CH_2)_3SMe$, R^2 = Et derivative is much higher (14659 g × g $(Cr)^{-1}$ × h^{-1}) than the one with the $(Et_2P)_2N(Me)$, bearing no supplemental donor group (4400 g × g $(Cr)^{-1}$ × h^{-1}). This is indicative of some stabilizing effect of the pendant donor group.

A similar stabilizing effect was also observed by Elowe *et al.*, who investigated the catalytic properties of dimeric Cr(III) complexes with pendant ether donors,[73] in an analogous fashion as reported by Hor and al., found these complexes to be primarily trimerization catalysts (between 45 and 66%), however, at a comparatively low ethylene pressure of only 1 bar. As will be seen later in the section on the kinetics of the tri- and tetramerization reaction (chapter 1), low pressures favor trimerization over tetramerization. The most stable over time catalytic system was obtained with the ligand **P10** (R^1 = CH_2-(*o*-MeO)C_6H_4, R^2 = Ph), which was seen as an analogue to the ligands **O**, used in the BP ethylene trimerization system.

A recently reported modification of the classic PNP ligands is the triple-site PNP ligand **P11**, which is prepared by the reaction of Ph_2PCl (6 equiv.) and tris(2-aminoethyl)amine (Scheme 26).[74]

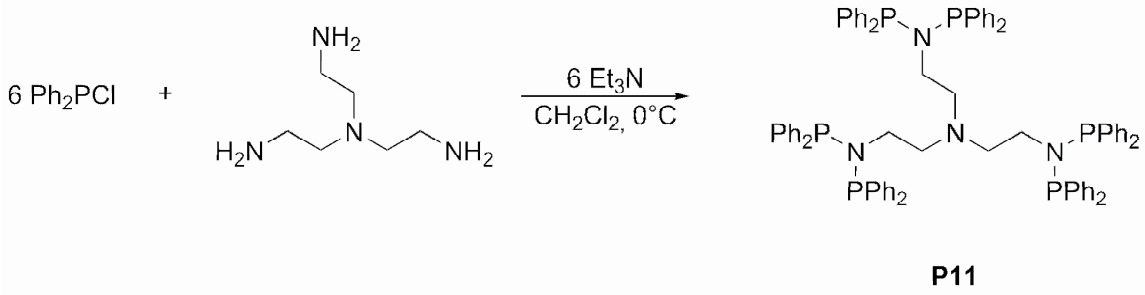

Scheme 26. Synthesis of the triple-site PNP ligand **P11**.

While the reported productivity and the observed selectivity lie within the range of PNP systems reported beforehand, the remarkable feature of the catalytic system is that it maintains its full activity at relatively MAO loadings as low as 100 equiv.

3.6.4.3.2.1.2 Carbon Substitution of the Central Nitrogen Bridge

As presented above, some insight has been gained on the relationship between structure of the PNP ligand and the observed selectivity of the catalytic system in which it is employed. In this context, it was found surprising that the ubiquitous bis(diphenylphosphino)methane ligand, despite its similarity to the PNP ligand, was inactive in selective ethylene tri- and tetramerization. Speculating on a need for rigidity in the central moiety of the diphosphine ligand, Overett *et al*. employed ligand **P12**-**P14** in the oligomerization reaction. For an unknown reason, with **P12**, only a low productivity was obtained stemming from an undefined product distribution.

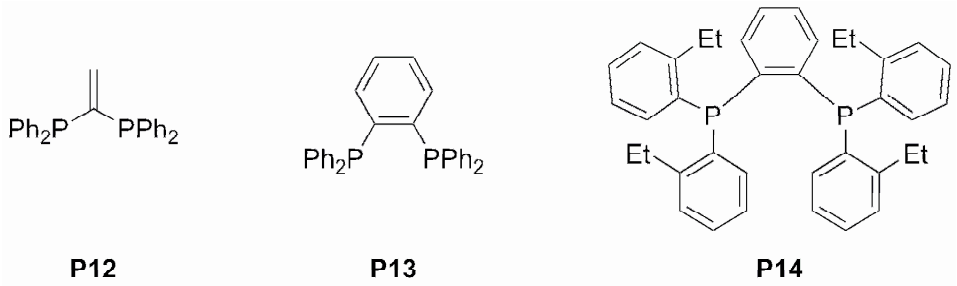

Figure 4.

On the other hand, a productivity of 2240000 g × g $(Cr)^{-1}$ × h^{-1} and an overall selectivity of 56.8% towards 1-octene (13.0% towards 1-hexene, 1-C_8/1-C_6 ratio = 4.4), with a polymeric fraction as low as 0.9%, was reported by Overett *et al.* with the complex [(**P13**)$CrCl_2(\mu_2$-Cl)]$_2$, when activated with 500 equiv. of MMAO-3A, at 60°C, and 50 bar of ethylene pressure. Essentially similar selectivities were reported with the analogous monomeric complex [(**P13**)$CrCl_3$(THF)], which was prepared from **P13** and [$CrCl_3(THF)_3$] in THF (Scheme 27), however, the productivity was somewhat lower (1543 g × g $(Cr)^{-1}$ × h^{-1}). Introduction of steric bulk in the *ortho* position of the P phenyl groups (ligand **P14**) induced a dramatic shift of selectivity from tetramerization to trimerization. The catalytic system [$Cr(acac)_3$]/**P14**/MMAO-3A, in a respective molar ratio of 1/1/500 yielded an overall selectivity of 59.2% towards 1-hexene (10.7% towards 1-octene, 1-C_8/1-C_6 ratio = 0.18). This result is supportive of the influence of the steric bulk of the diphosphine ligand on the selectivity towards either tri- or tetramerization.

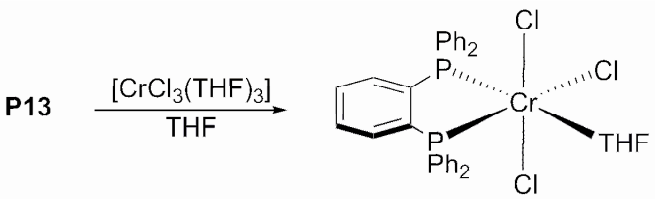

Scheme 27. Synthesis of the complex [(**P13**)$CrCl_3$(THF)].

Bis(diphenylphosphino)methane as the simplest PNP analogue was suspected to be non-innocent in the catalytic tri- and tetramerization reaction due to the relative acidity of the central methylene hydrogens and thus deprotonation in the presence of metal alkyl Lewis bases such as Me_3Al or even MAO.[75] Very recently, Wass and coworkers[76] reported on the preparation of the tetracarbonyl chromium complexes [$((Ph_2P)_2CHR)Cr(CO)_4$] (R = CH_3, *n*-hexyl, benzyl) bearing a substituted bis(diphenylphosphino)methane ligand, by deprotonation of the coordinated $(Ph_2P)_2CH_2$ ligand with *n*-BuLi,[77] and their subsequent cationization by reaction with a perfluorated silver aluminate (Scheme 28). The resulting complexes proved to be active in ethylene tri- and tetramerization after activation with 150 equiv. of carbonyl scavenger Et_3Al. The obtained overall 1-octene selectivities are not spectacular (approximately 33% depending on the substituent R), considering that important

polymeric fractions amounting to 17.0 to 64.3% of the total productivity were reported with this catalytic system.

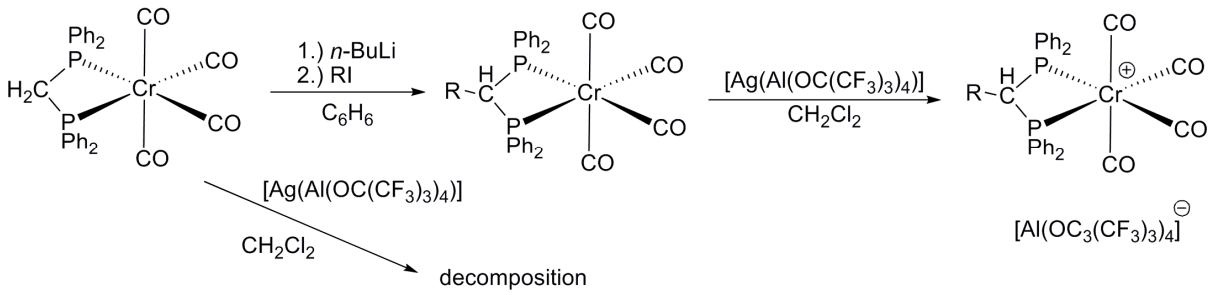

Scheme 28.

A direct comparison with the parent cationic complex $[((PPh_2)_2CH_2)Cr(CO)_4]^+$ was not possible, as it was prone to decomposition upon reaction with $[Ag(Al(OC(CF_3)_3)_4)]$.[78] However, a catalytic system prepared from $(Ph_2P)_2CHMe$ (**P15**) and $[Cr(acac)_3]$ (ligand/metal ratio = 1/1), and activated with 960 equiv. of MMAO proved to be active in ethylene tri-and tetramerization, however with a polymeric fraction, which accounted for 29.6% of the total productivity (219490 g × g $(Cr)^{-1}$ × h^{-1}) (Scheme 29).

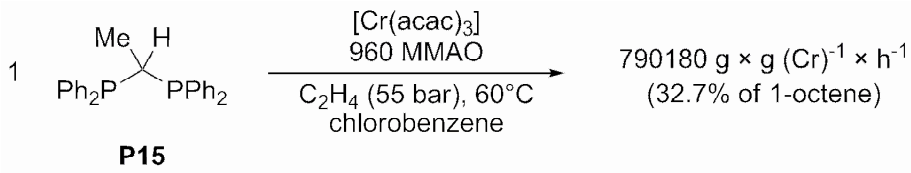

Scheme 29.

3.6.4.3.2.2 Other Transformations with the BP and the Sasol PNP System

The scope of the BP and the Sasol PNP oligomerization systems has been extended to (co)-oligomerization reactions. Bowen and Wass reported on the selective cotrimerization of styrene with ethylene.[79] A catalytic system consisting of $[CrCl_3(THF)_3]$ and ligand **O1** (metal/ligand ratio = 1/1), activated with 300 equiv. of MAO, yielded the best results (TOF(styrene) = 2674 h^{-1}), while the ligand **P1**, which had proven superior in the ethylene tetramerization reaction, yielded a catalytic system less than half as active as the one employing **O1**, as judged by the TOF(styrene) (1232 h^{-1}) (Scheme 30).

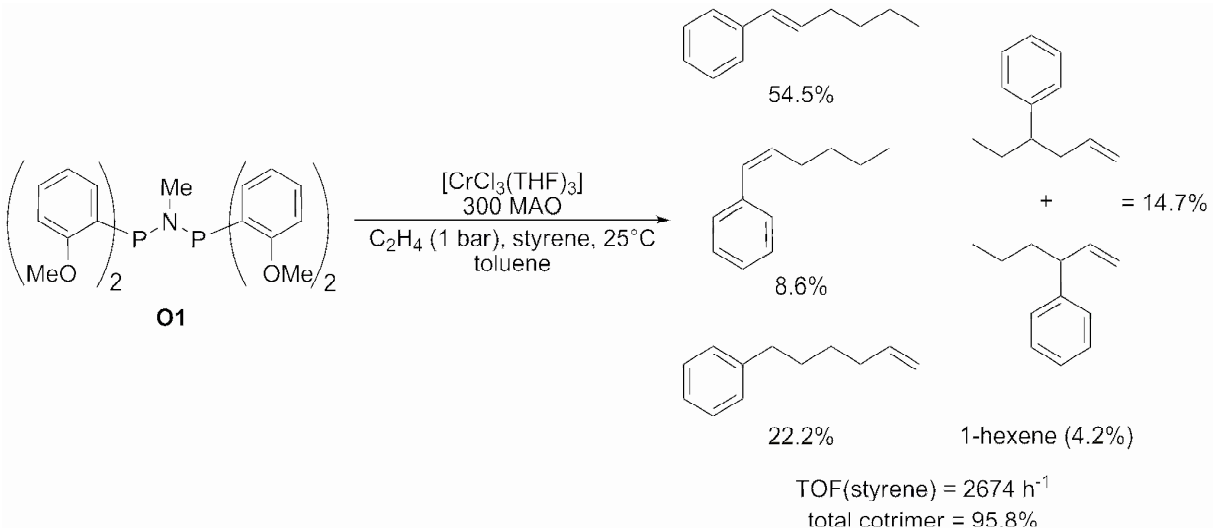

Scheme 30. Styrene/ethylene cotrimerization with the BP trimerization system.

Bowen *et al.* equally explored the selective trimerization of isoprene with catalytic systems employing $[CrCl_3(THF)_3]$ and either ligand **O1** or **P1** (ligand/metal ratio = 1/1), and MAO as activator.[80] The TOF reported with ligand **O1** was up to 660 h^{-1}, which is considerably higher than the activity of previously reported nickel-based isoprene trimerization catalysts (up to 20 h^{-1}).[81] Up to 79% of cyclic and linear isoprene trimerization products (C_{15} isomers) were found, the rest of the production accounted mainly for tetramer products.

After hydrogenation of the C_{15} fraction, only two structural isomers could be found, the linear 2,6,11-trimethyldodecane (approximately 70 to 85% of the C_{15} fraction) and the cyclic 1,4,8-trimethylcyclododecane (approximately 25 to 30% of the C_{15} fraction) (Scheme 31). Interestingly, catalytic runs using 1,3-butadiene instead of isoprene exclusively yielded polymerization products, a fact, which remains elusive to explanation up to now.

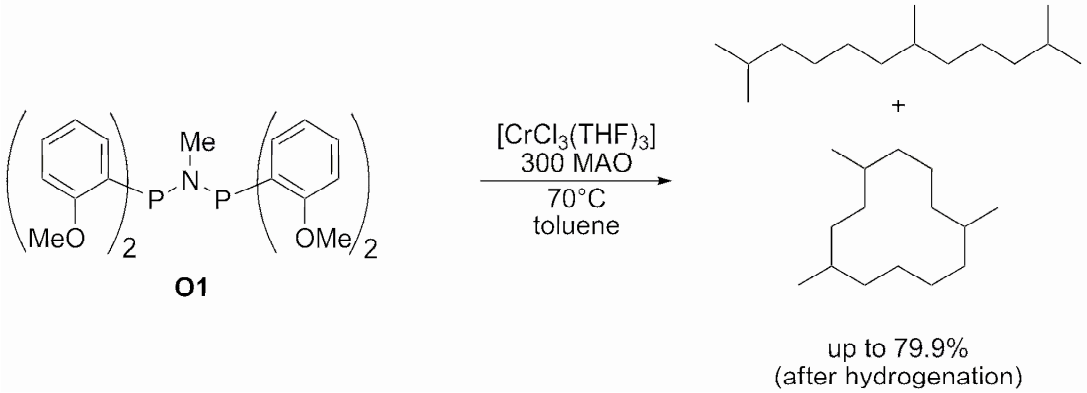

Scheme 31. Selective isoprene trimerization with the BP trimerization system.

4. Objectives of This Thesis

As can be seen from the preceding sections of the introduction, the catalyzed selective ethylene oligomerization has been a subject of ongoing research over the 40 years, with an explosion of studies emerging since approximately 2000 following the discovery of highly active chromium based catalytic systems employing neutral multidentate heteroatomic ligands to direct the selectivity of the oligomerization reaction towards the formation of either 1-hexene or, more recently, 1-octene.

The objectives of the present thesis are twofold: One major objective concerns the evaluation of new heteroatomic ligands in the ethylene oligomerization reaction. This involves the conception and preparation of these ligands, their coordination to relevant transition metals, and the catalytic testing towards oligomerization activity of the resulting complexes with ethylene and other α-olefins. Four major ligand classes have been evaluated, which are depicted in figure 5.

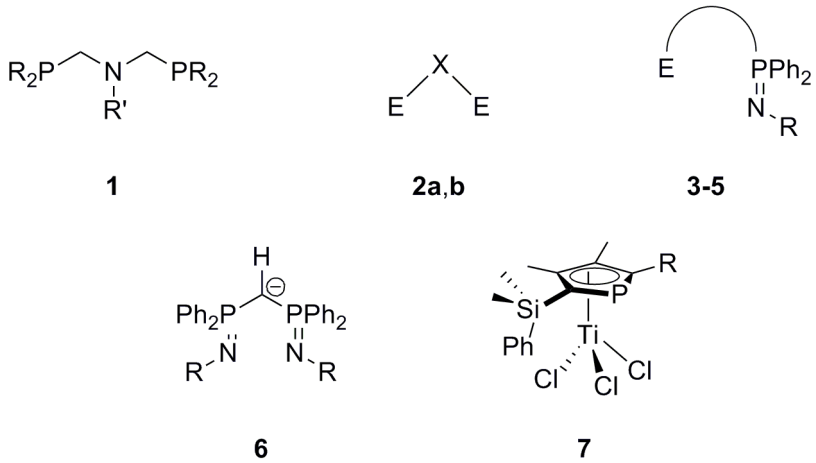

Figure 5. Evaluated ligands. **2a**: E = PR_2, X = NR', **2b**: E = SR, X = $C(Me)_2$.

One part of this work concerned the evaluation of symmetric bis(phosphinomethyl)amine (PCNCP) ligands (**1**) in the chromium-catalyzed selective tri- and tetramerization. The obtained results prompted us to take a closer look at some mechanistic aspects of this catalytic system, by means of theoretical chemistry and density functional methods (DFT), which constitutes the second major objective of this work.

Aside from this, a number of variations of the PNP ligand (**2a**) have been prepared and evaluated in ethylene oligomerization. This included the preparation of ligands bearing a similar geometry (notably an acute bite angle), but with different donor atoms (**2b**).

Mixed (P,N)-iminophosphorane ligands (**3**) were evaluated in the chromium- and nickel-catalyzed oligomerization reaction, and proved to be particularly efficient in nickel-catalyzed dimerization. It was therefore interesting to devise synthetic routes towards mixed (O,N)-iminophosphorane (**4**) and (S,N)-iminophosphorane ligands (**5**), to explore the coordination chemistry towards Ni(II), and to evaluate the resulting complexes in selective ethylene dimerization.

Symmetric monoanionic bis(iminophosphoranyl)methanides (**6**), which present some similarity to the bis(imino)pyridine ligands, whose complexes with iron proved to be highly active in ethylene oligomeriation and polymerization, could be prepared, and their coordination to Cr(III) was undertaken. The evaluation of these complexes revealed some unexpected product distributions.

The long-standing tradition of phosphorus-containing heterocycles in the laboratory tempted us to explore the catalytic activity of phosphatitanocene complexes with pendant aryl donors (**7**) in ethylene oligomerization and polymerization. This work was motivated by the precedent discovery by Deckers *et al.*, that the analogous cyclopentadienyl-titanium half sandwich complex yields a highly active ethylene trimerization catalyst when activated with MAO.

5. Bibliography

[1] K. Weissermel, H.-J. Arpe, in *Industrial Organic Chemistry*, 4. ed., Wiley-VCH, Weinheim, Germany, **2007**, pp. 59.
[2] H. A. Wittcoff, B. G. Reuben, J. S. Plotkin, in *Industrial Organic Chemicals*, 2. ed., John Wiley & Sons, Hoboken, New Jersey, **2004**.
[3] D. Morgan, in *PERP report 02/04*, Nexant Chem Systems, **2004**.
[4] J. T. Dixon, M. J. Green, F. M. Hess, M. D. H., *J. Organomet. Chem.* **2004**, *689*, 3641.
[5] H.-G. Elias, in *Macromolecules, Vol. 1*, **2005**, pp. 290.
[6] R. M. Manyik, W. E. Walker, T. P. Wilson, US3300458 (to Union Carbide Corporation), **1967**.
[7] W. K. Reagan, EP0417477 (to Phillips Petroleum Company), **1991**.
[8] A. Jabri, C. B. Mason, Y. Sim, S. Gambarotta, T. J. Burchell, R. Duchateau, *Angew. Chem. Intl. Ed.* **2008**, *47*, 9717.
[9] W. K. Reagan, J. W. Freeman, B. K. Conroy, P. T. M., E. A. Benham, EP0608447 (to Phillips Petroleum Company), **1994**.
[10] J. W. Freeman, J. L. Buster, R. D. Knudsen, US5856257 (to Phillips Petroleum Company), **1999**.
[11] E. Tanaka, H. Urata, T. Oshiki, T. Aoshima, R. Kawashima, S. Iwade, H. Nakamura, S. Katsuki, T. Okanu, EP0611743 (to Mitsubishi Chemical Corporation), **1994**.
[12] J. T. Dixon, J. J. C. Grove, A. Ranwell, WO0183477 (to Sasol Technology Pty. Ltd.), **2001**.
[13] in *Press Release*, Chevron Phillips Chemical Company, 31th Oct, **2005**.
[14] in *Chemical Engineering*, **2005**, p. 28.
[15] F. J. Karol, G. L. Karapinka, C. Wu, A. W. Dow, R. N. Johnson, W. L. Carrick, *J. Polymer Sci. Part A-1: Polymer Chem.* **1972**, *10*, 2621.
[16] G. J. P. Britovsek, V. C. Gibson, D. F. Wass, *Angew. Chem. Intl. Ed.* **1999**, *38*, 428.
[17] K. Theopold, H. , *Eu. J. Inorg. Chem.* **1998**, *1998*, 15.
[18] R. Emrich, O. Heinemann, P. W. Jolly, C. Kruger, G. P. J. Verhovnik, *Organometallics* **1997**, *16*, 1511.
[19] H. Mahomed, A. Bollmann, J. T. Dixon, V. Gokul, L. Griesel, C. Grove, F. Hess, H. Maumela, L. Pepler, *Appl. Catal. A: Gen.* **2003**, *255*, 355.
[20] J. J. C. Grove, H. Mahomed, L. Griesel, Pat. Appl. WO03/004158 (to Sasol Technology Pty. Ltd.), **2002**.
[21] Y. Yang, H. Kim, J. Lee, H. Paik, H. G. Jang, *Applied Catal. A: Gen.* **2000**, *193*, 29.
[22] T. Aoyama, H. Mimura, T. Yamamoto, M. Oguri, Y. Koei, JP09176299 (to Tosoh Corporation), **1997**.
[23] J. S. Rogers, G. C. Bazan, *Chem. Commun.* **2000**, 1209.
[24] J. S. Rogers, X. Bu, G. C. Bazan, *Organometallics* **2000**, *19*, 3948.
[25] T. Aoyama, H. Urata, JP11181016 (to Mitsubishi Chemical Industries), **1999**.
[26] D. C. Commereuc, R. M. Drochon, L. Saussine, US6031145 (to Institut Français du Pétrole), **1998**.
[27] D. C. Commereuc, R. M. Drochon, L. Saussine, EP1110930 (to Institut Français du Pétrole), **2001**.
[28] D. H. Morgan, S. L. Schwikkard, J. T. Dixon, J. J. Nair, R. Hunter, *Adv. Synth. Catal.* **2003**, *345*, 939.
[29] W. A. Herrmann, *Angew. Chem. Intl. Ed.* **2002**, *41*, 1290.
[30] C. W. Bielawski, R. H. Grubbs, *Angew. Chem. Intl. Ed.* **2000**, *39*, 2903.
[31] U. Frenzel, T. Weskamp, F. J. Kohl, W. C. Schattenmann, O. Nuyken, W. A. Herrmann, *J. Organomet. Chem.* **1999**, *586*, 263.
[32] A. Dohring, J. Gohre, P. W. Jolly, B. Kryger, J. Rust, G. P. J. Verhovnik, *Organometallics* **2000**, *19*, 388.
[33] M. Tilset, O. Andell, A. Dhindsa, M. Froseth, WO0249758 (to Borealis Technology OY), **2002**.

[34] D. S. McGuinness, W. Mueller, P. Wasserscheid, K. J. Cavell, B. W. Skelton, A. H. White, U. Englert, *Organometallics* **2001**, *21*, 175.
[35] D. S. McGuinness, V. C. Gibson, D. F. Wass, J. W. Steed, *J. Am. Chem. Soc.* **2003**, *125*, 12716.
[36] D. S. McGuinness, J. A. Suttil, M. G. Gardiner, N. W. Davies, *Organometallics* **2008**, *27*, 4238.
[37] D. S. McGuinness, *Organometallics* **2009**, *28*, 244.
[38] J. R. Briggs, US4668838 (to Union Carbide Corporation), **1987**.
[39] J. R. Briggs, *J. Chemical Soc.-Chem. Commun.* **1989**, 674.
[40] H. Sato, S. Suzuki, JP07215896 (to Idemitsu Chemical Company), **1995**.
[41] K. Kodoi, H. Sato, JP08183746 (to Idemitsu Chemical Company), **1996**.
[42] I. J. Levine, F. J. Karol, US4777315 (to Union Carbide Corporation), **1988**.
[43] F. J. Wu, EP0537609 (to Ethyl Corporation), **1992**.
[44] H. Maas, S. Mihan, R. D. Köhn, S. Guido, J. Tropsch, EP1171445 (to BASF AG), **1999**.
[45] R. D. Köhn, G. Kociok-Köhn, *Angew. Chem. Intl. Ed.* **1994**, *33*, 1877.
[46] P. Wasserscheid, S. Grimm, R. D. Köhn, M. Haufe, *Adv. Synth. Catal.* **2001**, *343*, 814.
[47] C. N. Nenu, B. M. Weckhuysen, *Chem. Commun.* **2005**, 1865.
[48] I. García-Orozco, R. Quijada, K. Vera, M. Valderrama, *J. Mol. Catal. A: Chem.* **2006**, *260*, 70.
[49] J. Zhang, A. Li, T. S. A. Hor, *Organometallics* **2009**, *28*, 2935.
[50] K. Iwanaga, M. Tamura, GB2314518 (to Sumitomo Chemical Corp.), **1997**.
[51] J. Zhang, P. Braunstein, T. S. A. Hor, *Organometallics* **2008**, *27*, 4277.
[52] D. S. McGuinness, P. Wasserscheid, W. Keim, D. Morgan, J. T. Dixon, A. Bollmann, H. Maumela, F. Hess, U. Englert, *J. Am. Chem. Soc.* **2003**, *125*, 5272.
[53] J. T. Dixon, P. Wasserscheid, D. S. McGuinness, H. F. M., H. Maumela, D. Morgan, A. Bollmann, EP1456152 (to Sasol Technology Pty. Ltd.), **2002**.
[54] D. S. McGuinness, P. Wasserscheid, D. H. Morgan, J. T. Dixon, *Organometallics* **2005**, *24*, 552.
[55] D. S. McGuinness, D. B. Brown, R. P. Tooze, F. M. Hess, J. T. Dixon, A. M. Z. Slawin, *Organometallics* **2006**, *25*, 3605.
[56] J. O. Moulin, J. Evans, D. S. McGuinness, G. Reid, A. J. Rucklidge, R. P. Tooze, M. Tromp, *Dalton Trans.* **2008**, 1177.
[57] D. de Wet-Roos, J. T. Dixon, *Macromolecules* **2004**, *37*, 9314.
[58] C. N. Temple, S. Gambarotta, I. Korobkov, R. Duchateau, *Organometallics* **2007**, *26*, 4598.
[59] F.-J. Wu, US5811618 (to Amoco Corporation), **1995**.
[60] D. S. McGuinness, P. Wasserscheid, W. Keim, C. Hu, U. Englert, J. T. Dixon, C. Grove, *Chem. Commun.* **2003**, 334.
[61] J. T. Dixon, C. Grove, P. Wasserscheid, D. S. McGuinness, F. Hess, H. Maumela, D. H. Morgan, A. Bollmann, WO03/053891 (to Sasol Technology Pty. Ltd.), **2003**.
[62] D. F. Wass, *Dalton Trans.* **2007**, 816.
[63] D. F. Wass, WO0204119 (to BP Chemicals Ltd.), **2002**.
[64] A. Carter, S. A. Cohen, N. A. Cooley, A. Murphy, J. Scutt, D. F. Wass, *Chem. Commun.* **2002**, 858.
[65] N. A. Cooley, S. M. Green, D. F. Wass, K. Heslop, A. G. Orpen, P. G. Pringle, *Organometallics* **2001**, *20*, 4769.
[66] S. J. Dossett, D. F. Wass, M. D. Jones, A. Gillon, A. G. Orpen, J. S. Fleming, P. G. Pringle, *Chem. Commun.* **2001**, 699.
[67] K. Blann, A. Bollmann, J. T. Dixon, F. M. Hess, E. Killian, H. Maumela, D. H. Morgan, A. Neveling, S. Otto, M. J. Overett, *Chem. Commun.* **2005**, 620.
[68] S. J. Schofer, M. W. Day, L. M. Henling, J. A. Labinger, J. E. Bercaw, *Organometallics* **2006**, *25*, 2743.
[69] A. Bollmann, K. Blann, J. T. Dixon, F. M. Hess, E. Killian, H. Maumela, D. S. McGuinness, D. H. Morgan, A. Neveling, S. Otto, M. Overett, A. M. Z. Slawin, P. Wasserscheid, S. Kuhlmann, *J. Am. Chem. Soc.* **2004**, *126*, 14712.

[70] K. Blann, A. Bollmann, J. T. Dixon, A. Neveling, D. H. Morgan, H. Maumela, E. Killian, F. M. Hess, S. Otto, L. Pepler, H. Mahomed, M. J. Overett, WO2004/056479 (to Sasol Technology Pty. Ltd.), **2003**.
[71] S. Kuhlmann, K. Blann, A. Bollmann, J. T. Dixon, E. Killian, M. C. Maumela, H. Maumela, D. H. Morgan, M. Prétorius, N. Taccardi, P. Wasserscheid, *J. Catal.* **2007**, *245*, 279.
[72] Z. Weng, S. Teo, T. S. A. Hor, *Dalton Transactions* **2007**, 3493.
[73] P. R. Elowe, C. McCann, P. G. Pringle, S. K. Spitzmesser, J. E. Bercaw, *Organometallics* **2006**, *25*, 5255.
[74] G. Mao, Y. Ning, W. Hu, S. Li, X. Song, B. Niu, T. Jiang, *Chin. Sci. Bull.* **2008**, *53*, 3511.
[75] M. J. Overett, K. Blann, A. Bollmann, R. de Villiers, J. T. Dixon, E. Killian, M. C. Maumela, H. Maumela, D. S. McGuinness, D. H. Morgan, A. Rucklidge, A. M. Z. Slawin, *J. Mol. Catal. A: Chem.* **2008**, *283*, 114.
[76] A. Dulai, H. t. de Bod, M. J. Hanton, D. M. Smith, S. Downing, S. M. Mansell, D. F. Wass, *Organometallics* **2009**, *28*, 4613.
[77] S. Al-Jibori, B. L. Shaw, *J. Chem. Soc. Dalton Trans.* **1982**, 286.
[78] A. J. Rucklidge, D. S. McGuinness, R. P. Tooze, A. M. Z. Slawin, J. D. A. Pelletier, M. J. Hanton, P. B. Webb, *Organometallics* **2007**, *26*, 2782.
[79] L. E. Bowen, D. F. Wass, *Organometallics* **2005**, *25*, 555.
[80] L. E. Bowen, M. Charernsuk, D. F. Wass, *Chem. Commun.* **2007**, 2835.
[81] S. Akutagawa, T. Taketomi, H. Kumobayashi, K. Takayama, T. Someya, S. Otsuka, *Bull. Chem. Soc. Jap.* **1978**, *51*, 1158.

Chapter 1. On the Mechanism of Selective Ethylene Tri- and Tetramerization

Chapter 1. On the Mechanism of Ethylene Oligomerization

In the first part of this chapter, different aspects of the mechanism of the chromium-catalyzed selective ethylene oligomerization, that is, the metallacyclic nature of the mechanism, the oxidation state of the catalytically active species, and the occurrence of C_6 cyclic byproducts in the Sasol tetramerization system are reviewed and our own experimental and theoretical contributions to some of these aspects are reported.

The second part of this chapter deals with a comprehensive experimental and theoretical treatment of substituent effects of the ligand used in a chromium-based system for ethylene tri- and tetramerization.

1. Introduction

1.1 The Cossee-Arlman Metal Hydride Mechanism

Unselective ethylene oligomerization leading to statistical distributions of LAOs, as observed with most historical processes (see section 2 of the introductory chapter) for this transformation, is known to follow a mechanism named "Cossee-Arlman" mechanism. Cossee and Arlman[1, 2] proposed a mechanism involving metal hydride and metal alkyl species, as shown in scheme 1.

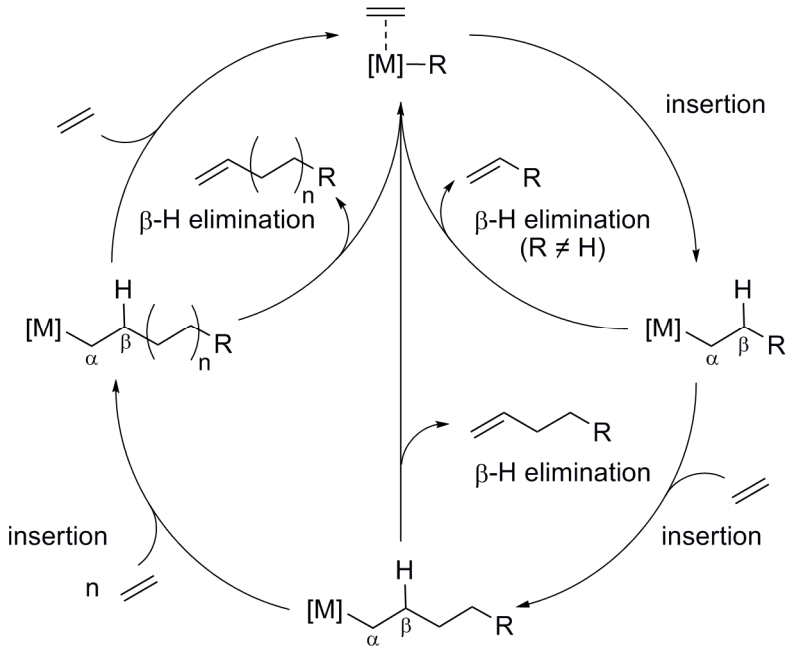

Scheme 1. Mechanism of LAO formation as proposed by Cossee and Arlman. [M] = transition metal, R = H, alkyl.

The active catalytic species is generated through reaction of a precatalyst with an activator, usually an organoaluminium compound such as Et_3Al, Et_2AlCl, $EtAlCl_2$, or an aluminoxane. Activation yields an

[M]-R (R = alkyl) species, which may either undergo direct β-hydride elimination to yield an equally active [M]-R (R = H) species, or insert further ethylene molecules into the M-R bond, until eventually β-hydride elimination occurs, the LAO is liberated, and an active [M]-H species is regenerated, which may insert ethylene molecules into its metal hydride bond, thus continuing the catalytic cycle.

As at each step either insertion of a further ethylene molecule or, alternatively, β-hydride elimination is a possible mechanistic option, the selectivity of the catalyst depends on the ratio between the rate of insertion k_{ins} and the rate of β-hydride elimination k_{elim}, and the factors (temperature, ethylene pressure, transition metal, ligand) influencing this ratio. Under the hypothesis that the rate of insertion is by far greater than the rate of elimination, long chain polyethylene is formed. If, on the other hand, the two rates are within the same order of magnitude, distributions of LAOs with different chain lengths $n \times 2$ are obtained. A mathematical model describing these distributions has been developed by Schulz and Flory, in which is assumed that the probability for chain growth does not depend on the chain length of the [M]-alkyl species, and that formed LAOs do not participate in the insertion reaction (which would yield branched α-olefins).

Thus, the probability p_{ins} of an insertion over elimination may be expressed as follows, provided that k_{ins} may be considered independent of the ethylene concentration:

$$p_{ins} = \frac{k_{ins}}{k_{ins} + k_{elim}} = \frac{x_{n+1}}{x_n}$$

Equation 1.

The so-called Schulz-Flory factor β is defined as the ratio between the rate of elimination and the rate of insertion reactions:

$$\beta = \frac{k_{elim}}{k_{ins}} = \frac{1 - p_{ins}}{p_{ins}} = \frac{x_n}{x_{n+1}} - 1$$

Equation 2.

In the literature, instead of Schulz-Flory factor β, distributions are often characterized conveniently directly by the Schulz-Flory coefficient K (= p_{ins}), which is defined by the following equation:

$$K = \frac{1}{\beta + 1} = \frac{x_{n+1}}{x_n}$$

Equation 3.

High K values thus signify broad distributions with long-chain oligomers, whereas small K values indicate tight distributions and thus shorter-chain oligomers.

A Cossee-Arlman mechanism is operative with most transition metals active in the ethylene oligomerization and polymerization reaction, however, depending on the nature of the coordination

sphere, the predominance of the Cossee-Arlman mechanism may be switched towards a mechanism involving metallacyclic intermediates. Evidence for a metallacyclic mechanism in ethylene oligomerization has been found for catalysts based on chromium, titanium, and tantalum.

1.2 Metallacyclic Mechanism in Ethylene Oligomerization

Manyik was the first to suggest the presence of metallacyclic intermediates in the chromium catalyzed oligomerization and polymerization of ethylene.[3] This was based on the observation of an increased amount of 1-hexene in the catalytic product stream with respect to the other products, which followed a classic Schulz-Flory distribution (see section 3 of the introductory chapter). After activation, the activated chromium center is believed to η^2-coordinate two ethylene molecules, which would subsequently form a chromacyclopentane intermediate (Scheme 2). This assumption was supported by the previous isolation of platinum metallacyclic intermediates. The chromacyclopentane intermediate was believed to evolve towards a chromium ethyl butenyl species via β-hydride transfer from one of the metallacyclic β-carbons to a third coordinated ethylene molecule (pathway 1, Scheme 2). 1-hexene should then be liberated by reductive elimination.

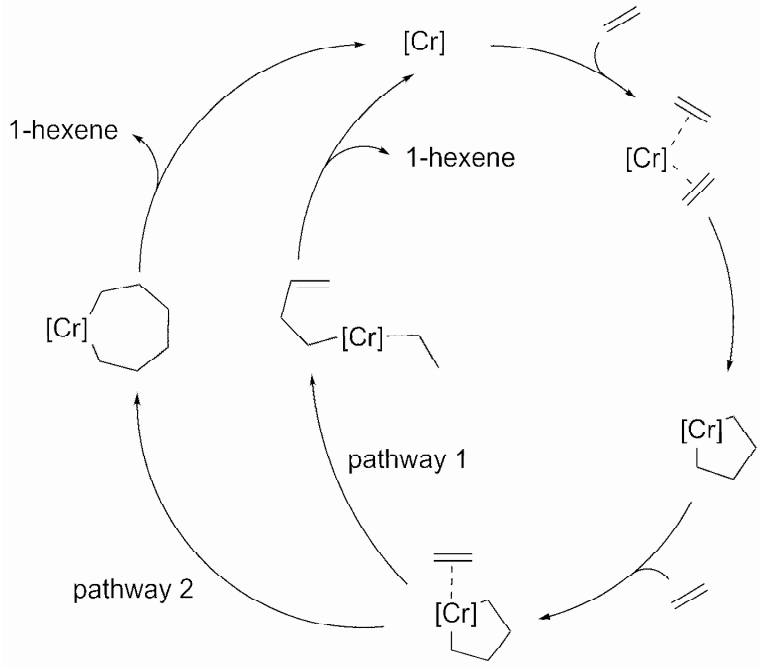

Scheme 2. Metallacyclic mechanism as proposed by Manyik (pathway 1) and Briggs (pathway 2).

The observation that thermal decomposition of platinacycloheptanes yields 1-hexene as the only product led Briggs to conclude that chromacycloheptanes might be intermediates in the ethylene trimerization reaction (pathway 2 in Scheme 2).[4] Liberation of 1-hexene should then proceed via the formation of a chromium hexenyl hydride species, which would reductively eliminate 1-hexene and regenerate the catalytically active species [Cr]. Seminal work by Jolly and colleagues, who prepared

and structurally characterized (η^5-C_5H_5)-chromacyclo-pentane and -heptane complexes further supported the viability of these intermediates in the catalytic cycle.[5]

With these general ideas set, further both experimental and mechanistic studies into the details of this mechanism appeared following the breakthrough discoveries of highly selective chromium catalysts bearing mixed heteroatomic ligands, notably the BP and Sasol PNP systems for ethylene tri- and tetramerization. Theoretical studies on the Phillips trimerization system,[6] as well as the titanium[7-9] and tantalum[10] based catalytic systems have equally been undertaken; reference to them is made in the following text when necessary.

2. The British Petroleum and the Sasol PNP Tri- and Tetramerization System

2.1 Establishment of a Metallacyclic Mechanism

Following the discovery by Wass and colleagues at British Petroleum (see section 3.6.4.3.1 of the introductory chapter), the Bercaw workgroup dedicated a number of studies towards the understanding of the mechanism of the selective ethylene trimerization reaction. One of their accomplishments was the preparation of a defined catalytic precursor complex,[11] of which two examples were prepared as outlined in scheme 3.

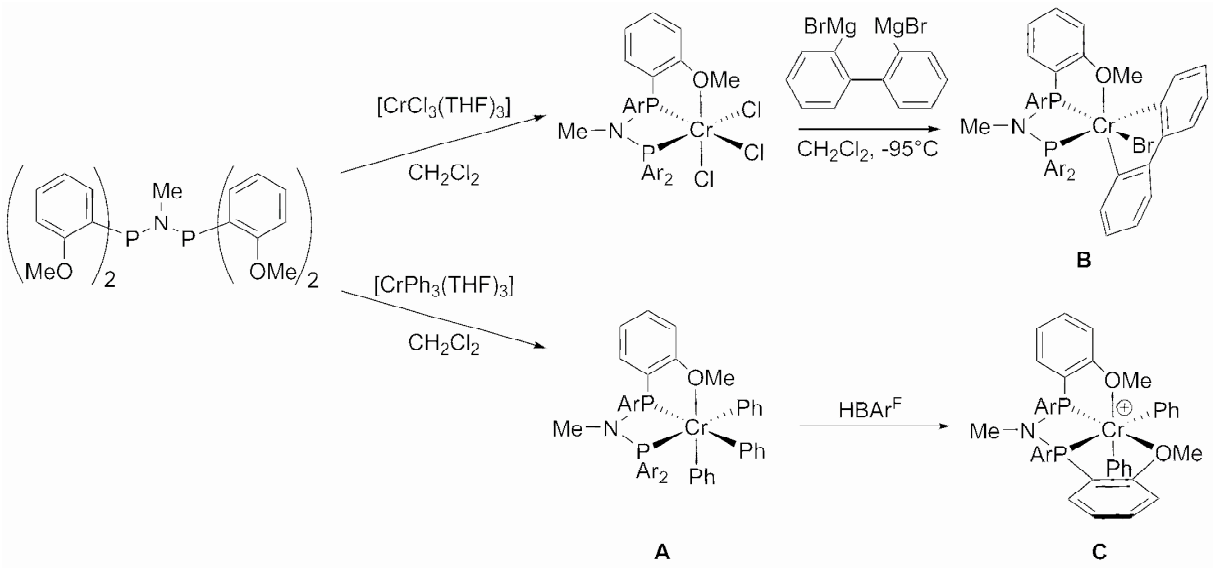

Scheme 3. Synthesis of well-defined catalyst precursors **A** and **B**. $HBAr^F$ = $[H(OEt_2)_2B((C_6H_3)$-$(CF_3)_2)_4]$. **C** is a suggested structure.

Activation of **A** with the Brønstedt acid $[H(OEt_2)_2(B(C_6H_3)$-$(CF_3)_2)_4]$ or activation of **B** with the halogen abstracting $[NaB((C_6H_3)$-$(CF_3)_2)_4]$ yielded presumably cationic chromium complexes (e.g. such as **C**) which were found to be active in ethylene trimerization.[12] Exposure of activated **A** or **B** to a 1:1 mixture of deuterated ethylene C_2D_4 and undeuterated C_2H_4 yielded exclusively C_6H_{12}, C_6D_{12},

$C_6H_8D_4$, and $C_6H_4D_8$. This result is consistent with a metallacyclic mechanism, whereas a Cossee-Arlman type mechanism would have involved H/D scrambling and thus the appearance of oligomers with uneven H and D numbers. Complex **C** does not decompose via the reductive elimination of biphenyl, but instead inserts ethylene into its Cr-Ph bonds, and eliminates styrene and benzene, as was found through a detailed analysis of the catalysis product mixture. On the other hand exposure of unactivated **A** to ethylene gave no reaction. This result was thus indicative of the necessity to have a cationic active species in the catalytic cycle. Further support for a metallacyclic mechanism was gained from the product analysis of the styrene/ethylene co-trimerisation[13] and the isoprene trimerization[14] with the BP PNP catalytic system (see section 3.6.4.3.2.2 of the introductory chapter). The resulting products of these reactions were found to stem exclusively from mechanistic scenarios involving metallacycles.

A similar analysis of the Sasol tetramerization system, equally involving a 1:1 mixture of deuterated C_2D_4 and undeuterated C_2H_4 came to the conclusion, that a metallacyclic mechanism was equally operative in the ethylene tetramerization reaction, and chromacycloheptanes were intermediates in this reaction.[15]

From these findings, the following general scheme for the mechanism of ethylene tri- and tetramerization could be established (Scheme 4):

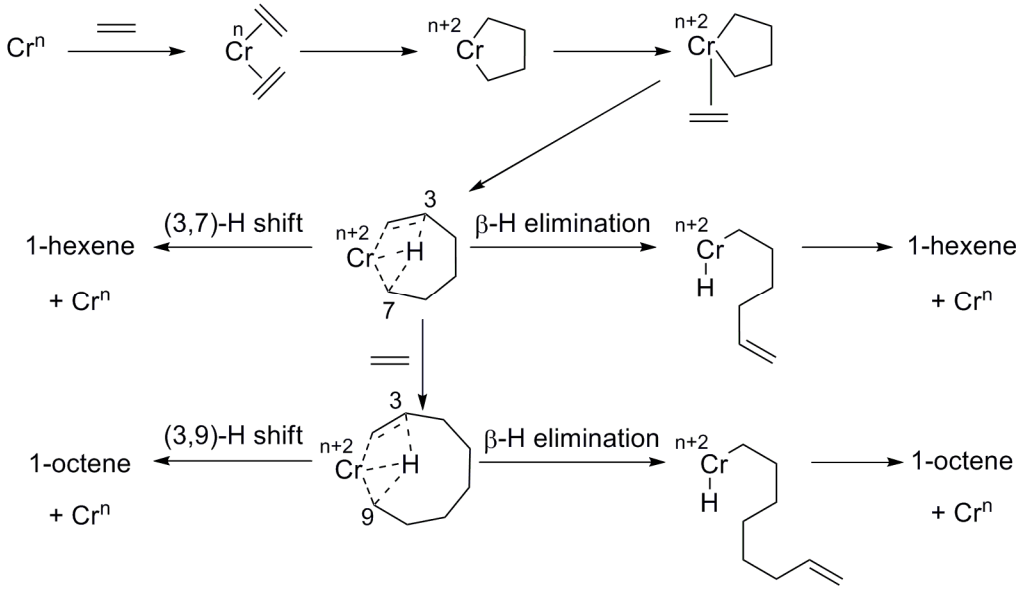

Scheme 4. Mechanism of the Ethylene Tri-and Tetramerization reaction as proposed in the literature.

The experimental studies, however, could not distinguish between the two possibilities which exist for the elimination of 1-hexene from the chromacycloheptane intermediate, or 1-octene from the chromacyclononane species. Both the chromacycloheptane and the chromacyclononane are sufficiently flexible to undergo rapid β-H elimination, yielding a chromium-alkenyl-hydride species, which reductively eliminates 1-hexene or 1-octene, respectively, to regenerate Cr^n and close the catalytic cycle. Theoretical calculations on this last step of the catalytic cycle, however, suggest that

the release of 1-hexene,[6-10, 16] and of 1-octene,[17] from the metallacyclic intermediate proceeds via a concerted (3,7)- or (3,9)-hydrogen shift, respectively, implicating a formal two-electron reduction of the metal center.

2.2 Kinetic Studies on the Chromium-Catalyzed Selective Oligomerization Reaction

Inspite of the growing number of contributions dealing with an improved understanding of the metallacyclic mechanism on chromium, and other metals, where this mechanism is operative, only relatively few studies deal with kinetic aspects of this reaction.

Early work of Manyik and coworkers indicated the reaction rate of the ethylene oligomerization reaction on chromium to be second-order dependent in ethylene concentration.[3] This same dependence was found for the BP trimerization system,[18] and the rate determining step was supposed to be the coordination and oxidative coupling of two ethylene molecules to form the chromacyclopentane intermediated.

Walsh *et al.* undertook a more detailed kinetic study on the Sasol PNP tri- and tetramerization system. Employing the ligand $(Ph_2P)_2N(i\text{-Pr})$, $[Cr(acac)_3]$, MAO, and cumene as solvent, both the dependence of the reaction rate on temperature and ethylene concentration was evaluated.[19]

The authors determined a kinetic model for the reaction rate $dc_{(oligo)}/dt$ following the relation described in equation 4, with k_i describing a temperature-dependent intrinsic rate (Equation 5).

$$\frac{dc_{(oligo)}}{dt} = k_i \times [Cr]^m \times [ethylene]^n \times e^{(-k_d \times t)}$$

Equation 4.

$$k_i = k_{i,0} \times e^{-\left(\frac{E_{Ai}}{RT}\right)}$$

Equation 5.

The exponential term in equation 4 contains the rate of desactivation k_d, whose temperature dependence is given by the following relation (equation 6):

$$k_d = k_{d,0} \times e^{-\frac{E_{Ad}}{RT}}$$

Equation 6.

Within the temperature (35-45°C), pressure (30-45 bar), and chromium charge range (5-15 µmol) of the study, E_{Ai} was determined to be 15.43 Kcal × mol^{-1}, E_{Ad} to 32.51 Kcal × mol^{-1}. While the rate dependence in chromium was found to be of first order (m = 1), a reaction rate dependence of n = 1.57 in ethylene concentration was found, indicating competing mechanistic alternatives of first and second order.

2.3 Oxidation State of the Chromium Metal Center

While it is now generally accepted that a metallacycle mechanism is operative in the selective tri- and tetramerization reaction, the oxidation state of the catalytically active species remains a subject of debate. Both the Cr(II)-Cr(IV) and the Cr(I)-Cr(III) two-electron redox couples have been suggested for different chromium based oligomerization systems.

Cr(II)-Cr(IV) was proposed to be the redox couple for the IFP phenoxide trimerization system (see section 3.4 of the introduction) by Morgan *et al.* on the basis of magnetic susceptibility measurements of catalytic mixtures.[20] The possibility of a Cr(II)-Cr(IV) redox couple to be operative was equally evoked for the two Sasol trimerization systems based on bis(sulphanylethyl)amine and bis(phosphinylethyl)amine ligands (sections 3.6.3.2 and 3.6.4.2 of the introduction), since Cr(II) complexes with these ligands proved equally active in the selective trimerization reaction.[21] The Gambarotta workgroup[22] equally speculated about a cationic divalent bis(sulphanyl)amine-chromium species to be the active species in the catalytic cycle, based on Cr(II) complexes **E** obtained by reaction of isobutylaluminoxane with Cr(III) complex **D** (Scheme 5). It should be noted that **E** was only active after addition of 300 equiv. of MAO, whose role was described not to be a further reductive agent, but a non-coordinating anion stabilizing the active cationic metal center.

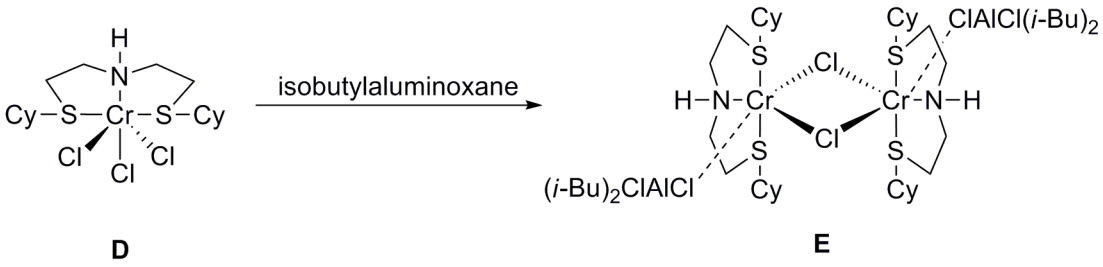

D **E**

Scheme 5.

From the dimeric Cr(III) precursor $[(((Ph_2P)_2NCy)CrCl_2(\mu_2\text{-}Cl))_2]$ (**F**) Jabri *et al.* obtained and structurally characterized the divalent cationic Cr(II) aluminate **G** bearing two $(Ph_2P)_2NCy$ ligands on a single metal center by reaction with a ten-fold excess of Me_3Al, as depicted in scheme 6.[23] Alongside with this, an unidentified black side product was formed in this reaction.

G showed no reactivity towards ethylene, even in the presence of excess Me_3Al. On the other hand, upon activation with 300 equiv. of MAO, **G** proved active in selective ethylene tri- and tetramerization.

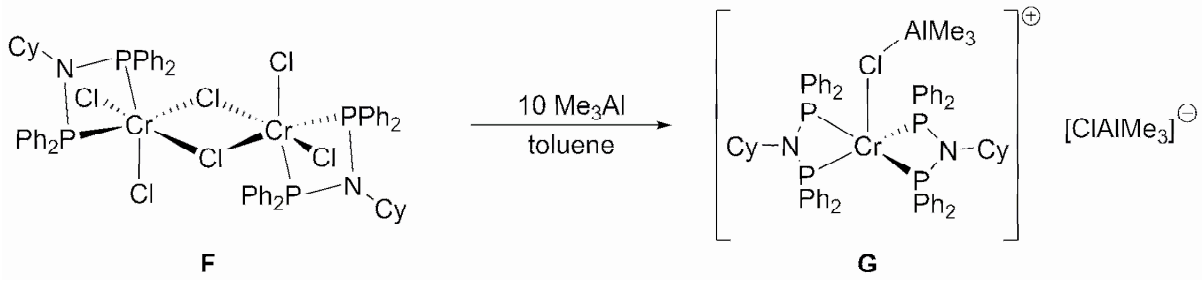

Scheme 6. Treatment of [(((Ph$_2$P)$_2$NCy)CrCl$_2$(μ$_2$-Cl))$_2$] (**F**) with excess Me$_3$Al (10 equiv.) as reported by Jabri *et al.*[23]

In our hands, the treatment of [(((Ph$_2$P)$_2$NPh)CrBr$_2$(μ$_2$-Br))$_2$] (**1**), with 5 equiv. of Me$_3$Al in toluene yielded the green divalent dimeric Cr(II) complex **2**, (scheme 7) of which crystals suitable for x-ray crystal structure analysis could be grown by layering cyclohexane over a saturated toluene solution of **2**. Figure 1 displays an Ortep plot of the molecular structure of **2** alongside with important bond lengths and angles.

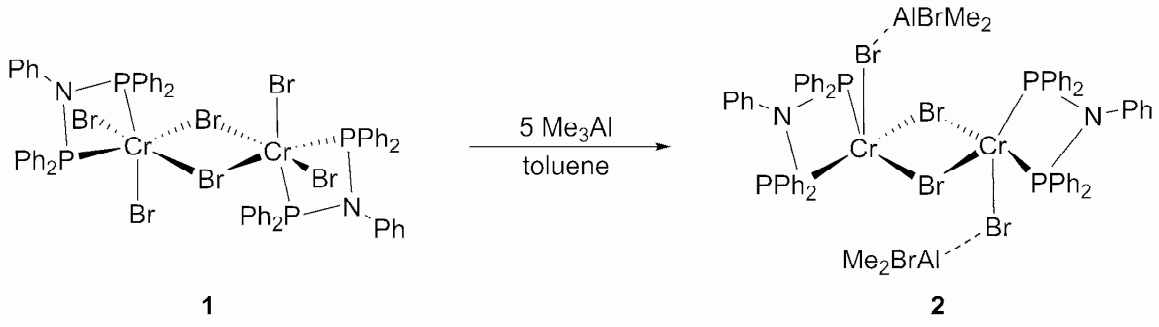

Scheme 7. Treatment of [(((Ph$_2$P)$_2$NPh)CrBr$_2$(μ$_2$-Br))$_2$] (**1**) with excess Me$_3$Al (5 equiv.).

In the solid state structure of **2**, the two Cr(II) centers each present a distorted square pyramidal coordination environment. The apical position is occupied by a [Me$_2$AlBr$_2$]$^-$ tetrahedral anion, which coordinates to the chromium center via one of its bromine atoms. The different halogen atoms and the different substituent on the central N atom render a direct comparison of the two structures **G** and **2** difficult, e.g. the Cr-(μ$_2$-Cl)AlMe$_3$ distance of 2.3682(19) Å in **G**, is much shorter than the corresponding Cr-(μ$_2$-Br)AlMe$_3$ distances (2.693(1) and 2.651(1) Å, respectively), probably simply due to the Cl/Br difference. On the other hand and not surprisingly, the P-Cr-P angles in **2** and **F** are very similar (66.39(6) and 66.57(5) Å for **F**, 66.95(5) and 67.09(5) Å for **2**).

The reactivity of **2** with ethylene was evaluated (Scheme 8). As with **G**, complex **2** shows no ethylene oligomerization activity even in the presence of 100 equiv. of Me$_3$Al, and only trace amounts of polymeric material were recovered under these conditions. In order to determine whether anion exchange with a weakly coordinating anion (WCA)[24] would help stabilizing the cationic Cr(II) center and thus promote reactivity with ethylene, one equiv. of the perfluorated lithium aluminate [Li(Al(OC(CF$_3$)$_3$)$_4$)],[25] whose trityl analogue combined with Et$_3$Al is an efficient activator of the

Sasol PNP tetramerization system,[26] was added, resulting in an immediate color change of the toluene solution to blue. No oligomerization products were detected with this catalytic mixture, however, a productivity of 1259 g × g $(Cr)^{-1}$ × h^{-1} exclusively towards polymeric material was observed. Upon activation with 300 equiv. of MAO, on the other hand, the usual tri- and tetramerization activity was observed.

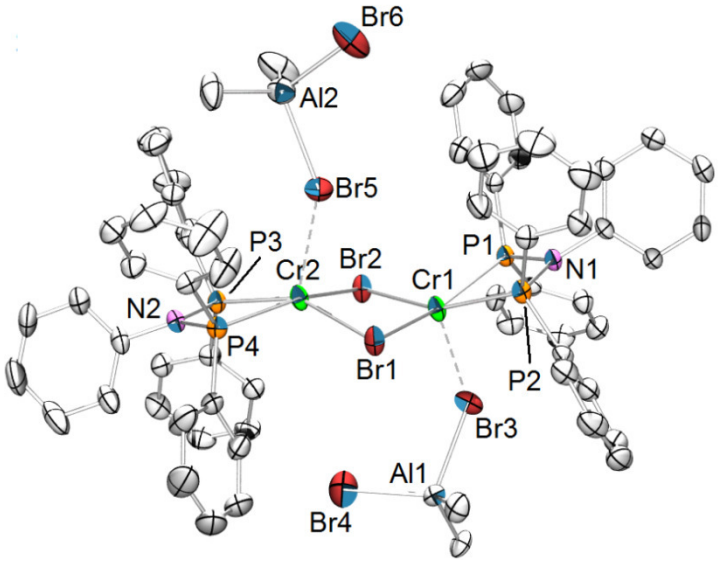

Figure 1. Ortep representation of the x-ray crystal structure of **2**. Hydrogen atoms have been omitted for clarity. Thermal ellipsoids are represented at the 50% level. Important bond lengths (Å) and angles (°): Cr1-Br1 = 2.510(1), Cr1-Br2 = 2.508(2), Cr1-Br3 = 2.693(1), Cr1-P1 = 2.461(1), Cr1-P2 = 2.474(1), Cr1···Cr2 = 3.430(1), Cr2-Br1 = 2.532(1), Cr2-Br2 = 2.548(2), Cr2-Br5 = 2.651(1), Cr2-P3 = 2.461(2), Cr2-P4 = 2.486(2), Al1-Br3 = 2.430(2), Al1-Br4 = 2.289(2), Al2-Br5 = 2.420(2), Al2-Br- = 2.300(2), Cr1-Br1-Cr2 = 85.73(3), Br1-Cr1-Br2 = 93.86(5), Cr1-Br2-Cr2 = 85.43(6), Br2-Cr2-Br1 = 92.39(5), P1-Cr1-P2 = 66.95(5), P3-Cr2-P4 = 67.09(5).

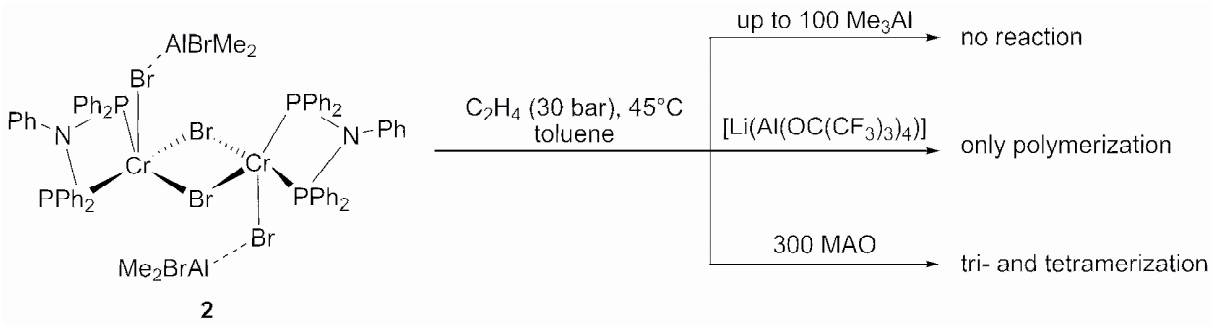

Scheme 8. Reactivity of complex **2** in ethylene oligo- and polymerization.

From the combination of both the results of Jabri *et al.*[23] and those obtained by ourselves, we can conclude that Me_3Al does not mimic the reduction ability of MAO. Furthermore, Cr(II) is probably not an active oxidation state in the tri- and tetramerization reaction, however, this oxidation state seems to

be active for polymerization,[27] when the cationic chromium species is stabilized with a well adapted counteranion.

Cr(I)-Cr(III) has been suggested to be the active redox couple in the selective trimerization reaction of higher α-olefins with 1,4,7-trialkyl-1,4,7-triazacyclononane chromium complexes devised by Köhn and coworkers (see section 3.6.2.1 of the introduction).[28, 29] Bercaw and colleagues deduced a Cr(I) active state to be active in the BP trimerization system as an implication of the reactivity of complex **C** (Scheme 3) with ethylene.

Subsequently, efforts have been made to isolate cationic Cr(I)-PNP complexes which would be active in the selective oligomerization without the need for cocatalysts. Both Rucklidge *et al.*[30] and the Wass workgroup[31] synthesized $[((Ph_2P)_2NR)Cr(CO)_4]$ complexes (R = *i*-Pr, Me), which were then oxidized with either $[(4\text{-}BrC_6H_4)(B(C_6F_5)_4)]$[31] or $[Ag(Al(OC(CF_3)_3)_4)]$[30] to their cationic counterparts $[((Ph_2P)_2NR)Cr(CO)_4]^+X^-$ (with X = $B(C_6F_5)_4$ (**H**) or $Al(OC(CF_3)_3)_4$ (**I**), respectively). These complexes are not active in ethylene oligomerization, but require a CO scavenger such as Et_3Al to liberate coordination sites on the Cr(I) metal center, to allow for ethylene molecules to coordinate to it and the catalytic cycle to start. While the catalytic system employing **H**, showed only very modest productivity in oligomerization (with 300 equiv. of Et_3Al: 710 g × g $(Cr)^{-1}$ × h^{-1}), productivities of up to 139800 g × g $(Cr)^{-1}$ × h^{-1} were reported with complex **I** and 200 equiv. of Et_3Al as CO scavenger. This difference in productivity underlines the necessity for sufficiently weak or non-coordinating counteranions for the generation of active catalysts.

In order to provide further support for the accessibility of the Cr(I) in the Sasol PNP system, we undertook room temperature ESR experiments on the MAO activated complex **F** in toluene as outlined in scheme 9.

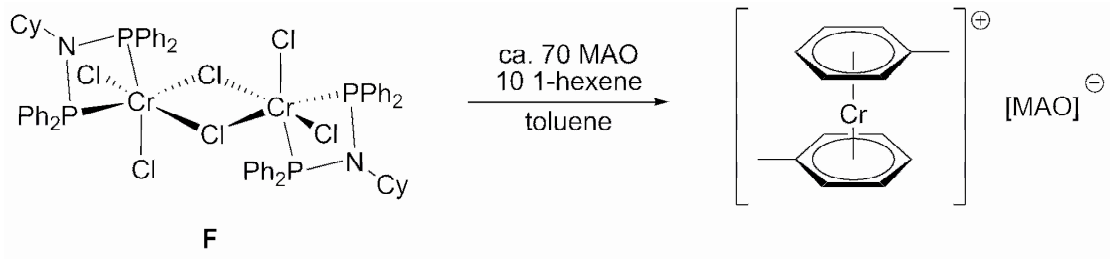

Scheme 9. ESR tube experiment.

1-hexene was equally added in an attempt to mimic the role of the ethylene, as the available ESR tubes could not be pressurized with ethylene. In the ESR spectrum, a single signal at g = 1.987 was observed, indeed indicative of a chromium (I) species. The hyperfine structure of the spectrum (Figure 2 - lower), recorded at ambient conditions, shows eleven major lines as well as satellites.

A satisfactory simulation of the hyperfine spectrum could be obtained (Figure 2 - upper). Since chromium is present in nature with four different isotopes, one has to consider the coupling of nuclear

and electronic spin. While ^{50}Cr, ^{51}Cr and ^{54}Cr are all $S = 0$ nuclei, ^{53}Cr with a natural abundance of 9.5% has a $S = 3/2$ nuclear spin.

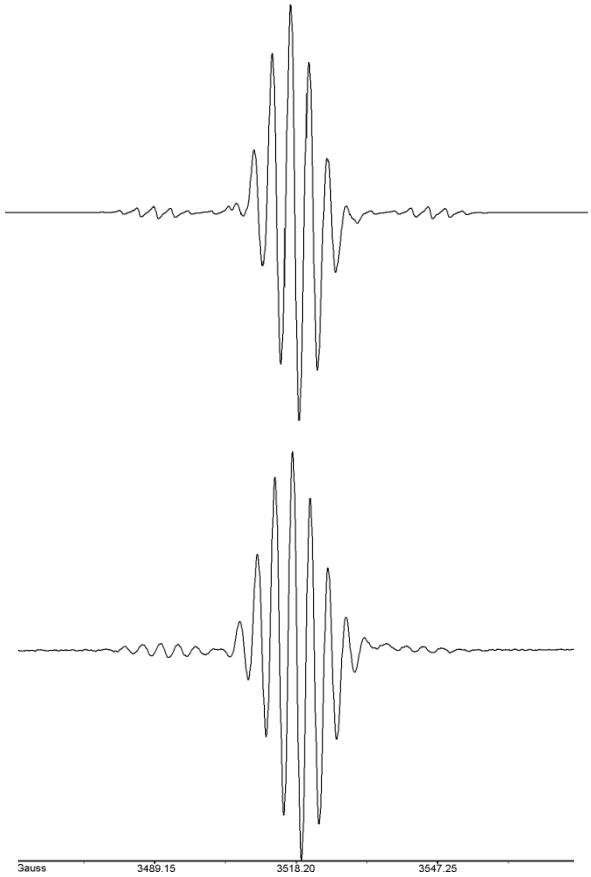

Figure 2. Simulated spectrum (upper) and recorded in-situ ESR spectrum of the catalytic mixture **F**/MAO/1-hexene (lower).

From the simulation, a chromium species with 90.5% abundance and $S = ½$ electronic spin was found to couple with ten $S = ½$ sites with a coupling constant of 3.57 Gauss. A second species with 9.5% abundance and $S = 3/2$ nuclear spin was found to couple with the electronic spin ($S = ½$) with a coupling constant of 18.00 Gauss, as well as with ten $S = ½$ sites with a coupling constant of 3.34 Gauss. This spectrum is consistent with a sandwich $[(\eta^6\text{-toluene})Cr]^+$ entity.[32] The ten equivalent $S = ½$ sites may be attributed to the aromatic ^1H nuclei of the toluene moieties.

No coupling to phosphorus or nitrogen nuclei could be observed.

Two major conclusions can be drawn from the ESR experiment. Firstly, the Cr(I) oxidation state is clearly accessible for a Cr(III)/MAO catalytic system. Secondly, it could be shown that the formation of η^6-bisarene-Cr^+ species is a degradation pathway of the catalytic species in aromatic solvents, following the loss of the bis(diphenylphosphino)amine ligand. We have affirmed this conclusion by catalytic evaluation of the catalytic system $[((\eta^6\text{-toluene})_2Cr)(BF_4)]$[33] with 300 equiv. MAO, which showed strictly no ethylene polymerization or oligomerization activity. Brückner *et al.* recently have drawn similar results with ESR experiments on the Sasol PNP tetramerization system.[34]

Given these indications, we believe that a Cr(I)-Cr(III) redox shuttle is operative in the BP and Sasol tri- and tetramerization system.

2.4 C_6 Cyclic Byproducts in the Sasol Tetramerization Reaction

Besides 1-hexene, two other C_6 byproducts are formed in quantities of up to 8% (and approximately in a 1:1 ratio) in a tetramerization experiment: methylenecyclopentane and methylcyclopentane. Overett *et al.*[15] suggested a number of possible mechanistic pathways for the formation of these products, all of them originating from a β-hydrogen elimination of the chromacycloheptane intermediate, leading to a Cr-hydride-hexenyl species. This species would then evolve further as depicted in scheme 10.

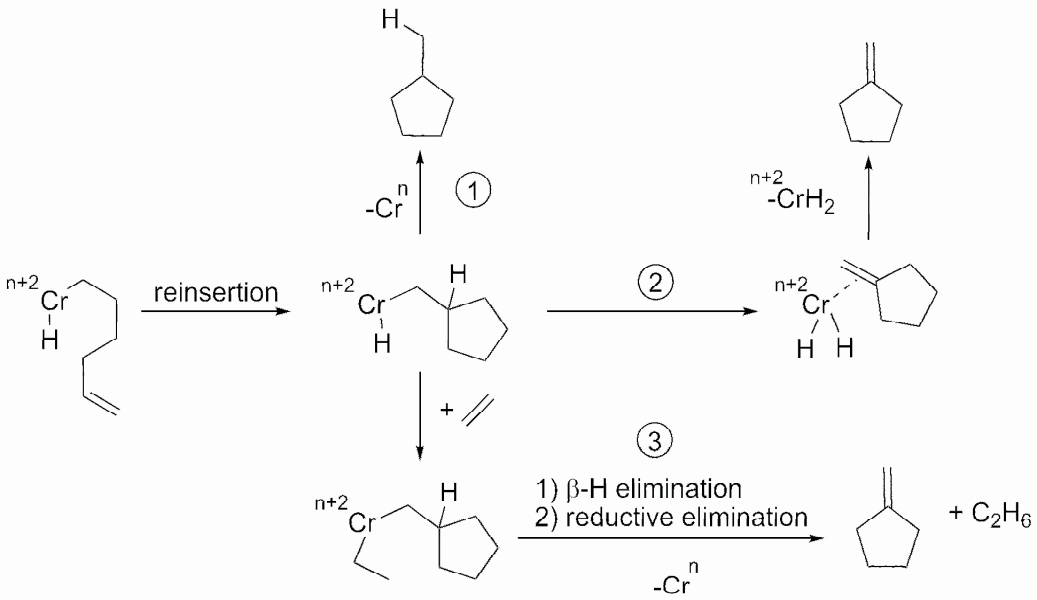

Scheme 10. Postulated mechanisms for the formation of methylenecyclopentane and methylcyclopentane.

The common precursor to both methylenecyclopentane and methylcyclopentane is suggested to be a Cr-hydride-methylenecyclopentane intermediate, which would be formed by reinsertion-cyclization of the Cr-hexenyl chain. Methylcyclopentane would be formed by reductive elimination (pathway 1, scheme 10), while two distinct mechanistic scenarios for the formation of methylenecyclopentane are imaginable. Pathway 2 would involve the β-hydride elimination from the methylenecyclopentane ligand and consequently the formation of a chromium dihydride species.

A further pathway 3 would involve insertion of ethylene in the Cr-hydride bond, leading to the intermediate formation of a Cr-ethyl-methylenecyclopentane species. β-hydrogen elimination from the methylenecyclopentane ligand, followed by reductive elimination of ethane would yield methylenecyclopentane. No dependence was found upon investigation of the influence of ethylene pressure on the quantity of cyclic C_6 byproducts in the tetramerization, which renders pathway 3 rather

implausible.[35] Furthermore, throughout catalytic runs undertaken with special care taken towards sample cooling (ethane boiling point = -88.6°C), no traces of ethane were detected by GC, rendering this pathway rather unlikely.

3. Theoretical Study on the Mechanism of Ethylene Tri- and Tetramerization with the Sasol PNP System

3.1 Objectives and Methods

In order to shed light on some important aspects of the mechanism of the tri- and tetramerization reaction, we have undertaken a complete theoretical study. This study had a multiple objectives: Firstly, we intended to elucidate the thermodynamics of the two competitive pathways leading either to 1-hexene release or chromacycle ring expansion with a fourth ethylene molecule to ultimately yield 1-octene. A second objective was to clarify which of the two mechanistic alternatives, either β-hydrogen elimination or (3,7) / (3,9)-hydrogen shift, were operative in the Sasol PNP system. Thirdly, the formation of the C_6 cyclic byproducts was investigated from a theoretical point of view.

Given the experimental evidence (see previous section), a Cr(I)-Cr(III) redox couple was assumed to be operative in the mechanism. Considering this, it must be borne in mind that Cr(III) complexes (s^1d^2) can adopt two possible electronic configurations, quartet (S = 3/2) or doublet (S = ½) state. Throughout this study, Cr(III) complexes were found to be more stable in the quartet electronic state. Cr(I) complexes, which may adopt either high-spin or low-spin configurations (S = ½ or 3/2 or 5/2), were equally found to be more stable in the quartet spin state.

Calculations were carried out at the quantum level using the Gaussian 03 set of programs[36] and using the B3PW91 functional. The standard 6-31G* basis set was used for all non-metallic atoms (H, C, N, and P), The basis set used on chromium was the Hay and Wadt[37] small-core quasi relativistic effective core potential with the double-ζ valence basis set (441s/2111p/41d) augmented with an f-polarization function (exponent = 1.941).[38]

The substitution on the bis(phosphino)amine (PNP) ligand was simplified in order to reduce computation time. On phosphorus, the phenyl substituents were systematically replaced by methyl groups, and on nitrogen, hydrogen replaced the hydrocarbyl substituent found in the real systems. This is justified, when at same time the effect of MAO is neglected, as a theoretical study on the role of MAO in the chromium catalyzed oligomerization of ethylene by van Rensburg *et al.* implies.[17]

The mechanism was thus explored following the steps of the catalytic cycle as outlined in scheme 4.

3.2 Ethylene Coordination to the Catalytically Active Species

In a first step, the relative stability of different $[(PNP)Cr(ethylene)_n]^+$ (n = 0 to 3) complexes was evaluated, as outlined in scheme 11.

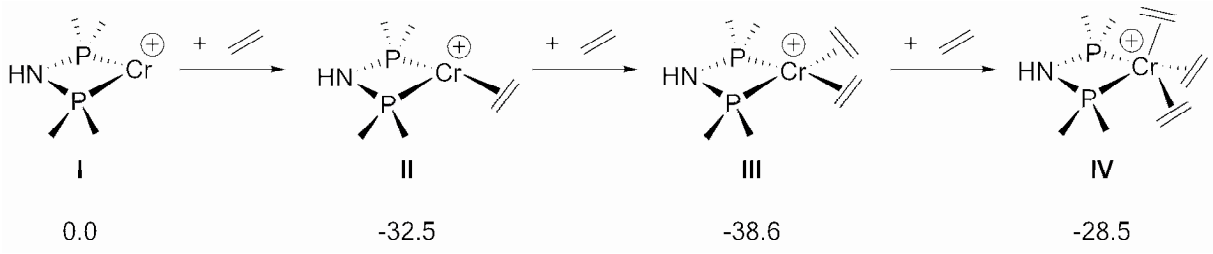

Scheme 11. Relative Stability of various $[(PNP)Cr(ethylene)_n]^+$ species. Gibbs free energies are given in Kcal × mol^{-1}.

Complex **III** bearing two coordinated ethylene moieties was found to be the thermodynamically most stable species, however, considering the high ethylene pressures (20-100 bar) used in catalysis, complex **IV** is probably the predominant species in solution. This is why throughout this study we considered the coordination sphere of the chromium center to be saturated with ethylene in most cases, yielding thus at least pentacoordinated species.

3.3 Formation of the Chromacyclopentane

The oxidative coupling of two coordinated ethylene molecules to form a chromacyclopentane **V** proved to be a process requiring an activation energy of 5.7 Kcal × mol^{-1} when starting from **III** (scheme 12a), and 9.0 Kcal × mol^{-1} when starting from **IV** (scheme 12b)with its ethylene saturated coordination sphere.

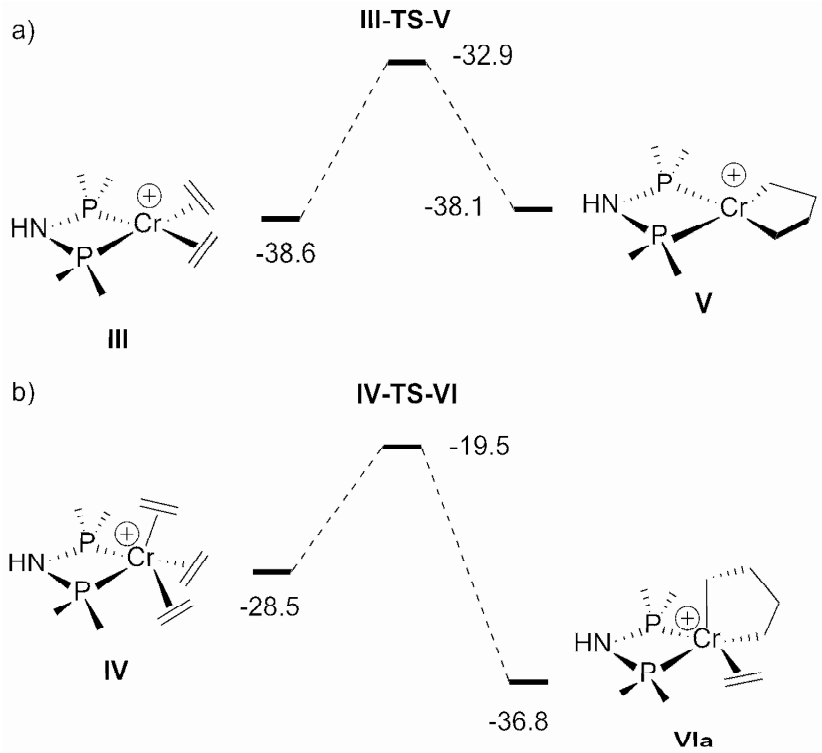

Scheme 12. Oxidative coupling to yield chromacyclopentane species.

Transformation of **V** to **VIa** is an energetically facile process, requiring only the coordination of a further ethylene molecule on the available axial coordination site.

We became aware that an important number of conformational isomers of the chromacyclopentane **VI** are possible (Figure 7), each of them only slightly different in energy. Upon comparison of for example **VIa** and **VIb**, which are different in terms of the relative orientation of the η^2-coordinated ethylene molecule, it became clear that these species must exist in a close equilibrium.

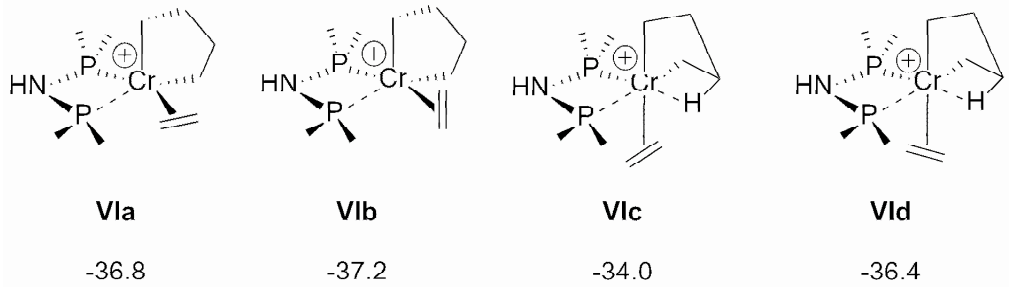

Figure 7. Stability of different chromacyclopentane conformational isomers **VIa**-**d**.

A closer look on the bond distances in the optimized structures revealed that the bis(phosphino)amine ligand is not symmetrically bond to the chromium center in the chromacyclopentane species **VIa**-**d**. Instead, the P-Cr bond situated *trans* to the metallacyclic Cr-C bond was found to be significantly longer than the P-Cr bond *trans* to the η^2-ethylene (e. g. 2.634 versus 2.492 Å in **VIa**, Figure 8).

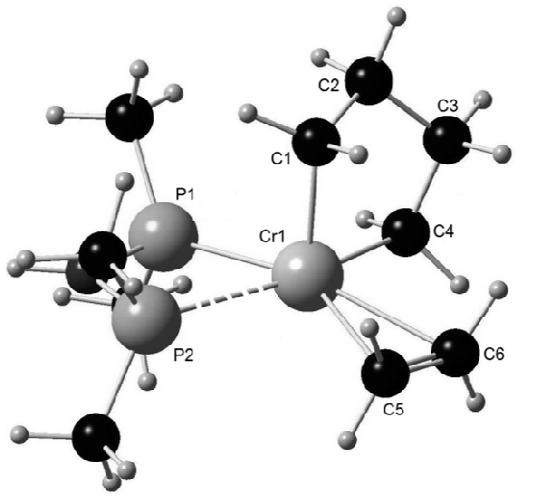

Figure 8. Optimized geometry of theoretical comlex **VIa**. Most significant bond distances (Å) and angles (°):: P1-Cr = 2.492, P2-Cr = 2.634, Cr-C1 = 2.049, Cr-C4 = 2.068, Cr-C5 = 2.509, Cr-C6 = 2.537 = C5-C6 = 1.348, P1-Cr-P2 = 66.412, C1-Cr-C4 = 86.614, C5-Cr-C6 = 30.987.

This difference in P-Cr bond length was considered as the reason for a possible hemilabile behavior of the bis(phosphine)amine ligand, i. e. decoordination from the metal center of one phosphine moiety. Then, rotation of the ligand around the remaining P-Cr bond, followed by recoordination of the pendant phosphine moiety, would become possible, a process, which was calculated to be energetically feasible and a way to explain interconversion between the different chromacyclopentane isomers (Scheme 13).

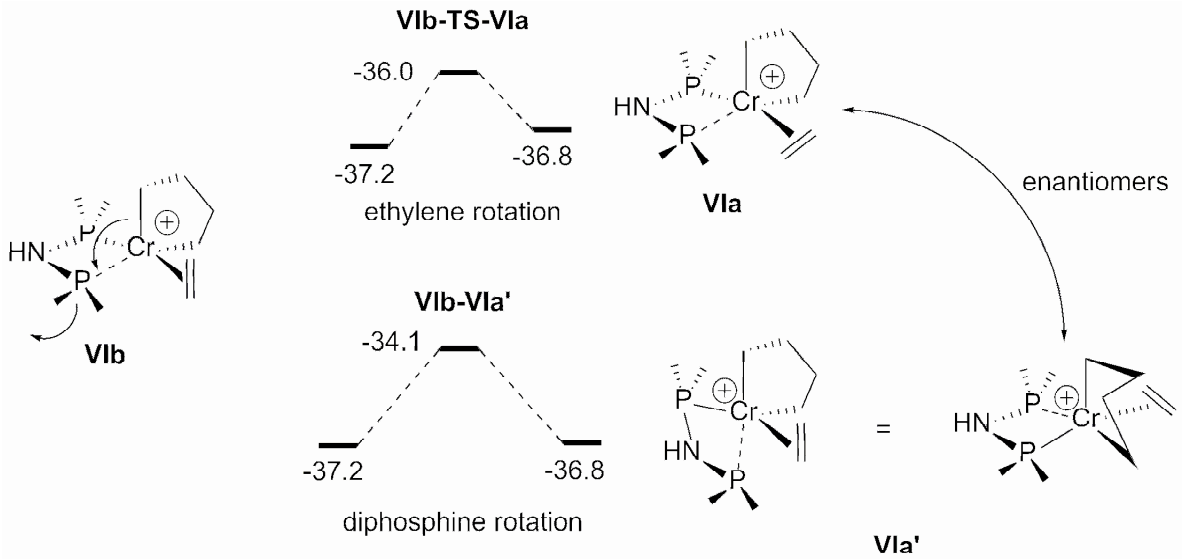

Scheme 13. VIb ↔ VIa (VIa') interconversion via either ethylene or diphosphine rotation.

3.4 The 1-Hexene Pathway

Complex **VIa** may undergo (1,2)-insertion of its η^2-coordinated ethylene molecule into the chromacycle. This process, which requires an activation energy of 6.4 Kcal × mol^{-1}, leads to the formation of chromacycloheptane **VIIa**, as depicted in scheme 14.

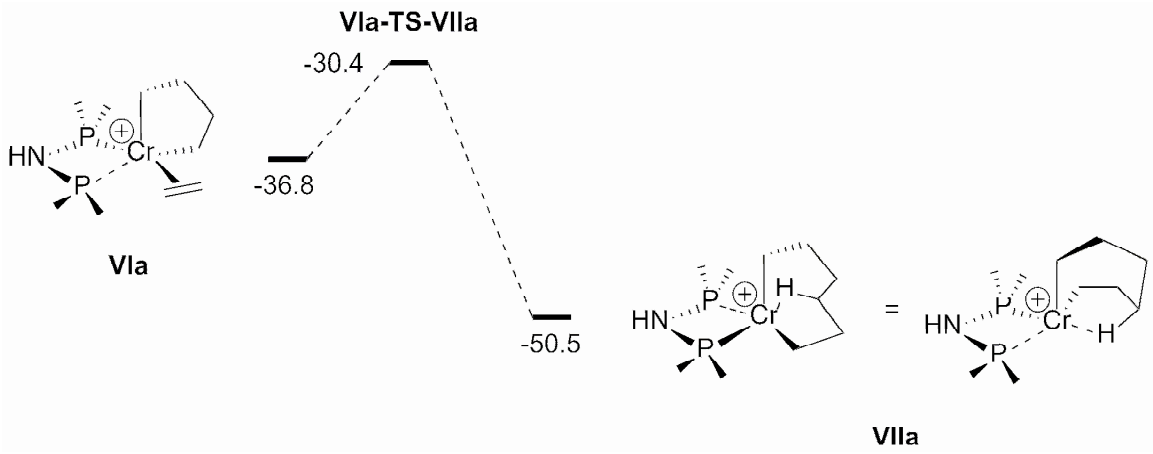

Scheme 14. (1,2)-ethylene insertion into the Cr-C bond.

Interestingly, **VIIa** features a γ-hydrogen agostic bond with the chromium center. However, the chromacycloheptane ring is sufficiently flexible, which leads to the occurrence of an important number of conformational isomers of **VIIa**, which are very similar in energy and require only a small activation energy for the isomerization process. For example, an activation energy of only 5.6 Kcal × mol^{-1} is necessary to convert **VIIa** into **VIIb**, which features a β-hydrogen agostic bond with the chromium center (Scheme 15).

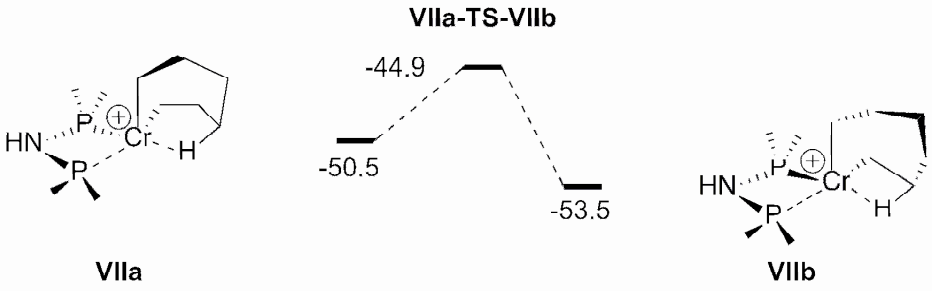

Scheme 15. Conformers of chromacycloheptane **VII**.

Apart from metallacycle flexibility, rotation around the P-Cr bond *trans* to the chromacycle Cr-C bond, as observed on the chromacyclopentane isomers **VI** (see section 3.3 above) was found to be an origin for even more conformational isomers of **VII**. Diphosphine rotation in complex **VIIa** yields **VIIc**, which features a boat like chromacycle conformation. Similar metallacycle conformations have equally been considered in Ti-,[7-9] Ta-,[10] and Cr(IV)-(η^5-pyrrole)[6] calculated trimerization mechanisms. After η^2-coordination of a further ethylene molecule to **VIIc**, which yielded **VIII**, a

suitable precursor for 1-hexene elimination was found. (3,7)-hydrogen transfer proceeds via the transition state **VIII**-**TS**-**IV**, which is accessible by an activation energy of 9.3 Kcal × mol^{-1} from **VIII**. **IX** ultimately releases 1-hexene and closes the catalytic cycle. (Scheme 16).

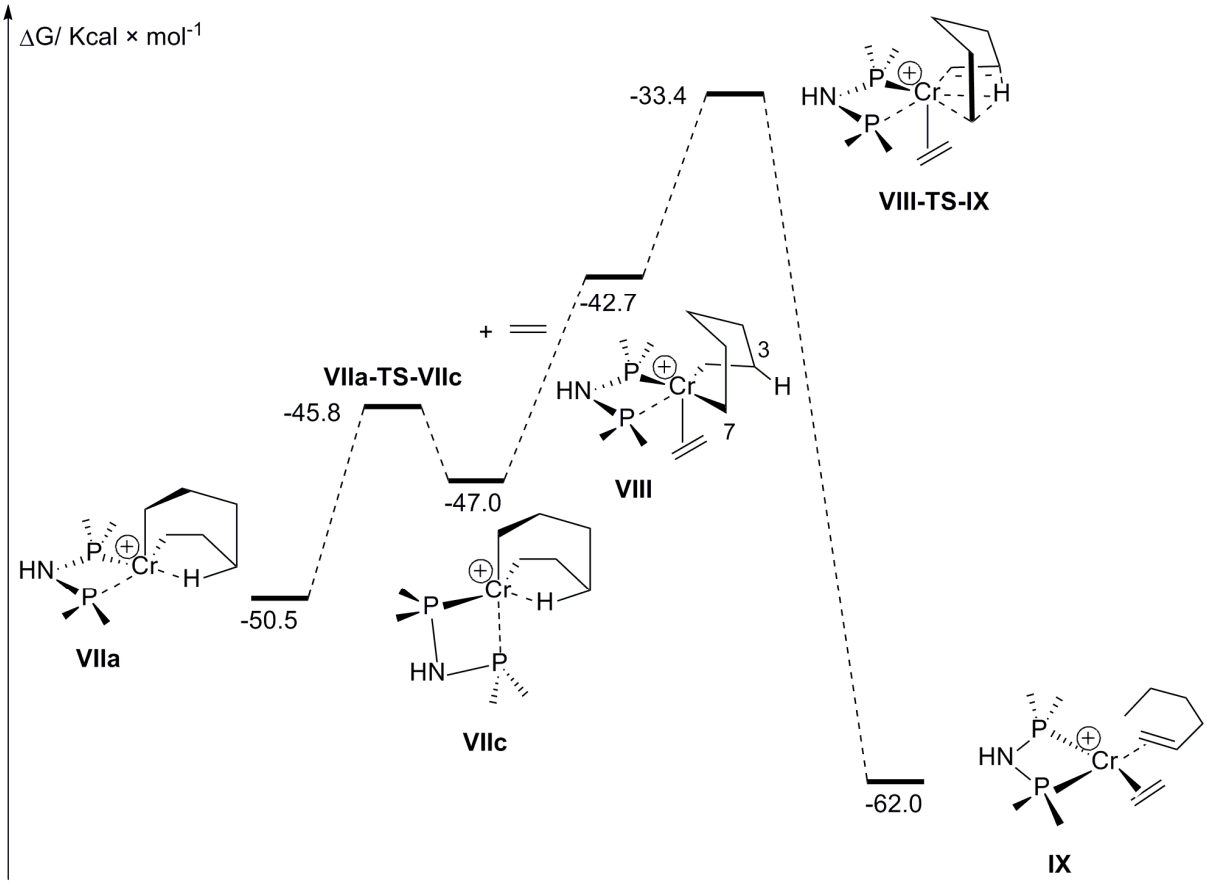

Scheme 16. 1-hexene elimination via (3,7)-hydrogen transfer.

As depicted in scheme 4, an alternative pathway implicating β-hydrogen elimination and the intermediate formation of Cr-hydride species has been proposed in the literature. We have considered this alternative starting from complex **VIIb**, which features a suitable β-hydrogen agostic bond. Coordination of a supplemental ethylene molecule to the free axial coordination site of **VIIb** yielded **X**. β-hydride abstraction from **X** involves an energy barrier of 11.9 Kcal × mol^{-1} (**X**-**TS**-**XI**) to obtain the Cr-hydride-hexenyl complex **XI**. Hydride transfer to the coordinated ethylene molecule of **XI** proved to require an activation energy of only 1.7 Kcal × mol^{-1} to yield the Cr-ethyl-hexenyl intermediate **XII**, which is probably a thermodynamic sink, given its exceptional stability (-55.5 Kcal × mol^{-1}) (Scheme 17). Consequently, 1-hexene elimination via transition state **XII**-**TS**-**IX** requires an important activation energy of 21.6 Kcal × mol^{-1}, which renders the β-hydrogen elimination pathway kinetically disfavored with respect to the (3,7)-hydrogen transfer pathway, whose realization from intermediate **VIII** involves an energy barrier of 9.3 Kcal × mol^{-1}.

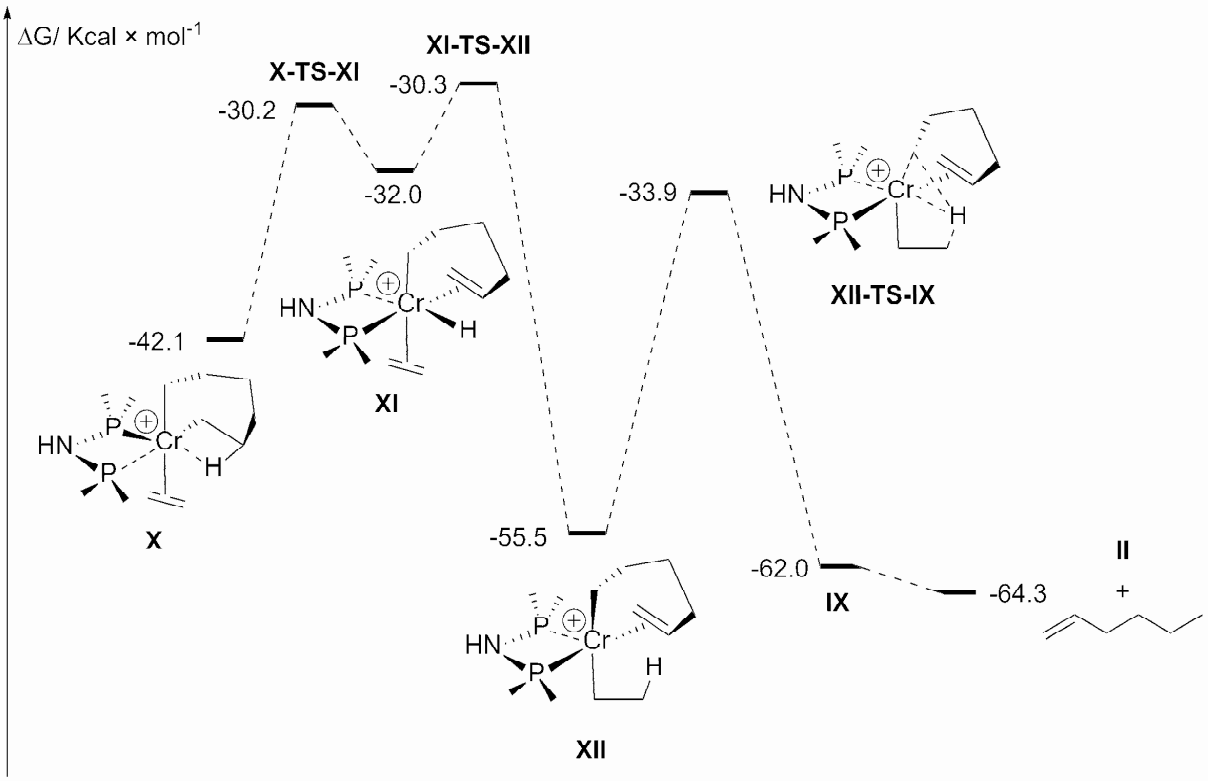

Scheme 17. Alternative Pathway for 1-hexene formation via an intermediate chromium hydride **XI**.

The Cr-ethyl-hexenyl intermediate **XII**, however, is believed to be a key intermediate in the formation of the cyclic C_6 byproducts (see section 2.4 above). A possible mechanistic scenario explaining their formation will be discussed in section 3.6.

3.5 The 1-Octene Pathway – Formation of a Chromacyclononane

In an analogous fashion as described in the previous section for the formation of the seven-membered chromametallacycle, the formation of chromacyclononane was found to proceed via (1,2)-insertion of a η^2-coordinated ethylene into a Cr-C metallacycle bond. A suitable chromacycloheptane conformer for this step was found in **XIII**, in which the ethylene molecule to be inserted occupies a coordination site *trans* to one of the phosphine moieties. The insertion step was found to require an activation energy of 11.5 Kcal × mol^{-1}, to yield the chromacyclononane isomer **XIV** (Scheme 18), which features a γ-hydrogen agostic bond similar to the one observed with the chromacycloheptane isomer **VIIa**.

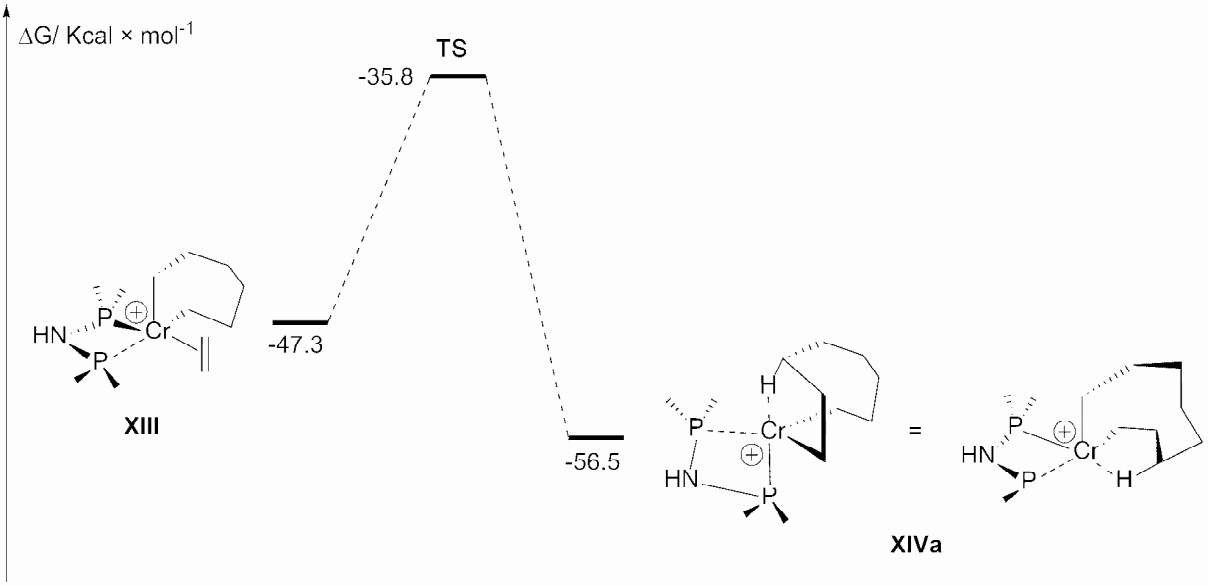

Scheme 18. Chromacyclononane formation.

The even greater conformational flexibility of the nine-membered metallacycle allows for a plethora of conformational isomers with very similar energy, which constituted a major difficulty in this study. Accordingly, the rearrangement of **XIVa** to complex **XIVb**, in which a β-hydrogen agostic bond to the chromium center has been found, is easily feasible. Decoordination of the phosphine *trans* to the metallacyclic Cr-C bond and rotation of the diphosphine ligand around the remaining P-Cr bond, followed by coordination of an ethylene molecule yields **XV**, which is a suitable precursor for the 1-octene elimination step (Scheme 19).

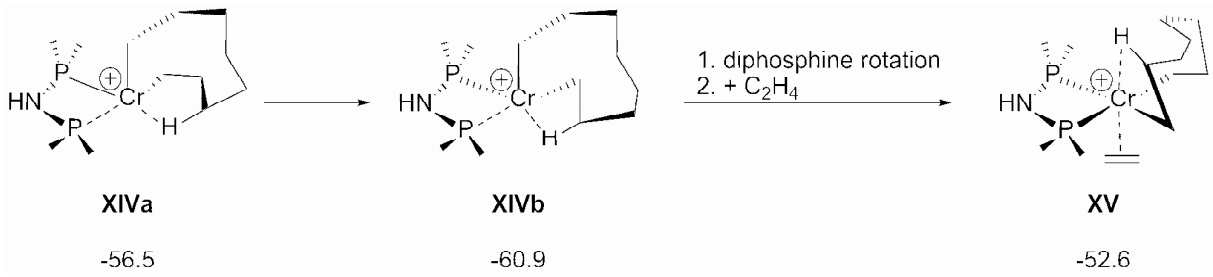

Scheme 19. Stability of different chromacyclononane isomers.

The mechanism accounting for the formation of 1-octene was found to proceed in an analogous to the one described for 1-hexene formation. A hydrogen is shifted from the C3 carbon to the C9 carbon of the metallacycle (thus a (3,9)-hydrogen transfer). The (3,9)-hydrogen transfer involves an activation energy of 15.9 Kcal × mol^{-1}, and yielded **XVI**, which upon the ultimate release of 1-octene, may restart a new catalytic cycle (Scheme 20).

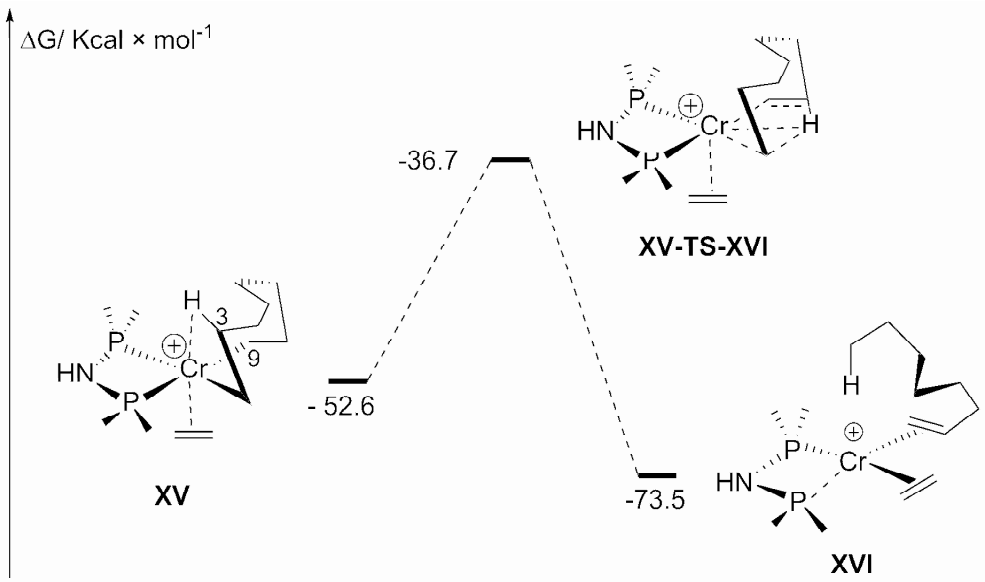

Scheme 20. (3,9)-hydrogen transfer in chromacyclononane complex **XV**.

An alternative β-hydrogen elimination pathway was equally explored, starting from a suitable chromacyclononane isomer such as **XIVb**, however, all attempts to find a transition state towards a Cr-hydride-octenyl species **XVII** failed and returned to **XIVb** (Scheme 21).

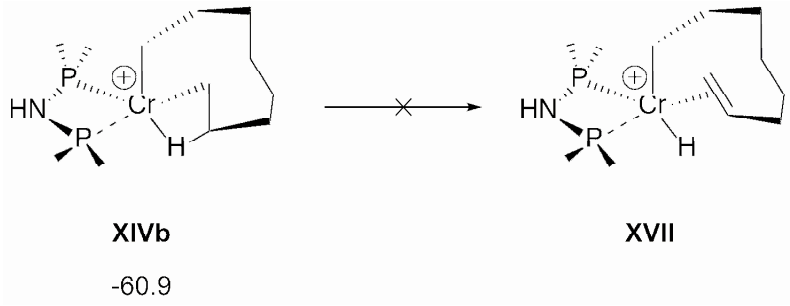

Scheme 21.

3.6 Formation of C_6 Cyclic Byproducts

As demonstrated in the previous sections, the formation of 1-hexene and 1-octene proceeds via intermediate chromacycloheptane and –nonane intermediates, which eliminated the olefin via (3,7)- or (3,9)-hydrogen transfer, respectively.

A second pathway for 1-hexene formation via β-hydrogen elimination was considered (see section 3.4). Even though this pathway is believed to be kinetically disfavored, the Cr-ethyl-hexenyl intermediate **XII** might be accessible in small quantities. We therefore considered **XII** as a suitable starting point to rationalize the formation of both methylcyclopentane and methylenecyclopentane. As outlined in scheme 10, the formation of methylcyclopentane was considered to proceed via intramolecular (1,2)-reinsertion-cyclization. The transition state of this transformation was located and the transformation was found to involve an energy barrier of 9.7 Kcal × mol^{-1}, rendering this process

accessible under the reaction conditions (Scheme 22). The subsequent step of this transformation, which consists in the β-hydrogen transfer from the ethyl ligand to the α-methylene group of the methylenecyclopentane ligand of **XVIII**, was equally found to be both kinetically and thermodynamically feasible ($\Delta G^{\ddagger}$ = 14.8 Kcal × mol^{-1}), yielding **II** and methylcyclopentane.

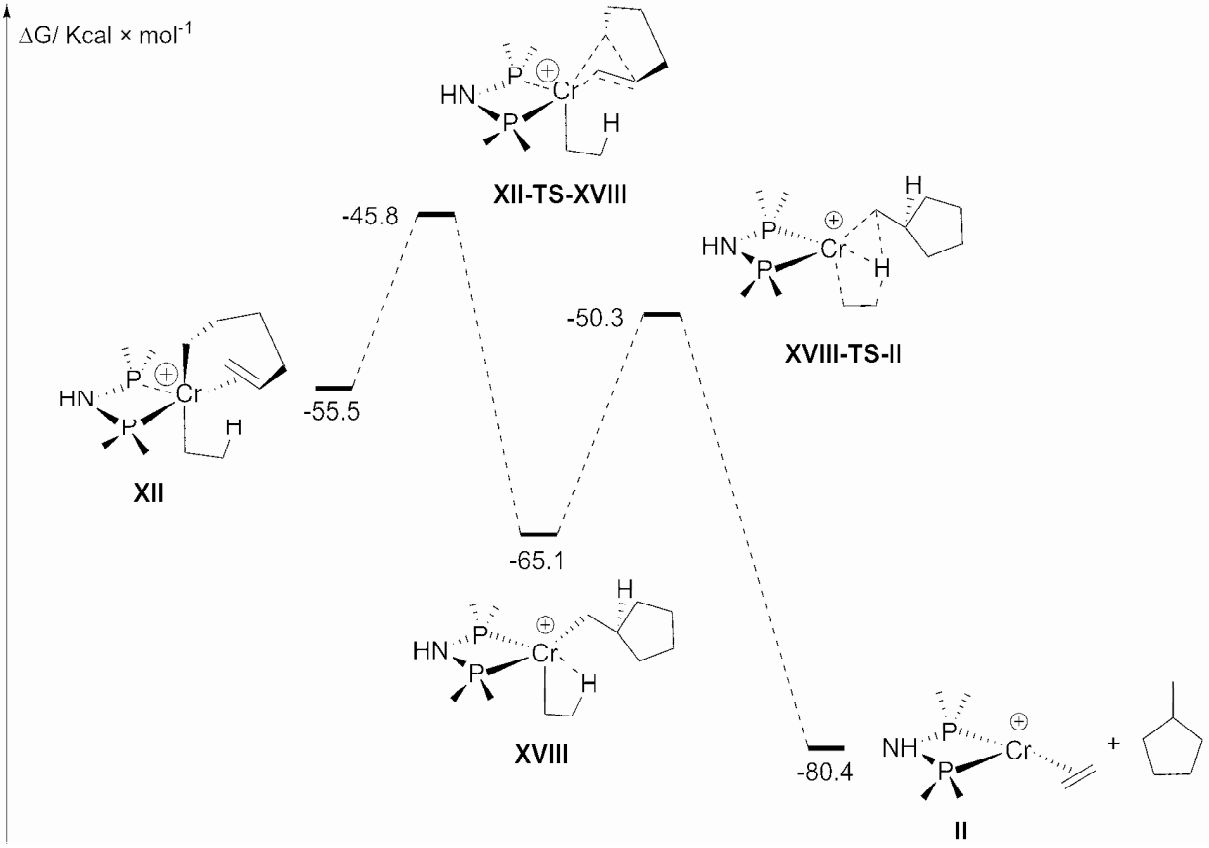

Scheme 22. Mechanism of methylcyclopentane formation.

The comparatively lower energy barrier of 9.7 Kcal × mol^{-1} for the formation of methylcyclopentane from **XII** compared to the higher energy barrier ($\Delta G^{\ddagger}$ = 21.6 Kcal × mol^{-1}, scheme 17) involved in the 1-hexene elimination complies with the findings of Kuhlmann *et al.*, who found a decreasing amount of C_6 cyclics, but an increased amount of 1-hexene, when conducting the oligomerization reaction at higher temperatures.[35] At higher temperatures, the β-elimination pathway for 1-hexene formation seems to compete with the formation of C_6 cyclics.

The formation of methylenecyclopentane may be rationalized starting from the common intermediate **XVIII** (Scheme 23). β-hydrogen transfer from the ethyl group to the chromium center forms intermediate **XIX**, which presents an agostic interaction between the chromium center and one of the methylene hydrogen atoms of the σ-bonded methylenecyclopentane ligand. β-hydrogen abstraction to the metal center then would yield the Cr-dihydride **XX**, which could subsequently release dihydrogen (**XXI**), then the formed η^2-bound methylenecyclopentane, to regenerate **II**.

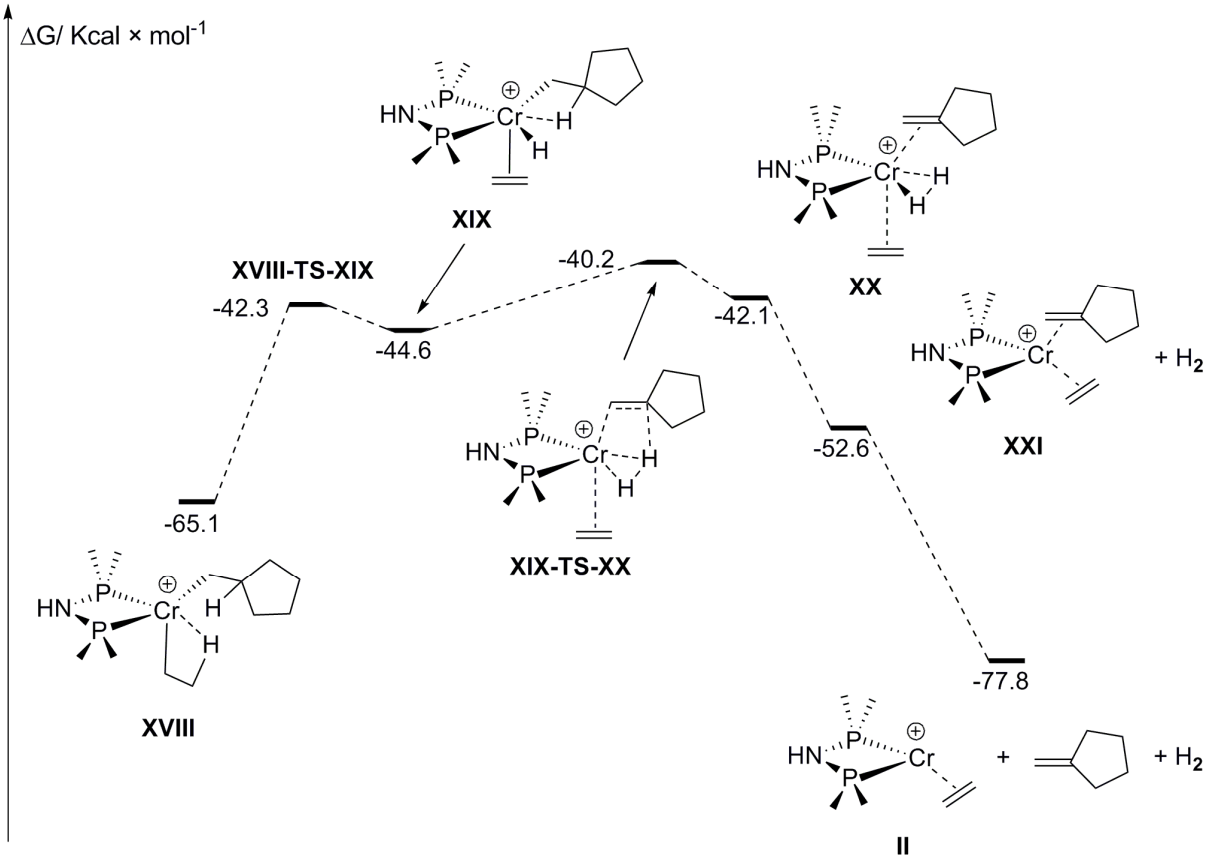

Scheme 23. Mechanism of methylenecyclopentane formation.

It should be borne in mind that this pathway is only one possible mechanistic alternative. Aside from the mechanism involving ethane formation (pathway 3, Scheme 10), other mechanistic alternatives may be envisaged. A bimolecular mechanism with a disproportionation reaction of two molecules of **XVIII**, as suggested by Overett *et al.*,[15] would give a good explanation for the 1:1 ratio observed between the quantities of the two cyclic byproducts, but were not accessible to theoretical investigation.

In conclusion, through this theoretical study, we were able to ascertain a number of steps of the metallacyclic mechanism operative in ethylene tri- and tetramerization on chromium, as well as the activation energies associated with these steps. While β-hydride elimination does not seem to be the predominant pathway for the release of the main products 1-hexene and 1-octene, a Cr-hydride intermediate was identified as a possible starting point for the formation of the C_6 cyclic byproducts.

4. The PCNCP Catalytic System – Tri- versus Tetramerization[39]

The present section deals with a new chromium-based catalytic system for ethylene tri- and tetramerization. The synthesis of the PCNCP (PCNCP = bis(phoshinomethyl)amine) ligands, their coordination to $[CrCl_3(THF)_3]$, and the evaluation of these complexes in the oligomerization reaction

is reported. In a second part, we take a closer look on the effect of the phosphine substituents' steric bulk on the selectivity of the oligomerization reaction towards either tri- or tetramerization.

4.1 PCNCP Ligand Synthesis

Symmetric bis(phosphinomethyl)amines with the general formula $(R_2PCH_2)_2NR'$ (PCNCP) **3a**-**g** were prepared following a new procedure adapted from a well-established route in the literature.[40, 41] This involved the reaction of a secondary phosphine R_2PH with formaldehyde, followed by a Mannich-type condensation of the resulting hydroxymethylphosphine R_2PCH_2OH with a primary amine $R'NH_2$, as outlined in scheme 24. Table 1 shows the R and R' substitution combinations alongside with the $^{31}P\{^1H\}$ chemical shifts of these ligands.

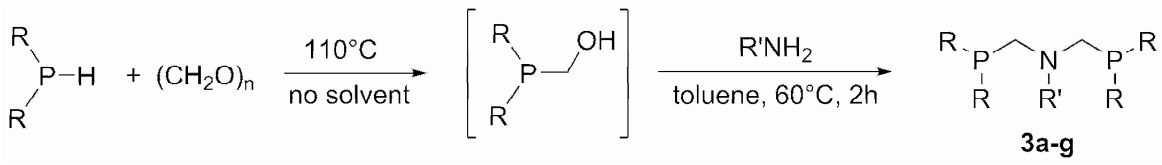

Scheme 24. General synthetic route to PCNCP ligands **3a**-**g**.

Table 1. Substituents in **3a**-**g**.

3	**a**	**b**[42]	**c**[40]	**d**	**e**	**f**	**g**
R	Ph	Ph	Ph	Cy	Cy	Cy	*n*-Bu
R'	*i*-Pr	*t*-Bu	Ph	*i*-Pr	*t*-Bu	Ph	*i*-Pr
δ ($^{31}P\{^1H\}$)[a]	-26.5	-27.2	-25.3	-14.9	-14.7	-15.0	-48.4

[a] in ppm

To assess the importance of the type of substituent on phosphorus on the activity of the corresponding catalyst, reactions were carried out with bis(phenylphosphine) (**3a**-**c**), bis(cyclohexylphosphine) (**3d**-**f**), and bis(*n*-butylphosphine)[43] (**3g**). Three different amines (isopropylamine, *t*-butylamine, and aniline) were employed in the case of the P-phenyl and P-cyclohexyl substituted ligands **3a**-**f**. The P-*n*-butyl substituted derivative **3g** proved more difficult to handle and therefore was only synthesized with isopropylamine.

4.2 Synthesis of $[(3)CrCl_3(THF)]$ Complexes

The chromium(III) complexes **4a**-**g** of the PCNCP ligands **3a**-**g** were easily prepared in almost quantitative yield by addition of $[CrCl_3(THF)_3]$ to a solution of **3a**-**g** in THF at room temperature, as depicted in scheme 25.

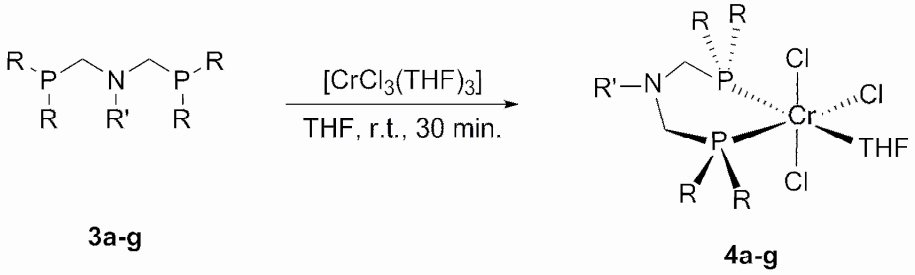

Scheme 25. Coordination of ligands **3a-g** to $[CrCl_3(THF)_3]$.

Coordination of the ligand to the Cr(III) metal center is indicated by the immediate color change of the reaction mixture from pink to dark blue. Due to the strong paramagnetic nature of the octahedral d^3 Cr(III) center, complexes **4a-g** are silent in ^{31}P NMR and their ^{1}H and ^{13}C NMR spectra exhibited only broad signals that could not be exploited to establish their structure, therefore, the complexes were primarily characterized by elemental analysis data. However, single crystals suitable for x-ray crystal structure determination could be grown in the case of **4d** by slow evaporation of a concentrated solution of **4d** in THF at room temperature. A view of the molecular structure of **4d** in the solid state is presented in figure 8 alongside with the most significant metric parameters.

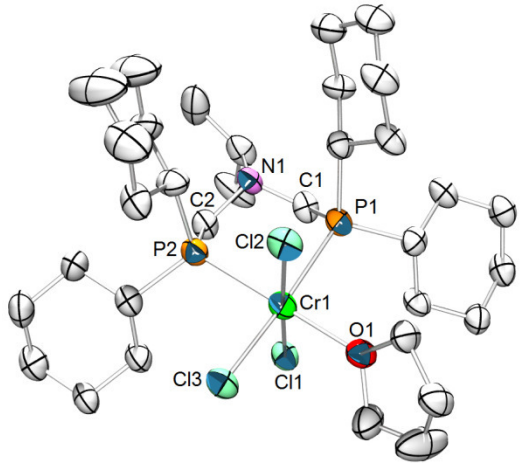

Figure 8. Molecular structure of one molecule of **4d** in the crystal. Thermal ellipsoids are drawn at the 30% probability level. Hydrogen atoms are omitted for clarity. Selected bond distances (Å) and angles (°): P1-Cr1 = 2.518(2), P1-C1 = 1.836(5), C1-N1 = 1.457(6), N1-C2 = 1.465(7), C2-P2 = 1.863(5), P2-Cr1 = 2.466(2), Cr1-Cl1 = 2.320(2), Cr1-Cl2 = 2.314(2), Cr1-Cl3 = 2.311(2), Cr1-O1 = 2.104(3), P1-C1-N1 = 116.3(4), C1-N1-C2 = 112.8(4), N1-C2-P2 = 116.1(4), C2-P2-Cr1 = 113.6(2), P2-Cr1-P1 = 85.90(5), P2-Cr1-Cl1 = 86.94(6), P2-Cr1-Cl3 = 90.16(6), P2-Cr1-Cl2 = 92.82(6), P2-Cr1-O1 = 177.4(1), P1-Cr1-Cl1 = 85.53(6), P1-Cr1-Cl2 = 89.72(6), Cl3-Cr1-Cl1 = 91.44(6).

As can be seen in figure 8, complex **4d** adopts a monomeric structure and the overall geometry around chromium is octahedral.

Interestingly, the PCNCP ligand behaves as a bidentate ligand and the central nitrogen donor does not participate in the coordination, as indicated by the very long Cr1-N1 distance of 4.017(1) Å.

Consequently, the coordination sphere is completed by coordination of a THF atom that is located *trans* to one of the phosphorus atoms (P2).

It should be noted that **4d** is not the first example of a bidentate [bis(phosphine)-$CrCl_3$(THF)] complex. Recently, Overett *et al.*[44] reported on the structure of a similar complex featuring 1,2-bis(diphenylphosphino)benzene as ligand (see section 3.6.4.3.2.1.2 of the introductory chapter). Metric parameters of complex **4d** are very close to those of this complex except for the P1-Cr1-P2 angle, which is larger in the case of **4d** (85.90(5) versus 77.82(2)°).

4.3 Evaluation of Complexes 4a-g in Ethylene Oligomerization

The catalytic activity of **4a-g** in ethylene oligomerization was then evaluated. Experiments were carried out at 45°C or 70°C in the presence of MAO (300 or 600 equiv.) and toluene was used as solvent. Catalytic performances are summarized in table 2. Importantly, we noted that no detectable polymeric material is formed in each experiment. Equally, no cyclic C_6 byproducts, as observed in the Sasol PNP tetramerization system, have been detected. Ligands with phenyl substitution on phosphorous systematically exhibit a lower activity than those with alkyl substitution (Cy and *n*-Bu) (entry 1-3 versus 4-7). Concomitantly, their selectivity towards trimerization is generally lower and oligomer distributions are observed. On the other hand, cyclohexyl substituted derivatives show higher activities alongside with high selectivities towards the formation of 1-hexene. Even though less pronounced, the great steric bulk of the *t*-Bu group on the central amine moiety seems to have a negative influence on the activity (entry 5). The most important observation concerns the effect of steric bulk at phosphorus atoms. Indeed, it becomes obvious that decreasing the steric bulk by replacing the cyclohexyl groups (**4d**-**f**) by the smaller *n*-Bu group (**4g**) results in a shift of the selectivity towards tetramerization, whereas α-selectivity is maintained. Finally, it clearly appears that the most satisfactory results are obtained with complex **4f** which shows an excellent selectivity towards trimerization (99%). Therefore, further experiments were carried out to optimize its performances. It was found that a temperature increase from 45°C to 70°C was beneficial for catalyst productivity (entry 6 versus 8). However an increase in ethylene pressure from 30 bars to 50 bars did not improve the productivity. Finally we found that improvement of the catalyst activity was achieved upon doubling of the MAO quantity and carrying out the oligomerization at 70°C (entry 10).

Table 2. Ethylene oligomerization with complexes **4a**-**g**.

	Precursor	T/°C	%C_4 (1-C_4)	%C_6 (1-C_6)	%C_8 (1-C_8)	%C_{10+} [c]	Productivity/ $g \times g(Cr)^{-1} \times h^{-1}$
1	**4a**	45	6(51)	88(98)	4(81)	2	2106
2	**4b**	45	4(59)	67(91)	20(85)	9	527
3	**4c**	45	3(57)	90(98)	4(87)	3	2335
4	**4d**	45	1(35)	97(95)	1(99)	1	4579
5	**4e**	45	1(20)	90(92)	2(99)	7	4003
6	**4f**	45	-	99(97)	1(99)	-	5300
7	**4g**	45	-	78(99)	21(98)	1	5127
8	**4f**	70	-	99(98)	1(99)	-	8535
9[b]	**4f**	45	-	98(98)	1(99)	1	4892
10[d]	**4f**	70	-	99(98)	1(99)	-	9783

[a] Conditions: $P(C_2H_4)$ = 30 bar, 30 min, MAO (300 eq.), [b] Conditions: $P(C_2H_4)$ = 50 bar, 30 min, [c] No polymeric material was recovered, [d] 600 eq. of MAO used.

4.4 Tri- versus Tetramerization – Theoretical Study

To gain insight into the influence of steric effects, calculations on selected steps of the catalytic cycle, with a particular focus on the competition between 1-hexene release from the catalytic species versus chromacyclononane formation.

A number of simplifications have again been introduced. As we were exclusively interested in the steric effects at phosphorus, the nitrogen substituent was systematically replaced by a methyl group. The *n*-butyl groups on the ligand **3f** in the experimental study of the catalytic system were replaced by ethyl groups assuming that the ending ethyl moiety of the *n*-butyl chains lie far away from the chromium metal center.

All calculations were again carried out at the quantum level using the Gaussian 03 suite.[36] The geometries were optimized using the Perdew-Burke-Ernzerhof (PBE) functional.[45-48] The standard 6-31G* basis set was used for all non-metallic atoms (H, C, N, and P) belonging to the cyclic part of the ligand and the chromacycles, whereas the 3-21G* basis set was used to describe the ethyl- and cyclohexyl substituents on the phosphorus atoms. The basis set used on chromium was the Hay and Wadt[37] small-core quasi relativistic effective core potential with the double-ζ valence basis set (441s/2111p/41d) augmented with an f-polarization function (exponent = 1.941).[38]

As in the previous theoretical study on tri- and tetramerization with Cr-bis(phosphino)amine complexes, the role of MAO was again neglected, which is supported by the van Rensburg study, which revealed dissociated ion pairs to be a prerequisite for the reaction to proceed.

Several chromacycloheptane rings adopting different geometries and conformations were computed both in the case of ethyl and cyclohexyl substituents. Indeed, it is important to keep in mind that, at

least, two geometries should be accessible in the case of chromacycloheptane complex. A first one, in which the bidentate ligand and the ring methylene susbtituents lie in the same plane (yielding a distorted square planar geometry), and a second one, in which the complex adopts a distorted tetrahedral geometry. Furthermore, one has to emphasize on the different conformations the chromacycloheptane ring may adopt. Despite many attempts to optimize a square planar structure, all our calculations converged towards the distorted tetrahedral structures **XXIa$_{R}$** (R = Et, Cy)**,** in which one of the metallacycle α-carbon atoms occupies the apical position. Notably, both structures feature a β-hydrogen agostic interaction (*d*(Cr-H) = 1.955 Å in **XXIa$_{Et}$** and *d*(Cr-H) = 1.971 Å in **XXIa$_{Cy}$**) in which the hydrogen atom occupies the remaining equatorial position. Several other conformations of the metallacycle, do not featuring this β-hydrogen agostic interaction, were computed but were found to be slightly higher in energy on the potential energy surface. A view of the chromacyclopentane **XXIa$_{Et}$** is presented in figure 9 and the most significant bond distances and bond angles are listed in the corresponding legend.

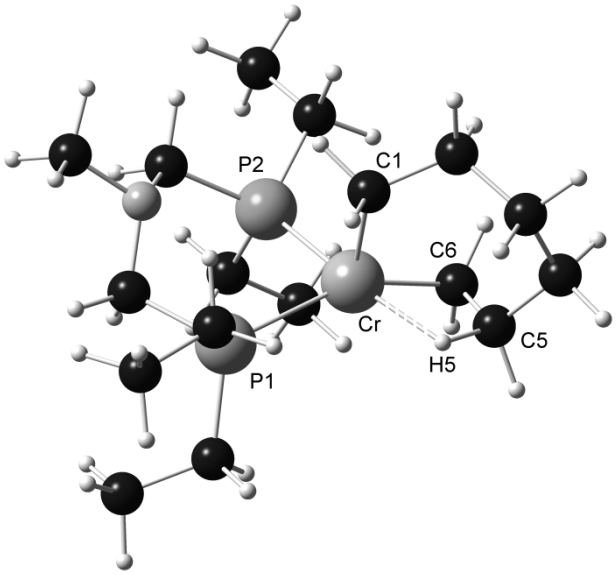

Figure 9. Optimized geometry of theoretical comlex **XXIa$_{Et}$**. Most significant bond distances (Å) and angles (°): P1-Cr = 2.505, P2-Cr = 2.411, Cr-C1 = 2.027, Cr-C6 = 2.010, C6-C5 = 1.516, C5-H5 = 1.171, H5-Cr = 1.956, P1-Cr-P2 = 90.630, Cr-C6-C5 = 83.523, C6-C5-H5 = 111.390, C5-H5-Cr = 95.676.

Coordination of one additional molecule of ethylene on **XXIa$_{R}$** was then studied. Two possibilities were considered. Indeed, one may consider that the ethylene molecule can attach to chromium on the remaining apical position to form a distorted octahedral complex, or by coordination on the equatorial site occupied by the β-agostic interaction to form a distorted square-pyramidal complex. Both structures **XXIb$_{Et}$** and **XXIb$_{Et}$'** were found as minima in the case of the ethyl derivative, but optimizations of the cyclohexyl complex only led to the distorted square-pyramidal complex **XXIb$_{Cy}$**. Attempts to minimize a structure analogous to **XXIb$_{Et}$'** in the case of the cyclohexyl derivative only

yielded a structure featuring no interaction between $\mathbf{XXIa_{Cy}}$ and the incoming molecule of ethylene (Scheme 26).

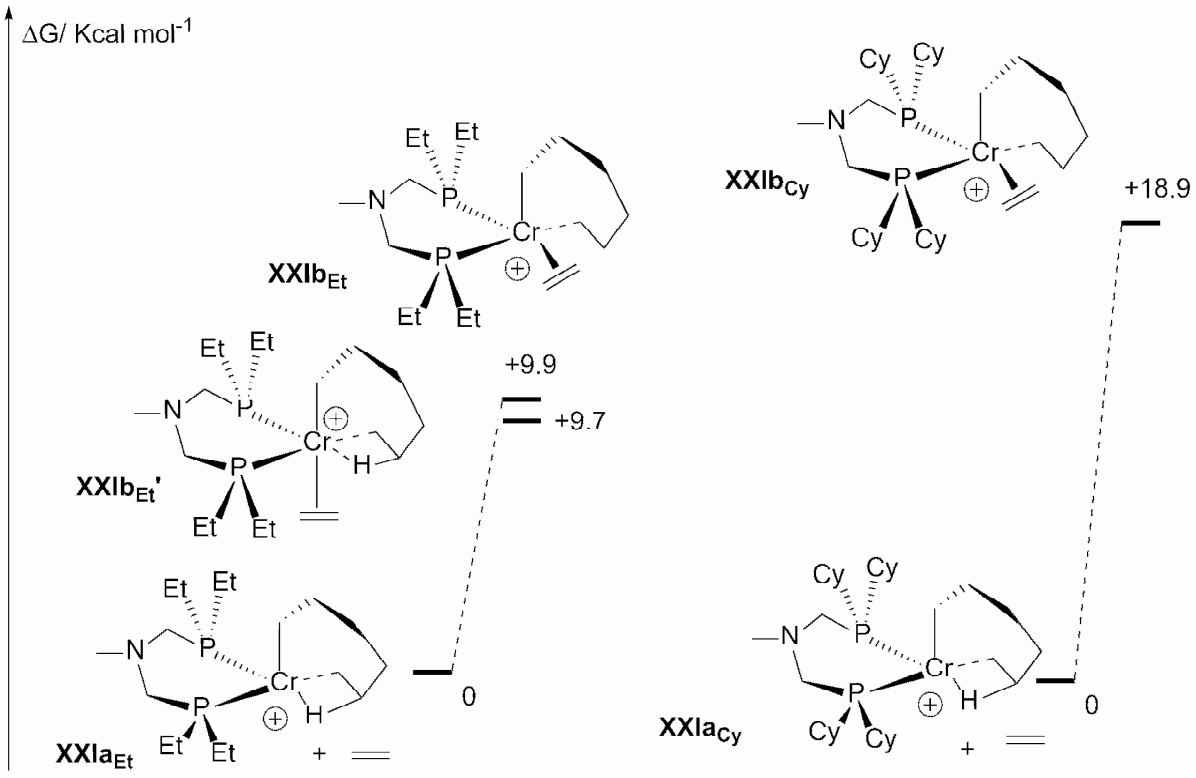

Scheme 26. Bonding of ethylene to structures $\mathbf{XXIa_{Et}}$ and $\mathbf{XXIa_{Cy}}$.

The energy required to coordinate one molecule of ethylene to $\mathbf{XXIa_{Cy}}$ to yield $\mathbf{XXIb_{Cy}}$ (ΔG = 18.9 kcal × mol^{-1}) was found to be much more important than the one needed to form $\mathbf{XXIb_{Et}}$ and $\mathbf{XXIb_{Et'}}$ (ΔG = 9.9 and +9.7 kcal × mol^{-1} respectively). This observation very likely reflects the stronger steric hindrance provided by the cyclohexyl groups in $\mathbf{Ib_{Cy}}$. Notably, in all complexes, bonding of the ethylene molecule to the cationic center is probably very weak as evidenced by the long Cr-$CC_{centroid}$ bond distances (2.396 Å in $\mathbf{Ib_{Et}}$; 2.567 Å in $\mathbf{Ib_{Et'}}$ and 2.395 Å in $\mathbf{Ib_{Cy}}$ and to the relatively short C=C bond lengths (1.360 Å in $\mathbf{Ib_{Et}}$, 1.355 Å in $\mathbf{Ib_{Et'}}$, and 1.359 Å in $\mathbf{Ib_{Cy}}$). These data are indicative of a weak π-back bonding from the chromium center to the π*-system of the ethylene ligand.

We then focused our study on the two main transformations that either lead to 1-hexene or to the chromacyclononane complexes. As in the preceeding study on the Sasol PNP system, two different processes were envisaged for the formation of 1-hexene, the (3,7)-intramolecular hydrogen transfer and the transient formation of an hydrido-hexenyl complex through a β-hydrogen transfer from carbon to chromium. Contrary to what was found with the Sasol PNP system, no such hydrido complexes could be successfully optimized in the case of the present PCNCP ligands, each attempt yielding back the starting precursors $\mathbf{XXIa_{Et}}$ and $\mathbf{XXIa_{Cy}}$. In each case, the (3,7)-hydrogen transfer process proved to be the only pathway to form the [Cr(I)(η^2-1-hexene)] complexes $\mathbf{XXIc_R}$ (R = Et, Cy). Thus the

formation of **XXIc$_{Et}$** was found to be only slightly endothermic (ΔG = 0.2 kcal × mol^{-1}), involving an energetic barrier of ($\Delta G^{\ddagger}$ = 13.3 kcal × mol^{-1}) (Scheme 27).

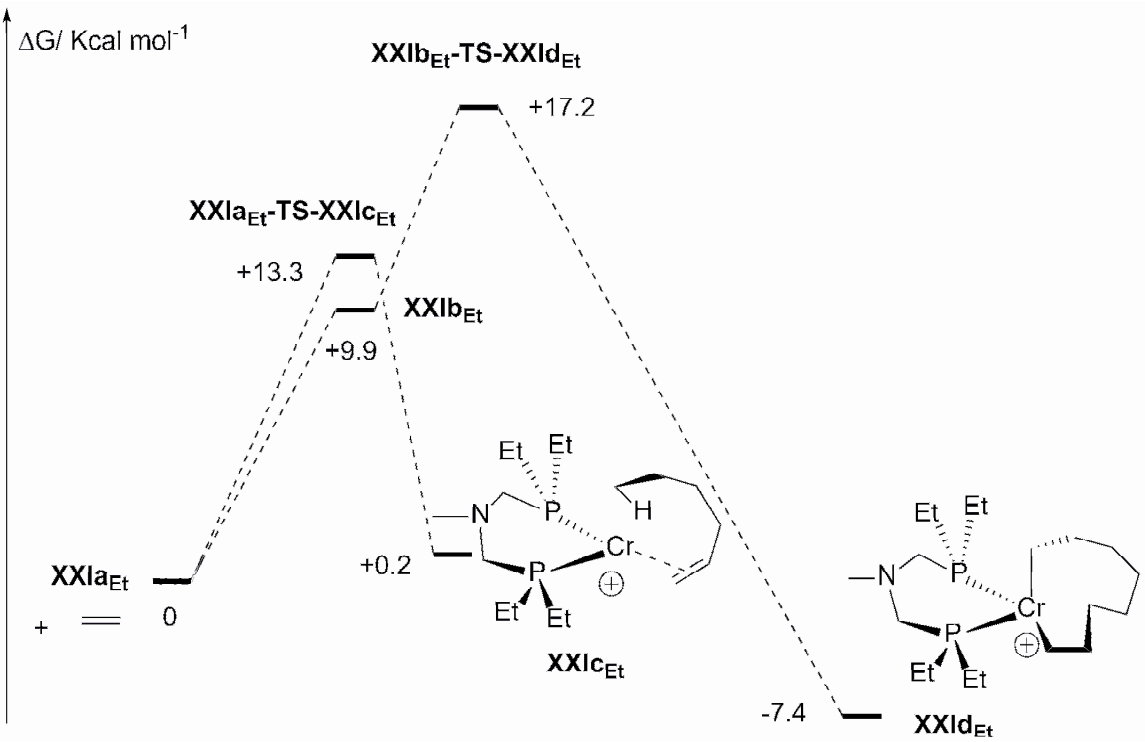

Scheme 27. Overall energetic pathway showing the transformation of **XXIa$_{Et}$** into the 1-hexene complex **XXIc$_{Et}$** and the chromacyclononane **XXId$_{Et}$**.

Note that both complexes **XXIc$_{Et}$** and **XXIc$_{Cy}$** were found as minima in the quadruplet spin state (the *S* = 2 state lying 16.5 and 16.6 kcal × mol^{-1} above for **XXIc$_{Et}$** and **XXIc$_{Cy}$**, respectively). A view of the transition state **XXIa$_{Et}$-TS-XXIc$_{Et}$** is presented in figure 10 (left) and the most significant bond lengths and bond angles are listed in the corresponding legend. As can be seen, if one does not take into account the C1-Cr bond which is significantly elongated, this transition complex adopts a distorted square planar pyramidal structure, only P1, P2, H5 and C6 being coordinated. As expected, the C5-H (1.443 Å) bond is elongated and close to the C1-H5 (1.482 Å) bond which is under formation. Concomitantly, the C5-C6 (future double bond of 1-hexene) is shortened to 1.452 Å. Most importantly, it appears that this hydrogen transfer is strongly assisted by chromium as attested by the relatively short Cr-H5 bond distance of 1.482 Å.

The ring expansion which leads to the chromacyclononane **XXId$_{Et}$** was also computed and the general energetic pathway is depicted in scheme 27. This transformation was found to be slightly exothermic (ΔG = -7.4 kcal × mol^{-1} versus **XXIa$_{Et}$** and -17.3 kcal × mol^{-1} versus **XXIb$_{Et}$**) and involves an activation barrier of ($\Delta G^{\ddagger}$ = 17.2 kcal × mol^{-1} from **XXIa$_{Et}$** and +7.3 kcal × mol^{-1} from **XXIb$_{Et}$**). A view of the transition state connecting **XXIb$_{Et}$** and **XXId$_{Et}$** is presented in figure 10 (right) as well as the most significant metric parameters.

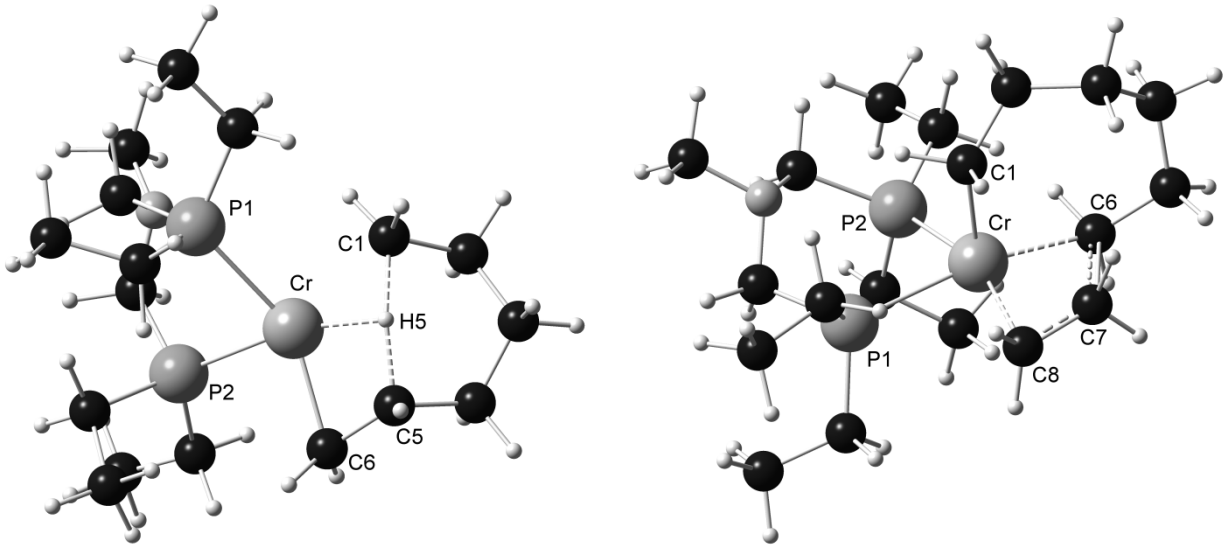

Figure 10. Optimized geometry of the transition structures **XXIa$_{Et}$-TS-XXIc$_{Et}$** (left) and **XXIb$_{Et}$-TS-XXId$_{Et}$** (right). Most significant bond distances (Å) and angles (°): For (**XXIa$_{Et}$-TS-XXIc$_{Et}$**): P1-Cr = 2.486, P2-Cr = 2.416, Cr-C1 = 2.219, Cr-C6 = 2.087, C6-C5 = 1.452, C5-H5 = 1.443, H5-Cr = 1.654, H5-C1 = 1.482, P1-Cr-P2 = 82.468, Cr-C6-C5 = 74.511, C6-C5-H5 = 114.532, C5-H5-Cr = 90.320, C1-H5-Cr = 89.844. **XXIa$_{Et}$-TS-XXIc$_{Et}$**: P1-Cr = 2.496, P2-Cr = 2.527, Cr-C1 = 2.039, Cr-C6 = 2.195, Cr-C8 = 2.121, C6-C7 = 2.168, C7-C8 = 1.450, P1-Cr-P2 = 82.988, P1-Cr-C8 = 82.321, Cr-C8-C7 = 78.094**,** C8-C7-C6 = 120.786, C6-C6-Cr = 63.504.

This ring expansion simply consists in a (1,2)-insertion process, the C6 carbon atom of the ring attacking the C7 carbon atom of the coordinated ethylene moiety. Not surprisingly, if we take into account the high exothermicity of the process, the overall geometry around chromium is closer to that of the starting precursor **XXIb$_{Et}$** than to that of **XXId$_{Et}$**. The most significant information are given by the C6-C7 (2.168 Å) bonds and Cr-C8 (2.121 Å) bonds length which are still rather long and the C7-C8 (1.419 Å) bond which is slightly lengthened. Note that to complete this first part of the study, additional calculations were done postulating the hexacoordinated **XXIb$_{Et}$**, complex as starting precursor for the synthesis of a chromacyclononane, but all attempts proved unsuccessful. We conclude that both pathways starting from **XXIa$_{Et}$**, which lead to **XXIc$_{Et}$** and **XXId$_{Et}$**, require an activation energy of 13.3 and 17.2 kcal × mol^{-1}, respectively, and therefore are both kinetically accessible.

The same approach was followed in the case of the cyclohexyl derivatives **XXIa$_{Cy}$** and **XXIb$_{Cy}$** and the complete energetic pathways leading to the 1-hexene **XXIc$_{Cy}$** and chromocyclononane **XXId$_{Cy}$** complexes were computed. In each case, transition states **XXIa$_{Cy}$-TS-XXIc$_{Cy}$** and **XXIb$_{Cy}$-TS-XXId$_{Cy}$** were localized and were found to be geometrically close to that computed in the case of the ethyl derivatives. These two energetic pathways are presented in scheme 28. Two conclusions can be drawn comparing schemes 27 and 28. It appears that the kinetic formation of 1-hexene is slightly favored in the case of the cyclohexyl substituent compared to the ethyl derivative ($\Delta G^{\ddagger}$ = 10.9 kcal ×

mol^{-1} versus 13.3 kcal × mol^{-1}) while the formation of the chromacyclononane is slightly exothermic in comparison (ΔG = -1.0 kcal × mol^{-1} versus -7.4 kcal × mol^{-1}).

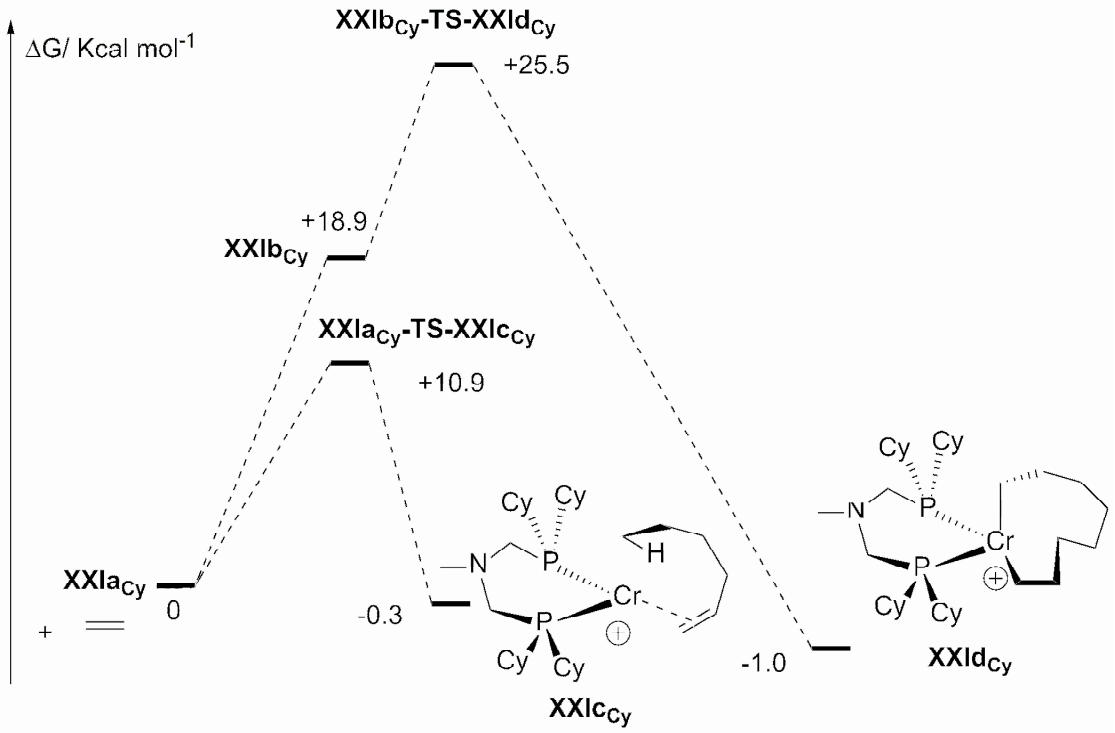

Scheme 28. Overall energetic pathway showing the transformation of $\mathbf{Ia_{Cy}}$ into the 1-hexene complex $\mathbf{Ic_{Cy}}$ and the chromacyclononane $\mathbf{Id_{Cy}}$.

However, the most important information is given by the comparison of the two processes in the case of the cyclohexyl substituent. Contrary to what is observed with the ethyl derivative, formation of 1-hexene is favored ($\Delta G^{\ddagger}$ = 10.9 kcal × mol^{-1}) over the formation of complex $\mathbf{XXIb_{Cy}}$ which is the key intermediate to allow the growth of the metallacycle ($\Delta G^{\ddagger}$ = 25.5 kcal × mol^{-1} with $\mathbf{XXIa_{Cy}}$ as reference). Examination of scheme 28 led us to conclude that formation of the chromacyclononane is strongly disfavored when cyclohexyl substituents are present. Note that these conclusions are in good agreement with experimental results which show that only 1-hexene is formed.

To complete this study, we then envisaged the existence of a second type of pentacoordinated ethylene complex $\mathbf{XXIIb_R}$ (R = Et, Cy), which could be formed by coordinating one molecule of ethylene on the apical position of the unsaturated square pyramidal derivative $\mathbf{XXIIa_R}$, though this latter unsaturated complex could not be optimized in the case of our PCNCP ligands (see above). Optimizations of the structures $\mathbf{XXIIb_R}$ were successful and both complexes were found to be energetically close to isomers $\mathbf{XXIb_R}$ (+13.5 kcal × mol^{-1} for $\mathbf{IIb_{Et}}$ versus +9.9 and +9.7 kcal × mol^{-1} for $\mathbf{Ib_{Et}}$ and $\mathbf{XXIb_{Et}}$, respectively and +17.0 kcal × mol^{-1} for $\mathbf{XXIIb_{Cy}}$ versus +18.9 kcal × mol^{-1} for $\mathbf{XXIb_{Cy}}$) (Scheme 29). A view of one molecule of complex $\mathbf{XXIIb_{Cy}}$ is shown in figure 11.

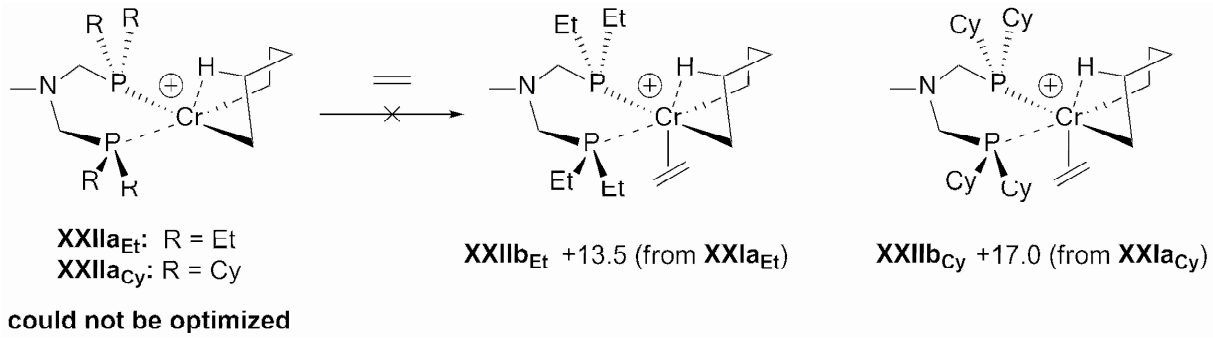

Scheme 29. Relative energies of **XXIIb$_{Et}$** and **XXIIb$_{Cy}$**.

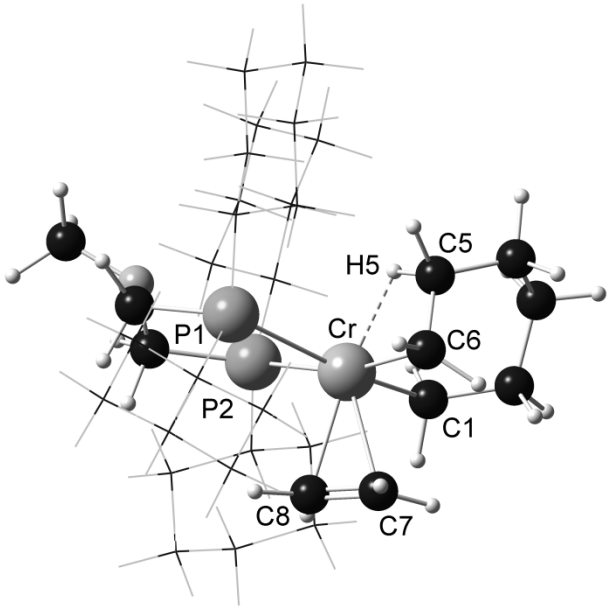

Figure 11. Optimized geometry of complex **IIb$_{Cy}$**. Cyclohexyl substituents are drawn in wireframe for the sake of clarity. Most significant bond lengths (Å) and angles (°): P1-Cr = 2.764, P2-Cr = 2.593, Cr-C1 = 2.089, Cr-C6 = 2.0675, C5-H5 = 1.164, H5-Cr = 1.946, Cr-C7 = 2.284, Cr-C8 = 2.261, P1-Cr-P2 = 87.766, Cr-C6-C5 = 82.393, C6-C5-H5 = 112.496, C5-H5-Cr = 97.789.

Though we have no experimental evidence about the formation of these ethylene complexes, two hypotheses may account for their formation. First, one may propose that one MAO counteranion interacts with this unsaturated complex and forces it to adopt a distorted square pyramidal geometry, with an incoming ethylene molecule then substituting this MAO anion in a second step (Scheme 30). A second hypothesis would be that complexes **XXIa$_R$** may rearrange to yield complexes **XXIIb$_R$**. These complexes are obviously energetically close to the **XXIb$_R$** isomers and could be relevant intermediates in the mechanism. It was therefore important to verify whether **XXIIb$_R$** could indeed be formed from the pentacoordinated chromacycloheptane **XXIa$_R$**.

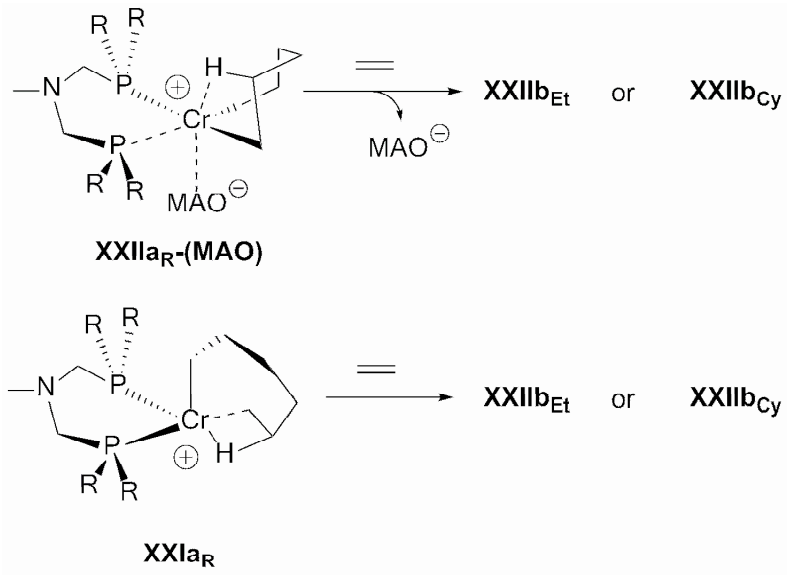

Scheme 30. Possible precursors for the formation of **IIb$_{Et}$** and **IIb$_{Cy}$**.

Pursuing our investigations we found a plausible mechanism that may possibly account for transformation of complexes **XXIa$_R$** into complexes **XXIIb$_R$** (R = Et, Cy). This mechanism, which is depicted in the scheme 31 involves, as a first step, the decoordination of the ligand's phosphine moiety located *trans* to the β-agostic hydrogen and, in a subsequent second step, the coordination of the incoming ethylene molecule on the vacant site created.

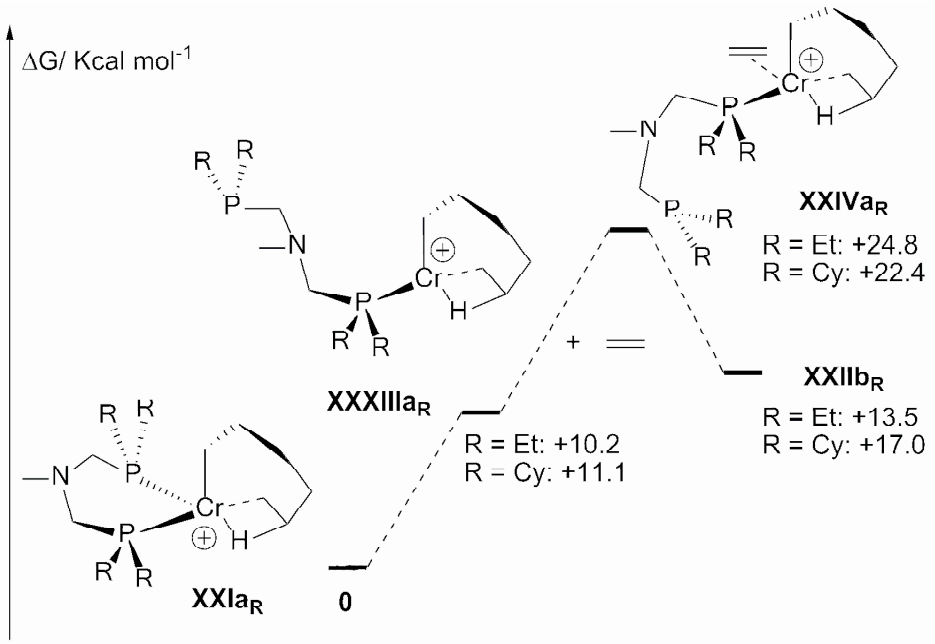

Scheme 31. Overall energetic pathway showing the possible formation of **XXIIb$_R$** (R = Et, Cy) ethylene complexes from the pentacoordinated **XXIa$_R$** chromacycloheptanes.

Interestingly, the creation of this vacant site only requires a small energy (ca. 10.6 kcal × mol^{-1}). Finally the last step of this mechanism involves the recoordination of the pendant phosphine moiety to

chromium *trans* to the apical alkyl substituent to yield $\mathbf{XXIIb_R}$. However, these pathways involve important free energies higher than 22 kcal × mol^{-1} and are probably disfavored, in both cases, compared to the formation of 1-hexene and chromacyclononanes complexes. (Schemes 27 and 28)

Nevertheless, to be exhaustive, we considered complexes $\mathbf{XXIIb_R}$ (R = Et, Cy) as possible intermediates in the ring expansion process to chromacyclononanes. The two corresponding structures $\mathbf{XXIId_{Et}}$ and $\mathbf{XXIId_{Cy}}$ were successfully optimized as well as the two corresponding transition states $\mathbf{XXIIb_{Et}}$**-TS-**$\mathbf{XXIId_{Et}}$ and $\mathbf{XXIIb_{Cy}}$**-TS-**$\mathbf{XXIId_{Cy}}$ which connect them to the two ethylene complexes $\mathbf{XXIIb_R}$. The energetic pathways of these two transformations are depicted in scheme 32.

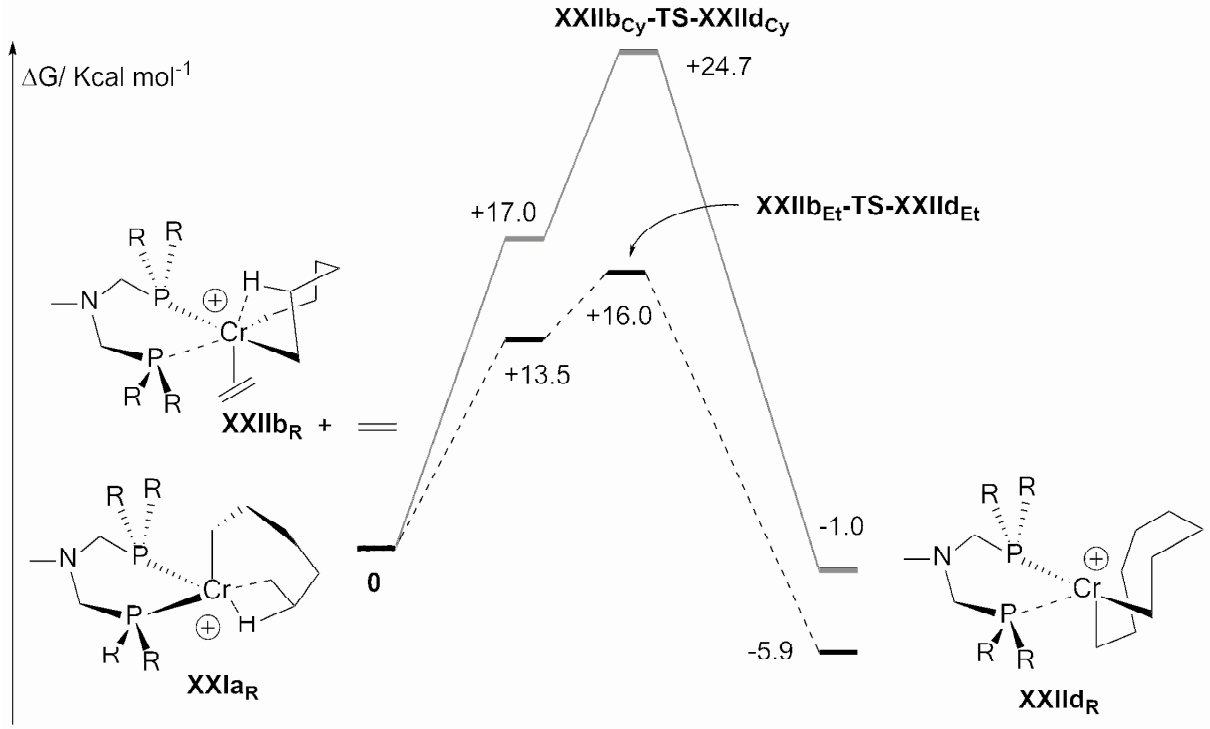

Scheme 32. Overall energetic pathways explaining the formation of chromacyclononanes $\mathbf{IId_R}$ from the ethylene complexes $\mathbf{XXIIb_R}$ (R = Et, Cy).

In the case of the ethyl substituent, formation of the chromacyclononane is competitive with the elimination leading to 1-hexene ($\Delta G^{\ddagger}$ between $\mathbf{XXIa_{Et}}$ and ($\mathbf{XXIIb_{Et}}$**-TS-**$\mathbf{XXIId_{Et}}$) = +16.0 kcal × mol^{-1} versus $\Delta G^{\ddagger}$ between $\mathbf{XXIa_{Et}}$ and ($\mathbf{XXIa_{Et}}$**-TS-**$\mathbf{XXIc_{Et}}$) = +13.3 kcal × mol^{-1}) and compares with the energetic barrier needed to form chromacyclononane XX$\mathbf{Id_{Et}}$ from $\mathbf{XXIa_{Et}}$ ($\Delta G^{\ddagger}$ between $\mathbf{XXIa_{Et}}$ and ($\mathbf{XXIb_{Et}}$**-TS-**$\mathbf{XXId_{Et}}$) = +17.2 kcal × mol^{-1}). However, when cyclohexyl substituents are present at phosphorus, the formation of the chromacyclononane is disfavored with respect to the formation of the 1-hexene complex. Indeed, +24.7 kcal × mol^{-1} are needed to reach the transition state $\mathbf{XXIIb_{Cy}}$**-TS-**$\mathbf{XXIId_{Cy}}$ whereas formation of 1-hexene requires an activation energy of only 10.9 kcal × mol^{-1}. Here also we note that the formation of chromacyclononanes $\mathbf{XXId_{Cy}}$ and $\mathbf{XXIId_{Cy}}$ roughly require the same activation barriers (+24.7 kcal × mol^{-1} for isomer **XXII** versus +25.5 kcal × mol^{-1} for isomer **XXI**).

These last series of results led us to conclude that isomers $\mathbf{IIb_R}$, if they are formed, can lead to 1-hexene complexes through a (3,7)-elimination and the corresponding chromacyclononanes through the insertion of the ethylene molecule. However, as stated in the case of isomers $\mathbf{XXIb_R}$ formation of chromacyclononanes is strongly disfavored when cyclohexyl groups are present. Even though no additional detailed studies were undertaken in the case of the two isomers considered, we may reasonably propose that this difference does not stem from electronic effects since both substituents are alkyl groups, but rather results from steric effects which limit the access of incoming ethylene molecules to the cationic chromium center.

5. Conclusion

In this chapter on the mechanism of the chromium catalyzed tri- and tetramerization reaction of ethylene, we have presented our contributions to the establishment of the redox couple present in the metallacyclic mechanism of this transformation. The results point towards a Cr(I)-Cr(III) couple, an alternative, which has been equally affirmed through the studies of various other workgroups.

The different possible steps of the mechanism of the tri- and tetramerization reaction with the Sasol PNP system was studied using DFT calculations, and allowed to establish a viable reaction pathway. Two possible ways of 1-hexene elimination from the intermediate chromacycloheptane (either (3,7)-hydrogen transfer or β-hydrogen elimination), as well as a possible mechanistic scenario for the formation of the C_6 cyclic byproducts methylenecyclopentane and methylcyclopentane found in the catalytic product stream. (3,9)-hydrogen transfer from a chromacyclononane was shown to be the only viable pathway for 1-octene elimination.

In the second part of this chapter, the preparation of new chromium(III) complexes bearing bidentate bis(phosphinomethyl)-amines (PCNCP) ligands was described. Monomeric octahedral complexes were obtained, in which the bisphosphine ligand adopts a facial coordination mode. Those complexes were evaluated towards their activity in the selective ethylene oligomerization reaction upon activation with excess MAO. Activities of up to 9783 $g \times g(Cr)^{-1} \times h^{-1}$ were observed, with concomitant selectivities of up to 99% towards 1-hexene. The selectivity towards the ethylene trimerization product was found to be strongly dependent on the steric bulk on the phosphine moieties, and, to a lesser extent, on the basicity of the phosphinyl groups, and the substitution on the central nitrogen of the ligands. Bulky dicyclohexylphosphinyl groups led to high selectivities towards 1-hexene, whereas less bulky di-*n*-butylphosphinyl substituents led to the apparition of 21% of 1-octene during catalysis.

The relation between steric bulk on phosphorous and the oligomer product distribution was studied through DFT calculations concentrating on the key steps of the metallacyclic mechanism which are decisive for the selectivity towards either 1-hexene or 1-octene. The results obtained from these theoretical investigations clearly show that in the case of these PCNCP based systems, formation of Cr(I)-(1-hexene) complexes results from an intramolecular (3,7)-hydrogen transfer and not from a β-

hydrogen transfer followed by a reductive elimination. Contrary to what was found with the Sasol PNP system, hydrido-(PCNCP)Cr(III)-(1-hexenyl) complexes were found unstable. The final important conclusion concerns the selectivities observed. Our calculations clearly demonstrate that, though the two substituents considered (ethyl and cyclohexyl) are probably not very different from an electronic point of view, the formation of chromacyclononane is strongly disfavoured when cyclohexyl groups are present at phosphorus, compared to the formation Cr(I)-(1-hexene) complexes. This result, which is in very good agreements with experimental data, reveals that steric bulk at phosphorus is a very important factor that can probably be further exploited to finely tune selectivites in this important catalytic transformation.

6. Bibliography

[1] P. Cossee, *J. Catal.* **1964**, *3*, 80.
[2] E. J. Arlman, P. Cossee, *J. Catal.* **1964**, *3*, 99.
[3] R. M. Manyik, W. E. Walker, T. P. Wilson, *J. Catal.* **1977**, *47*, 197.
[4] J. R. Briggs, *J. Chem. Soc.-Chem. Commun.* **1989**, 674.
[5] R. Emrich, O. Heinemann, P. W. Jolly, C. Kruger, G. P. J. Verhovnik, *Organometallics* **1997**, *16*, 1511.
[6] W. Janse van Rensburg, C. Grove, J. P. Steynberg, K. B. Stark, J. J. Huyser, P. J. Steynberg, *Organometallics* **2004**, *23*, 1207.
[7] S. Tobisch, T. Ziegler, *Organometallics* **2003**, *22*, 5392.
[8] A. N. J. Blok, P. H. M. Budzelaar, A. W. Gal, *Organometallics* **2003**, *22*, 2564.
[9] T. J. M. de Bruin, L. Magna, P. Raybaud, H. Toulhoat, *Organometallics* **2003**, *22*, 3404.
[10] Z.-X. Yu, K. N. Houk, *Angew. Chem. Interl. Ed.* **2003**, *42*, 808.
[11] T. Agapie, S. J. Schofer, J. A. Labinger, J. E. Bercaw, *J. Am. Chem. Soc.* **2004**, *126*, 1304.
[12] S. J. Schofer, M. W. Day, L. M. Henling, J. A. Labinger, J. E. Bercaw, *Organometallics* **2006**, *25*, 2743.
[13] L. E. Bowen, D. F. Wass, *Organometallics* **2006**, *25*, 555.
[14] L. E. Bowen, M. Charernsuk, D. F. Wass, *Chem. Commun.* **2007**, 2835.
[15] M. J. Overett, K. Blann, A. Bollmann, J. T. Dixon, D. Haasbroek, E. Killian, H. Maumela, D. S. McGuinness, D. H. Morgan, *J. Am. Chem. Soc.* **2005**, *127*, 10723.
[16] B. Blom, G. Klatt, J. C. Q. Fletcher, J. R. Moss, *Inorg. Chim. Acta* **2007**, *360*, 2890.
[17] W. Janse van Rensburg, J.-A. van den Berg, P. J. Steynberg, *Organometallics* **2007**, *26*, 1000.
[18] A. Carter, S. A. Cohen, N. A. Cooley, A. Murphy, J. Scutt, D. F. Wass, *Chem. Commun.* **2002**, 858.
[19] R. Walsh, D. H. Morgan, A. Bollmann, J. T. Dixon, *Appl. Catal. A: Gen.* **2006**, *306*, 184.
[20] D. H. Morgan, S. L. Schwikkard, J. T. Dixon, J. J. Nair, R. Hunter, *Adv. Synth. Catal.* **2003**, *345*, 939.
[21] D. S. McGuinness, D. B. Brown, R. P. Tooze, F. M. Hess, J. T. Dixon, A. M. Z. Slawin, *Organometallics* **2006**, *25*, 3605.
[22] C. N. Temple, S. Gambarotta, I. Korobkov, R. Duchateau, *Organometallics* **2007**, *26*, 4598.
[23] A. Jabri, P. Crewdson, S. Gambarotta, I. Korobkov, R. Duchateau, *Organometallics* **2006**, *25*, 715.
[24] I. Krossing, I. Raabe, *Angew. Chem. Interl. Ed.* **2004**, *43*, 2066.
[25] I. Krossing, *Chem. Eur. J.* **2001**, *7*, 490.
[26] D. S. McGuinness, A. J. Rucklidge, R. P. Tooze, A. M. Z. Slawin, *Organometallics* **2007**, *26*, 2561.
[27] K. Theopold, H. , *Eur. J. Inorg. Chem.* **1998**, *1998*, 15.
[28] R. Köhn, D., M. Haufe, G. Kociok-Köhn, S. Grimm, P. Wasserscheid, W. Keim, *Angew. Chem.* **2000**, *39*, 4337.
[29] R. D. Köhn, D. Smith, M. F. Mahon, M. Prinz, S. Mihan, G. Kociok-Köhn, *J. Organomet. Chem.* **2003**, *683*, 200.
[30] A. J. Rucklidge, D. S. McGuinness, R. P. Tooze, A. M. Z. Slawin, J. D. A. Pelletier, M. J. Hanton, P. B. Webb, *Organometallics* **2007**, *26*, 2782.
[31] L. E. Bowen, M. F. Haddow, A. G. Orpen, D. F. Wass, *Dalton Trans.* **2007**, 1160.
[32] E. Angelescu, C. Nicolau, Z. Simon, *J. Am. Chem. Soc.* **1966**, *88*, 3910.
[33] D. Braga, A. L. Costa, F. Grepioni, L. Scaccianoce, E. Tagliavini, *Organometallics* **1996**, *15*, 1084.
[34] A. Brückner, J. K. Jabor, A. E. C. McConnell, P. B. Webb, *Organometallics* **2008**, *27*, 3849.
[35] S. Kuhlmann, J. T. Dixon, M. Haumann, D. H. Morgan, J. Ofili, O. Spuhl, N. Taccardi, P. Wasserscheid, *Adv. Synth. Catal.* **2006**, *348*, 1200.
[36] M. J. Frisch, G. W. Trucks, H. B. Schlegel, G. E. Scuseria, M. A. Robb, J. R. Cheeseman, J. J. A. Montgomery, T. Vreven, K. N. Kudin, J. C. Burant, J. M. Millam, S. S. Iyengar, J. Tomasi, V. Barone, B. Mennucci, M. Cossi, G. Scalmani, N. Rega, G. A. Petersson, H. Nakatsuji, M. Hada, M. Ehara, K. Toyota, R. Fukuda, J. Hasegawa, M. Ishida, T. Nakajima, Y. Honda, O.

Kitao, H. Nakai, M. Klene, X. Li, J. E. Knox, H. P. Hratchian, J. B. Cross, C. Adamo, J. Jaramillo, R. Gomperts, R. E. Stratmann, O. Yazyev, A. J. Austin, R. Cammi, C. Pomelli, J. W. Ochterski, P. Y. Ayala, K. Morokuma, G. A. Voth, P. Salvador, J. J. Dannenberg, V. G. Zakrzewski, S. Dapprich, A. D. Daniels, M. C. Strain, O. Farkas, D. K. Malick, A. D. Rabuck, K. Raghavachari, J. B. Foresman, J. V. Ortiz, Q. Cui, A. G. Baboul, S. Clifford, J. Cioslowski, B. B. Stefanov, G. Liu, A. Liashenko, P. Piskorz, I. Komaromi, R. L. Martin, D. J. Fox, T. Keith, M. A. Al-Laham, C. Y. Peng, A. Nanayakkara, M. Challacombe, P. M. W. Gill, B. Johnson, W. Chen, M. W. Wong, C. Gonzalez, J. A. Pople, Gaussian 03, Revision B.05, Gaussian Inc., Pittsburgh PA, **2003**.

[37] P. J. Hay, W. R. Wadt, *The J. Chem. Phys.* **1985**, *82*, 299.

[38] A. W. Ehlers, M. Böhme, S. Dapprich, A. Gobbi, A. Höllwarth, V. Jonas, K. F. Köhler, R. Stegmann, A. Veldkamp, G. Frenking, *Chem. Phys. Lett.* **1993**, *208*, 111.

[39] C. Klemps, E. Payet, L. Magna, L. Saussine, X. F. Le Goff, P. Le Floch, *Chem. Eur. J.* **2009**, *15*, 8259.

[40] A. L. Balch, M. M. Olmstead, S. P. Rowley, *Inorg. Chim. Acta* **1990**, *168*, 255.

[41] L. Maier, *Helv. Chim. Acta* **1965**, *48*, 1034.

[42] M. Keles, Z. Aydin, O. Serindag, *J. Organomet. Chem.* **2007**, *692*, 1951.

[43] C. A. Busacca, J. C. Lorenz, N. Grinberg, N. Haddad, M. Hrapchak, B. Latli, H. Lee, P. Sabila, A. Saha, M. Sarvestani, S. Shen, R. Varsolona, X. Wei, C. H. Senanayake, *Org. Lett.* **2005**, *7*, 4277.

[44] M. J. Overett, K. Blann, A. Bollmann, R. de Villiers, J. T. Dixon, E. Killian, M. C. Maumela, H. Maumela, D. S. McGuinness, D. H. Morgan, A. Rucklidge, A. M. Z. Slawin, *J. Mol. Cat. A: Chem.* **2008**, *283*, 114.

[45] J. P. Perdew, K. Burke, M. Ernzerhof, *Phys. Rev. Lett.* **1996**, *77*, 3865.

[46] A. D. Becke, *J. Chem. Phys.* **1993**, *98*, 5648.

[47] J. P. Perdew, Y. Wang, *Phys. Rev. B* **1992**, *45*, 13244.

[48] A. K. Rappe, C. J. Casewit, K. S. Colwell, W. A. Goddard, W. M. Skiff, *J. Am. Chem. Society* **1992**, *114*, 10024.

Chapter 2. Variations on the PNP Ligand

Chapter 2. Variations on the PNP Ligand

1. Introduction

The present chapter presents and describes some strategies taken to find alternatives to the Sasol chromium tri- and tetramerization system and its bis(phosphino)amine (PNP) ligand. As described below, the ideas for the devised ligand systems stem from conclusions drawn either from advancements reported in the current literature on the (selective) oligomerization reaction, or, alternatively, from knowledge acquired through the theoretical studies on both the Sasol PNP system and the new PCNCP ligand system (see chapter 1). Our work on various ligands may be divided in two parts: The first part concernes the elaboration of new derivatives of the Sasol PNP ligand,[1] in order to elucidate some of the structural parameters decisive for performance in the oligomerization reaction.

The second part is dedicated to the synthesis and evaluation of other potentially bidentate ligands in the chromium-catalyzed oligomerization reaction, which to some point resemble the PNP ligand from a sterical point of view. In the last part of this chapter, the synthesis and catalytic evaluation of a Mn-PNP complex are described.

2. PNP Derivatives

The best performance of the Sasol PNP system in terms of selectivity and productivity towards the formation of 1-octene is achieved with the ligand $(Ph_2P)_2N(i\text{-Pr})$, bearing acceptor substituents of medium steric bulk on its phosphine moieties. Donor substituted ligands such as $(Et_2P)_2N(Me)$ were reported to be considerably less active and less productive in the oligomerization reaction.[2]

Considering these reported results, we decided to elaborate bis(phosphino)amine ligands with acceptor properties and both excessive and minimum steric bulk in order to evaluate the influence of these two factors on the outcome of the oligomerization reaction on chromium. Accordingly, three new bis(phosphole)amine ligands **1a**-**c**, which through their cyclic π-system exhibit very pronounced acceptor properties, and a bis(dialkynephosphino)amine ligand **2** (Figure 1) were prepared and catalytically tested.

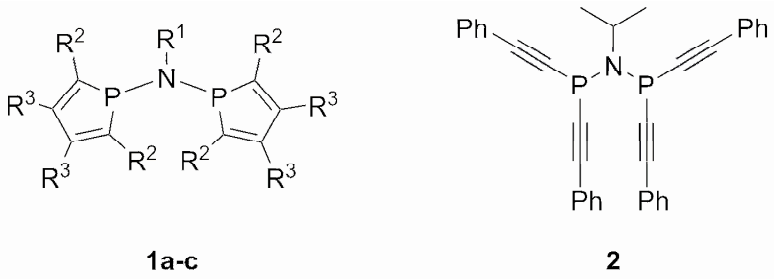

Figure 1. Evaluated PNP ligands. **1a**: $R^1 = R^2 = Ph$, $R^3 = H$, **b**: $R^1 = i$-Pr, $R^2 = Ph$, $R^3 = H$, **c**: $R^1 = Ph$, $R^2 = SiMe_3$, $R^3 = Me$.

2.1 Bis(phosphole)amine Ligands

Following the established synthetic route for bis(phosphine)amines,[3-5] ligands **1a**-**c** were easily prepared from the corresponding 1-bromo-phosphole (cases **1a**,**b**) or chlorophosphole (case of **1c**), and 0.5 equiv. of the respective primary amine R^1NH_2 in the presence of Et_3N in 67 to 73% yield as outlined in scheme 1.

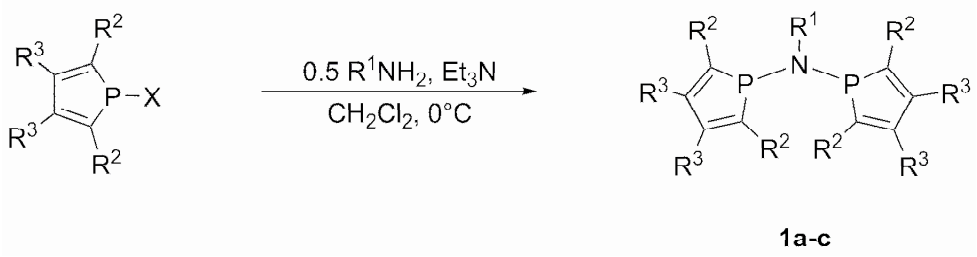

Scheme 1. Synthesis of bis(phosphole)amines **1a**-**c**. X = Cl, Br.

Phosphole ligands have rarely been employed in ethylene oligomerization reactions,[6] and to the best of our knowledge, no catalytic systems with chromium and phosphole ligands are known in the literature.

The prepared ligands **1a**-**c** were evaluated by preparing a catalytic mixture of the ligand and $[CrCl_3(THF)_3]$ in toluene (ligand/Cr ratio = 1.7), followed by activation with 300 equiv. of MAO. The catalytic tests, whose results have been summarized in table 1, were carried out at 35 bar of ethylene pressure and at a temperature of 45°C.

Table 1. Oligomerization results with $[CrCl_3(THF)_3]$ and ligand **1a**-**c**.

Entry	Ligand	%C_4 (%1-C_4)	%C_6 (%1-C_6)	%C_8 (%1-C_8)	%C_{10+}	%Polymer	Productivity/ $g \times g(Cr)^{-1} \times h^{-1}$
1	**1a**	3(75)	4(72)	2(83)	6	85	17300
2	**1b**	1(72)	5(83)	2(91)	4	88	16450
3	**1c**	traces	3(86)	1(78)	3	93	22180
4	**-**	2(33)	15(82)	7(81)	32	44	1523

Conditions: [Cr] = 8 µmol, 45°C, ligand/metal ratio = 1.7/1, 300 equiv. of MAO, 35 bar of ethylene pressure, solvent toluene, 1 h.

All three bis(phosphole)amine ligands **1a**-**c** did not promote the selectivity towards a particular oligomer. Instead, a distribution of oligomer products was observed in each catalytic experiment, while the overall productivity in the liquid fraction was comparatively low. Significant quantities of polymeric material were produced, which accounted for up to 93% of the total productivity. The catalyst prepared in-situ from **1c** exhibited the greatest activity towards polymerization, which may be a result of the great steric bulk provided by the two $SiMe_3$ groups in 2- and 5- positions of the ligand's phosphole heterocycles, which most effectively suppress the possibility of a metallacyclic mechanism on the chromium metal center, and instead direct towards a Cossee-Arlman type insertion mechanism, leading to polymerization.

A bis(phosphino)amine ligand **2** with strong acceptor properties and minimal steric bulk in the vicinity of the metal center was thus conceived.

2.2 Bis(dialkynylphosphino)amine Ligand

Ligand **2** was prepared in a four-step synthesis using conventional synthetic procedures as outlined in scheme 2. Reaction of $(i\text{-Pr})_2NH$ and PCl_3 in the presence of Et_3N yielded $(i\text{-Pr})_2NPCl_2$, which is a suitable precursor for the generation of chlorophosphines R_2PCl (R = hydrocarbyl substituent). Addition of $i\text{-Pr}_2NPCl_2$ to two equivalents of lithio-phenylacetylene at -78°C yielded the phosphinoamine compound **3**, whose complete formation was indicated by a single peak in the $^{31}P\{^1H\}$ NMR spectrum at -16.1 ppm. **3** was not isolated, but treated with a concentrated solution of HCl in diethyl ether to obtain the desired chloro-dialkynylphosphine **4** in 78% yield ($\delta(^{31}P\{^1H\}$ = -19.4 ppm). In an analogous fashion as described for the bis(phosphole)amines **1a**-**c**, compound **2** was obtained upon reaction of **4** with 0.5 equiv. of $i\text{-PrNH}_2$ in the presence of Et_3N in 62% yield as a white-yellow powder.

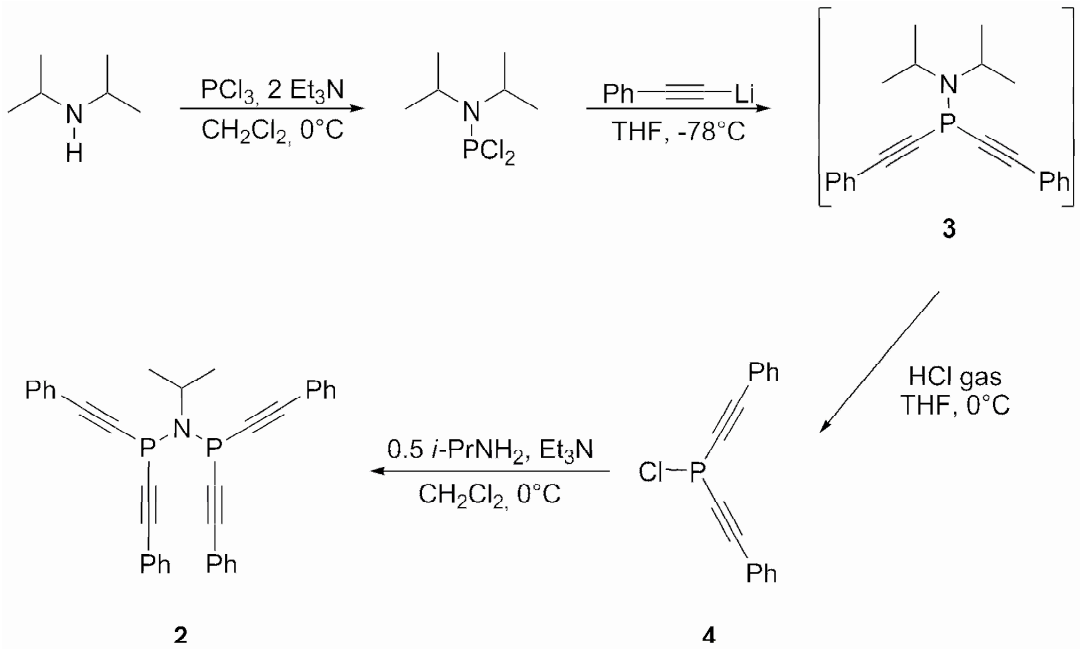

Scheme 2. Preparation of bis(dialkynylphosphino)amine **2**.

As described for the bis(phosphole)amine ligands **1a**-**c**, ligand **2** was tested in an in-situ fashion with a ligand/Cr ratio of 1.7, at 45°C and at 35 bars of ethylene pressure, using 300 equiv. of MAO. $[Cr(acac)_3]$ was used as metallic precursor. The catalytic results are presented in table 2. The second entry in table 2 presents the results obtained with a catalytic mixture of the "Sasol" ligand $(Ph_2P)_2N(i\text{-}Pr)$ and $[Cr(acac)_3]$ tested under the same conditions.

Interestingly, both the C_6 and C_8 selectivities as well as the overall activity of both catalytic mixtures are indeed very similar. However, with respect to the α-selectivity, the catalytic mixture containing **2** exhibited considerably lower performance than the $(PPh_2)_2N(i\text{-}Pr)$ analogue (e.g. 77 versus 99% in 1-octene). While further experiments at different catalytic conditions (temperature, ethylene pressure, MAO quantity) would have been necessary, it emerges from this single test, that acceptor-substituted bis(phosphino)amines with moderate to low steric bulk are the ligands of choice for an oligomerization reaction with a selectivity shift towards tetramerization. On the other hand, excessive steric bulk such as found on the tested bis(phosphole)amines **1a**-**c** seems to favor mechanistic pathways leading to mainly polymers alongside with unselective oligomerization.

Table 2. Oligomerization with $[Cr(acac)_3]$ and ligand **2**.

Entry	Ligand	$\%C_4$ ($\%1\text{-}C_4$)	$\%C_6$ ($\%1\text{-}C_6$)	$\%C_8$ ($\%1\text{-}C_8$)	$\%C_{10+}$	%Polymer	Productivity/ $g \times g(Cr)^{-1} \times h^{-1}$
1	**2**	1(62)	32(33)	52(77)	5	10	17400
2	$(PPh_2)_2N(i\text{-Pr})$	1(66)	30(39)	54(99)	5	10	19000
3	-	4(33)	17(82)	9(81)	37	33	2600

Conditions: [Cr] = 8 µmol, 45°C, ligand/metal ratio = 1.7/1, 300 equiv. of MAO, 35 bar of ethylene pressure, solvent toluene, 1h.

2.3. A PCP Ligand

As described in the introductory chapter (section 3.6.4.3.2.1.2), some insight has been gained on the relationship between the structure of the PNP ligand and the observed selectivity of the catalytic system in which it is employed. Given the η^2-P,P diphosphine coordination of the bis(phosphine)amines, we found it surprising that the ubiquitous bis(diphenylphosphino)methane, in which the amine bridge is replaced by a C_1 spacer, gives very poor catalysis results (unselective Schulz-Flory distribution),[7, 8] inspite of similar bite angle, donor strength,[9] and steric constraint.

One assumed important difference between $(Ph_2P)_2CH_2$ and the PNP ligand is the relatively greater rigidity of the latter, which hinders free rotation around the P-N bond, whereas rotation around the P-C bond in $(Ph_2P)_2CH_2$ has a relatively low barrier. In order to quantify this effect, the rotation barrier of the two stripped parent molecules $(H_2P)_2CH_2$ (**I**) and $(H_2P)_2NH$ (**II**) was evaluated by means of density functional theory using the B3LYP functional and the 6-31G* basis set. Scheme 3 summarizes the obtained result, confirming the greater hindrance of rotation around the P-N bond.

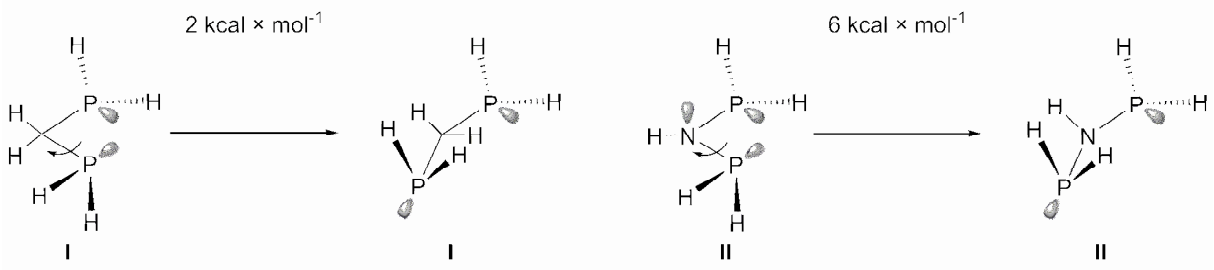

Scheme 3. Rotation barrier around the P-C bond (in **I**, left) and around the P-N bond (in **II**, right). Free energies ΔG are reported.

In order to imitate the backbone rigidity of the PNP ligand, the diphosphine ligand $(Ph_2P)_2CCPh_2$ (**5**) with a planar sp^2 central carbon bridge was synthesized in high yield (95%) (Scheme 4) by desulfurization of the 1,1-bis(disulfinophosphine)alkene **6**,[10] which was prepared following a method devised by Cantat *et al.* from our work group.[11]

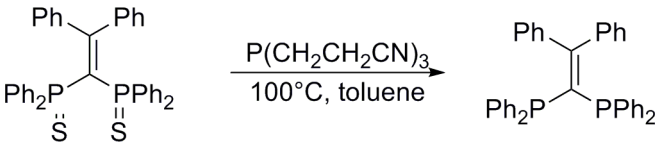

6 **5**

Scheme 4. Synthesis of the diphosphine **5**.

An x-ray crystal structure of **5** revealed a PCP angle of 112.72(6)°, which is comparable to the PNP angle of 114.6(1)° found in $(Ph_2P)_2N(Me)$.[12]

Upon evaluation of ligand **5** in the ethylene oligomerization reaction, the catalytic system prepared either from $[CrCl_3(THF)_3]$ or $[Cr(acac)_3]$ (metal/ligand ratio = 1.7/1) only exhibited deceivingly low productivities and no selectivity towards a particular oligomer could be observed (Table 3). Instead, a major part of the productivity accounted for polymeric material. The slightly higher productivity obtained when using $[Cr(acac)_3]$ as metal precursor is probably due to the higher solubility of this precursor in toluene.

Table 3. Catalytic results with diphosphine ligand **5**.

Entry	Precursor	%C_4 (%1-C_4)	%C_6 (%1-C_6)	%C_8 (%1-C_8)	%C_{10+}	%Polymer	Productivity/ g × g(Cr)$^{-1}$ × h^{-1}
1	$[CrCl_3(THF)_3]$	6(66)	13(33)	20(51)	1	60	192
2	$[Cr(acac)_3]$	2(66)	12(39)	20(89)	15	51	333

Conditions: [Cr] = 8µmol, 45°C, ligand/metal ratio = 1.7/1, 300 equiv. of MAO, 35 bar of ethylene pressure, solvent toluene, 1h.

This result is in line with the findings of Overett *et al.*,[8] who reported very low productivity and an unselective distribution of oligomers with a Cr(III) complex formed from the diphosphine ligand $H_2CC(PPh_2)_2$, which is very similar to our ligand **1**.

3. Bidentate Ligands with Sulfur Donors

3.1 Dithioacetals

Chromium-based catalytic systems comprising tridentate bis(sulphanylethyl)amine ligands (see section 3.63.2 of the introductory chapter) are highly effective in selective ethylene trimerization to 1-hexene with selectivities in excess of 98%. These ligands feature a meridional coordination around the chromium metal center (S-Cr-S approx. 180°), occupying thus one hemisphere around the chromium center, which is a possible reason for their selectivity towards the trimerization product and the impossibility of further metallacycle growth towards chromacyclononane.

The activity achieved with bis(sulphanylethyl)amines triggered our interest towards bidentate dithioethers, which would feature a more acute chelate angle with the chromium metal similar to the one observed with the bis(diphosphino)amines (66-68° on Cr(III)[1, 13]).

We therefore turned out interest towards two dithioacetals **7a**,**b**, which were prepared by reaction of 2 equiv. of either *n*-butylthiol or thiophenol on acetone in the presence of catalytic quantities of BF_3·THF, as outlined in scheme 5.[14, 15]

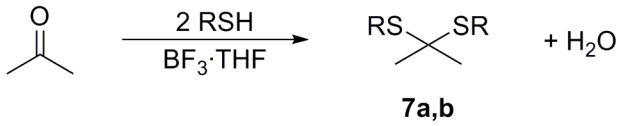

Scheme 5. Synthesis of dithioacetals **7a**,**b**. **a**: R = *n*-Bu, **b**: R = Ph.

Both compounds **7a** and **7b** were obtained in 89 and 95% yield, respectively. In a first step, coordination to $[CrCl_3(THF)_3]$ (scheme 6) was tried, but proved unsuccessful, even at higher reaction temperatures of up to 90°C.

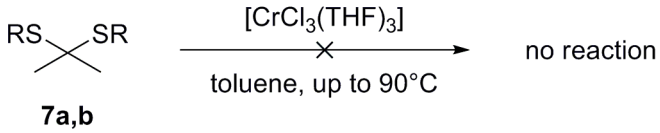

Scheme 6. Coordination attempts with dithioacetals **7a**,**b**.

Therefore, in a second step, thioacetals **7a**,**b** were employed in the formulation of a in-situ activated catalytic mixture in the same fashion as described for the catalytic tests with ligand **5** (see above), employing $[Cr(acac)_3]$ as chromium source (ligand/metal ratio = 1.7), 300 equiv. of MAO, toluene as solvent and ethylene at 35 bar pressure (run time = 1 h). Unfortunately, the resulting catalytic mixtures produced only trace amounts of oligomers as indicated by GC analysis alongside with a polymer production of 455 g × g(Cr)$^{-1}$ × h^{-1} (catalytic system employing **7a**) and 420 g × g(Cr)$^{-1}$ × h^{-1} (catalytic system employing **7b**). This is lower than the activity observed with $[Cr(acac)]_3$ alone (see Table 2).

This result is indicative of an inhibitor effect of the dithioacetal ligands on the catalytic activity of the Cr metal center, and the modest polymer production is probably due to naked metal centers activated by MAO, which are either poisoned by the ligand or its degradation products, or are quickly deactivated to form stable Cr(I)-bisarene complexes, as indicated by the yellowish color of the organic phase at the end of the catalytic run. Probably, dithioacetals are not sufficiently strong ligands to stabilize chromium in its active state for oligomerization.

3.2 Thiocarboxylates

Due to the apparently low affinity between Cr(III) and the dithioacetals **7a**,**b**, we turned our interest towards anionic dithiocarboxylates, since their coordination geometry, notably an expected small S-

Cr-S angle similar to the P-Cr-P angle and thus a suitable geometry for metallacycle growth seemed to be achievable with these compounds. While, to the best of our knowledge, no structurally characterized Cr-thiocarboxylate complex has been reported so far; the average of the three S-Cr-S angles in the homoleptic $[(C_6H_5)_4P]^+_3[Cr(S_2CO)_3]^{3-}$ complex is 73.3(1)°[16] and thus approx. 6° greater than the values found with bis(phosphino)amine ligands. The lithio-thiocarboxylate **8** was prepared via a well established synthetic route from CS_2 and MeLi in THF. Subsequent addition of a THF solution of the thiocarboxylate (1 equiv.) on a THF solution of $[CrCl_3(THF)_3]$ (1 equiv.) at ambient temperature resulted in the immediate precipitation of a brown solid **9** from the reaction mixture, which, due to its insolubility in all common organic solvents, was inaccessible for further analysis.

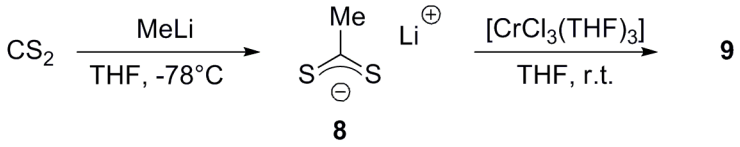

Scheme 7. Synthesis of compound **9**.

Despite this lack of structural information, the solid **9** was submitted to an ethylene oligomerization test (300 equiv. of MAO, 35 bar ethylene pressure, 45°C, toluene solvent). Strictly no activity towards either polymerization or oligomerization was found in this catalytic run, even though dissolution of complex **9** in toluene was observed upon addition of MAO. This rather disappointing result led us to abandon this class of ligands.

4. A Manganese-PNP Complex and its Evaluation in Ethylene Oligomerization

The method of introducing bis(phosphino)amine ligands on Cr(0)-hexacarbonyl complexes by carbonyl/phosphine exchange, as described in section 3.6.4.3.2.1.2 of the introductory chapter prompted us to use this strategy on $[MnBr(CO)_5]$, since oligomerization of ethylene with manganese-based catalysts has never been reported before. Heating of an equimolar mixture of $[MnBr(CO)_5]$ and $(Ph_2P)_2N(Ph)$ in toluene at 110°C over 16 h yielded complex **10** in 71% yield as a yellow powder (scheme 8).

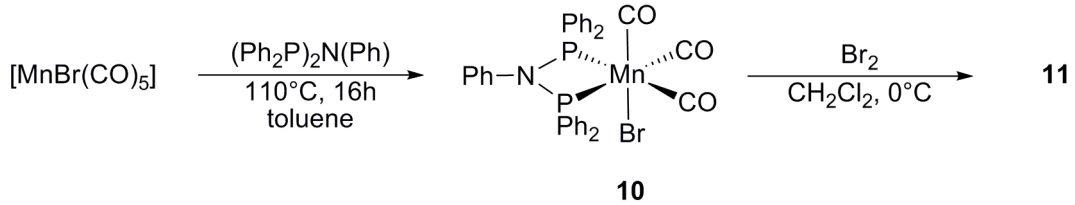

Scheme 8. Synthesis of complex **10** and its oxidation with Br_2.

Crystals suitable for x-ray crystal structure analysis could be grown from a concentrated CH_2Cl_2 solution of **10**. Figure 2 displays an Ortep plot of the molecular structure of **10** alongside with selected bond lengths and distances.

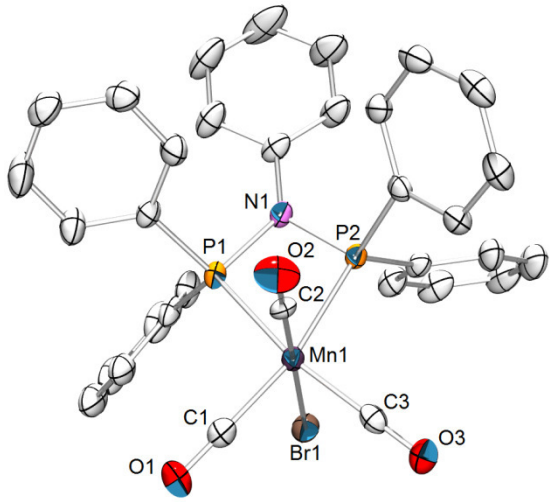

Figure 2. Ortep representation of the x-ray crystal structure of **10**. A positional disorder of the axial Br and CO ligand was found in the single crystal, and only one isomer is displayed here; hydrogen atoms have been omitted for clarity. Thermal ellipsoids are represented at the 50% level. Important bond lengths (Å) and angles (°): Mn1-Br1 = 2.5233(5), Mn1-P1 = 2.2990(8), Mn1-P2 = 2.3130(8), Mn1-C1 = 1.841(3), Mn1-C2 = 1.838(2), Mn1-C3 = 1.840(3), C1-O1 = 1.120(3), C2-O2 = 1.108(2), C3-O3 = 1.100(4), P1-Mn1-P2 = 70.15(3), Mn1-P1-N1 = 94.43(8), P1-N1-P2 = 101.4(1), N1-P2-Mn1 = 93.82(8), Br1-Mn1-C1 = 81.95(8), Br1-Mn1-C2 = 168.6(1), Br1-Mn1-C3 = 85.6(1), P1-Mn1-C1 = 95.6(1), P2-Mn1-C3 = 98.8(1).

The x-ray crystal structure reveals a coordination mode identical to the one observed with the analogous Cr-PNP-$(CO)_4$ complexes. As with these complexes, no activity in ethylene oligomerization or polymerization was observed upon activation with 300 equiv. of MAO. Consequently, and in analogy to what has been reported with said Cr-PNP-$(CO)_4$ complexes, **10** was oxidized with Br_2 in CH_2Cl_2 to yield **11** (Scheme 8). Compound **11**, a highly air- and moisture-sensitive yellow powder was found to have lost all its CO ligands as indicated by IR spectroscopy, however, no ^{31}P-NMR of the reaction mixture could be recorded, which is indicative of coordination to a paramagnetic metal center, speculatively Mn(IV). Equally, ^{1}H and ^{13}C NMR spectra of **11** yielded only broad unexploitable signals.

Unfortunately, no activity in ethylene oligomerization and/or polymerization could be observed with **11** in the presence of MAO.

5. Conclusion and Perspectives

In the present chapter, a number of strategies towards new ligands for the chromium-catalyzed selective oligomerization of ethylene have been described. It could be shown that bulky bis(phosphole)amine ligands direct the selectivity towards polymerization rather than oligomerization. On the other hand, the propinyl-substituted PNP ligand **2** was, when employed in an in-situ fashion, comparable in terms of its overall productivity, however, its α-selectivity both in the C_6 and the C_8 fraction was significantly lower than the selectivity obtained with the Ph-substituted analogue. Ligand **5** was prepared to evaluate the effect of the "backbone rigidity" found in the PNP ligand, as evidences by the relatively high rotation barrier around the P-N bond. Unfortunately, ligand **5**, featuring a rigid central sp^2 carbon atom, led to unselective oligomerization only, for a reason yet to be determined. The result obtained was later confirmed in a literature report.[8]

Both neutral and anionic bidentate sulfur-based ligands with putatively small bite angles were equally prepared and evaluated, however, without much success in terms of ethylene oligomerization activity.

A last attempt was directed towards the preparation towards a Mn-PNP complex and its catalytic evaluation. While the synthesis starting from $[MnBr(CO)_5]$ proved successful, the resulting complex **10**, as well as its bromine-oxidized analogue **11**, which could not be properly characterized, were found to be inactive in ethylene oligomerization/polymerization. A closer look should be taken towards complex **10**, taking into account recent results from the literature. It has been shown that the activation of $Cr(CO)_4$-PNP complexes requires the use of Et_3Al as effective CO scavenger combined with a weakly coordinated anion to stabilize the active cationic metal center (see section 2.3 of chapter 1).[17, 18] Applying this strategy, the combined use of Et_3Al as CO scavenger and alkylating agent, as well as $[(Ph_3C)(Al(OC(CF_3)_3)_4)]$ as alkyl abstractor and weakly coordinating anion to generate a cationic manganese metal center from complex **10** should be tried.

The application of a special class of bidentate N,N ligands in chromium-catalyzed oligomerization is presented in the next chapter.

6. Bibliography

[1] A. Bollmann, K. Blann, J. T. Dixon, F. M. Hess, E. Killian, H. Maumela, D. S. McGuinness, D. H. Morgan, A. Neveling, S. Otto, M. Overett, A. M. Z. Slawin, P. Wasserscheid, S. Kuhlmann, *J. Am. Chem. Soc.* **2004**, *126*, 14712.

[2] D. S. McGuinness, M. Overett, R. P. Tooze, K. Blann, J. T. Dixon, A. M. Z. Slawin, *Organometallics* **2007**, *26*, 1108.

[3] S. J. Dossett, D. F. Wass, M. D. Jones, A. Gillon, A. G. Orpen, J. S. Fleming, P. G. Pringle, *Chem. Commun.* **2001**, 699.

[4] M. S. Balakrishna, T. K. Prakasha, S. S. Krishnamurthy, U. Siriwardane, N. S. Hosmane, *J. Organomet. Chem.* **1990**, *390*, 203.

[5] N. A. Cooley, S. M. Green, D. F. Wass, K. Heslop, A. G. Orpen, P. G. Pringle, *Organometallics* **2001**, *20*, 4769.

[6] G. Mora, S. van Zutphen, C. Klemps, L. Ricard, Y. Jean, P. Le Floch, *Inorg. Chem.* **2007**, *46*, 10365.

[7] K. Blann, A. Bollmann, J. T. Dixon, A. Neveling, D. H. Morgan, H. Maumela, E. Killian, F. M. Hess, S. Otto, L. Pepler, H. Mahomed, M. J. Overett, WO2004/056479 (to Sasol Technology Pty. Ltd.), **2003**.

[8] M. J. Overett, K. Blann, A. Bollmann, R. de Villiers, J. T. Dixon, E. Killian, M. C. Maumela, H. Maumela, D. S. McGuinness, D. H. Morgan, A. Rucklidge, A. M. Z. Slawin, *Journal of Molecular Catalysis A: Chemical* **2008**, *283*, 114.

[9] J. N. L. Dennett, A. L. Gillon, K. Heslop, D. J. Hyett, J. S. Fleming, C. E. Lloyd-Jones, A. G. Orpen, P. G. Pringle, D. F. Wass, J. N. Scutt, R. H. Weatherhead, *Organometallics* **2004**, *23*, 6077.

[10] T. Cantat, *Ph. D. Thesis*, Ecole Polytechnique, Palaiseau, France, **2007**.

[11] T. Cantat, F. Biaso, A. Momin, L. Ricard, M. Geoffroy, N. Mezailles, P. L. Floch, *Chem. Commun.* **2008**, 874.

[12] A. F. Cotton, F. E. Kühn, A. Yokochi, *Inorg. Chim. Acta* **1996**, *252*, 251.

[13] T. Agapie, M. W. Day, L. M. Henling, J. A. Labinger, J. E. Bercaw, *Organometallics* **2006**, *25*, 2733.

[14] T. C. Whitner, E. E. Reid, *J. Am. Chem. Soc.* **1921**, *43*, 638.

[15] A. Schönberg, K. Praefcke, *Chem. Ber.* **1967**, *100*, 778.

[16] S. C. O'Neal, J. W. Kolis, *Inorg. Chem.* **1989**, *28*, 2780.

[17] L. E. Bowen, M. F. Haddow, A. G. Orpen, D. F. Wass, *Dalton Trans.* **2007**, 1160.

[18] A. J. Rucklidge, D. S. McGuinness, R. P. Tooze, A. M. Z. Slawin, J. D. A. Pelletier, M. J. Hanton, P. B. Webb, *Organometallics* **2007**, *26*, 2782.

Chapter 3. (Bisiminophosphoranyl)-methanide Ligands in the Ethylene Oligomerization and Polymerization Reaction

Chapter 3. (Bisiminophosphoranyl)-methanide Ligands in the Ethylene Oligomerization and Polymerization Reaction

1. Introduction

Polydentate nitrogen N,N ligands have attracted increased interest during the last few years as suitable alternatives to the dominant and ubiquitous metallocene-based catalyst precursors, which have found widespread application as single-site catalyst notably in olefin polymerization.[1] In this context, notably bis-imine type ligands and complexes of these ligands with late transition metals Fe, Co, and Ni have been found to exhibit exceptional activities in ethylene polymerization catalysis. Following the initial discovery by Brookhart, Gibson, and other researchers at DuPont, the tridentate bis(imino)pyridines **A** have received most extensive attention due to the exceptional activities in ethylene polymerization of the five-coordinate iron (II) complexes **B**[2, 3] (activities up to 2.1×10^7 g(PE) × mol(Fe)$^{-1}$ × bar^{-1} × h^{-1}) (with R^1 = Me, R^2 = R^3 = 2,6-*i*-Pr-C_6H_3) upon activation with excess quantities of MAO (Figure 1). It should be noted that, if the substituents R^2 and R^3 are either small, or $R^2 \neq R^3$, thus yielding unsymmetrical ligands, complex **C** is an excellent catalyst for ethylene oligomerization, again upon activation with excess quantities of MAO.[4] The isostructural Co(II) complexes were found to be an active polymerization and/or oligomerization catalysts upon activation with MAO, albeit with activities roughly one magnitude lower than their Fe(II) counterparts.[5] Influences of the ligand's sterics on the selectivity of the catalytic system towards either polymerization or oligomerization generally follow the same tendency both on Fe(II) and Co(II) bis(imino)pyridine complexes.[6] This same dependence of the oligomerization/polymerization behavior on the substitution pattern of the aryl group has also been observed with the equally highly active chromium (III) complexes **C**.[7, 8] Polymerization activities of up to 4.14×10^7 g(PE) × mol(Cr)$^{-1}$ × bar^{-1} × h^{-1} were reported (with R^1 = Me, R^2 = R^3 = 2,4,6-Me-C_6H_2). Smaller R^2 and R^3 substituents lead to higher activities upon MAO activation, but yield polyethylene with low molecular weight.

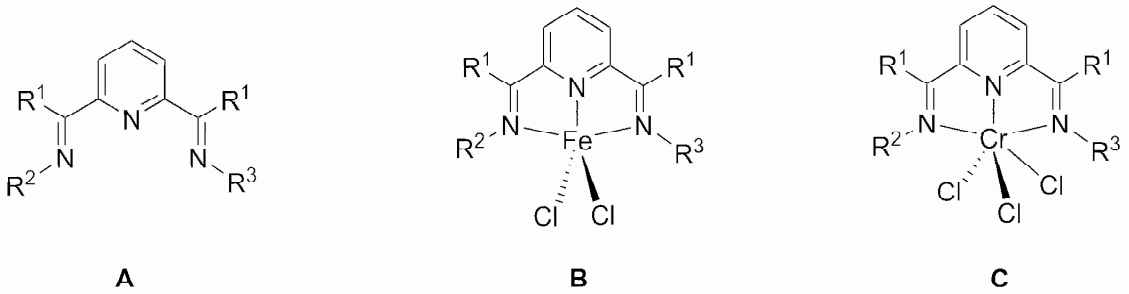

Figure 1. Bis(imino)pyridine ligands and complexes.

Pd(II) and Ni(II) complexes bearing diazabutadiene ligands **D** for the polymerization of ethylene, α-olefins, and cyclic olefins have been devised by Brookhart and coworkers. Their discovery was a starting point for extensive follow-up developments by numerous research groups. Amongst these, one has to cite the commercialization of the Ni-diazabutadiene catalyst system under the Versipol® trademark by DuPont.[9]

Activities in ethylene polymerization of up to 1.1×10^7 g(PE) × mol(Ni)$^{-1}$ × bar^{-1} × h^{-1} are obtained with square-planar Ni(II) complexe **E1** (with R, R' = Me, Ar = 2,6-*i*-Pr-C_6H_3),[5, 10] when activated with MAO (Figure 2). Alternatively, dimethyl-Ni complexes **E2** may be activated with alkyl abstracting agents such as $[(H(OEt_2)_2)B(C_6H_3(CF_3)_2)_4]$ to yield highly electrophilic cationic Ni(II) complexes, which are the active species in the catalytic cycle.

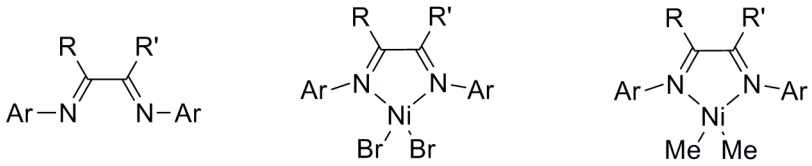

D **E1** **E2**

Figure 2. Diazabutadiene ligand and complexes.

The application of diazabutadiene ligands in the chromium catalyzed trimerization has been disclosed by Sumitomo Chemical Corp.[11] Their best result was obtained using the symmetric sterically bulky diazabutadiene $(CH{=}NC(CH_3)_2CH_2C(CH_3)_3)_2$ and Cr(III)-2-ethylheptanoate as metal precursor, the catalytic species being formed *in situ*. Activities of up to 22995 g × g(Cr)$^{-1}$ × h^{-1} and an overall 1-hexene content of 58.3% were reported upon activation with triethylaluminium and conducting the catalytic run at 120°C and 40 bars.

Chromium complexes with anionic β-diketiminate ligands have equally been evaluated in ethylene polymerization reactions. Both the Gibson[12] and Theopold's[13] workgroups reported on the binuclear complexes Cr(III) **F**, (Figure 3) which were found to yield high molecular weight polyethylene. The monomeric complexes **G1**[12, 14] and **G2**[15] were found to be considerably more active when activated with Et_2AlCl rather than MAO.

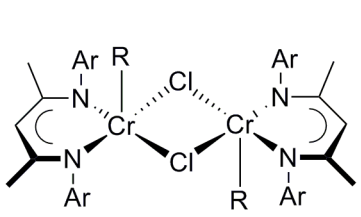

F

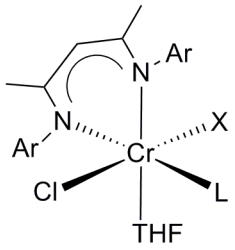

G

Figure 3. Cr(III)-β-ketiminate complexes. **F**: R = Me, Ar = Ph, 2,6-*i*-Pr-C_6H_3, **G1**: Ar = 2,6-*i*-Pr-C_6H_3, X∩L = PhCOO, **G2**: Ar = Ph, X = Cl, L = THF.

Compared to this, the phosphorous analogues of bis-imines, the bis(imino)phosphoranes have received less attention, even though the combination of a similar steric environment and profoundly different electronic properties such as a great σ donor strength and a high π acceptor capacity makes them an interesting target for evaluation as ligands, particularly for olefin oligomerization and polymerization catalysts. Kreischer *et al.*[16] as well as Bochmann and colleagues[17] have reported on ethylene polymerization employing bis(iminophosphorane)pyridine analogues of complex **B** which were found to feature only moderate polymerization activities.

The symmetric bis(iminophosphoranyl)methanes $CH_2(P(R^2)_2{=}NR^1)_2$ **H** have been subject to extensive research over the last years with respect to their coordination properties towards main group and transition metals, but naturally also the catalytic properties of the resulting complexes in a variety of catalytic transformations. (See also the following chapter 4 for some examples) **H** may be derivatized either by single or double abstraction of the central methylene protons with a sufficiently strong base, to obtain the monoanionic species **I** or the dianionic species **J**, respectively (Scheme 1).[18]

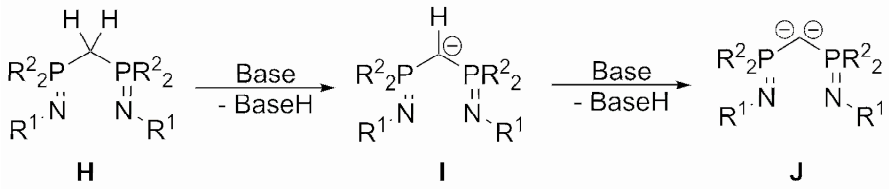

H **I** **J**

Scheme 1. Deprotonation of bis(iminophosphorane)methanes **H** to their monoanionic (**I**) and dianionic (**J**) derivatives.

The monoanionic bis(iminophosphoranyl)methanides **I** have attracted our particular attention. Whereas formally and from a structural point of view, these anions may be regarded as analogues to the before mentioned β-diketiminates, however, as has been shown by Boubekeur through theoretical calculations, the strict comparison between β-diketiminates and bis(iminophosphoranyl)methanides is unjustified.[19] While the negative charge of the central carbon is delocalized over the entire π system of the planar β-diketiminate structure, the structure of the bis(iminophosphoranyl)methanides is best

described by localized negative charges on the nitrogen atoms and the central carbon moiety, and positive charges on the phosphorus sites.

Coordination complexes of the monoanions **I** with a wide range of alkaline metals, alkaline earth metals, transition metals, and lanthanides, have been synthesized.[20] With regard to the ethylene polymerization and oligomerization reaction, Al(III),[21] Cr(II),[22] have been evaluated. Aparna *et al.*[23] synthesized dialkyl aluminium bis(iminophosphoranyl)methanides, which were found to be moderately active (up to 68×10^3 g(PE) mol(Al)$^{-1}$ bar^{-1} h^{-1}) in the polymerization of ethylene upon activation with methyl abstracting trityl tetrafluoroborate. Interestingly, the analogous aluminium bis(iminophosphoranyl)methanediides presented much higher polymerization activities (up to 2×10^6 g(PE) × mol(Al)$^{-1}$ × bar^{-1} × h^{-1}).[21] Wei and Stephan[22] synthesized in 2002 the first chromium (II) bis(iminophosphoranyl)methanide complexes. The dimeric compound **K** was found to exist in two different isomers $\mathbf{K^a}$ and $\mathbf{K^b}$, which coexist in the single crystal structure, when crystallization is carried out from a benzene solution (Figure 4).

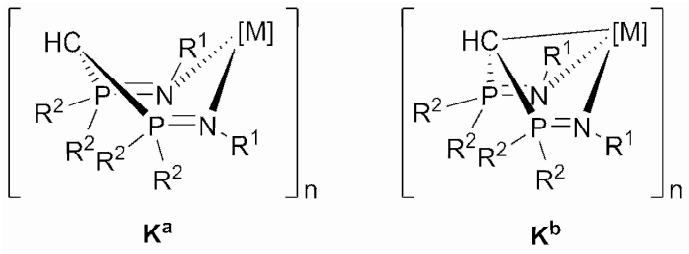

Figure 4. Coordination modes of monoanion **I**. $\mathbf{K^a}$, $\mathbf{K^b}$: [M] = Cr-μ_2-(Cl), R^1 = $SiMe_3$, R^2 = Ph, n = 2.

Upon crystallization from THF, only the isomer $\mathbf{K^b}$ is present in the crystal lattice. Wheras the coordination geometry around the chromium center is best described as pseudo-square planar for $\mathbf{K^a}$, a trigonal bipyramid is adopted by the isomer $\mathbf{K^b}$. These two types of coordination modes have equally been reported earlier by the Elsevier group upon their studies of the coordination of bis(iminophosphoranyl)methanides towards iridium,[24, 25] and were found to be dependent on both oxidation state and the steric bulk of the supplemental ligands coordinated to the central metal. **K** was evaluated for its activity in the ethylene polymerization reaction and was found to produce 59×10^3 g(PE) × mol(Cr)$^{-1}$ × bar^{-1} × h^{-1} upon activation with 500 equivalents of MAO. The presence of different isomers and possibly multi-site catalysis were evoked as possible reasons for the broad molecular weight distribution (polydispersity index = 47) observed in the obtained polymer.[22]

Gambarotta and colleagues[26] recently reported on a divergent catalytic behavior towards either ethylene oligomerization or polymerization of chromium pyrrolide complexes derived from the Phillips ethylene trimerization system. From this work, it emerged that the chromium oxidation state of the catalyst precursor would be decisive on the selectivity of the catalyst towards either polymerization or oligomerization via a metallacyclic mechanism. Cr(II) precursors were found to

give rise to polymerization reactions, whereas Cr(I) complexes, obtained through reduction with organoaluminium activators, yielded mainly trimerization products (hexenes), and Cr(III) led to unselective oligomerization.

Prompted by this, we decided to explore the coordination chemistry of bis(iminophosphoranyl)methanide anions towards Cr(III) and to evaluate the obtained complexes in the ethylene oligomerization/polymerization reaction after activation with MAO and other organoaluminium activators. A further incentive for the evaluation of these ligands in this reaction is the ease of access and the good availability of the starting materials to synthesize a broad range of derivatives, as is shown the next section.

2. Synthesis Starting from Bis(diphenylphophino)methane via Bromination

The Kirsanov method[27, 28] was the synthetic strategy of choice for the synthesis of the bis(iminophosphorane) ligands as it has the advantage of providing a wide range of possible substitutions on the nitrogen moiety. In the following chapter 4, the different strategies of iminophosphorane synthesis are discussed in detail, and the advantage of the Kirsanov method for the preparation of mixed (N,P), (N,O), and (N,S) ligands will be exposed, since the scope of these ligands, as will be shown, could be extended to nickel-catalyzed selective ethylene oligomerization.

Following a synthesis protocol previously devised by Demange *et al.*,[18] bis(aminophosphonium)methanes are prepared by the addition of bromine to a solution of 1,2-bis(diphenylphosphino)methane in dichloromethane at -78°C (Scheme 2).

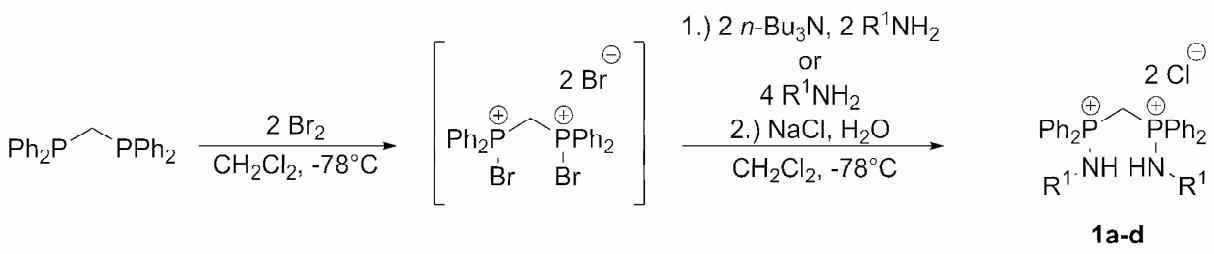

1a-d

Scheme 2. Synthesis of bis(aminophosphonium) chlorides **1a-d** by the Kirsanov method. **a**: R^1 = *i*-Pr, **b**: R^1 = *t*-Bu, **c**: R^1 = Ph, **d**: R^1 = *o*-MeO-C_6H_4.

The completeness of this reaction is checked by $^{31}P\{^1H\}$ NMR, where the peak of the intermediate product $[(Ph_2P)_2CH_2Br_2]^{2+}$ 2$[Br]^-$ appears at 48 ppm (s). Subsequent addition of either four equivalents (with respect to 1,2-bis(diphenylphosphino)methane) of a primary amine or of two equivalents of *n*-Bu_3N followed by two equivalents of a primary amine yields the desired bis(aminophosphonium) bromides, which, through aqueous workup with brine may be recovered as the corresponding dichloride salts **1** in yields of up to 72%. This is advantageous, when during subsequent coordination

steps to transition metal halide precursors, chloride-bromide exchange reactions would yield product mixtures.

3. Deprotonation and Coordination to $CrCl_3(THF)_3$[29]

The bis(aminophosphonium) salts **1** are conveniently deprotonated using three equivalents of a strong base such as MeLi, NaH, KH or KHMDS in a coordinating solvent such as THF, following the works of Babu *et al.*[30] The use of KH or KHMDS is particularly advantageous, as the two equivalents of potassium chloride formed during the reaction may easily be removed by simple filtration or centrifugation of the reaction mixture. Furthermore, *ortho*-lithiation reactions on the N-phenyl group, which were observed with the *ortho*-anisidine derivative **2d**, yielding complex product mixtures, as indicated by $^{31}P\{^1H\}$ NMR, can be avoided.

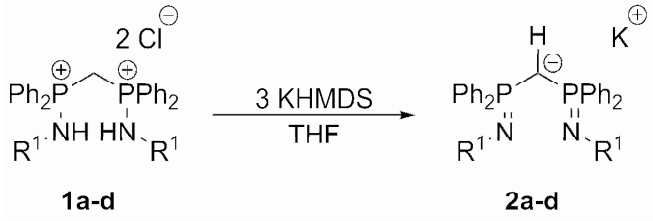

Scheme 3. Synthesis of potassium bis(iminophosphoranyl)methanides **2a**-**d**.

Completeness of the reaction is checked by $^{31}P\{^1H\}$ NMR; the displacements of both the parent bis(aminophosphonium) chlorides **1** and their monoanionic derivatives **2** are displayed for convenience in Table 1. Subsequently, the corresponding monoanions **2** are recovered as pale yellow powders after removal of KCl by filtration and evacuation of the THF solvent (Scheme 3).

Table 1: $^{31}P\{^1H\}$ chemical shifts of **1** and **2** (in ppm).

δ ($^{31}P\{^1H\}$)	**a**	**b**	**c**	**d**
1 (in CH_2Cl_2)	33.7	29.5	29.8	34.9
2 (in THF)	21.1	3.9	15.2	11.5

Addition of $CrCl_3(THF)_3$ to a THF solution of the monoanions **2a**-**d**, which may either be freshly prepared, or isolated beforehand, affords the blue (**3a**-**c**) and brown (**3d**) complexes, respectively. The potassium salts formed during the reaction have to be removed quickly by filtration or centrifugation, as the formed complexes **3a**-**d** are present in solution only at the beginning of the reaction, and precipitate subsequently from either THF or CH_2Cl_2 solution. This renders separation from the potassium salts difficult. Due to the strong paramagnetic nature of the octahedral d^3-Cr (III) center, no exploitable signals could be observed for any of these complexes in ^1H, ^{13}C, and ^{31}P NMR. However, the complete disappearance of the ligands signal can be used as an indicator of the completeness of the

reaction. Crystals of sufficient quality for x-ray structure analysis could be grown of **3a**-**d** either from concentrated CH_2Cl_2 or THF solutions (Figures 5 and 6).

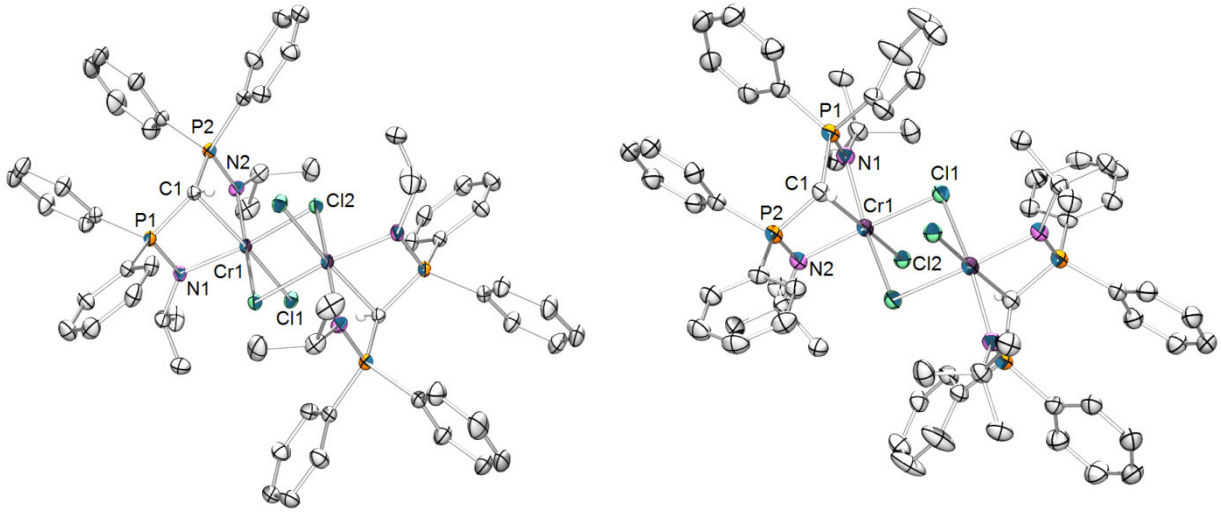

Figure 5. Ortep representation of the x-ray crystal structure of **3a** (left) and **3b** (right). Hydrogen atoms (except the one on C1) have been omitted for clarity. Thermal ellipsoids are represented at the 50% level. Important bond lengths (Å) and angles (°): **3a**: Cr1···Cr1' = 3.6306(5), Cr1-N1 = 2.039(1), Cr1-N2 = 2.040(1), Cr1-Cl1 = 2.3699(5), Cr1-Cl2 = 2.4120(4), Cr1-C1 = 2.231(1), N1-P1 = 1.602(1), P1-C1 = 1.755(1), C1-P2 = 1.755(1), P2-N2 = 1.601(1), N1-Cr1-N2 = 92.28(5), Cl1-Cr1-Cl2 = 92.40(1), N1-Cr1-C1 = 73.35(5), Cr1-N1-P1 = 98.06(6), N1-P1-C1 = 99.03(7), P1-C1-P2 = 118.5(1), C1-P2-N2 = 99.50(7); **3b**: Cr1···Cr1' = 3.7231(8), Cr1-N1 = 2.100(2), Cr1-N2 = 2.077(2), Cr1-Cl1 = 2.4212(8), Cr1-Cl2 = 2.397(1), Cr1-C1 = 2.192(3), N1-P1 = 1.604(2), P1-C1 = 1.751(3), C1-P2 = 1.765(2), P2-N2 = 1.604(2), N1-Cr1-N2 = 97.00(8), Cl1-Cr1-Cl2 = 92.20(3), N1-Cr1-C1 = 72.1(1), Cr1-N1-P1 = 95.7(1), N1-P1-C1 = 97.7(1), P1-C1-P2 = 122.8(1), C1-P2-N2 = 100.1(1).

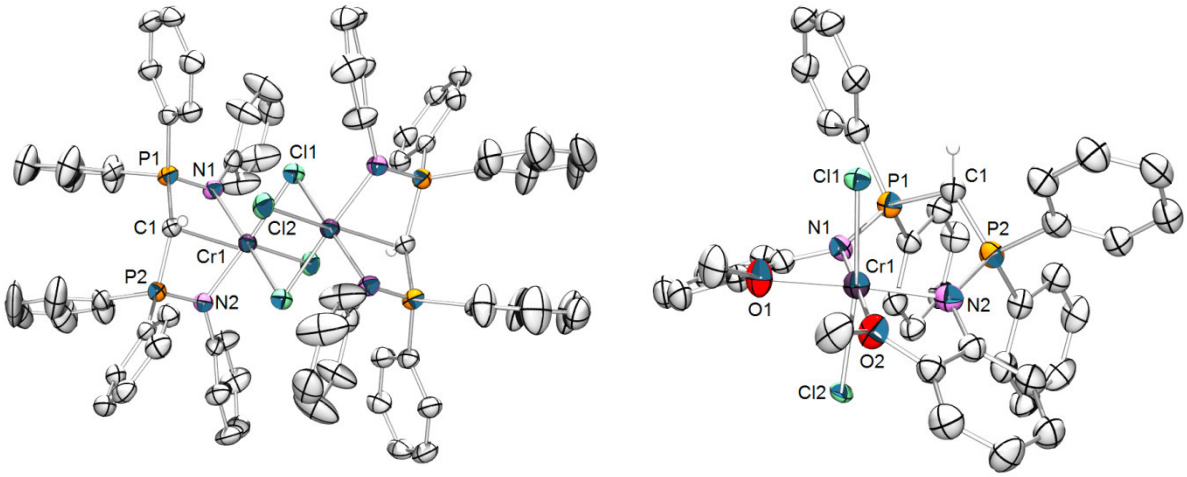

Figure 6. Ortep representation of the x-ray crystal structure of **3c** (left) and **3d** (right). Hydrogen atoms (except the one on C1) have been omitted for clarity. Thermal ellipsoids are represented at the 50% level. Important bond lengths (Å) and angles (°): **3c**: Cr1···Cr1' = 3.5020(5), Cr1-N1 = 2.031(3), Cr1-N2 = 2.035(3), Cr1-Cl1 = 2.388(1), Cr1-Cl2 = 2.335(1), Cr1-C1 = 2.258(4), N1-P1 = 1.616(3),

P1-C1 = 1.757(4), C1-P2 = 1.741(4), P2-N2 = 1.615(3), N1-Cr1-N2 = 96.4(1), Cl1-Cr1-Cl2 = 92.69(4), N1-Cr1-C1 = 73.7(1), P1-C1-P2 = 121.3(2), C1-P2-N2 = 98.8(1); **3d**: Cr1-N1 = 2.014(4), Cr1-N2 = 2.000(5), Cr1-O1 = 2.087(4), Cr1-O2 = 2.094(4), Cr1-Cl1 = 2.374(2), Cr1-Cl2 = 2.364(2), Cr1···C1 = 3.366(6), N1-P1 = 1.636(5), P1-C1 = 1.701(6), C1-P2 = 1.726(6), P2-N2 = 1.627(5), N1-Cr1-N2 = 101.5(2), O1-Cr1-O2 = 85.8(1), Cl1-Cr1-Cl2 = 168.56(6), Cr1-N1-P1 = 122.5(3), N1-P1-C1 = 112.2(3), P1-C1-P2 = 118.6(3), C1-P2-N2 = 111.9(3), P2-N2-Cr1 = 122.5(3).

3a-**c** present a dimeric structures similar to the one reported by Wei and Stephan[22] for the Cr(II) complex $[(HC(PPh_2NSiMe_3)_2Cr(\mu_2\text{-}Cl)]_2$. The anionic nature of the bis(iminophosphoranyl)methanide ligand was confirmed by the location and subsequent refinement of the single central proton in the x-ray structures. Structures **3a**-**c** show coordination of the central carbon atom to the chromium center with Cr1-C1 bond lengths of 2.231(1) Å (**3a**), 2.192(3) Å (**3b**), and 2.258(4) Å (**3c**), respectively. These lengths are intermediate between the short Cr1-C1 distance of 2.148(5) Å found in the $[C(PPh_2NSiMe_3)_2Cr]_2$ bridging carbene complex and the one 2.264(3) Å observed for $[(HC(PPh_2NSiMe_3)_2Cr(\mu_2\text{-}Cl)]_2$. The Cr···Cr separation measured at 3.6306(5) Å for **3a**, 3.7231(8) Å for **3b**, and 3.5020(5) Å for **3c** compares with what was found by Wei and Stephan for the Cr(II) dimeric isomers (3.504(1) Å for $\mathbf{K^b}$). The ligands adopts a slightly distorted octahedral geometry around each of the chromium central atoms as evidenced by a N1-Cr1-N1 angle of 92.88(5)° in **3a**, 97.00(8)° in **3b**, and 96.4(1)° in **3c**, respectively. As expected from their inherent similarity, all three structures present essentially identical structural features.

The potential pentadentate coordination of **2d**, owing to the presence of two methoxy groups, is confirmed in the x-ray crystal structure of **3d**. Complex **3d** is indeed a monomeric species in the solid state with a distorted octahedral geometry around the chromium center. The methoxy groups occupy two equatorial coordination sites with a very short average Cr1-O bond length of 2.091(4) Å, and complete thus the coordination sphere. The Cr-N distances are 2.014(4) Å and 2.000(5) Å long, respectively. Both nitrogen and oxygen atoms form an equatorial coordination plane with a mean deviation of only 0.41°. No Cr1···C1 bond was observed in the structure of **3d**. Moreover, the Cr1-N1-P1-C1-P2-N2 ring system exhibits a boat-like geometry which differs strongly from the structures recorded for **3a**-**c**, implying a delocalization of the negative charge over said ring system. Figure 7 displays a representation of the two geometries observed.

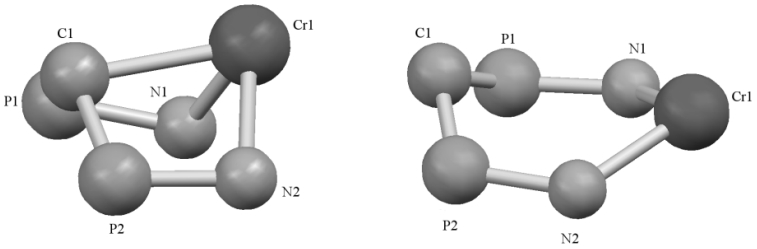

Figure 7. Diagram of the bis(iminophosphoranyl)methanide geometry on the Cr(III) center of **3b** (left) and **3d** (right).

This type of structural element was observed by Wei and Stephan for the isomer $\mathbf{K}^{a}$ in the solid state structure of $[(HC(PPh_2NSiMe_3)_2Cr(\mu_2\text{-}Cl)]_2$ upon recrystallization from benzene.[22] Nevertheless, there the Cr1···C1 distance of 2.921(3) Å is much shorter than that of 3.366(6) Å measured for **3d**.

4. Coordination to $[NiBr_2(DME)]$

Given the easy availability of the monoanionic ligand derivative, and the potential of Ni in ethylene oligomerization, coordination to $[NiBr_2(DME)]$ and catalytic evaluation of the formed complex was equally carried out. Addition of $[NiBr_2(DME)]$ to a THF solution of the bis(iminophosphoranyl)methanide anion **2b** resulted in an immediate color change of the reaction mixture to deep red (Scheme 4).

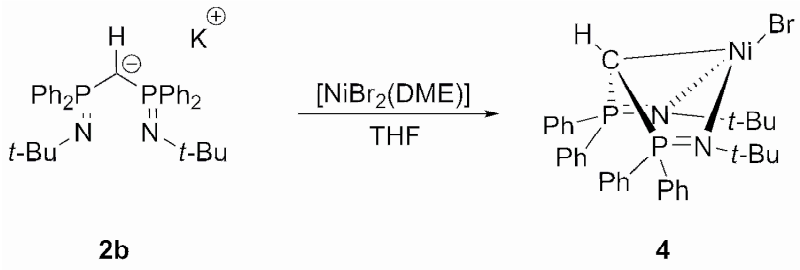

Scheme 4. Synthesis of Ni(II) complex **4**.

Extraction with toluene and cooling the saturated toluene solution yielded green/red single crystals, whose x-ray crystal structure analysis revealed the molecular structure displayed in figure 8.

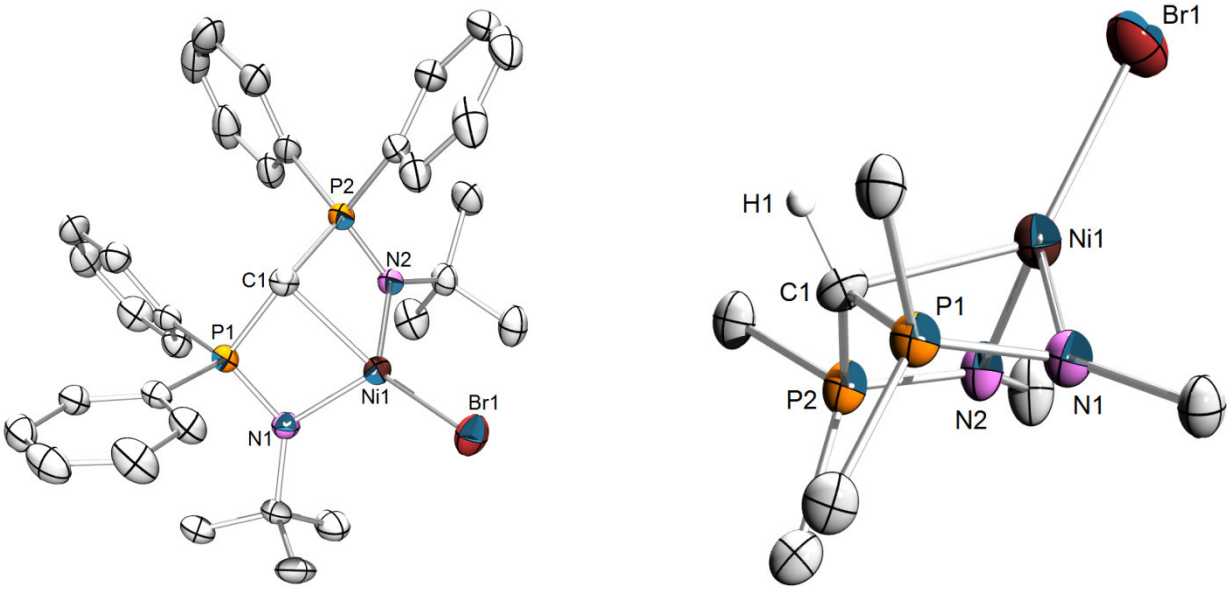

Figure 8. Two views of the x-ray crystal structure of **4**. Hydrogen atoms (except the one on C1) have been omitted for clarity. Thermal ellipsoids are represented at the 50% level. Important bond lengths (Å) and angles (°): Ni1-Br1 = 2.3297(4), Ni1-C1 = 2.175(2), Ni1-N1 = 2.005(2), N1-P1 = 1.598(2), P1-C1 = 1.743(3), C1-P2 = 1.752(2), P2-N2 = 1.594(2), N2-Ni1 = 1.979(2), N1-Ni1-Br1 = 127.47(6), N1-Ni1-C1 = 75.8(1), C1-Ni1-N2 = 77.70(8), N2-Ni1-Br1 = 123.32(6), N1-Ni1-N2 = 102.9(1), C1-Ni1-Br1 = 133.22(7), N1-P1-C1 = 100.6(1), P1-C1-P2 = 123.9(2), C1-P2-N2 = 102.5(1).

A side view of the core structure (figure 8, right) shows a tetrahedral coordination around the Ni(II) center comparable to the Cr(III) complexes **3a**-**c** and $\mathbf{K^b}$, which have been discussed in the previous section. This structural feature, which, due to the paramagnetic nature of tetrahedrally coordinated Ni(II), confirms the silence of complex **4** in ^{1}H, ^{13}C and ^{31}P{^{1}H} NMR spectroscopy, differs dramatically from the structure of the analogous complex [HC(P(Ph)$_2$=N(2,6-*i*-Pr-C$_6$H$_3$))$_2$NiBr] (**L**). This complex, reported in 2000 by Al-Benna *et al.*,[17] exhibits a strictly square-planar coordination sphere (angle sum = 360.8°), alongside with exploitable NMR signals, as expected for this coordination geometry. The Ni1-C1 bond length of 2.175(2) Å in **4** is significantly longer than the one observed in **L** (2.008(2) Å).

A preliminary test in ethylene oligomerization/polymerization, however, revealed the inactivity of complex **4**. No polymeric material and solely trace amounts of butenes were detected upon activation with 300 equiv. of MAO. This result agrees with the findings of Al-Benna *et al.*, who equally reported inactivity of complex **L** in ethylene polymerization upon activation with 200 equiv. of MAO.

5. Ethylene Oligomerization and Polymerization with Complexes 3a-d[29]

The catalytic activities of the complexes **3a**-**d** in ethylene oligomerization and polymerization were investigated and the results are compiled in Table 2. Experiments were carried out at both 45°C and 20°C in the presence of excess quantities of MAO. Alternatively, tests were carried out using either Et_3Al or Me_3Al combined with the alkyl abstracting perfluoroalkylaluminate $[Ph_3C][Al(OC(CF_3)_3)_4]$.[31] The ethylene pressure was maintained constant at either 30 or 55 bar throughout the catalytic run (0.5 or 2h). Activation with Et_2AlCl did not yield an active catalytic mixture (entry 6), whereas the use of 10 equiv. of $MeAl_3$ gave only a very modest productivity and mainly polymeric material (entry 7). Two important common features of all catalyst precursors **3a**-**d** were observed. First, the overall productivity increased, when the oligomerization reactions were carried out at lower temperatures. This effect is most pronounced for **3a**, for which the productivity increased from 19877 $g \times g(Cr)^{-1} \times h^{-1}$ at 45°C to 21354 $g \times g(Cr)^{-1} \times h^{-1}$ at 20°C (entries 1 and 8). A further improvement was achieved, when the catalytic reaction was carried out at 55 bar (entry 9). Secondly, all catalysts exhibit two distinct product distributions in the liquid phase with one maximum production of 1-hexene and a second tight distribution in the C_{14}-C_{24} range, alongside with a significant fraction of polymeric material, which account for 12-85% depending on the type of cocatalyst employed. Figure 9 shows a GC trace of the catalytic run 1 (**3a**). Most surprisingly, no C_{10} and C_{12} products were detected and the C_{14}-C_{24} fraction was found to contain α-olefins with odd carbon numbers. This unprecedented bimodal distribution might be due to the presence of two competing oligomerization mechanisms. The C_4-C_8 fraction would be the result of a metallacyclic mechanism, whereas the higher C_{14}-C_{24} fraction would be the result of a degenerative polymerization mechanism. However, the distribution follows neither a Poisson nor Schultz-Flory type distribution.

Table 2. Ethylene oligomerization/polymerization with complexes **3a**-**d**.

Entry	Precursor	T/°C	%C_4 (%1-C_4)	%C_6 (%1-C_6)	%C_8 (%1-C_8)	%C_{14}-C_{24}	%Polymer	Productivity/ $g \times g(Cr)^{-1} \times h^{-1}$
1	**3a**	20	3(95)	11(98)	5(99)	65	16	21354
2[a]	**3a**	20	3(95)	11(98)	7(95)	67	12	8267
3[b]	**3a**	45	1(99)	3(73)	2(95)	4	90	3227
4[c]	**3a**	45	4(93)	8(99)	10(99)	62	17	13289
5[d]	**3a**	45	2(96)	5(99)	6(99)	66	21	12648
6[e]	**3a**	45	traces	traces	traces	traces	-	-
7[f]	**3a**	45	2(99)	3(52)	3(92)	7	85	426
8	**3a**	45	2(91)	8(98)	3(99)	69	18	19877
9[g]	**3a**	20	2(90)	9(88)	3(90)	70	16	23552
10[h]	**3a**	20	2(93)	10(98)	5(99)	66	17	20741
11	**3b**	45	2(90)	5(97)	2(99)	69	19	18172
12	**3b**	20	2(90)	6(98)	3(99)	66	23	19305
13	**3c**	20	4(97)	9(99)	7(99)	68	12	18761
14	**3d**	45	6(95)	13(98)	3(99)	63	15	19708
15	**3d**	20	6(95)	14(98)	3(99)	61	16	20470

Conditions: [Cr] = 8 µmol, 30 bar ethylene pressure, 300 equiv. of MAO, solvent = toluene, run time 0.5 h. [a] run time 2 h, [b] activator Et_3Al (4 equiv.), [c] activator Me_3Al (50 equiv.) + $[Ph_3C][Al(OC(CF_3)_3)_4]$ (1 equiv.), [d] activator Et_3Al (50 equiv.) + $[Ph_3C][Al(OC(CF_3)_3)_4]$ (1 equiv.), [e] activator Et_2AlCl (10 equiv.), [f] activator $MeAl_3$ (10 equiv.), [g] $P(C_2H_4)$ = 55 bar, [h] 600 equiv. of MAO.

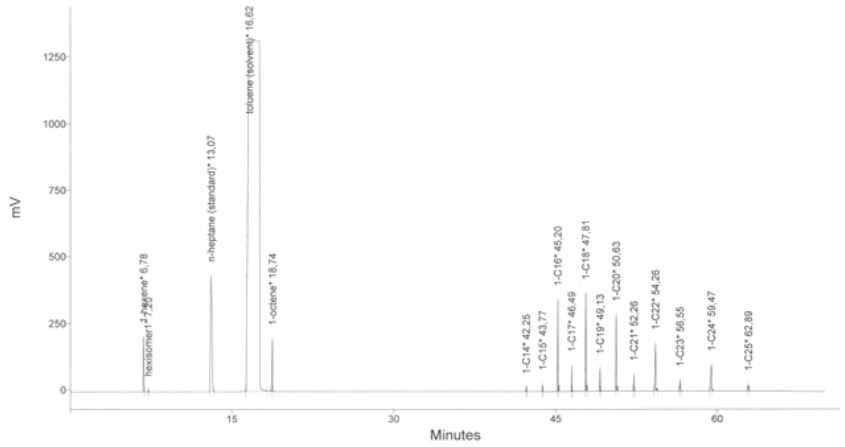

Figure 9. GC trace of catalytic run with complex **3a** (entry 1 of table 2) This analysis was made from an effluent recovered by flash vacuum distillation of the product mixture at the end of the catalytic

run. This resulted in the complete loss of the C_4 fraction and partial loss of the C_6 fraction, which thus cannot be quantified from this GC trace.

To understand the origin of the α-olefins with uneven carbon number, one may envisage two possible mechanistic alternatives. First, insertion of ethylene into a Cr^+-Me bond and further chain growth, followed by chain transfer from chromium to an Al-methyl species is possible. This has been described by Bazan *et al.*[32] upon activation of $[Cp^*Cr(Me)_2(PMe)_3]$ with either excess quantities of MAO or with mixtures of $B(C_6F_5)_3$ and excess trimethylaluminium. In this case *n*-alkanes with odd carbon numbers were obtained in Schultz-Flory type distributions after quenching with water. However, since β-hydride abstraction in an Al-alkyl species is rather implausible, one would have to consider re-transfer (after a possible chain growth) of the alkyl chain to chromium, followed by β-hydride abstraction and release of an α-olefin with an odd carbon number.

Wöhl *et al.*[33] have recently described the apparition of odd-numbered α-olefins within a Schultz-Flory product distribution in the Cr (III)/(diphenylphosphino)amine (PNP) catalytic system upon activation with MAO and use of substoichometric quantities of PNP ligand (e.g. 0.5 equivalents) with respect to the employed chromium (III) precursor, typically $[CrCl_3(THF)_3]$. A mechanism involving bimetallic $PNPCr_2$ complexes with a bridging PNP ligands is suggested to be operative. Those bimetallic species are supposed to be alkylated by the MAO forming $PNPCr_2(Me)_n$ intermediates, which in turn eliminate methane to yield a chromium carbene, which undergoes metathesis with even numbered α-olefins formed via the metallacyclic mechanism by monomeric $PNPCr^+$ sites. Scheme 5 outlines this mechanistic alternative. Bimetallic species are imaginable in our system, when one considers ligand transfer to an aluminium species. As in the introductory section above, aluminium dialkyl bis(iminophosphoranyl)methanide complexes have been described[23] and have been found to be moderately active in ethylene polymerization after activation with trityl tetrafluoroborate.[21] This ligand transfer might thus account for the polymeric fraction found in the catalytic runs.

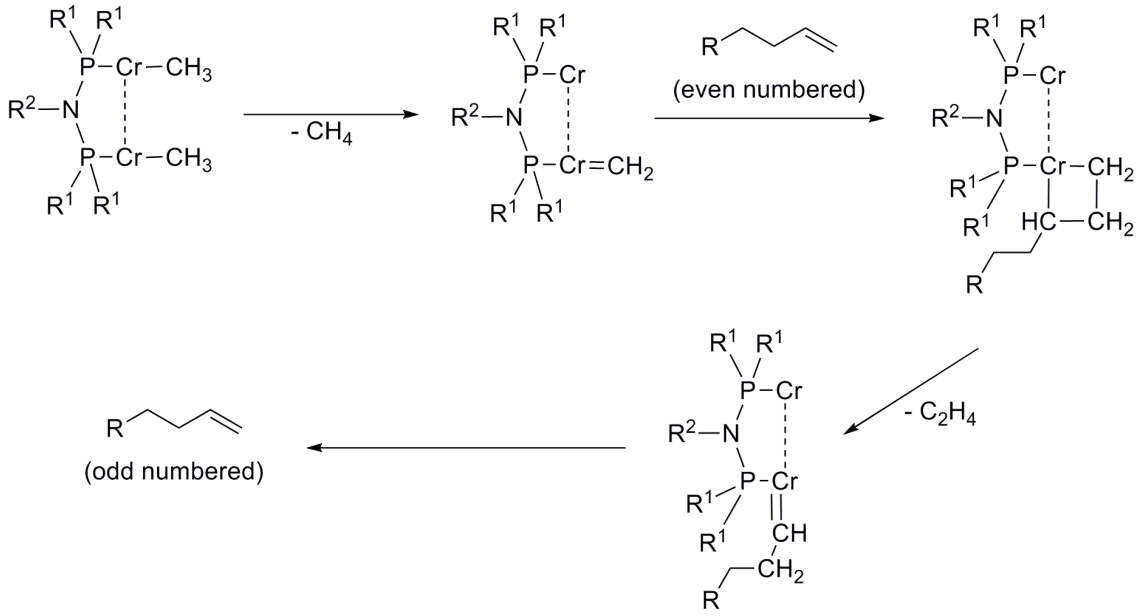

Scheme 5. Formation of odd-numbered α-olefins as suggested by Wöhl *et al*. R^1 is typically Ph, R^2 is typically *i*-Pr.

Both of these two mechanistic alternatives rely on an Al-Me species which serves as source for the additional carbon atom in the α-olefin product mixture. Therefore, supplemental tests were carried out, in order to attempt elucidation of the phenomenon of odd-numbered carbon atoms. One catalytic run (entry 10) was carried out using 600 equivalents of MAO instead of 300. However, no change in the ratio between odd-numbered and even-numbered olefin products was observed. Equally, no change in this ratio was obtained through a prolongation of the duration of the catalytic run from 0.5 to 2 h (entry 2). This result is probably due to the relatively quick deactivation of the catalytic species, mainly due to the rapid enclosure with polymeric material, which inhibits the access of supplemental MAO as methylating agent to the active chromium center.

The polymeric material produced during the runs was analyzed by differential scanning calorimetry. All polymers presented a unique melting point between 127.1 and 149.8°C, which is indicative of a highly linear unbranched polyethylene of high molecular weight. Figure 6 shows the obtained melting diagram of the polymer obtained from entry 1. The high molecularity precluded further analysis by high temperature ^{13}C NMR, as the polymer samples presented only a minimum solubility in 1,3,5-trichlorobenzene at 130°C.

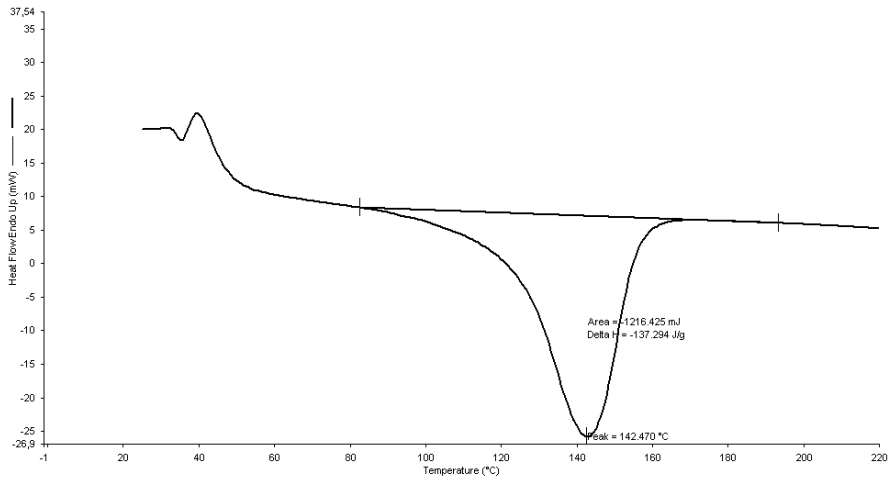

Figure 10. DSC thermogram graph of polymer obtained from run 1.

6. Conclusion and Perspectives

In the present chapter, we have presented four representatives of novel Cr(III) bis(iminophosphoranyl)methanide complexes, which were shown to adopt either dimeric μ_2-Cl bridged or monomeric structures, depending on the availability of supplemental donor sites. A representative example of a Ni(II) complex was equally synthesized; its x-ray crystal structure revealed a tetrahedral coordination around the nickel central atom. The prepared complexes were evaluated towards their activity in the ethylene oligomerization/polymerization reaction. While the Ni(II) complex showed no activity (when activated with MAO), the chromium bis(iminophoshoranyl)methanides were found to be active both in ethylene oligomerization and polymerization upon activation with either MAO, Et_3Al, or mixtures of Et_3Al and $[Ph_3C][Al(OC(CF_3)_3)_4]$ or Me_3Al and $[Ph_3C][Al(OC(CF_3)_3)_4]$, respectively. Three product fractions were obtained: besides a solid polymer fraction, a C_4-C_8 liquids fraction containing mainly α-olefins, and a second liquid fraction in the range C_{14}-C_{24}, which contained mainly α-olefins with both even and odd carbon numbers. The origin of these olefins with odd-numbered carbon number could not be fully established, just as the "C_{10}-C_{12} gap" in the distribution. Two possible mechanistic alternatives have been brought forward as partial explanations for the observed mechanism.

However, the obtained C_{14}-C_{24} fraction is highly interesting from a commercial point of view, as these carbon chain lengths fall within the range of heavy fuels, which up to today, are not accessible in an on-purpose fashion via ethylene oligomerization. Future work will have to concentrate on minimizing the part of the undesired polymers, which constitute a major obstacle to the industrialization of an oligomerization process.

7. Bibliography

[1] G. J. P. Britovsek, V. C. Gibson, D. F. Wass, *Angew. Chem. Intl. Ed.* **1999**, *38*, 428.
[2] V. C. Gibson, C. Redshaw, G. A. Solan, *Chem. Rev.* **2007**, *107*, 1745.
[3] G. J. P. Britovsek, V. C. Gibson, B. S. Kimberley, P. J. Maddox, S. J. McTavish, G. A. Solan, A. J. P. White, D. J. Williams, *Chem. Commun.* **1998**, 849.
[4] B. L. Small, M. Brookhart, *J. Am. Chem. Soc.* **1998**, *120*, 7143.
[5] S. D. Ittel, L. K. Johnson, M. Brookhart, *Chem. Rev.* **2000**, *100*, 1169.
[6] C. Bianchini, G. Mantovani, A. Meli, F. Migliacci, F. Laschi, *Organometallics* **2003**, *22*, 2545.
[7] M. A. Esteruelas, A. M. Lopez, L. Mendez, M. Olivan, E. Onate, *Organometallics* **2003**, *22*, 395.
[8] H. Sugiyama, G. Aharonian, S. Gambarotta, G. P. A. Yap, P. H. M. Budzelaar, *J. Am. Chem. Soc.* **2002**, *124*, 12268.
[9] L. Johnson, A. Bennett, P. Butera, K. Dobbs, N. Drysdale, E. Hauptman, A. Ionkin, S. Ittel, E. McCord, S. McLain, C. Radzewich, A. Rinehart, R. S. Schiffino, K. J. Sweetman, J. Uradnisheck, L. Wang, Y. Wang, Z. H. Yin, in *225th National Meeting of the American-Chemical-Society*, Amer Chemical Soc, New Orleans, Louisiana, **2003**, pp. 356.
[10] L. K. Johnson, C. M. Killian, M. Brookhart, *J. Am. Chem. Soc.* **1995**, *117*, 6414.
[11] K. Iwanaga, M. Tamura, GB2314518 (to Sumitomo Chemical Corp.), **1997**.
[12] V. C. Gibson, C. Newton, C. Redshaw, G. A. Solan, A. J. P. White, D. J. Williams, *Eur. J. Inorg. Chem.* **2001**, *2001*, 1895.
[13] L. A. MacAdams, W.-K. Kim, L. M. Liable-Sands, I. A. Guzei, A. L. Rheingold, K. H. Theopold, *Organometallics* **2002**, *21*, 952.
[14] V. C. Gibson, C. Newton, C. Redshaw, G. A. Solan, A. J. P. White, D. J. Williams, P. J. Maddox, *Chem. Commun.* **1998**, 1651.
[15] W.-K. Kim, M. J. Fevola, L. M. Liable-Sands, A. L. Rheingold, K. H. Theopold, *Organometallics* **1998**, *17*, 4541.
[16] K. Kreischer, J. Kipke, M. Bauerfeind, J. Sundermeyer, *Z. Anorg. Allgem. Chem.* **2001**, *627*, 1023.
[17] S. Al-Benna, M. J. Sarsfield, M. Thornton-Pett, D. L. Ormsby, P. J. Maddox, P. Bres, M. Bochmann, *J. Chem. Soc., Dalton Trans.* **2000**, 4247.
[18] M. Demange, L. Boubekeur, A. Auffrant, N. Mezailles, L. Ricard, X. L. Goff, P. L. Floch, *New J. Chem.* **2006**, *30*, 1745.
[19] L. Boubekeur, *Ph. D. Thesis*, Ecole Polytechnique, Palaiseau, France, **2006**.
[20] T. K. Panda, P. W. Roesky, *Chem. Soc. Rev.* **2009**, 3125.
[21] R. G. Cavell, K. Aparna, R. P. K. Babu, Q. Y. Wang, *J. Mol. Catal. A: Chem.* **2002**, *189*, 137.
[22] P. Wei, D. W. Stephan, *Organometallics* **2002**, *21*, 1308.
[23] K. Aparna, R. McDonald, M. Ferguson, R. G. Cavell, *Organometallics* **1999**, *18*, 4241.
[24] P. Imhoff, R. van Asselt, J. M. Ernsting, K. Vrieze, C. J. Elsevier, W. J. J. Smeets, A. L. Spek, A. P. M. Kentgens, *Organometallics* **1993**, *12*, 1523.
[25] P. Imhoff, J. H. Gulpen, K. Vrieze, W. J. J. Smeets, A. L. Spek, C. J. Elsevier, *Inorg. Chim. Acta* **1995**, *235*, 77.
[26] A. Jabri, C. B. Mason, Y. Sim, S. Gambarotta, T. J. Burchell, R. Duchateau, *Angew. Chem. Intl. Ed.* **2008**, *47*, 9717.
[27] A. V. Kirsanov, *Izvestiya Akademii Nauk Sssr-Seriya Khimicheskaya* **1950**, 426.
[28] I. N. Zhmurova, A. V. Kirsanov, *J. Gen. Chem. USSR* **1962**, *32*, 2540.
[29] C. Klemps, A. Buchard, R. Houdard, A. Auffrant, N. Mézailles, X. F. Le Goff, L. Ricard, L. Saussine, L. Magna, P. Le Floch, *New J. Chem.* **2009**, *33*, 1748.
[30] R. P. K. Babu, K. Aparna, R. McDonald, R. G. Cavell, *Organometallics* **2001**, *20*, 1451.
[31] I. Krossing, H. Brands, R. Feuerhake, S. Koenig, *J. Fluorine Chem.* **2001**, *112*, 83.
[32] G. C. Bazan, J. S. Rogers, C. C. Fang, *Organometallics* **2001**, *20*, 2059.
[33] A. Wöhl, W. Müller, N. Peulecke, B. H. Müller, S. Peitz, D. Heller, U. Rosenthal, *J. Mol. Catal. A: Chem.* **2009**, *297*, 1.

Chapter 4. Mixed (N,E) (E = O,P,S) Iminophosphorane Ligands in the Ethylene Oligomerization and Polymerization Reaction

Chapter 4: Mixed (N,E) (E = O,P,S) Iminophosphorane Ligands in the Ethylene Oligomerization and Polymerization Reaction

1. Introduction to the Chemistry of Iminophosphoranes

Iminophosphoranes, whose general formula is $R_3P{=}NR'$ (**A**), also known as phosphinimides, phosphinimines, or λ^5-phosphazenes, have first been described by Staudinger and Meyer as early as 1919.[1] Since then, the P=N structural motif has found application in a vast variety of applications in all parts of synthetic organic chemistry,[2-5] coordination chemistry and catalysis[6,7] as well as in material sciences.[8,9]

A

Figure 1. Resonance structures of an iminophosphorane.

This introduction aims to present the reader some important synthetic approaches to the iminophosphorane functionality, to describe briefly the electronic structure of the P=N moiety, and to outline some examples of iminophosphorane coordination chemistry relevant to catalytic applications, notably in olefin oligomerization and polymerization reactions.

1.1 Synthesis of Iminophosphoranes

Whereas an extensive number of approaches towards the iminophosphorane moiety exist in the literature, however, only a few of them are of relevance from a synthetic viewpoint. The two most important routes are the before mentioned Staudinger reaction, and the route devised by Kirsanov, thus known as the Kirsanov reaction. The common principle of both reactions is the employment of a phosphine PR_3 as starting material in the reaction, whereas the nitrogen is incorporated either through an azide $R'N_3$ or a primary amine $R'NH_2$. A further relevant synthetic route is the aza-Mitsunobu reaction, whose scope and limitations are presented below.

1.1.1 The Staudinger Reaction

The Staudinger reaction, which is based upon the reaction of an azide $R'N_3$ with a phosphine R_3P, is the most ancient synthetic approach to iminophosphoranes,[1] yet it is still by far the most used method.[10,11] (Scheme 1) This may in part be ascribed to the fact, that during this reaction, nitrogen N_2 is released as the only side product, thus rendering unnecessary further purification of the

iminophosphorane product. However, the major inconvenient is the risk of explosion associated with most azide derivatives, which is a major drawback to the variation of the nitrogen substituent R'. The mechanism of the Staudinger reaction has been investigated theoretically using DFT methods,[12,13] and was found to proceed via a phosphazide intermediate $R_3PN{=}N{=}NR'$, however, in the normal synthetic conduct of the Staudinger reaction, this intermediate cannot be isolated.

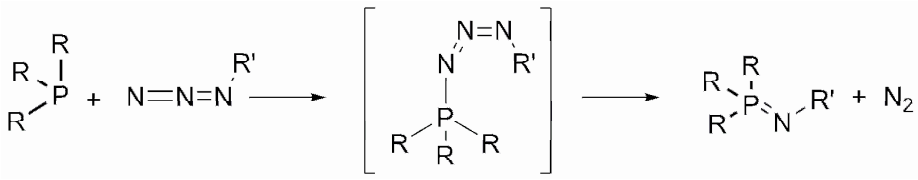

Scheme 1. The Staudinger reaction.

1.1.2 The Kirsanov Reaction

An alternative method towards the iminophosphorane functionality was devised by Kirsanov in 1950.[14] It is based upon the reaction of phosphorous pentachloride PCl_5 with phenylsulfonamide, followed by treatment with a Grignard reagent PhMgBr.[15-17] (Scheme 2)

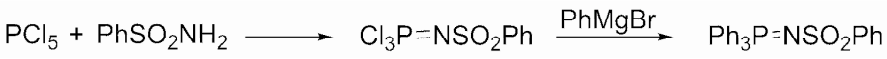

Scheme 2. The original Kirsanov reaction.

This reaction has subsequently been modified by Horner and Oedinger.[18] Bromination of a tertiary phosphine, followed by reaction with a primary amine $R'NH_2$ in the presence of one equivalent of a base (e. g. triethylamine) yields an aminophosphonium bromide salt $[R_3PNHR']^+[Br]^-$, which, upon formal elimination of HBr with a further equivalent of a well-adapted base, yields the corresponding iminophosphorane. (Scheme 3)

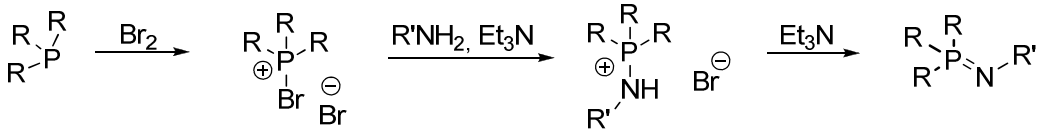

Scheme 3. The Horner/Oedinger variation of the Kirsanov reaction.

It should be noted that in the case of R' = alkyl, triethylamine, as displayed in scheme 3, does not constitute a sufficiently strong base to allow deprotonation of the aminophosphonium bromide, stronger bases such as potassium hexamethyldisilazane, or organolithium compounds have to be employed in a separate second step after intermediate isolation and purification of the aminophosphonium salts. But this intermediate additional step does not constitute an inconvenient in the preparation of iminiophosphoranes. On the contrary: aminophosphonium salts, as opposed to their

iminophosphorane analogues, are air- and water stable, and thus easy to manipulate and in most cases easy to isolate from the reaction mixture. They can be prepared in great quantities via the method outlined in scheme 3. Another further advantage over the Staudinger reaction is the variability brought to the nitrogen residue R', as virtually any primary amine may be employed in this reaction. This opens the route towards a great variety of derivatives, including chiral iminophosphoranes, which is important notably for catalysis.

1.1.3 The Aza-Mitsunobu Reaction

A more recent access to iminophosphoranes constitutes the aza-Mitsonubo reaction,[19] which is outlined in scheme 4. This method is based on the reaction of triphenylphosphine with diethylazodicarboxylate and a primary amine R'NH_2.

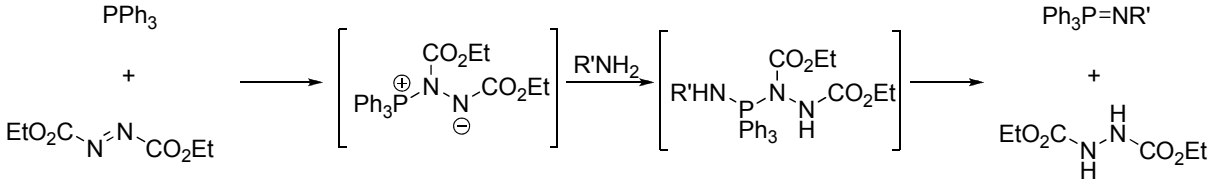

Scheme 4. The aza-Mitsunobu reaction.

Even though this one-pot reaction proceeds with excellent yields, its scope is limited amines with electron withdrawing groups, with a proton sufficiently acidic to allow its abstraction by the azodicarboxylate.

1.2 Electronic Structure of the P=N function

Iminophosphoranes, which are isoelectronic analogues to phosphine oxides ($R_3P=O$) and phosphine sulfides ($R_3P=S$), are often noted for convenience reasons with a formal double bond connecting the phosphorous and the nitrogen moiety, or as a resonance hybrid **A** (Scheme 1) between an aza-ylene $R_3P=NR'$ and the ionic ylidic form R_3P^+-N^-R'.[6] The P-E (E = N, C, O, S) bonding situation being a subject of debate over the last years,[20] both calculations and evidence gained from the experimental determination of charge density[21] seem to exclude the participation of d-orbitals in the bonding of these "hypervalent" compounds. Alternatively, negative hyperconjugation[22] has been suggested to stabilize the bonding in these compounds and to be responsible for any π bond character.[23-25] Both Boubekeur[26] and Cao[27] from our group have carried out DFT calculations on iminophosphoranes and the analogous phosphonium ylides. Due to the paramount importance of imines $RN=CR'_2$, which may be regarded as carbon analogs of iminophosphoranes, as ligands in homogeneous catalysis, the relevant parameters to the description of the electronic structure have equally been calculated and

discussed. Table 1 presents NBO charges and Wiberg bond indices, as calculated for these three cases. Simplified models, with R, R' = H have been employed for these calculations.

Table 1. NBO charges and Wiberg bond indices as calculated by Boubekeur (a) and Cao (b). (a): rb3lyp functional, 6-31G* basis set; (b): b3pw91 functional, 6-31G* basis set.

Compound	NBO charges	Wiberg bond indices
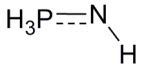	(a) charge(P) = 1.07, charge(N) = -1.32	1.34
	(b) charge(P) = 1.03, charge(N) = -1.26	
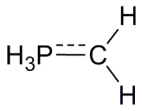	(a) charge(P) = 0.79, charge(C) = -1.22	1.37
	(b) charge(P) = 0.78, charge(C) = -1.20	
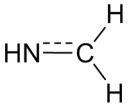	(a) charge(N) = -0.63, charge(C) = -0.10	2.03
	(b) charge(N) = -0.62, charge(C) = -0.11	

While the Wiberg bond index of 2.03 for the imine $HN{=}CH_2$ clearly indicates the double bond character of the N-C bond and partial charge distribution on the N and C moieties, the situation is consequently different in the case of the phosphonium ylide and the iminophosphorane: NBO charges indicate the presence of a zwitterionic form in these species, thus $H_3P^+\text{-}C^-H_2$ and $H_3P^+\text{-}N^-H$, respectively, represent the predominant resonance structures for these species. This explains the similar Wittig type reactivity of both phosphonium ylides and iminophosphoranes.

1.3 Iminophosphorane Ligands in the Ethylene Oligomerization and Polymerization Reaction

Compared to their carbon analogs, the imines, ligands incorporating the iminophosphorane moiety have found only a relatively sparse application in catalysis. This might be due to the fact that iminophosphoranes are hard ligands (following the Pearson HSAB concept)[28], which makes them bad ligands towards late electron-rich transition metals, which however, take a predominant role in most known catalytic reactions. In order to stabilize different transition metal oxidation states with iminophosphoranes, as required in order to establish a working catalytic cycle, the design of multidentate ligands is the concept of choice. The two most common realizations of this concept are either chelating coordination of a bis- or tris-iminophosphorane, the incorporation of a coordination site with different electronic properties (soft), or the combination of these two approaches. Figure 2

shows some examples of iminophosphorane-based ligands and complexes, which have found application in catalysis.

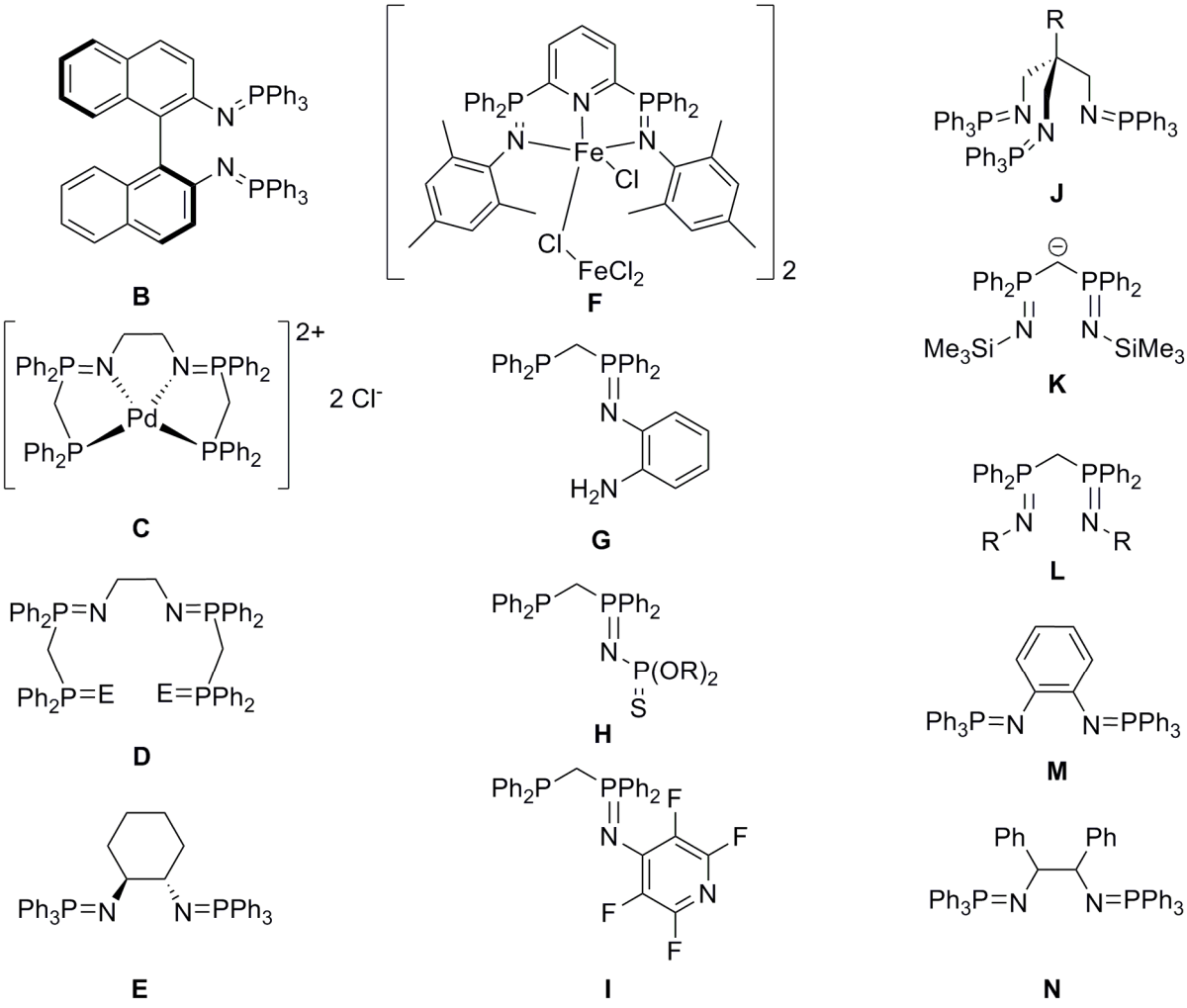

Figure 2. Some iminophosphorane ligands and complexes which have found applications in homogeneous catalysis processes. **D** (E = O, S, lone pair).

In 1998, the stereoselective cyclopropanation of styrene employing the Cu(I) complex of the bis(iminophosphorane) **B**, was reported as the first example of a catalytic application.[29] Recently, the application of the Pd(II) complex **C** in the Suzuki-Miyaura coupling reaction, which bears a tetradentate phosphine-iminophosphorane ligand prepared from dppm and ethylene diamine, has been reported to be effective both in water and in toluene/water biphasic medium.[30] Fe(II) of mixed ligands **D** were found to be effective in transfer hydrogenation of acetophenone at 82° with *i*-PrOH as hydrogen source.[31] Activity in Ru catalyzed hydrogen transfer reactions to ketones has equally been reported with the corresponding complexes of the phosphine-iminophosphorane ligands **G**,[32] **H**,[33] and **I**.[34,35] Ligand **E** was successfully tested in Pd catalyzed nucleophilic allylic substitution.[36]

However, the main application of iminophosphoranes in catalysis has been the ethylene oligomerization and polymerization reaction. Sauthier *et al*. reported on Ni(II) complexes of ligands **E**, **M** and **N** and their activity in ethylene dimerization upon activation with Et_2AlCl.[37,38] Selectivities of up to 90% towards dimerization were observed with $NiCl_2$(**N**), however, this major fraction was found to contain only 1% of the desired 1-butene. Ni(II) and Fe(II) complexes of the tripodal ligand **J** were activated with MMAO, Et_2AlCl, or $EtAlCl_2$, and found to yield broad oligomer distributions, while the overall activity was significantly influenced by the nature of the ligand substituent R, which was either Ph or Me. More promising, the analogous palladium complex $PdCl_2$(**J**) with R = Ph, exhibited a selectivity towards ethylene trimerization of 93%, however, the α-selectivity was not reported.[39,40] The bis-iminophosphorane-pyridine Fe(II) complex **F** showed a modest activity of 62×10^2 g(PE) × mol(Fe)$^{-1}$ × bar^{-1} × h^{-1} upon activation with 1000 equivalents of MAO and 10 equivalents of triisobutylaluminium.[41] Coordination and catalytic activity in ethylene oligomerization and polymerization of complexes comprising ligands **K** and **L** have been discussed in chapter 3.

2. Nickel Catalyzed Selective Ethylene Dimerization with N,E (E = O, S, P) mixed Iminophosphorane Ligands

Nickel based catalyst play an outstandingly important role in the oligomerization[42] and polymerization[43,44] of ethylene. The most prominent example in this catalyst class constitutes what is called today the "Keim's" catalyst,[45-49] a square-planar Ni(II) phosphinyl-enolato complex [NiPh{Ph_2PCH=C(O)Ph}(PPh_3)],[50] which is prepared by oxidative addition of $Ni(cod)_2$ into a P-Ph bond of the ylide in the presence of PPh_3 (Scheme 5).

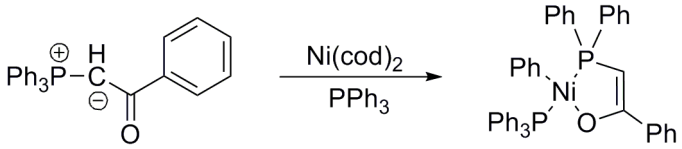

Scheme 5. Preparation of the Keim's complex for ethylene oligomerization and polymerization.

It was shown by Klabunde *et al.*, that addition of a phosphine scavenger led to a polymerization catalyst.[51,52] Keim's complex has found large-scale industrial application in the Shell Higher Olefin Process (SHOP), and it has been this industrial interest, which has triggered further interest in nickel based catalytic systems bearing mixed heteroatomic ligands with mixed anionic and/or neutral (P,O) donor combinations.[53-57] (N,O) and (N,P) donor combinations will be treated in the following sections.

2.1 N,O-Iminophosphorane Ligands

Prime examples of SHOP-type catalysts with a mixed (N,O) donor combination are the neutral salicylaldiminato Ni(II) complex **O**, developed by Grubbs and coworkers,[58,59] the related amido aldehyde system **P**, developed by Novak and coworkers,[60] and the keto-amido Ni(II) complex **Q** disclosed by the Brookhart group,[61] which are all highly active ethylene polymerization catalysts, without requiring organoaluminium activators. (Figure 3)

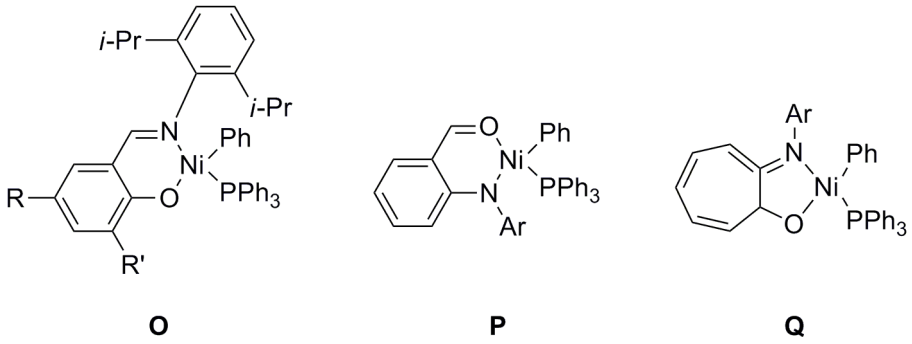

O **P** **Q**

Figure 3. (N,O) based nickel systems for ethylene polymerization.

Whereas these three (N,O) systems proved highly active in polymerization at low pressures (typically 1 bar), studies by Carlini *et al.* revealed selectivity switches of these N,O and related systems towards the formation of linear oligomers at higher pressures.[62] Cr(III)-salicylaldiminato complexes, upon activation with excess quantities of MAO, were found to be active in ethylene oligomerization, yielding mainly α-olefins.[63]

Based on these findings, we became interested in the evaluation of analogous anionic phenolato-iminophosphorane (**1**) and neutral ether-iminophosphorane (**2**) ligands and their coordination to various metal centers. (Figure 4)

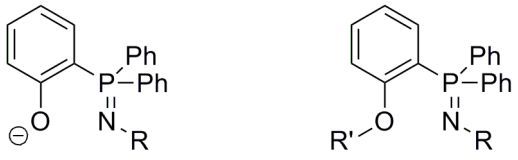

1 **2**

Figure 4. Phenolato-iminophosphorane (**1**) and ether-iminophosphorane (**2**) ligands.

It should be noted that a Staudinger synthesis of ligand **1**, and its coordination to Ti(IV) and Zr(IV) has been reported before by Sun and coworkers.[64] Due to the inherent limitation of the Staudinger synthesis with respect to the hazards associated with most azides, only the derivatives with R = Ph, $SiMe_3$ were accessible. Two ligands per metal center coordinated to yield $(\mathbf{1})_2MCl_2$ (M = Ti, Zr) complexes, which proved to be essentially inactive in ethylene polymerization and oligomerization

upon activation with either 2000 equiv. of MMAO or i-$Bu_3Al/Ph_3CB(C_6F_5)_4$ (100/1 equiv.). The excessive steric congestion around the metal center trough the presence of two chelating ligands was evoked as a possible reason for the inactivity of said complexes.[64]

2.2.1 Synthesis of Phenolato-Iminophosphoranes 1

Our synthetic approach was based on the Kirsanov reaction using a protocol, which has previously been devised in our group.[26] Via well established synthetic protocols, and employing a protecting group strategy, the ethoxy-methyl protected phenol **3** was ortho-lithiated in diethylether at -78°C, then reacted with Ph_2PCl to yield the triphenylphosphine derivative **4**.[65] Reaction with one equivalent of bromine in CH_2Cl_2 at -78°C led to the highly sensitive bromophosphonium bromide **5**, which was not isolated. Addition of one equivalent of triethylamine, followed by one equivalent of a primary amine RNH_2, cleanly yielded the aminophosphonium salt **6**,[66] whose deprotection was easily carried out by treatment with a concentrated HCl solution in methanol. (Scheme 6)

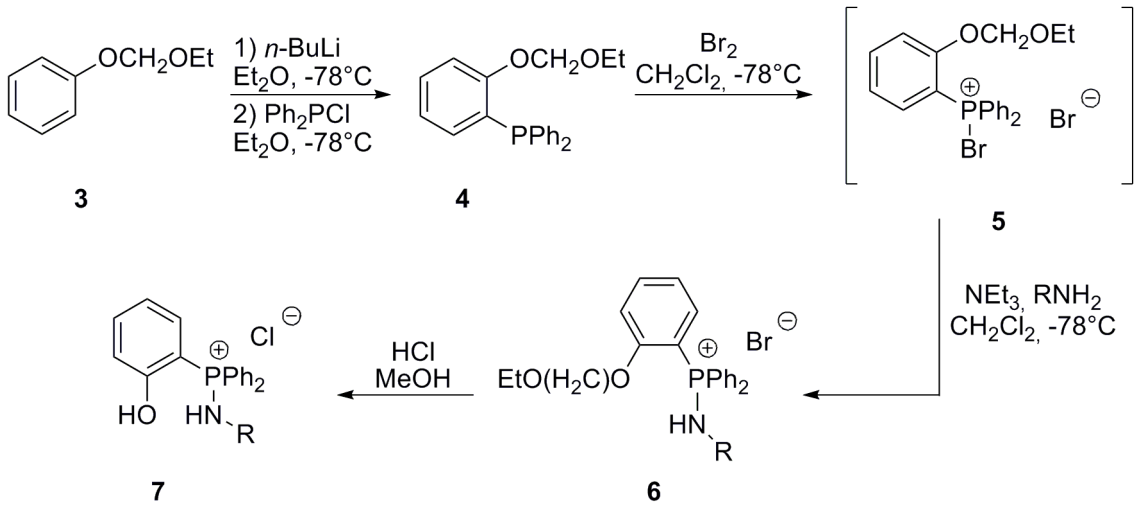

Scheme 6. Synthesis of phenol-aminophosphonium chlorides **7a**-**c**. (**a**: R = *t*-Bu, **b**: R = $CH_2C(CH_3)_3$, **c**: R = Ph).

The desired phenol-aminophosphonium chlorides **7** were thus obtained in overall yields of 40 to 52%. Single crystals of the N-*t*-Bu derivative **7a** suitable for x-ray structure analysis could be obtained by slow diffusion of hexanes into a concentrated solution of **7a** in CH_2Cl_2. An Ortep representation of the compound is presented in figure 5. The P1-N1 bond length of 1.616(5) Å and the P1-N1-C19 angle of 131.3(4)° are both characteristically within the range found for aminophosphonium salts.[26]

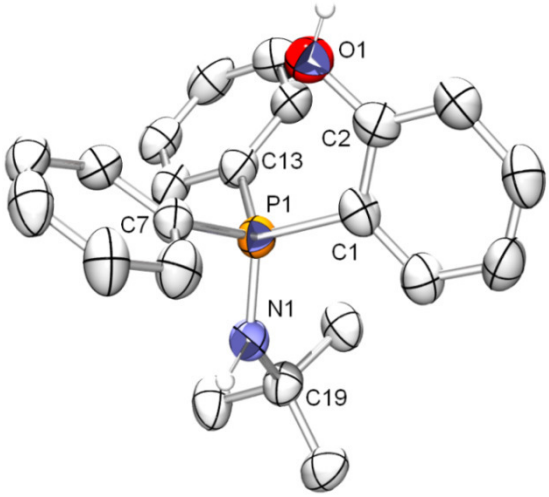

Figure 5. Ortep representation of the x-ray crystal structure of **7a**. Hydrogen atoms (except those on N1 and O1) and the chloride counteranion have been omitted for clarity. Thermal ellipsoids are represented at the 50% level. Important bond lengths (Å) and angles (°): P1-N1 = 1.616(5), P1-C1 = 1.806(6), P1-C7 = 1.799(6), P1-C13 = 1.798(6), N1-C19 = 1.513(7), O1-C2 = 1.380(8), N1-P1-C1 = 112.4(3), N1-P1-C13 = 109.8(3), C1-C2-O1 = 116.8(6), P1-N1-C19 = 131.3(4).

Due to their stability towards air and water, the salts **7** serve as convenient starting materials for the in situ preparation of iminophosphoranes and their coordination to various group 9 and 10 metal centers. Double deprotonation of **7a**-**c** with two equivalents of either KHMDS or *n*-BuLi in THF yielded as intermediates the potassium- (**1a**) or lithio- phenolate iminophosphoranes **1b**-**d**, respectively, whose formation was only checked by ^{31}P NMR. Its coordination properties towards $[PdCl_2(PPh_3)_2]$, $[Rh(cod)Cl]_2$, and $[NiBr_2(DME)]$ were tested.

2.2.2 Coordination to Rh(I) and Pd(II)

In order to assess the coordination properties of this new class of ligands, coordination to Rh(I) and Pd(II) was carried out using the aminophosphonium ligand precursor **7a**. Double deprotonation of **7a** was undertaken with KHMDS, to yield the potassium phenolate iminophosphorane **1a**, which was not isolated, but immediately employed for coordination to $[Rh(cod)Cl]_2$ as well as $[PdCl_2(PPh_3)_2]$. (Scheme 7) Double deprotonation with *n*-BuLi yielded the lithio phenolate iminophosphorane **1b**. However, coordination attempts with $[Rh(cod)Cl]_2$ and $[PdCl_2(PPh_3)_2]$ employing **1a** proved unsuccessful.

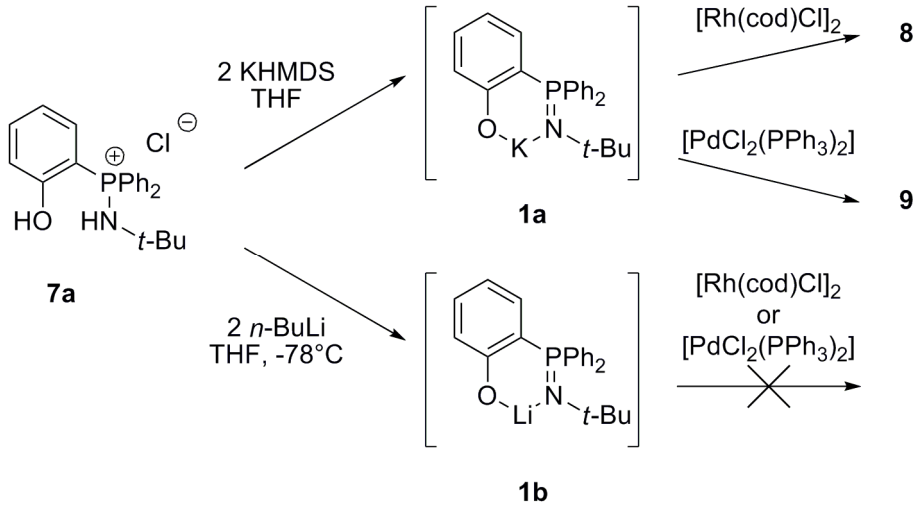

Scheme 7. Coordination of **1a** to $[Rh(cod)Cl]_2$ and $[PdCl_2(PPh_3)_2]$.

By complete characterization of complex **8** by ^{1}H, ^{13}C and ^{31}P NMR a monomeric structure could be as depicted in figure 6 established. Interestingly, no ^{2}J (Rh-P) coupling was found in the ^{31}P spectrum, instead a single peak at 21 ppm (in THF) was observed. Unfortunately, crystals suitable for x-ray crystal structure could not be obtained despite numerous trials in various solvent systems.

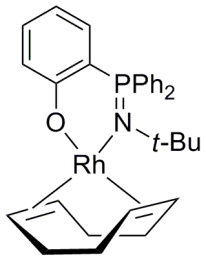

8

Figure 6. Structure of Rh(I) complex **8** as established by NMR spectroscopy.

The Pd(II) complex **9** was obtained as an orange solid by simple addition of $[PdCl_2(PPh_3)_2]$ to a THF solution of **1a** as outlined in scheme 7. Coordination of the ligand was followed by ^{31}P NMR. Besides the appearance of free PPh_3 at -5.4 ppm, two coupling phosphorus nuclei at 10.7 ppm (attributed to coordinated PPh_3) and 25.4 ppm (attributed to the coordinated iminophosphorane) were observed ($^{3}J_{PP}$ = 5.6 Hz). After removal of removal of KCl by filtration, which is insoluble in THF, the complex **9** was purified and separated from free PPh_3 by precipitation from a THF/toluene mixture. Monocrystals suitable for x-ray crystal analysis were obtained by layering a concentrated THF solution of **9** with hexane.

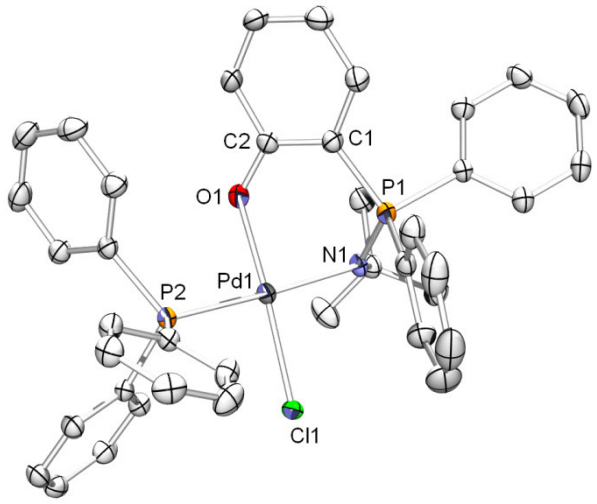

Figure 7. Ortep representation of the x-ray crystal structure of **9**. Hydrogen atoms have been omitted for clarity. Thermal ellipsoids are represented at the 50% level. Important bond lengths (Å) and angles (°): Pd1-O1= 2.008(2), Pd1-N1 = 2.129(2), Pd1-Cl1 = 2.3333(6), Pd1-P2 = 2.2716(6), P1-N1 = 1.603(2), P1-C1 = 1.804(2), C1-C2 = 1.416(3), C2-O1 = 1.315(2), N1-Pd1-Cl1 = 92.96(5), O1-Pd1-N1 = 88.74(6), O1-Pd1-P2 = 89.29(4), P2-Pd1-Cl1 = 89.57(2), Pd1-N1-P1 = 103.6(1), P1-C1-C2 = 120.3(2), C1-C2-O1 = 125.4(2), C2-O1-Pd1 = 123.8(1).

2.2.3 Coordination to Ni(II)

[$NiBr_2$(DME)] was added to in-situ prepared solutions of phenolato-iminophosphoranes **1b-d** to obtain the corresponding complexes **10b-d**. The complete disappearance of the ^{31}P NMR signal in the reaction mixture in all cases was indicative of coordination of **1b-d** to the Ni(II) center and formation of a paramagnetic complex. (Scheme 8)

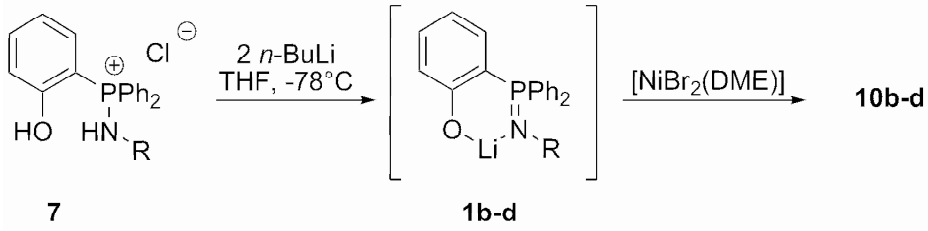

Scheme 8. Synthesis of phenolato-iminophosphorane complexes **10b-d**. **b**: R = *t*-Bu, **c**: R = $CH_2C(CH_3)_3$, **d**: R = Ph.

In the case of **10b**, single crystals suitable for x-ray crystal structure analysis could be obtained by diffusion of hexane into the reaction mixture in THF. (Figure 7) The structure reveals a tetrahedral geometry around the Ni(II) center, with one molecule of **1b** coordinated both trough the anionic phenolato site O1 and the neutral iminophosphorane. A striking feature of the structure is the co-coordination of a LiCl/Br$(THF)_2$ unit, which completes the coordination sphere of the Ni(II) center

through μ_2 coordination of Cl1. Li1 completes its equally tetrahedral coordination sphere with μ_2-O1. The Ni1-O1-Li1-Cl1 four-membered metallacycle is a feature, which to our knowledge has only rarely been reported before. Eckert *et al.*[67] reported on a similar structural motif incorporating a Fe(II)-β-diketiminate moiety, while a tertbutylate unit exhibits a similar μ_2-O coordination. A μ_2 coordinated tertbutylate is equally present in the structure of the Cr(II) complex [Cr(μ_1-O*t*-Bu)(μ_2-O*t*-Bu)Li(μ_2-Cl)(THF)$_2$].[68] All other structural features of compound **10b** lie within the range observed for tetrahedral Ni(II) iminophosphorane complexes[69] and do not deserve further comment.

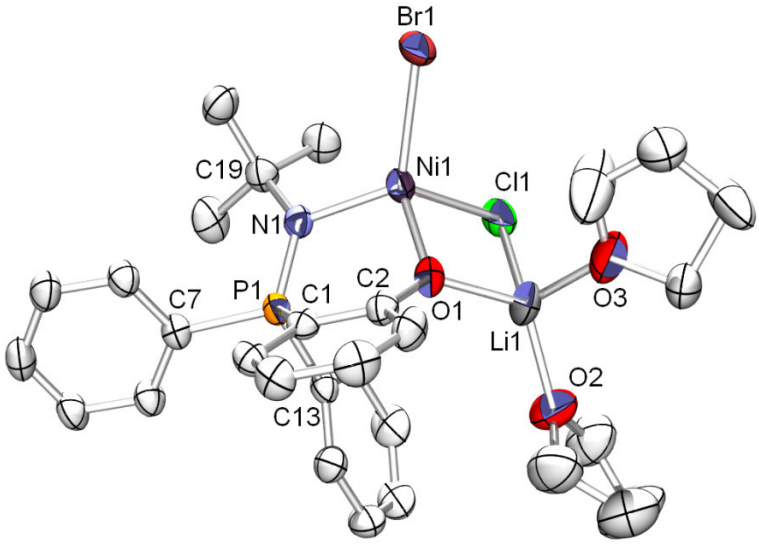

Figure 8. Ortep representation of the x-ray crystal structure of **10b**. Partial chloride bromide exchange has been observed on this structure and the Br/Cl occupation factors refine to a value close to 0.8/0.2. Hydrogen atoms have been omitted for clarity. Thermal ellipsoids are represented at the 50% level. Important bond lengths (Å) and angles (°): P1-N1 = 1.601(2), P1-C1 = 1.802(3), N1-C19 = 1.506(3), C2-O1 = 1.323(3), O1-Ni1 = 1.954(2), Ni1-N1 = 1.981(2), Ni1-Br1 = 2.382(2), Ni1-Cl1 = 2.32(1), Cl1-Li1 = 2.32(1), Li1-O1 = 1.894(5), Li-O2 = 1.871(6), Li1-O3 = 1.930(7), O1-Ni1-N1 = 98.7(1), O1-Ni1-Br1 = 119.19(7), P1-N1-C19 = 129.4(2), P1-N1-Ni1 = 113.4(1), O1-Ni1-Cl1 = 88.6(3), O1-Li1-Cl1 = 90.1(3), O2-Li1-O3 = 106.4(3).

2.2.4 Application in the Selective Dimerization of Ethylene

Complexes **10b-d** were employed in the ethylene oligomerization reaction after activation with 300 equiv. of MAO at either 45°C or 20°C. Table 2 lists the obtained activities. Importantly, only short chain oligomers in the C_4-C_8 range were observed and no polymeric material was detected. **10b** proved to be the most active catalyst with a TOF of up to 177.6 mol(C_2H_4) × mol(Ni)$^{-1}$ × h^{-1} when running the catalysis at 45°C, however, within the butenes fraction, an α-selectivity of only 78% was achieved. Whereas this selectivity could only be insignificantly increased to 79%in the case of **10b**, even when lowering the temperature to 20°C, this selectivity dependence was more pronounced in the case of **10c** and **10d**, where the α-selectivity in the butenes fraction raised from 76 to 85% (run 3 and 4), and from

73 to 88% (run 5 and 6), respectively, when conducting the oligomerization reaction at 20°C instead of 45°C. **10d** has equally been evaluated with Et_2AlCl (10 equiv.) and $EtAlCl_2$ (10 equiv.), but both cocatalysts proved inactive with the present system (run 7 and 8).

Table 2. Results in the Ethylene Oligomerization reaction with complexes **10a-c**. (Ratio Al/Ni = 300)

Entry	Precursor	$\%C_4$ ($\%1\text{-}C_4$)	$\%C_6$ ($\%1\text{-}C_6$)	$\%C_8$ ($\%1\text{-}C_8$)	TOF / $10^3 \times$ mol(C_2H_4) $\times$ mol(Ni)$^{-1} \times h^{-1}$.
1[a]	**10b**	92 (78)	7 (25)	1 (69)	177.6
2[b]	**10b**	92 (79)	7 (25)	1 (75)	176.0
3[a]	**10c**	93 (76)	5 (30)	2 (77)	152.3
4[b]	**10c**	93 (85)	4 (32)	3 (77)	148.7
5[a]	**10d**	89(73)	10 (35)	1 (80)	124.3
6[b]	**10d**	90 (88)	10 (37)	traces	120.7
7[b,c]	**10d**	traces	-	-	-
8[b,d]	**10d**	traces	-	-	-

[a] reaction at 45°C; [b] reaction at 20°C; [c] Et_2AlCl (10 equiv.); [c] $EtAlCl_2$ (10 equiv.)

2.2.5 Synthesis of Ether-Iminophosphoranes 2

In an analogous fashion to the synthesis of the phenolato-iminophosphoranes **1**, the ether-aminophosphonium salt **13** was prepared starting from the methyl ether-functionalized triphenylphosphine **11** in 64% overall yield. (Scheme 9)

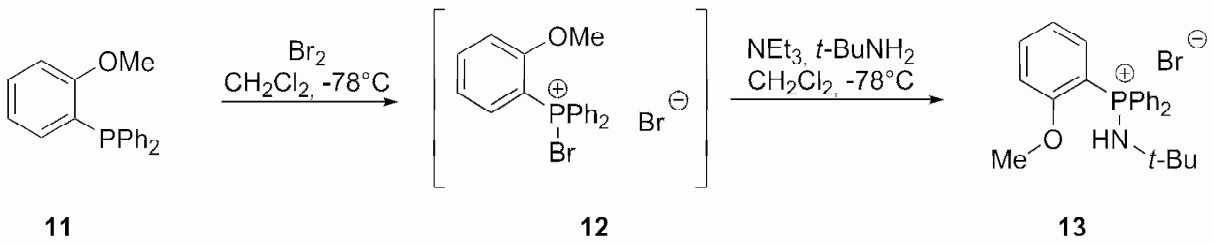

11 **12** **13**

Scheme 9. Synthesis of ether-aminophosphonium salt **13**.

Deprotonation of **13** to yield the corresponding ether-iminophosphorane proceeded smoothly both with *n*-BuLi and KHMDS (1 equiv.) Unfortunately, subsequent coordination to Pd(II), Rh(I), and Ni(II) was unsuccessful. This is ascribed to the low donor strength of the ether oxygen donor, and the unfavourable interaction between the soft late transition metals and the hard iminophosphorane donor. Work with **13** was therefore not further pursued.

2.3 (N,P)-Iminophosphorane Ligands

(N,P) mixed heteroatomic ligands play an important role both in transition metal coordination chemistry and in catalysis.[70-73] Accordingly, their application in transition-metal catalyzed ethylene oligomerization, polymerization, and copolymerization has attracted attention.[42,43,74] Notably phosphino-imine, phosphito-imine, phosphino-oxazoline, phosphito-oxazoline, and phosphino-pyridine ligands, in numerous variations and with various degrees of steric bulk, coordinated to group 10 metal centers, have been studied in this reaction. Figure 9 displays a selection of P,N mixed donor ligands and complexes which have found application in the ethylene oligomerization reaction.

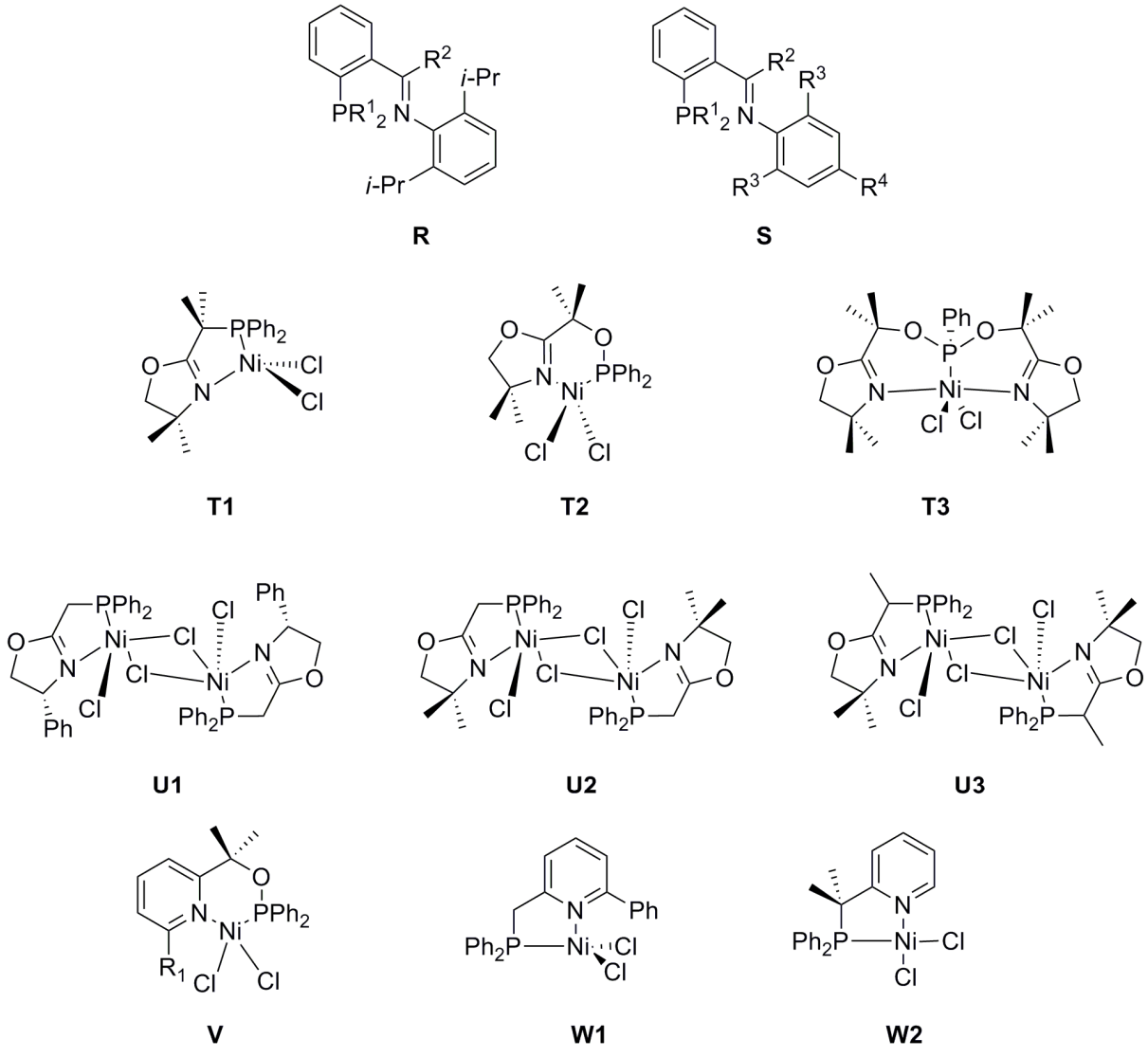

Figure 9. Some ligands and Ni(II) complexes employed in the ethylene oligomerization and polymerization reaction.

Phosphino imine ligands **R**, which have been disclosed by Shell[75] and Eastman Chemical Corporation,[76] and their corresponding Ni(II) complexes were found to be active in polymerization

only. Polymerization activity was found to be best upon the use of highly basic phosphine moieties (R^1 = *i*-Pr, *t*-Bu) and R^2 = Ph. On the other hand, the [Pd(**S**)OTf_2] complexes were found to be active in the oligomerization of ethylene, however, Schultz-Flory distributions of short- to medium chain length oligomers were obtained. Substitution of R^4 with electron-donating groups (e.g. OMe) was found to be beneficial towards overall activity.[77]

The tetrahedral phosphite-oxazoline complex **T1** was found to yield up to 45900 mol(C_2H_4) × mol(Ni)$^{-1}$ × h^{-1} upon activation with 6 equiv. of $EtAlCl_2$ (P_{C2H4} = 10 bar, T = 30°C), the C_4-selectivity obtained was 54%, of which 20% was 1-butene.[78] The analogous complex **T2** was found to exhibit an activity of 49500 mol(C_2H_4) × mol(Ni)$^{-1}$ × h^{-1}, under equal reaction conditions while the C_4-selectivity increased to 64% (8% 1-butene).[79] This rather low α-selectivity could be increased to 18% upon reducing the activator quantity to only 2 equiv. Concomitantly, the total fraction of C_4 products raised to 81%. Complex **T3**, reported by Speiser *et al.* in 2004,[80] features a trigonal-bipyramidal coordination geometry. Remarkably, this complex catalyzed ethylene oligomerization upon activation with only 1.3 equiv. of $EtAlCl_2$, which is highly interesting from an economical point of view. An activity of 17000 mol(C_2H_4) × mol(Ni)$^{-1}$ × h^{-1} was reported. Comparison of the bidentate phosphite-oxazoline on **T2** with the tridentate ligand on **T3**, shows that bidentate ligation is beneficial towards catalyst activity, however, it was reported that **T3** features greater stability towards heat and decomposition, which is important for industrial applications.

The dimeric Ni(II) complexes **U1**, **U2**, **U3** bearing phosphine-oxazoline ligands were reported by Braunstein and colleagues.[78] Remarkably, all three complexes were reported to be inactive upon activation with 400 eq. of MAO. Increasing alkyl substitution on the α-carbon atom next to the PPh_2 moiety proved beneficial towards activity even with low quantities of cocatalyst: Whereas **U2** produced only traces of oligomeric products after activation with 6 equiv. of $EtAlCl_2$, the methyl-substituted complex **U3** showed an activity of 18400 mol(C_2H_4) × mol(Ni)$^{-1}$ × h^{-1} (64% of C_4 products, of these 13% butenes) under these same conditions.

Square-planar complex **V**, which was equally reported by Braunstein and colleagues,[79,81] exhibited an activity of 43700 mol(C_2H_4) × mol(Ni)$^{-1}$ × h^{-1} (64% of C_4 products, of these 5% butenes), when activated with $EtAlCl_2$ (6 equiv.), while activation of this complex with MAO resulted in decomposition and no activity in oligomerization. Upon comparison of the catalytic activities of **W1** and **W2**, the positive effect of increased α-substitution on the α-carbon next to the phosphine functionality is obvious: **W1** (47300 mol(C_2H_4) × mol(Ni)$^{-1}$ × h^{-1}) versus 58100 mol(C_2H_4) × mol(Ni)$^{-1}$ × h^{-1} for **W2**, both activated with 6 equiv. of $EtAlCl_2$.[82-84]

In the light of these results, we decided to employ two types of phosphine-iminophosphorane ligands (Figure 10), whose straightforward synthesis had been devised previously in our laboratory, in the

nickel-catalyzed selective dimerization of ethylene. The coordination to Cr(III) metal centers and the activity of the resulting complexes in the oligomerization reaction was equally evaluated.

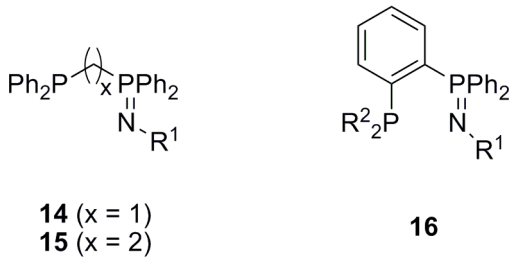

14 (x = 1)
15 (x = 2)

16

Figure 10.

2.3.1 Synthesis of Mixed Phosphine-Iminophosphorane Ligands

Via the above described Kirsanov method, and following the protocol devised by Boubekeur *et al.*,[85] the aminophosphonium salt precursors to compounds **14** and **15** are accessible by monobromination, followed by treatment with a primary amine R^1NH_2, of dppm (x = 1) and dppe (x = 2), respectively. (Scheme 10)

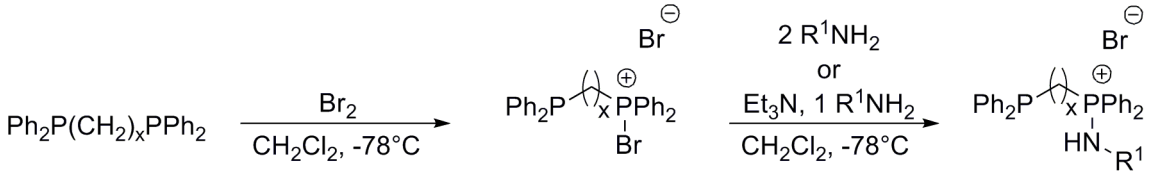

17a-e (x = 1)
18 (x = 2)

Scheme 10. Synthesis of phosphine-aminophosphonium bromides **17a**-**e**, **18**. **a**: $R^1 = CH_2$-*t*-Bu, **b**: R^1 = *p*-$CH_2C_6H_4OMe$, **c**: R^1 = Ph, **d**: R^1 = *o*-MeO-C_6H_4, **e**: R^1 = *o*-NH_2-C_6H_4, R^1 = Ph.

Both bidentate (N,P) ligands as well as tridentate (N,N',P) ligands with a supplemental amine donor or (O,N,P) ligands, containing a supplemental ether oxygen donor site are accessible through this method, which bears as its major advantages both the simple availability of the starting materials, and the easy scale up of the synthesis to quantities of 10 g and above.

As described by Boubekeur *et al.*, the monobromination strategy proved unsuccessful when applied to 1,2-bis(diphenylphosphino)benzene, yielding only unusable product mixtures.[66] Phosphine-iminophosphoranes of the general structure **16** (or their corresponding phosphine-aminophosphonium salts) were thus made accessible via another synthetic approach, taking advantage of the excellent *ortho*-directing properties of the iminophosphorane function in the lithiation reaction of arenes, which has first been described by Stuckwisch in 1976.[86] In 1995, the x-ray crystal structure of the ortho-

lithiated iminophosphorane $[(Ph_2(Li\text{-}C_6H_4)P{=}NSiMe_3]_2(Et_2O)_2$ was reported.[87] Boubekeur *et al.* described the reaction of chlorophoshines ($R^2{}_2PCl$) with the lithiated iminophosphorane to yield mixed (N,P) ligands **16**.[66] (Scheme 11).

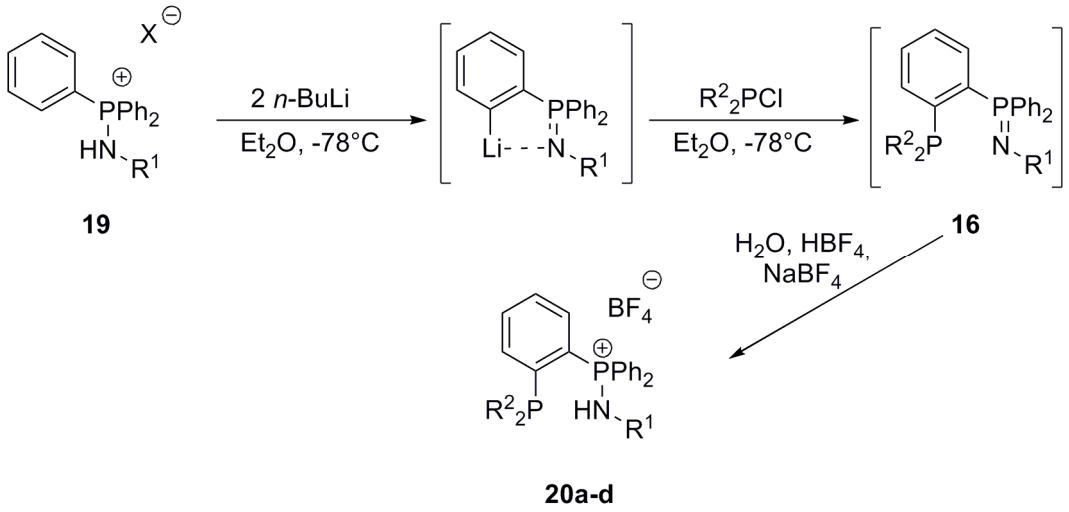

Scheme 11. Access to phosphine-iminophosphoranes **16** and phosphine-aminophosphonium tetrafluorborates **20a**-**d** as described by Boubekeur *et al.* X = Cl, Br, **a**: $R^1 = CH_2$-*t*-Bu, R^2 = Ph, **b**: R^1 = *i*-Pr, R^2 = Ph, **c**: R^1 = *t*-Bu, R^2 = Ph **d**: R^1 = *t*-Bu. R^2 = *i*-Pr.

The aminophosphonium halides are conveniently synthesized from PPh_3, bromine, and primary amine R^1NH_2 by the Kirsanov method, as outlined in scheme 3. Subsequent double-deprotonation yields the ortho-lithiated iminophosphorane intermediate, which is not isolated, but quenched with $R^2{}_2PCl$. The "free" and quite moisture sensitive iminophosphorane **16** does not need to be stored, instead, through the acidic aqueous workup, one obtains the corresponding phosphine-aminophosphonium tetrafluoroborates **20a**-**d**, which have an unlimited shelf life.

To obtain the corresponding phosphine-iminophosphoranes *in-situ*, a simple deprotonation step, either with KHMDS, *n*-BuLi, or MeLi in either THF or Et_2O is required. Metal precursors may then be added directly to this solution for coordination, as outlined in scheme 12. This direct coordination sequence avoids the need to isolate the iminophosphorane. However, some restrictions apply to the choice of base. When deprotonating **17b**,**d** with organolithium bases, unidentifiable product mixtures were obtained, which is ascribed to *ortho*-lithiation reactions due to directing ether groups on the N-aryl moiety. KHMDS was then the base of choice.

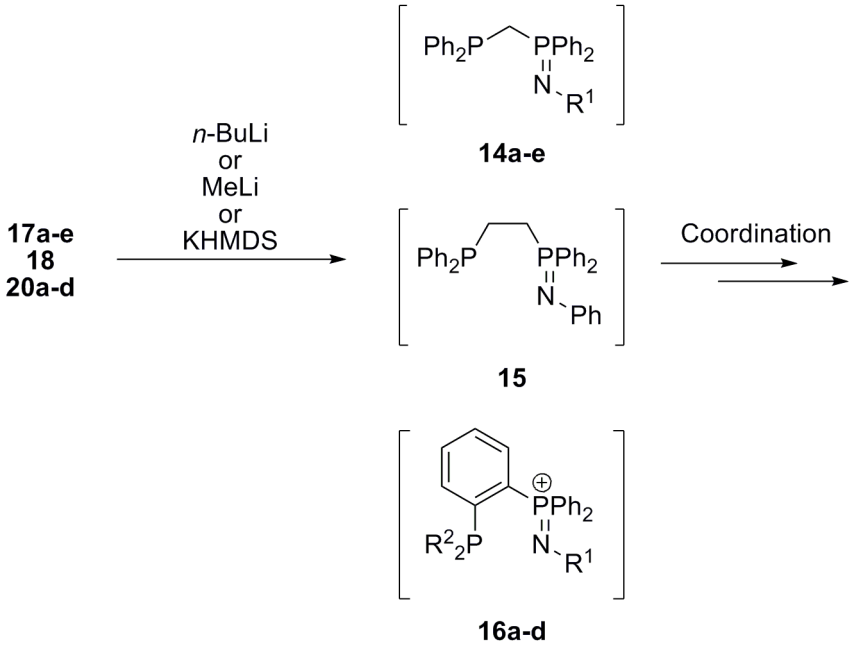

Scheme 12. Deprotonation-coordination sequence.

With ligands precursors **17a-e**, **18**, and **20a-d** at hand, the coordination properties of these ligands towards Ni(II) and Cr(III) and the activity of the resulting complexes was investigated.

2.3.2 Coordination to $[CrX_3(THF)_3]$ (X = Cl, Br)

Coordination of to **14a**-**e**, **15**, and **16a**-**d** to $[CrX_3(THF)_3]$ (X = Cl, Br) was attempted using the deprotonation-coordination sequence described above. It turned out that the bidentate ligands **14a**-**c** did not coordinate to the Cr(III) center, instead the corresponding aminophosphonium salts **17a**-**c**, **18**, and **20a**-**d** were recovered, as indicated by ^{31}P NMR spectroscopy. This reaction, which implies the presence of at least one equivalent of acid HX in the reaction mixture, was equally observed when reacting the simple iminophosphorane $Ph_3P{=}N$*t*-Bu with $[NiBr_2(DME)]$, and remains unclear, as follow-up experiments under inert atmosphere, and thorough exclusion of all traces of acids in the metal precursors used, invariably led to the same result. On the other hand, with **14d**,**e**, coordination to $[CrCl_3(THF)_3]$ and $[CrBr_3(THF)_3]$, respectively, proceeded smoothly (Scheme 13), as indicated by the complete disappearance of the signal in the ^{31}P NMR due to the paramagnetism of the Cr(III) metal center.

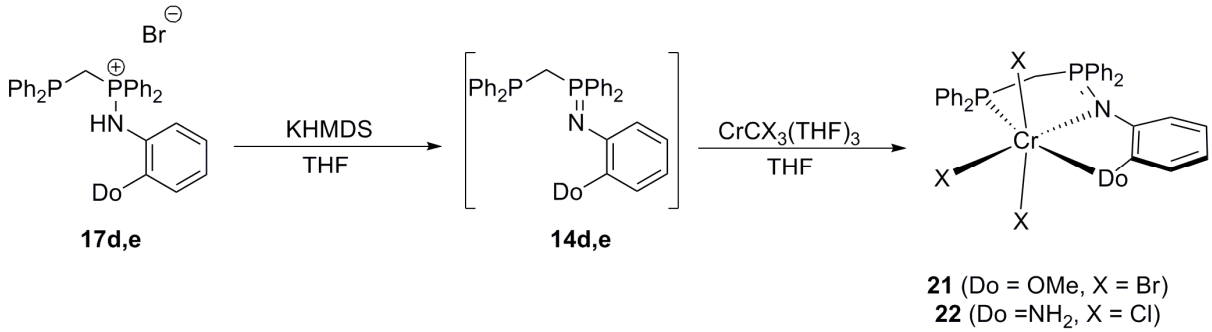

Scheme 13. Coordination of **14d** (Do = OMe) and **14e** (Do = NH_2) to Cr(III).

Of both complexes **21** and **22**, crystals suitable for x-ray structure analysis could be obtained by slow diffusion of hexane into concentrated THF (**21**) or CH_2Cl_2 (**22**) solutions of the respective compound. Figures 11 and 12 display Ortep drawings of **21** and **22**, respectively.

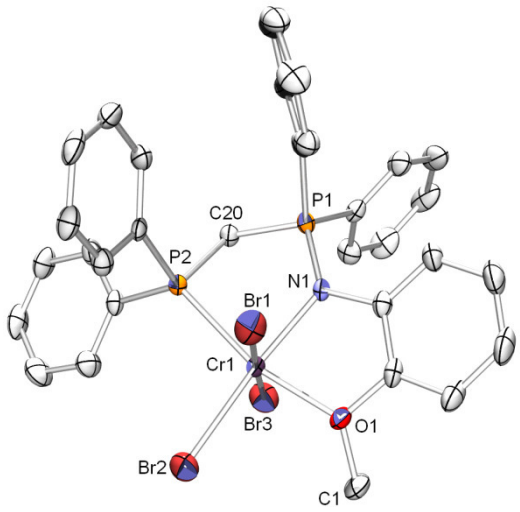

Figure 11. Ortep representation of the x-ray crystal structure of **21**. Hydrogen atoms and two THF solvent molecules present in the crystal lattice have been omitted for clarity. Thermal ellipsoids are represented at the 50% level. Important bond lengths (Å) and angles (°): Cr1-Br1 = 2.437(1), Cr1-Br2 = 2.454(1), Cr1-Br3 = 2.450(1), Cr1-O1 = 2.057(4), Cr1-N1 = 2.064(5), Cr1-P2 = 2.432(2), N1-P1 = 1.610(5), P1-C20 = 1.799(6), P2-C20 = 1.830(6), O1-Cr1-N1 = 79.7(2), O1-Cr1-P2 = 165.0(1), Br1-Cr1-Br2 = 92.26(4), Br2-Cr1-Br3 = 90.52(4), P2-Cr1-N1 = 85.5(2), Br2-Cr1-P2 = 95.85(5), N1-P1-C20 = 105.3(3), P1-C20-P2 = 112.6(3), C20-P2-Cr1 = 98.9(2).

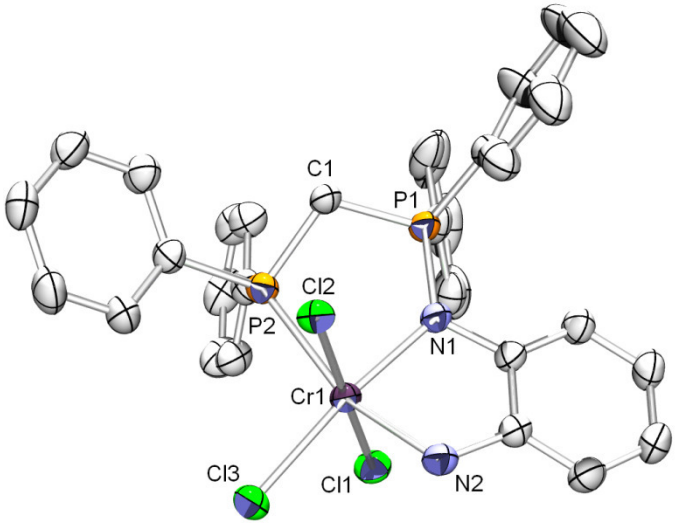

Figure 12. Ortep representation of the x-ray crystal structure of **22**. Hydrogen atoms and two THF solvent molecules present in the crystal lattice have been omitted for clarity. Thermal ellipsoids are represented at the 50% level. Important bond lengths (Å) and angles (°): Cr1-N1 = 2.054(2), Cr1-N1 = 2.064(2), Cr1-P2 = 2.5131(8), Cr1-Cl1 = 2.3117(7), Cr1-Cl2 = 2.3453(7), Cr1-Cl3 = 2.3287(7), P1-N1 = 1.612(2), P1-C1 = 1.795(2), P2-C1 = 1.834(3), N1-Cr1-N2 = 80.07(8), N1-Cr1-P2 = 84.22(6), Cr1-N1-P1 = 125.2(1), N2-Cr1-Cl1 = 90.31(7), Cl1-Cr1-C3 = 89.36(3), P1-C1-P2 = 110.7(1).

The crystal structures reveal the expected meridional tridentate (O,N,P) (in **21**) and (N,N',P) (in **22**) coordination mode of the phosphine-iminophosphorane, within a slightly distorted octahedral coordination geometry. To the best of our knowledge, **21** and **22** are the first known examples of Cr(III) complexes with mixed phosphine-iminophosphorane ligands.

2.3.3 Evaluation of 21 and 22 in Ethylene Oligomerization/Polymerization

The catalytic activity of the complexes **21** and **22** was then evaluated in the oligomerization of ethylene. The experiments were conducted at 45°C, using 300 equiv. of MAO as cocatalyst, 30 bar of ethylene pressure and toluene as solvent (catalysis runtime 30 min.). Unfortunately, only trace amounts of liquid oligomers were formed, instead, the catalysts both proved active in ethylene polymerization, yielding 6730 g(PE) × g(Cr)$^{-1}$ × h^{-1} (**21**) and 5240 g(PE) × g(Cr)$^{-1}$ × h^{-1} (**22**), respectively, of a highly insoluble polyethylene, which was not further analyzed.

2.3.4 Coordination to [$NiBr_2$(DME)][69]

As described above, Ni(II) complexes were prepared in an analogous fashion as described for the Cr(III) complexes, by addition of [$NiBr_2$(DME)] to a THF solution of the *in-situ* formed phosphine.

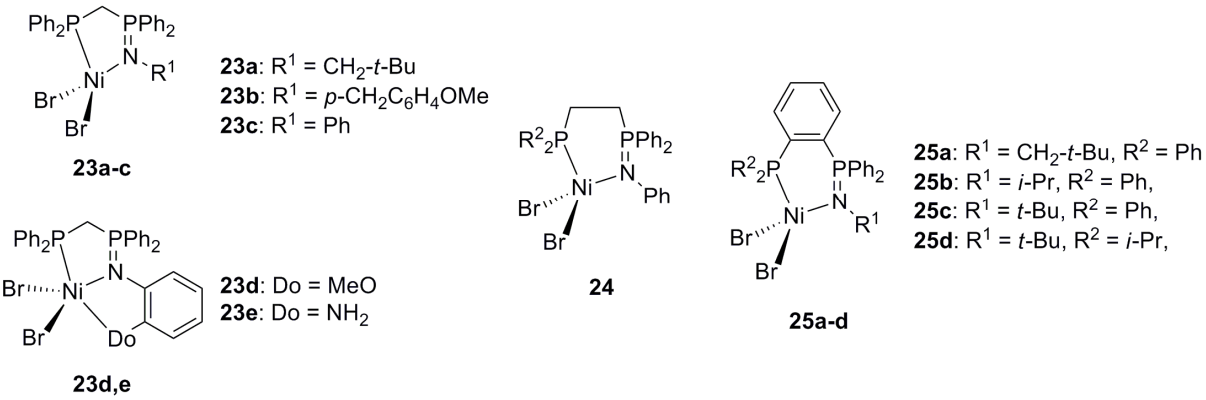

Figure 13. Prepared Ni(II)-phosphine-iminophosphorane complexes.

All coordination attempts were successful, and x-ray crystal structure could be obtained in most cases. In the case of the bidentate ligands **14a**-**c**, **15**, and **16a**-**d**, the complexes adopted invariably distorted tetrahedral geometries, whereas in the case of the tridentate ligands **14d**,**e**, a meridional coordination mode was found, the complexes adopting an overall distorted trigonal-bipramidal geometry. The paramagnetic nature of the obtained complexes precluded analysis by ^{1}H, ^{13}C, and ^{31}P NMR spectroscopy, indeed, the complete disappearance of the ^{31}P NMR signal was a good indicator for the completeness of the reaction. It should be noted here, that complex **23b** was described before by Boubekeur *et al.*[85] Figures 14 and 15 show Ortep drawings of two representative examples of the two coordination geometries obtained.

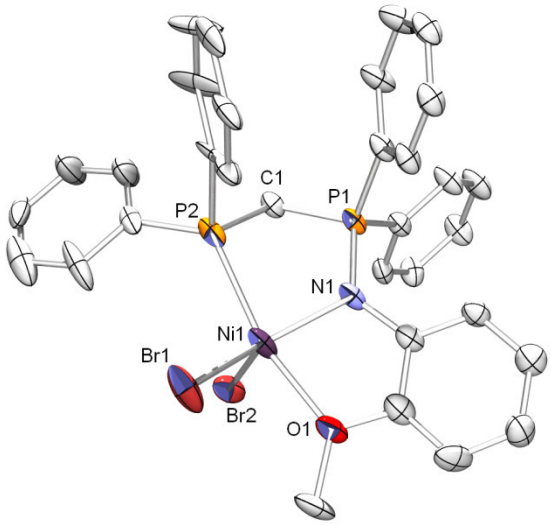

Figure 14. Ortep representation of the x-ray crystal structure of **23d**. Hydrogen atoms and disorder on one of the P2 phenyl rings have been omitted for clarity. Thermal ellipsoids are represented at the 30% level. Important bond lengths (Å) and angles (°): Ni1-Br1 = 2.438(1), Ni1-Br2 = 2.408(1), Ni1-N1 = 2.030(4), Ni1-O1 = 2.112(5), N1-P1 = 1.625(5), Ni1-P2 = 2.352(2), P1-C1 = 1.783(6), P2-C1 = 1.836(5), Br1-Ni1-Br2 = 110.37(3), Br1-Ni1-N1 = 143.0(1), O1-Ni1-N1 = 77.4(1), O1-Ni1-P2 = 165.6(1), N1-P1-C1 = 106.3(1), P1-C1-P2 = 110.4(3).

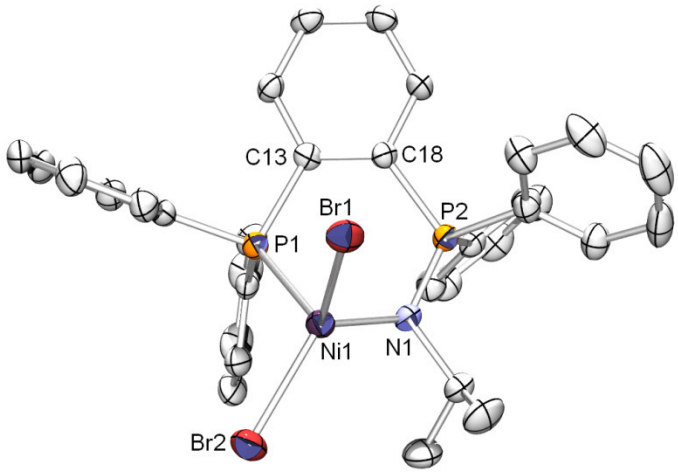

Figure 15. Ortep representation of the x-ray crystal structure of **25b**. Hydrogen atoms and two THF solvent molecules present in the crystal lattice have been omitted for clarity. Thermal ellipsoids are represented at the 50% level. Important bond lengths (Å) and angles (°): Ni1-Br1 = 2.3912(4), Ni1-Br2 = 2.3667(4), Ni1-N1 = 1.969(2), Ni1-P1 = 2.2741(7), P1-C13 = 1.824(2), P2-N1 = 1.600(2), P2-C18 = 1.813(3), C13-C18 = 1.407(3), N1-Ni1-P1 = 91.43(6), N1-Ni1-Br2 = 122.94(6), P1-Ni1-Br2 = 107.26, N1-Ni1-Br1 = 107.35(6), P1-Ni1-Br1 = 103.87(2), Br1-Ni1-Br2 = 118.68(2), C13-P1-Ni1 = 107.46(8), N1-P2-C18 = 114.1(1) P2-N1-Ni1 = 123.7(1), C18-C13-P1 = 122.(2), C13-18-P(2) = 127.2(2).

2.3.5 Evaluation of Complexes 23-25 in the Selective Dimerization of Ethylene[69]

The catalytic activities of complexes **23**-**25** in the oligomerization reaction of ethylene were evaluated. In a first set of experiments, the catalytic reactions were carried out at 45°C, at 30 bar of ethylene pressure, and in the presence of 300 equiv. of MAO as cocatalyst and toluene as solvent. Table 3 summarizes the obtained results.

Table 3. Results in the Ethylene Oligomerization reaction with complexes **23**-**25**.

Entry	Precursor	%C_4 (%1-C_4)	%C_6 (%1-C_6)	TOF / 10^3 × mol(C_2H_4) × mol(Ni)$^{-1}$ × h^{-1}.
1	**23a**	93.9 (83.4)	6.1 (32.7)	45.3
2	**23b**	92.8 (77.0)	7.2 (29.4)	65.8
3	**23c**	94.6 (85.9)	5.4 (45.1)	42.0
4	**23d**	93.7 (82.7)	6.3 (33.2)	43.9
5	**23e**	94.3 (81.7)	5.7 (37.2)	42.6
6	**24**	96.7 (57.1)	3.3 (36.3)	44.1
7	**25a**	96.3 (67.5)	3.7 (39.8)	96.7
8	**25b**	97.7(61.4)	2.3 (73.9)	106.5
9	**25c**	95.1 (67.9)	4.9 (45.8)	21.1
10	**25d**	89.8 (55.4)	10.2 (58.6)	23.6

Concerning the product distribution, only butenes and hexenes were formed, whereas only trace amounts of octenes were detected by GC in some experiments. The oligomerization process turned out to be highly selective towards the formation of butenes, with C_4 selectivities of up to 97.7%, whereas the C_6 fraction amounted to 2.3 – 10.2% of the total activity. While these selectivities lie within the range of the best performances of known catalytic systems, the observed activities are equally within the range of prior art systems or above. A closer look on the obtained results reveals that catalysts **25**, which feature a rigid six-membered ring structure (Ni-N-P-C-C-P), show higher activities than their five-membered analogs **23** and the relatively flexible structure of complex **24**. However, from the comparison of **23a** and **25a**, which have identical substitution patterns on both phosphorous and nitrogen, it becomes clear that the increased activity of **25** is accompanied by a decrease in α-selectivtiy (83.4% for **23a** vs. 67.5% for **25a**). While the nature of the nitrogen substituent R^1 does not seem to have a decisive influence on both catalyst activity and selectivity, and even the presence of the third supplemental donor group in both the (O,N,P) complex **23d** and the (N,N',P) complex **23e** does not alter significantly the catalytic properties, the influence of R^1 was significant with complexes **25a**-**d**. The presence of a bulky *t*-Bu group in **25c**,**d** significantly decreased the catalysts' activity, compared to the analogous **25a** (N-CH_2-*t*-Bu) and **25b** (N-*i*-Pr), which exhibit less bulky substitution in vicinity to the Ni metal center (entries 9, 10 vs. 7, 8 in table 3).

The basicity of the phosphine moiety in complexes **25** does not seem to have a great influence on both the C_4 and the α-selectivity of the oligomerization reaction, which becomes apparent upon comparison of the catalytic results obtained with complexes **25c** and **25d** (entries 9 and 10 in table 3).

On the basis of these results we then focused on catalyst lifetime issues as well as the effect of temperature on the catalysis outcome. Complex **25b** was chosen due to its superior performance. Oligomerization runs were carried out both at room temperature and at 45°C and the reactions were quenched either after 20 minutes or 1 h, using 300 equiv. of MAO. The results of these catalytic runs are presented in table 4.

Table 4. Oligomerization results for **25b** at 45°C and r.t. and at different catalysis run times.

Entry	T/°C	run time	$\%C_4$ ($\%1\text{-}C_4$)	$\%C_6$ ($\%1\text{-}C_6$)	TOF / $10^3 \times mol(C_2H_4) \times mol(Ni)^{-1} \times h^{-1}$.
1	45	1 h	97.7 (61.4)	2.3 (73.9)	106.5
2	r.t.	1 h	97.1 (73.6)	2.9 (59.3)	166.0
3	45	20 min.	96.6 (68.0)	3.4 (52.1)	248.8
4	r.t.	20 min	96.7 (72.9)	3.3 (49.7)	324.5

The first obvious result is the activity increase obtained when lowering the temperature from 106.5 × 10^3 mol(C_2H_4) × mol(Ni)$^{-1}$ × h^{-1} at 45°C to 166.0 × 10^3 mol(C_2H_4) × mol(Ni)$^{-1}$ × h^{-1} at r.t. at 20°C, accompanied by a slight improvement in 1-butene selectivity (61.4% to 73.6%). This result might be due to an improved solubility of the gaseous ethylene in the reaction mixture at lower temperature. However, the activity increase by factor 2 (324.5 × 10^3 mol(C_2H_4) × mol(Ni)$^{-1}$ × h^{-1} vs. 166.0 × 10^3 mol(C_2H_4) × mol(Ni)$^{-1}$ × h^{-1}) upon shortening the catalysis run time to 20 minutes is indicative of either a short catalyst lifetime, or, possibly due to product accumulation and thus a concomitant decrease in ethylene concentration, as the catalytic runs were carried out in a semi-batch mode.

2.4 (N,S)-Iminophosphorane Ligands

As mentioned in the previous sections, (N,O) and (N,P) mixed ligand systems have found relatively widespread application in nickel catalyzed ethylene oligomerization and polymerization. Compared to this, (N,S) systems have attracted much less attention. DuPont disclosed a series of imine-thioether and imine-thiophene ligands, whose complexes with late transition metal centers were claimed to be active ethylene oligomerization/polymerization.[88] McGuinness *et al.*[89] devised a symmetrical tridentate $(RS(CH_2)_2)_2NH$ (R = alkyl) ligand, coordinated to Cr(III), which shows excellent activity in the selective ethylene trimerization reaction, while Zhang *et al.* reported on Cr(III) complexes **X** (Figure 16) with bis(pyrazolyl) ligands bearing a pendant thioether group, which were found to selectively trimerize ethylene (98.9%, α-selectivty: up to 99.6%).[90] Carpentier and colleagues reported on a pentacoordinated Ni(II) complex **Y** (Figure 16), bearing a sulfur-bridged tridentate bis(pyrazolyl) ligand, which was found to be highly active (81.0 × 10^3 mol(C_2H_4) × mol(Ni)$^{-1}$ × h^{-1}) in the selective

dimerization of ethylene.[91] Upon activation with 250 equiv. of MAO, and at 40 bar of ethylene pressure, a C_4 selectivity of 98.6% (82.2% of 1-butene) was achieved.

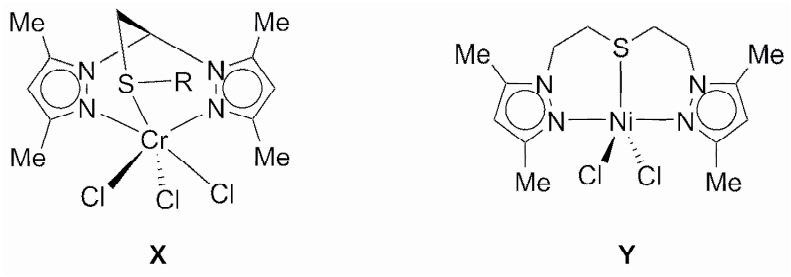

Figure 16.

However, aside the mentioned systems, to the best of our knowledge, no Ni based catalytic system with mixed unsymmetrical (N,S) ligands has yet been disclosed. Given the established *ortho*-lithiation strategy of iminophosphoranes described above, we decided to enlarge the range available of iminophosphoranes with supplemental donor sites by the (N,S) type of mixed ligands (Figure 17).

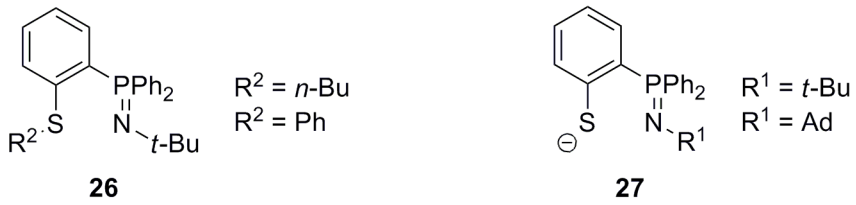

Figure 17. Neutral thioether-iminophosphorane (**26**) and anionic thiophenolato-iminophosphorane (**27**) ligands.

2.4.1 Synthesis of Thioether-Iminophosphoranes 26

Starting from the stable aminophosphonium salts $[Ph_3P\text{-}N(H)\text{-}t\text{-}Bu]^+[X]^-$, (X = Cl, Br) which is easily obtained by the above described Kirsanov reaction, the addition of two equivalents of either *n*-BuLi or MeLi yields a *ortho*-lithiated iminophosphorane, which is, in an analogous fashion to the syntheses described above, not isolated, but immediately quenched with the corresponding disulfide $R^2\text{-}S\text{-}S\text{-}R^2$ (Scheme 14).

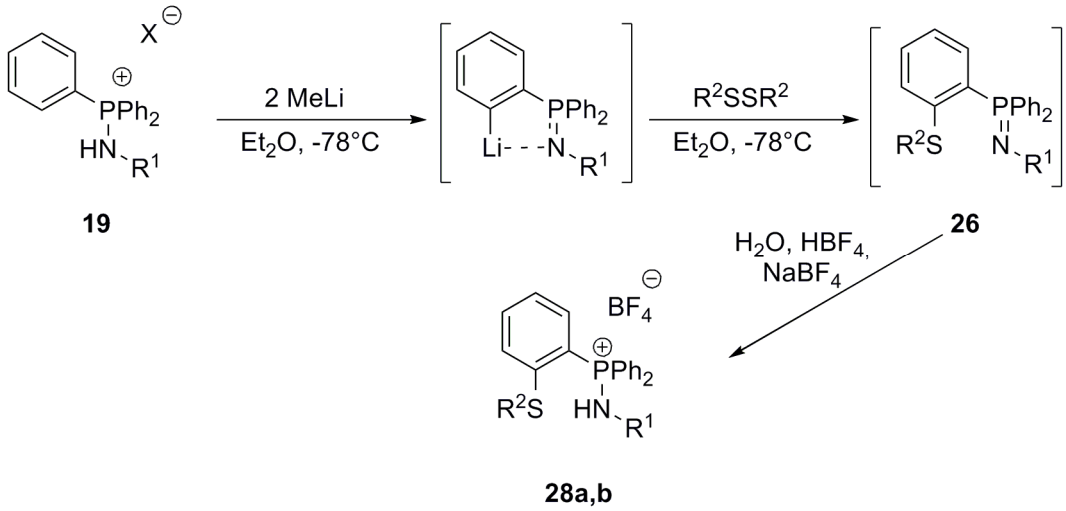

Scheme 14. Access to thioether-iminophosphoranes **26** and thioether-aminophosphonium tetrafluorborates **28a**,**b**. X = Cl, Br, **a**: R^1 = *t*-Bu, R^2 = Ph, **b**: R^1 = *t*-Bu, R^2 = *n*-Bu.

As described in the previous sections on N,O and N,P mixed iminophosphorane ligands, the obtained aminophosphonium salts **28a**,**b** again represent convenient precursors, stable to air and water, which can easily transformed to the free iminophosphorane **26** by simple deprotonation. Of compound **28a**, crystals suitable for x-ray crystal structure analysis could be obtained by slow evaporation of a concentrated CH_2Cl_2 solution. An Ortep drawing is presented in figure 17.

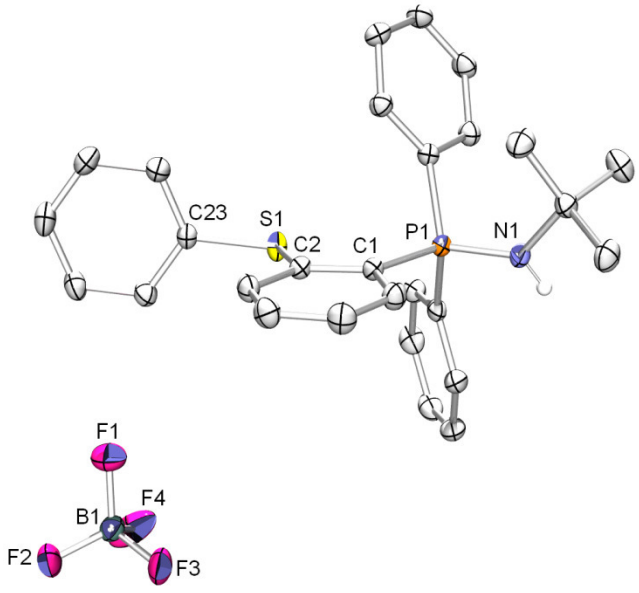

Figure 17. Ortep representation of the x-ray crystal structure of **28a**. Hydrogen atoms (except the one on N1) have been omitted for clarity. Thermal ellipsoids are represented at the 50% level. Important bond lengths (Å) and angles (°): P1-N1 = 1.628(1), P1-C1 = 1.813(1), C1-C2 = 1.418(2), C2-S2 = 1.777(1), S1-C23 = 1.775(1), N1-P1-C1 = 111.27(6), P1-C1-C2 = 123.6(1), C1-C2-S1 = 120.2(1), C2-S1-C23 = 102.34(6).

However, as in the case of the neutral ether-iminophosphoranes **2**, subsequent coordination attempts of the in-situ formed **26** to various group 10 metal precursors ($[Pd(allyl)Cl]_2$, $[PdCl_2(SMe)_2]$, $[NiBr_2(DME)]$) proved unsuccessful, even after prolonged reaction times and at reaction temperatures of up to 60°C. The probably rather low affinity of the hard-donor iminophosphorane moiety with electron-rich late metal centers and the weak donor strength of the thioether group is presumably at the origin of his failure. Work on this ligand class was thus discontinued.

2.4.2 Synthesis of Thiophenolato-Iminophosphoranes 27

Quenching of the free *ortho*-lithiated iminophosphorane with elemental sulfur was successfully employed to gain access to a new class (N,S) mixed iminophosphorane ligands. (Scheme 15) While in the above cited cases the *ortho*-lithiation reaction and the subsequent quenching either with a chlorophosphine $R^2{}_2PCl$ or a disulfide R^2-S-S-R^2 could be either carried out in Et_2O or THF, the quenching reaction with S_8 has necessarily to be carried out in THF, probably due to the even poorer solubility of sulfur in Et_2O compared to THF. Completeness of the reaction is checked by $^{31}P\{^1H\}$ NMR with the appearance of a characteristic peak at δ = 12.9 ppm (R^1 = *t*-Bu) and δ = 12.6 ppm (R^1 = Ad), respectively. Acidic workup with $HBF_4/NaBF_4/H_2O$ yields the tetrafluoroborate salts **29a**,**b** as off-white colored powders.

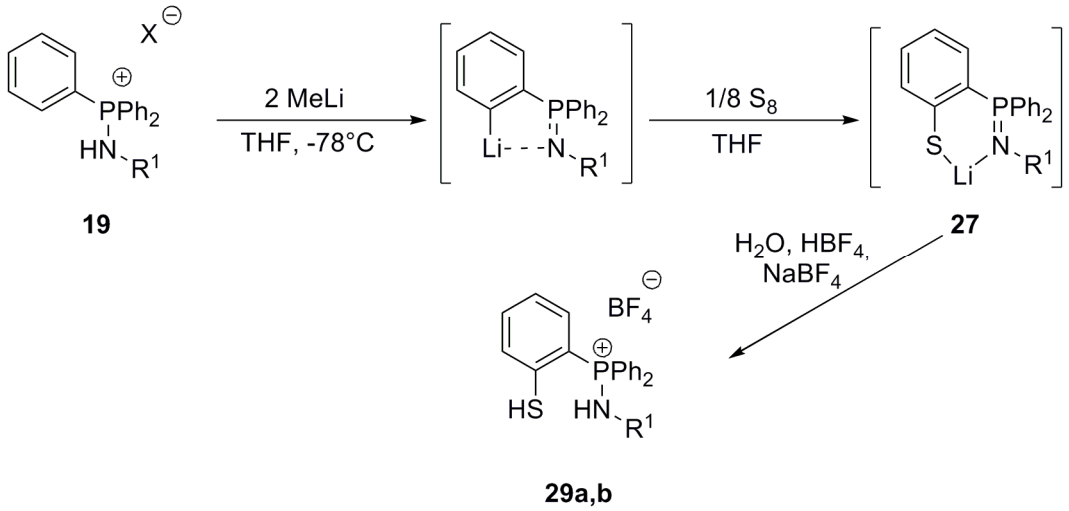

Scheme 15. Access to thiophenolato-iminophosphoranes (Li^+)**27** and thioether-aminophosphonium tetrafluorborates **29a**,**b**. X = Cl, Br, **a**: R^1 = *t*-Bu, **b**: R^1 = Ad.

Single crystals suitable for x-ray crystal structure analysis could be obtained by slow evaporation of a concentrated CH_2Cl_2 solution of **29a**, confirming the thiol functionalization. (Figure 18).

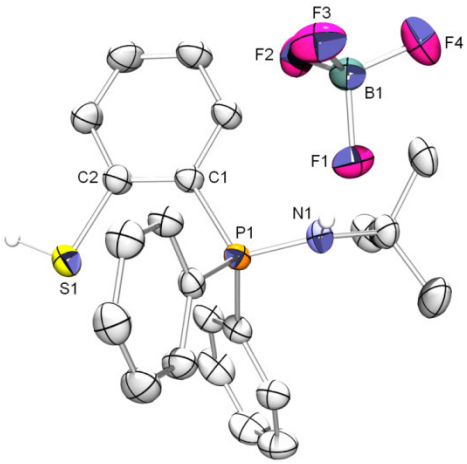

Figure 18. Ortep representation of the x-ray crystal structure of **29a**. Hydrogen atoms (except those on N1 and S1) have been omitted for clarity. Thermal ellipsoids are represented at the 50% level. Important bond lengths (Å) and angles (°): P1-N1 = 1.623(1), P1-C1 = 1.807(2), C1-C2 = 1.405(2), C2-S1 = 1.781(2), N1-P1-C1 = 113.66(7), P1-C1-C2 = 123.4(1), C1-C2-S1 = 120.6(1).

While the lithiation reaction proceeded in the desired fashion with the N-alkyl derivatives of the aminophosphonium salts **19**, a peculiar reactivity was observed with the N-Ph derivative, as only the lithiation with MeLi was successful, whereas the otherwise successful use of *n*-BuLi led to unidentifiable product mixtures. One first indication of this was the comparatively low field shift of δ = 24.2 ppm in $^{31}P\{^{1}H\}$ NMR of the lithiated species **30**,[92] compared to the chemical shift of the N-*t*-Bu (9 ppm) and the N-Ad (8.6 ppm) derivatives, as well as the precipitation of this species as a white powder from the THF solution. ^{1}H and ^{13}C spectroscopy are consistent with the structure **30** displayed in scheme 16 and those reported by Lopez-Ortiz *et al.*[92] Reaction with elemental sulfur and subsequent work up with $HBF_4/NaBF_4/H_2O$ led to the thiomethyl-aminophosphonium tetrafluoroborate **31**. Quenching with Ph_2PCl, followed by acidic aqueous work up yielded the phosphine-aminophosphonium salt **17c** in 75% yield (Scheme 16).

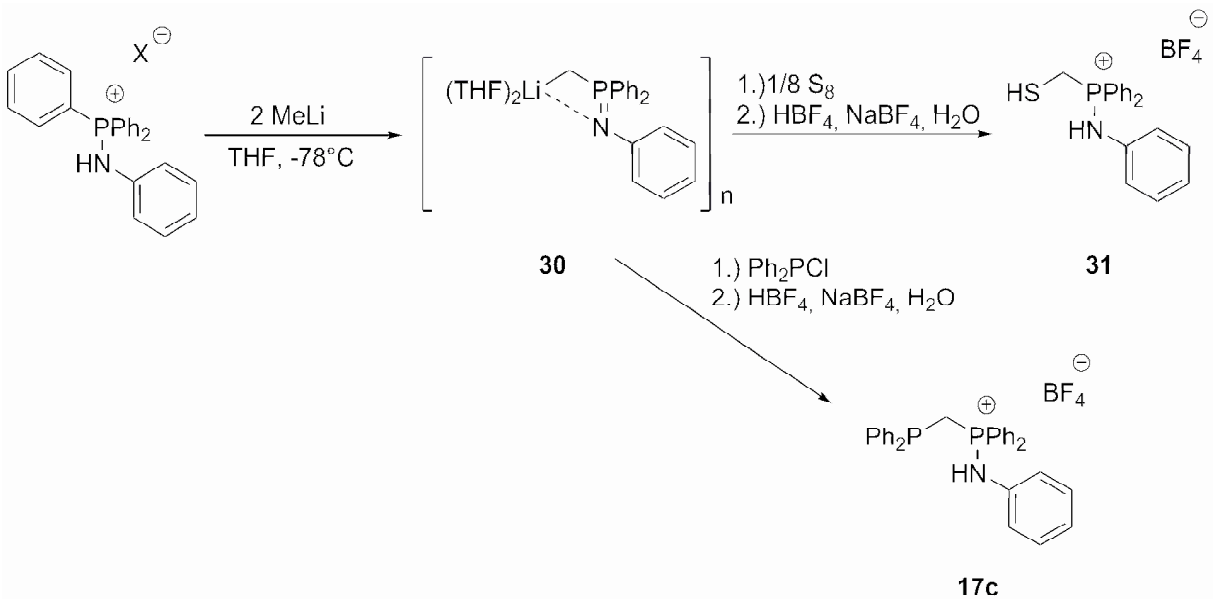

Scheme 16. Lithiation of $[Ph_3P\text{-}N(H)Ph]^+[X]^-$ (X = Cl, Br) with MeLi and subsequent quenching reactions.

While this reaction, to the best of our knowledge, has not been reported on iminophosphoranes, similar reactivities have been reported by Seyferth *et al.* upon reaction of triphenylphosphine oxide or triphenylphosphine sulfide with benzylmagnesium compounds.[93,94]

The observed products **30**, **31**, and **17c** point towards a mechanism involving nucleophilic attack of a methyl anion on the pentavalent tetracoordinated phosphonium center, which is probably facilitated by the charge accepting property of the N-Ph group across the iminophosphorane nitrogen atom (Scheme 17). Either in a concerted fashion with the approach of the Me^- anion via a pentacoordinated transition state ("S_N2 type mechanism"), or subsequent to the Me^- attack ("S_N1 type mechanism"), one P-Ph bond is cleaved, liberating a Ph^- anion, which deprotonates the newly formed P-CH_3 group. This being only a putative mechanistic scenario, further studies using theoretical methods are necessary to ascertain these proposals.

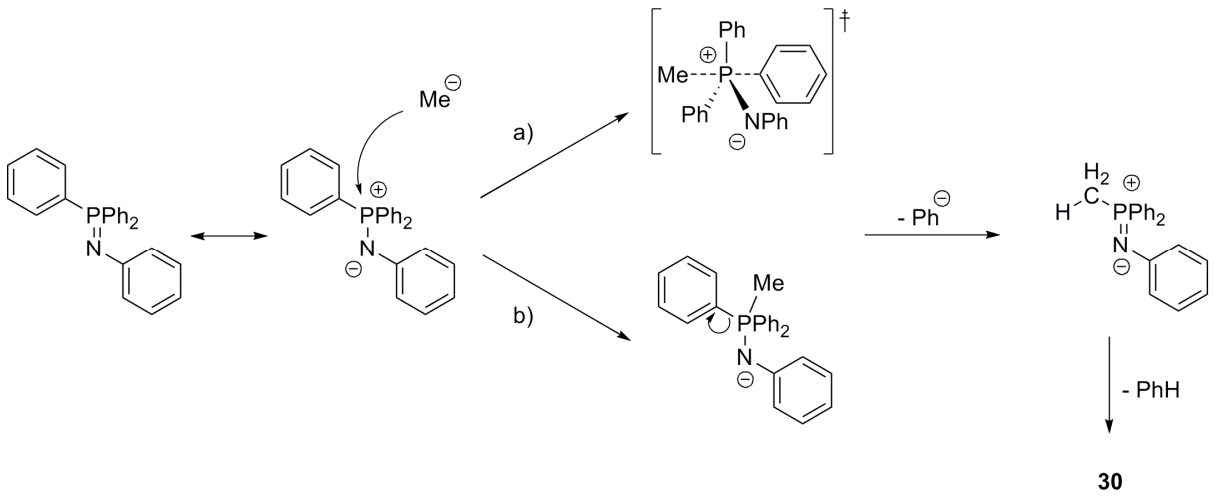

Scheme 17. Putative mechanism for the formation of **30** via (a) a concerted "S_N2-type" or (b) a stepwise "S_N1-type" pathway.

2.4.3 Coordination of 29a,b to Pd(II) and Rh(I)

As with the before mentioned (N,O) mixed iminophosphorane ligands, the coordination behavior of the novel (N,S) mixed iminophosphoranes towards Pd(II) and Rh(I) metal centers was evaluated (Scheme 18). Contrary to the case of the (N,O) ligands, double deprotonation with MeLi, and thus formation of a lithio-thiolate did not hinder subsequent coordination to the transition metal centers. Coordination of $[PdCl_2(PPh_3)_2]$ was carried out in THF; completeness of the reaction was indicated by the apparition of two doublet peaks for the coordinated PPh_3 and the iminophosphorane moiety, respectively, at δ = 15.39 ppm and δ = 31.77 ppm (^3J(P,P) = 3.4 Hz) in the $^{31}P\{^1H\}$ NMR, apart from the singulet peak of the liberated PPh_3, indicating the formation of the palladium complex **32a**. In order to simplify the synthetic procedure, $[PdCl_2(PPh_3)_2]$ was directly added to a solution of (Li^+)**27** (R^1 = *t*-Bu), which had been prepared freshly from aminophosphonium salt **19** (R^1 = *t*-Bu, X = Br) via the procedure outlined in scheme 15. A second set of doublets at δ = 15.49 ppm and 31.27 ppm (^3J(P,P) = 3.4 Hz) was observed in $^{31}P\{^1H\}$ NMR, which became the only signal (besides the PPh_3 signal), when excess quantities of LiBr were added.

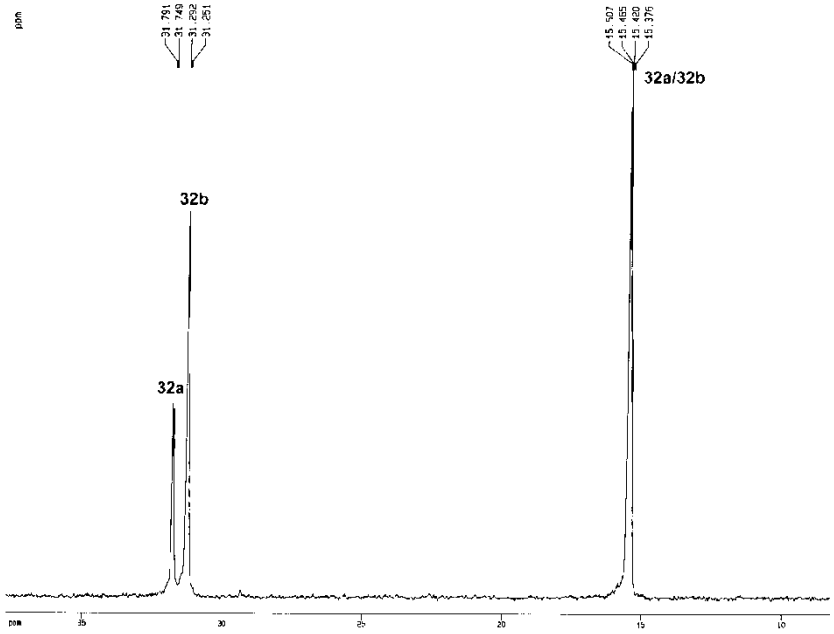

Scheme 18. $^{31}P\{^{1}H\}$ NMR spectrum (in THF) of the **32a/32b** product mixture.

This second doublet was thus attributed to the product **32b**, resulting from the complete Cl/Br exchange reaction on the palladium center. Single crystals of **32b** could be grown by diffusion of hexane into a concentrated CH_2Cl_2 solution of **32b**. Figure 19 displays an Ortep representation of the molecular structure.

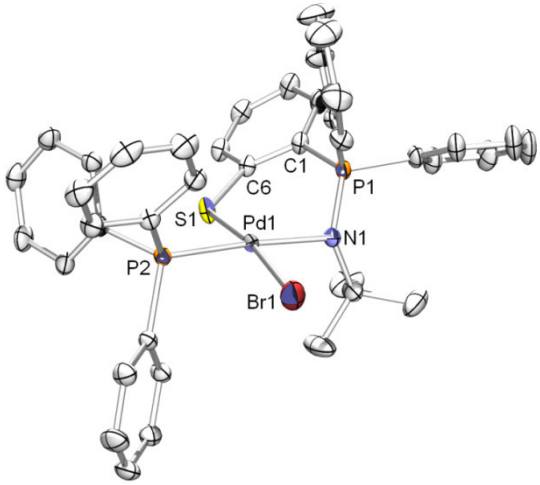

Figure 19. Ortep representation of the x-ray crystal structure of **32b**. Hydrogen atoms and a CH_2Cl_2 solvent molecule present in the crystal lattice have been omitted for clarity. Thermal ellipsoids are represented at the 50% level. Important bond lengths (Å) and angles (°): Pd1-N1 = 2.116(2), Pd1-S1 = 2.283(1), Pd1-P2 = 2.2676(8), Pd1-Br1 = 2.4781(6), N1-P1 = 1.608(3), P1-C1 = 1.809(3), C1-C6 = 1.409(4), C6-S1 = 1.757(3), S1-Pd1-P2 = 90.51(3), S1-Pd1-N1 = 92.53(8), N1-Pd1-Br1 = 91.97(8), P2-Pd1-Br1 = 84.65(3), Pd1-N1-P1 = 109.3(1), P1-C1-C6 = 119.7(2), C1-C6-S1 = 128.3(2), C6-S1-Pd1 = 115.4(1).

Coordination of (Li^+)**27** (R^1 = *t*-Bu) to $[Rh(cod)Cl]_2$ in THF proceeded smoothly, as indicated by the immediate color change of the reaction mixture to yellow and the appearance of a singulet peak at 22.9 ppm in the $^{31}P\{^1H\}$ NMR spectrum of the reaction mixture. After purification, complex 33 could be obtained as a yellow powder in 61% yield. Crystals suitable for x-ray crystal analysis could be obtained by slow diffusion of hexane into a concentrated CH_2Cl_2 solution of the complex. An Ortep presentation of the molecular structure of **33** is presented in figure 20.

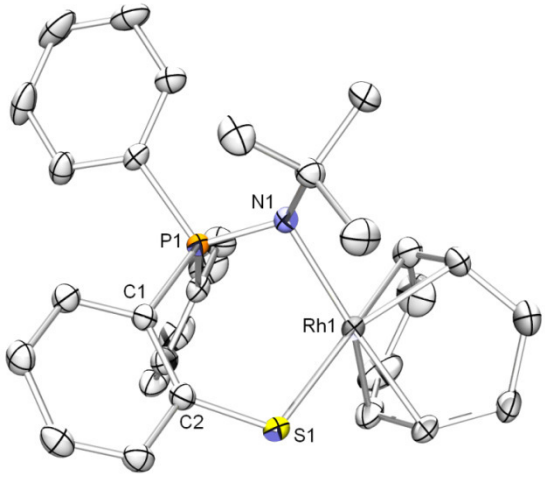

Figure 20. Ortep representation of the x-ray crystal structure of **33**. Hydrogen atoms have been omitted for clarity. Thermal ellipsoids are represented at the 50% level. Important bond lengths (Å) and angles (°): Rh1-N1 = 2.205(1), Rh1-S1 = 2.3397(5), N1-P1 = 1.600(1), P1-C1 = 1.814(2), C1-C2 = 1.418(2), C2-S1 = 1.748(2), S1-Rh1-N1 = 94.11(4), Rh1-N1-P1 = 103.13(7), N1-P1-C1 = 116.36(8), P1-C1-C2 = 118.1(1), C1-C2-S1 = 126.0(1), C2-S1-Rh1 = 117.75(6).

2.4.4 Coordination of 29a,b to Ni(II) and Evaluation in the Oligomerization of Ethylene

Ligands **29a**,**b** were equally evaluated with respect to their coordination properties towards $[NiBr_2(DME)]$ after double deprotonation with MeLi. A color change to green of the reaction mixture in the case of **29a**,**b** accompanied by a complete disappearance of the ^{31}P NMR signal indicated coordination. Probably due to the paramagnetism of the Ni(II) metal center, ^1H and ^{13}C NMR spectroscopy yielded only broad unexploitable signals. Unfortunately, attempts to grow single crystals of **34a**,**b** have remained futile despite numerous attempts with various solvent systems and crystallization techniques.

Assuming a molecular structure analogous to **10b**, complexes **34a**,**b** were preliminarily evaluated in the ethylene oligomerization reaction in the presence of excess quantities of MAO (300 equiv.) and Et_2AlCl (10 equiv.) at 45°C in toluene (run time 30 min.) (Table 5).

Table 5. Results in the Ethylene Oligomerization reaction with complexes **34a**,**b**.

Entry	Precursor	$\%C_4$ ($\%1\text{-}C_4$)	$\%C_6$ ($\%1\text{-}C_6$)	$\%C_8$ ($\%1\text{-}C_8$)	TOF / $10^3 \times mol(C_2H_4) \times mol(Ni)^{-1} \times h^{-1}$.
1[a]	**34a**	94 (81)	4 (43)	2 (68)	77.3
2[b]	**34a**	traces	traces	-	-
3[a]	**34b**	94 (81)	5 (33)	1 (64)	62.6

[a] MAO (300 equiv.); [b] Et_2AlCl (10 equiv.)

While Et_2AlCl was found not to be an effective activator, and only trace amounts of butenes and hexenes were formed, an activity of 77.3 $10^3 \times mol(C_2H_4) \times mol(Ni)^{-1} \times h^{-1}$ was observed with catalyst **34a**. Whereas the activity of the bulkier N-Ad derivative **34b** was slightly lower (62.6 $10^3 \times mol(C_2H_4) \times mol(Ni)^{-1} \times h^{-1}$), the C_4 selectivity (94%) and the selectivity towards 1-butene (81%) were essentially equal. This activity variation depending on the steric bulk of the nitrogen substituent R^1, is analogous to the one observed with (N,P) mixed iminophosphorane-Ni complexes **25**.

3. Conclusion and Perspectives

Novel bidentate mixed (N,O) and (N,S) iminophosphorane ligands were prepared via two different synthetic approaches. The coordination behavior of these new ligands towards Pd(II), Rh(I), and Ni(II) was investigated. Whereas coordination of the neutral (N,O) ether-iminophosphorane and (N,S) thioether-iminophosphoranes ligands, respectively, proved unsuccessful, their anionic phenolato-iminophosphoranes and thioether-iminophosphorane analogues did coordinate to the metal halides under elimination of alkali metal halides. The Ni-(N,O), Ni-(N,S), and the related Ni-(N,P) phosphine-iminophosphorane complexes were evaluated in the ethylene oligomerization reaction after activation with either MAO or Et_2AlCl. While Et_2AlCl was found not to be effective as activator to these complexes, catalytic tests with excess quantities of MAO revealed high activities in oligomerization and good selectivities towards the formation of butenes and α-selectivities (towards 1-butene) of up to 88%. These results compare favorably with the best reported catalytic systems for this transformation. Further work is necessary to optimize these results, mainly by careful adaption of the catalysis reaction conditions (temperature, pressure) and of the process regime.

It was furthermore found that the iminophosphorane $Ph_3P{=}NPh$ undergoes cleavage of the P-Ph bond upon reaction with MeLi, followed by addition of the Me group to the phosphorous moiety. Due to its inherent acidity, this methyl group is lithiated. Subsequent quenching with electrophiles, which has been demonstrated here with sulfur and Ph_2PCl, opens an access to a new class of mixed iminophosphorane ligands, whose potential will have to be evaluated.

The synthetic access to the (N,O) phenolato-iminophosphorane ligands may be extended further by the use of diamines, to yield polydentate (N,N,O,O)-type ligands, whose, diimine analogs, known as salen ligands,[95] have found widespread application in various catalytic transformations, notably in the (stereoselective) Jacobsen epoxidation.[96,97] Through the use of enatiomerically pure amines, ligands acting as steric inductors for asymmetric catalytic transformations are accessible. We have prepared a representative bis(aminophosphonium) salt ligand precursor **35**, using the protected triphenylphosphine derivative **4** and the racemic (*1R*,*2R*) and (*1S*,*2S*) mixture of *trans*-1,2-diaminocyclohexane (Scheme 19).

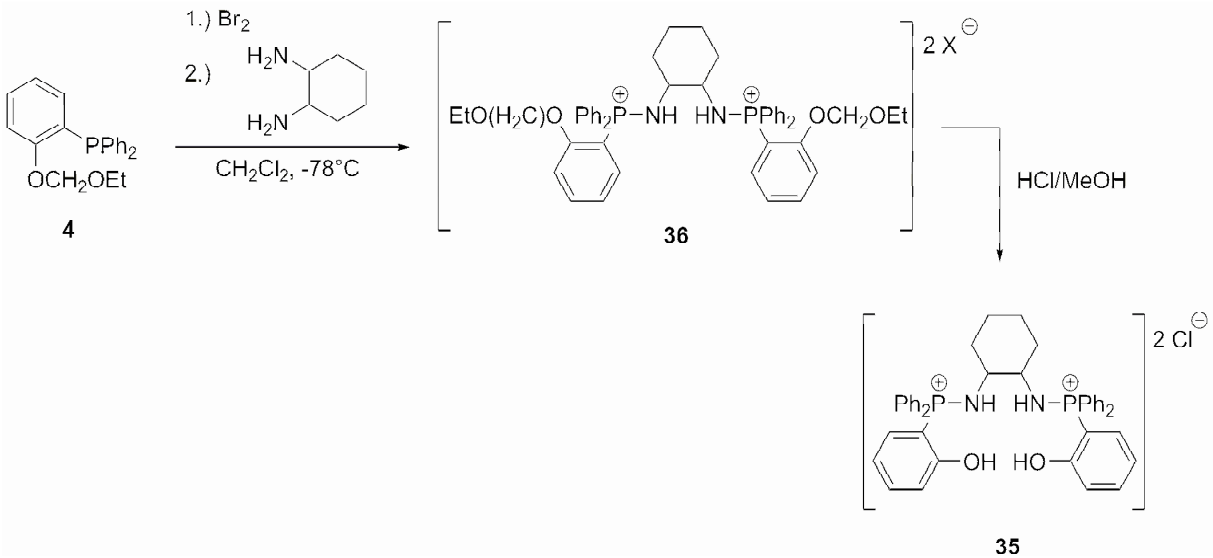

Scheme 19. Synthesis of bis(aminophosphonium) salen analogues. X may be Cl, Br, depending on workup procedure.

Crystals suitable for x-ray structure analysis could be grown from a concentrated THF solution of the protected bis(aminophosphonium) intermediate **36** (Figure 21). Since the enantiopure form of this diamine is equally available, this synthesis could potentially furnish an enatiopure form of this ligand, whose coordination properties would have to be evaluated.

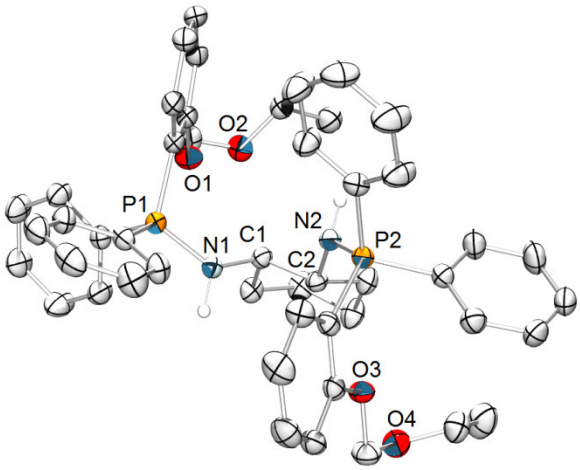

Figure 21. Ortep representation of the x-ray crystal structure of **36**. Only the (*1R*,*2R*) enantiomer is displayed. Two chloride counteranions and hydrogen atoms (except those on N1 and N2) have been omitted for clarity. Thermal ellipsoids are represented at the 50% level. Important bond lengths (Å) and angles (°): P1-N1 = 1.616(2), P2-N2 = 1.617(2), N1-C1 = 1.480(3), N2-C2 = 1.491(3), C1-C2 = 1.534(3), P1-N1-C1 = 127.2(2), P2-N2-C2 = 128.8(2), N1-C1-C2 = 108.1(2), N2-C2-C1 = 107.9(2).

4. Bibliography

[1] H. Staudinger, J. Meyer, *Helv. Chim. Acta* **1919**, *2*, 635.
[2] R. Schwesinger, H. Schlemper, *Angew. Chem. Interl. Ed.* **1987**, *26*, 1167.
[3] R. Schwesinger, J. Willaredt, H. Schlemper, M. Keller, D. Schmitt, H. Fritz, *Chem. Ber.* **1994**, *127*, 2435.
[4] F. Palacios, C. Alonso, D. Aparicio, G. Rubiales, J. M. de los Santos, *Tetrahedron* **2007**, *63*, 523.
[5] S. Shah, J. D. Protasiewicz, *Coord. Chem. Rev.* **2000**, *210*, 181.
[6] A. Steiner, S. Zacchini, P. I. Richards, *Coord. Chem. Rev.* **2002**, *227*, 193.
[7] V. Chandrasekhar, P. Thilagar, B. Murugesa Pandian, *Coord. Chem. Rev.* **2007**, *251*, 1045.
[8] H. R. Allcock, *Curr. Op. Sol. St. Mat. Sci.* **2006**, *10*, 231.
[9] M. Gleria, R. De Jaeger, *J. Inorg. Organomet. Polym. Mat.* **2001**, *11*, 1.
[10] Y. G. Gololobov, I. N. Zhmurova, L. F. Kasukhin, *Tetrahedron* **1981**, *37*, 437.
[11] Y. G. Gololobov, L. F. Kasukhin, *Tetrahedron* **1992**, *48*, 1353.
[12] M. Alajarin, C. Conesa, H. S. Rzepa, *J. Chem. Soc. Perkin Trans. 2* **1999**, 1811.
[13] C. Widauer, H. Grutzmacher, I. Shevchenko, V. Gramlich, *Eur. J. Inorg. Chem.* **1999**, 1659.
[14] A. V. Kirsanov, *Izvestiya Akademii Nauk Sssr-Seriya Khimicheskaya* **1950**, 426.
[15] I. N. Zhmurova, A. V. Kirsanov, *J. Gen. Chem. USSR* **1961**, *31*, 3440.
[16] I. N. Zhmurova, A. V. Kirsanov, *J. Gen. Chem. USSR* **1962**, *32*, 2540.
[17] I. N. Zhmurova, A. V. Kirsanov, *J. Gen. Chem. USSR* **1963**, *33*, 1004.
[18] L. Horner, H. Oediger, *Just. Lieb. Ann. Chem.* **1959**, *627*, 142.
[19] H. J. Niolas, D. Martin, *Tetrahedron Lett.* **1978**, 4031.
[20] D. G. Gilheany, *Chem. Rev.* **2002**, *94*, 1339.
[21] N. Kocher, D. Leusser, A. Murso, D. Stalke, *Chem. Eur. J.* **2004**, *10*, 3622.
[22] W. Kutzelnigg, *Angew. Chem. Intl. Ed.* **1984**, *23*, 272.
[23] A. E. Reed, P. v. R. Schleyer, *J. Am. Chem. Soc.* **2002**, *112*, 1434.
[24] E. Magnusson, *J. Am. Chem. Soc.* **2002**, *115*, 1051.
[25] J. A. Dobado, H. Martinez-Garcia, Molina, M. R. Sundberg, *J. Am. Chem. Soc.* **1998**, *120*, 8461.
[26] L. Boubekeur, *Ph. D Thesis*, Ecole Polytechnique, Palaiseau, France, **2006**.
[27] T. P. A. Cao, *M. Sc. report*, Ecole Polytechnique, Palaiseau, **2009**.
[28] R. G. Pearson, *J. Am. Chem. Soc.* **1963**, *85*, 3533.
[29] M. T. Reetz, E. Bohres, R. Goddard, *Chem. Commun.* **1998**, 935.
[30] A. Buchard, B. Komly, A. Auffrant, X. F. Le Goff, P. L. Floch, *Organometallics* **2008**, *27*, 4380.
[31] A. Buchard, H. Heuclin, A. Auffrant, X. F. L. Goff, P. L. Floch, *Dalton Transactions* **2009**, 1659.
[32] L. Boubekeur, S. Ulmer, L. Ricard, N. Mezailles, P. Le Floch, *Organometallics* **2005**, *25*, 315.
[33] V. Cadierno, P. Crochet, J. Diez, J. Garcia-Alvarez, S. E. Garcia-Garrido, S. Garcia-Granda, J. Gimeno, M. A. Rodriguez, *Dalton Trans.* **2003**, 3240.
[34] V. Cadierno, P. Crochet, J. Garcia-Alvarez, S. E. Garcia-Garrido, J. Gimeno, *J. Organomet. Chem.* **2002**, *663*, 32.
[35] V. Cadierno, J. Diez, S. E. Garcia-Garrido, S. Garcia-Granda, J. Gimeno, *J. Chem. Soc. Dalton Trans.* **2002**, 1465.
[36] M. Sauthier, J. Fornies-Camer, L. Toupet, R. Reau, *Organometallics* **2000**, *19*, 553.
[37] M. Sauthier, F. Leca, R. F. de Souza, K. Bernardo-Gusmao, L. F. T. Queiroz, L. Toupet, R. Reau, *New J. Chem.* **2002**, *26*, 630.
[38] K. Bernardo-Gusmão, L. F. Trevisan Queiroz, R. F. de Souza, F. Leca, C. Loup, R. Réau, *J. Catal.* **2003**, *219*, 59.
[39] L. Beaufort, F. Benvenuti, L. Delaude, A. F. Noels, *J. Mol. Catal. A: Chem.* **2008**, *283*, 77.
[40] L. Beaufort, D. Jan, F. Benvenuti, A. F. Noels, Pat. Appl. EP1402949 (to Solvay), **2004**.
[41] K. Kreischer, J. Kipke, M. Bauerfeind, J. Sundermeyer, *Z. Anorg. Allgem. Chem.* **2001**, *627*, 1023.

[42] F. Speiser, P. Braunstein, L. Saussine, *Acc. Chem. Res.* **2005**, *38*, 784.
[43] S. D. Ittel, L. K. Johnson, M. Brookhart, *Chem. Rev.* **2000**, *100*, 1169.
[44] G. J. P. Britovsek, V. C. Gibson, D. F. Wass, *Angew. Chem. Intl. Ed.* **1999**, *38*, 428.
[45] W. Keim, A. Behr, B. Limbäcker, C. Krüger, *Angew. Chem. Intl. Ed.* **1983**, *22*, 503.
[46] P. W. Glockner, W. Keim, R. F. Mason, R. S. Bauer, DE2053753 (to Shell Internationale Research Maatschappij N. V.), **1969**.
[47] R. F. Mason, US3737475 (to Shell Oil Co.), **1973**.
[48] W. Keim, A. Behr, G. Kraus, *J. Organomet. Chem.* **1983**, *251*, 377.
[49] W. Keim, *Angew. Chem. Intl. Ed.* **1990**, *29*, 235.
[50] W. Keim, F. H. Kowaldt, R. Goddard, C. Kruger, *Angew. Chem. –Intl. Ed.* **1978**, *17*, 466.
[51] U. Klabunde, S. D. Itten, *J. Mol. Catal.* **1987**, *41*, 123.
[52] U. Klabunde, R. Mulhaupt, T. Herskovitz, A. H. Janowicz, J. Calabrese, S. D. Ittel, *J. Polym. Sci. Part A: Polym. Chem.* **1987**, *25*, 1989.
[53] Z. J. A. Komon, X. Bu, G. C. Bazan, *J. Am. Chem. Soc.* **2000**, *122*, 12379.
[54] Z. J. A. Komon, X. Bu, G. C. Bazan, *J. Am. Chem. Soc.* **2000**, *122*, 1830.
[55] R. Soula, J. P. Broyer, M. F. Llauro, A. Tomov, R. Spitz, J. Claverie, X. Drujon, J. Malinge, T. Saudemont, *Macromolecules* **2001**, *34*, 2438.
[56] V. C. Gibson, A. Tomov, A. J. P. White, D. J. Williams, *Chem. Commun.* **2001**, 719.
[57] P. Kuhn, D. Sémeril, C. Jeunesse, D. Matt, P. Lutz, R. Welter, *Eur. J. of Inorg. Chem.* **2005**, *2005*, 1477.
[58] T. R. Younkin, E. F. Connor, J. I. Henderson, S. K. Friedrich, R. H. Grubbs, D. A. Bansleben, *Science* **2000**, *287*, 460.
[59] C. Wang, S. Friedrich, T. R. Younkin, R. T. Li, R. H. Grubbs, D. A. Bansleben, M. W. Day, *Organometallics* **1998**, *17*, 3149.
[60] M. Nodono, B. M. Novak, P. T. Boyle, *Polym. J.* **2004**, *36*, 140.
[61] F. A. Hicks, M. Brookhart, *Organometallics* **2001**, *20*, 3217.
[62] C. Carlini, M. Isola, V. Liuzzo, A. M. R. Galletti, G. Sbrana, *Appl. Catal. A: Gen.* **2002**, *231*, 307.
[63] E. Kirillov, T. Roisnel, A. Razavi, J.-F. o. Carpentier, *Organometallics* **2009**, *28*, 2401.
[64] C.-H. Qi, S.-B. Zhang, J.-H. Sun, *J. Organomet. Chem.* **2005**, *690*, 3946.
[65] A. Bianchi, A. Bernardi, *J. Org. Chem.* **2006**, *71*, 4565.
[66] L. Boubekeur, L. Ricard, N. Mezailles, M. Demange, A. Auffrant, P. Le Floch, *Organometallics* **2006**, *25*, 3091.
[67] N. A. Eckert, J. M. Smith, R. J. Lachicotte, P. L. Holland, *Inorg. Chem.* **2004**, *43*, 3306.
[68] J. Hvoslef, H. Hope, M. B. D., P. P., *Chem. Commun.* **1983**, 1438.
[69] A. Buchard, A. Auffrant, C. Klemps, L. Vu-Do, L. Boubekeur, X. F. L. Goff, P. L. Floch, *Chem. Commun.* **2007**, 1502.
[70] P. Espinet, K. Soulantica, *Coord. Chem. Rev.* **1999**, *193-195*, 499.
[71] P. Braunstein, F. Naud, *Angew. Chem. Intl. Ed.* **2001**, *40*, 680.
[72] P. J. Guiry, C. P. Saunders, *Adv. Synth. Catal.* **2004**, *346*, 497.
[73] P. Braunstein, *J. Organomet. Chem.* **2004**, *689*, 3953.
[74] V. C. Gibson, S. K. Spitzmesser, *Chem. Rev.* **2003**, *103*, 283.
[75] E. van den Beuken, E. Drent, B. L. Feringa, WO 98/42440 (to Shell International Research), **1998**.
[76] C. M. Killian, J. P. McDevitt, P. B. Mackenzie, L. S. Moody, J. A. Ponasik, WO98/40420 (to Eastman Chemical Company), **1998**.
[77] P.-Y. Shi, Y.-H. Liu, S.-M. Peng, S.-T. Liu, *Organometallics* **2002**, *21*, 3203.
[78] F. Speiser, P. Braunstein, L. Saussine, R. Welter, *Organometallics* **2004**, *23*, 2613.
[79] F. Speiser, P. Braunstein, L. Saussine, R. Welter, *Inorg. Chem.* **2004**, *43*, 1649.
[80] F. Speiser, P. Braunstein, L. Saussine, *Dalton Transactions* **2004**, 1539.
[81] A. Kermagoret, P. Braunstein, *Organometallics* **2007**, *27*, 88.
[82] H.-P. Chen, Y.-H. Liu, S.-M. Peng, S.-T. Liu, *Organometallics* **2003**, *22*, 4893.
[83] F. Speiser, P. Braunstein, L. Saussine, *Organometallics* **2004**, *23*, 2633.
[84] J. Flapper, H. Kooijman, M. Lutz, A. L. Spek, P. W. N. M. van Leeuwen, C. J. Elsevier, P. C. J. Kamer, *Organometallics* **2009**, *28*, 3272.

[85] L. Boubekeur, L. Ricard, N. Mezailles, P. Le Floch, *Organometallics* **2005**, *24*, 1065.
[86] C. G. Stuckwisch, *J. Org. Chem.* **1976**, *41*, 1173.
[87] A. Steiner, D. Stalke, *Angew. Chem. Intl. Ed.* **1995**, *34*, 1752.
[88] A. M. A. Bennet, E. B. Coughlin, D. S. Donald, J. Feldman, L. K. Johnson, K. A. Kreutzer, S. J. McLain, L. T. J. Nelson, A. Parthasarathy, X. Shen, W. Tam, Y. Wang, US5714556 (to DuPont), **1998**.
[89] D. S. McGuinness, P. Wasserscheid, W. Keim, D. Morgan, J. T. Dixon, A. Bollmann, H. Maumela, F. Hess, U. Englert, *J. Am. Chem. Soc.* **2003**, *125*, 5272.
[90] J. Zhang, P. Braunstein, T. S. A. Hor, *Organometallics* **2008**, *27*, 4277.
[91] F. Junges, M. C. A. Kuhn, A. H. D. P. dos Santos, C. R. K. Rabello, C. M. Thomas, J.-F. Carpentier, O. L. Casagrande, *Organometallics* **2007**, *26*, 4010.
[92] F. Lopez-Ortiz, E. Pelaez-Arango, B. Tejerina, E. Perez-Carreno, S. Garcia-Granda, *J. Am. Chem. Soc.* **1995**, *117*, 9972.
[93] D. Seyferth, D. E. Welch, J. K. Heeren, *J. Am. Chem. Soc.* **1963**, *85*, 642.
[94] D. Seyferth, D. E. Welch, J. K. Heeren, *J. Am. Chem. Soc.* **1964**, *86*, 1100.
[95] P. Pfeiffer, E. Breith, E. Lübbe, T. Tsumaki, *Just. Lieb. Ann. Chem.* **1933**, *503*, 84.
[96] W. Zhang, J. L. Loebach, S. R. Wilson, E. N. Jacobsen, *J. Am. Chem. Soc.* **1990**, *112*, 2801.
[97] E. N. Jacobsen, W. Zhang, A. R. Muci, J. R. Ecker, L. Deng, *J. Am. Chem. Soc.* **1991**, *113*, 7063.

Chapter 5. Phosphatitanocenes – Application in the Catalyzed Polymerization of Ethylene

Chapter 5. Phosphatitanocenes – Application in the Catalyzed Polymerization of Ethylene

1. Introduction

Titanium-based catalyst systems play an outstanding role in the field of olefin transformation. The Ziegler-Natta-type catalyst system employing [$TiCl_4$], usually activated with an organoaluminium compound, is one of the most ubiquitous systems for the polymerization of ethylene. Another industrially important application of titanium-based catalyst is the dimerization of ethylene to 1-butene, as realized in the IFP Alphabutol process, where a homogeneous titanium catalyst $Ti(OR)_4$, typically activated by $AlEt_3$, yields 1-butene in high selectivities.[1, 2]

The catalytic activity of [Cp^RTiX_3] (R = hydrocarbyl, X = monoanionic ligand) upon activation with MAO in the polymerization of styrene to yield syndiotactic polystyrene, was discovered by Ishihara *et al.*[3-5] and triggered numerous investigations of the catalytic properties of titanocene piano stool compounds of the type [Cp^RTiX_3] or [Cp^RTiR_3] in olefin polymerization reactions, both in industry and academia. This led to the development and disclosure of a multitude of catalysts with variations both on the substitution pattern of the cyclopentadienyl ligand, mostly by the inclusion of either anionic or neutral supplemental donors or by the implementation of ligands isoelectronic to the cyclopentadienyl ligand and with similar steric bulk. Figure 1 shows some examples. The constrained cyclopentadienyl-amide complex **A**, disclosed by Dow Chemical Company, figures amongst the first examples of titanium half sandwich complexes, which have found commercial application, primarily in the ethylene copolymerization reaction with higher α-olefins.[6]

Other developments relying on the modification of the Cp substitution pattern include the amine substituted indenyl-amide complex **B**, which was reported to yield a polymeric material of higher molecular weight in the ethylene/1-octene copolymerization than its analogue **A**. At the same time, the molecular weight was found to be highly dependent on the position of the pyrrolidine substituent.[7] Equally highly active in ethylene/1-octene copolymerization were the η^5-cyclohexadienyl complexes **C** (M = Ti, Zr), and the η^6-boratabenzene complexes **D** (M = Ti, Zr).[8] With the bridged phospholyl-amide complex **E**, very high activities of up to 41.3 kg (PE) × mmol $(Ti)^{-1}$ × min^{-1} in the ethylene polymerization reaction under steady state conditions at 103 bar, and upon activation with MAO, were reported by researchers at Nova S.A.[9] However, the obtained polymer is of lower molecular weight than the material obtainted with **A**.

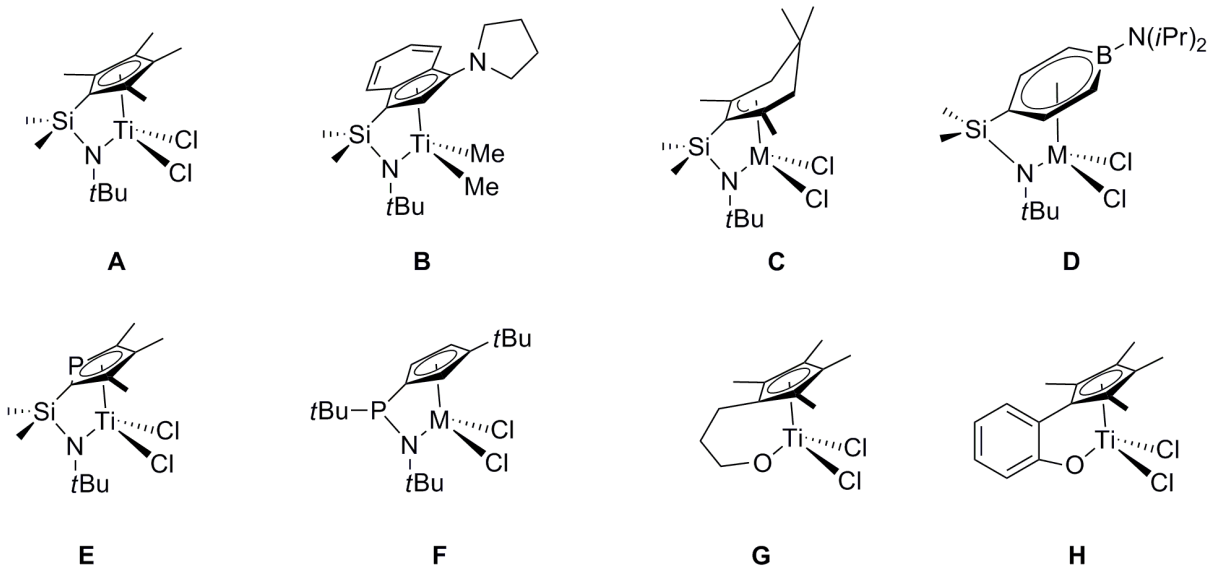

Figure 1. Bridged-cyclopentadienyl and related group IV catalysts for olefin polymerization. **C**,**D**,**F** (M = Ti, Zr).

Complexes **F** features a phosphine-bridged cyclopentadienyl-amide ligand; **F** (M = Ti) was reported to yield high-molecular polyethylene with an activity of 100 g (PE) × mmol (Ti)$^{-1}$ × h^{-1},[10] while its analogue with the neutral diethylamino donor was found to be only modestly active, which was found to be the case with other Cp-Ti complexes with neutral pendant amino donors.[10] **G**[11] and **H**[12] are examples of bridged cyclopentadienyl-alkoxy titanium complexes with high activities in the polymerization of ethylene, propylene (**G** and **H**), and styrene (**G**).

Whereas a Cossee-Arlman[13, 14] coordination-migratory insertion mechanism has been generally accepted to be operative in the olefin polymerization reaction, the oxidation state of the metal, Ti(III) or Ti(IV),[15-18] has been a subject of debate. A study directed towards this controversy, employing well-defined Ti(III) and Ti(IV) precursors, identified Ti(III) to be operative in the syndiotactic styrene polymerization, whereas Ti(IV) exhibits a complementary selectivity towards the polymerization of 1-alkenes.[19] In 1999, Pellecchia *et al.* reported on the polymerization of ethylene catalyzed with [Cp*TiMe$_3$] activated with equimolar quantities of B(C$_6$F$_5$)$_3$ in toluene solution.[20] Surprisingly, the obtained polymer was found to contain significant butyl branching (up to 50 butyl chains per 1000 carbon atoms of the main chain), which differs from the highly linear polyethylene usually obtained with half-sandwich titanocene systems. Concomitantly, 1-hexene was detected in the liquid phase of the catalytic runs. This result, and the observation, that the attempted co-polymerization of styrene and ethylene with the [Cp*TiMe$_3$]/B(C$_6$F$_5$)$_3$ catalytic system yields both phenylhexenes and 4-phenyl-1-butyl branched polyethylene,[21, 22] is suggestive of an olefin trimerization reaction. A metallacyclic mechanism analogous to the one proposed by Manyik[23] and later by Briggs[24] for chromium-based ethylene trimerization, was suggested and a Ti(II)/Ti(IV) couple was presumed to be active in the

mechanism.[20] Based on these findings, Deckers *et al.* disclosed in 2001 a catalytic system employing [(η^5-$C_5H_4CMe_2Ph$)$TiCl_3$] (**I**), which upon activation with excess quantities of MAO yields selectively 1-hexene (up to 93 wt%) with virtually no concomitant polymer formation (Scheme 1).[25-28] An number of derivatives of this catalytic system with different pendant groups were subsequently reported.[29, 30]

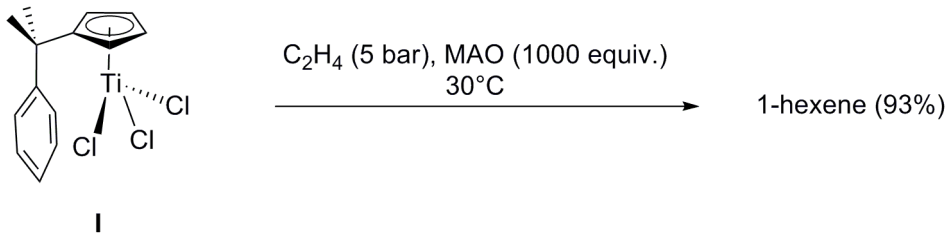

I

Scheme 1. Selective ethylene trimerization with [(η^5-$C_5H_4CMe_2Ph$)$TiCl_3$] (**I**)

The active species in this reaction appears to be a cationic titanium complex, in which a pendant arene group coordinates in a hemilabile fashion to the metal center (Scheme 2).[31] The trimerization has equally been the subject of some theoretical investigations.[32-36] Blok *et al.* found the olefin elimination step to proceed via a direct sigmatropic 3,7 hydrogen shift rather than by the intermediate formation of a Ti-hydride species,[32] a conclusion, which had previously been drawn by Yu *et al*. for the metallacyclic mechanism which governs the ethylene trimerization with tantalum based catalysts.[37]

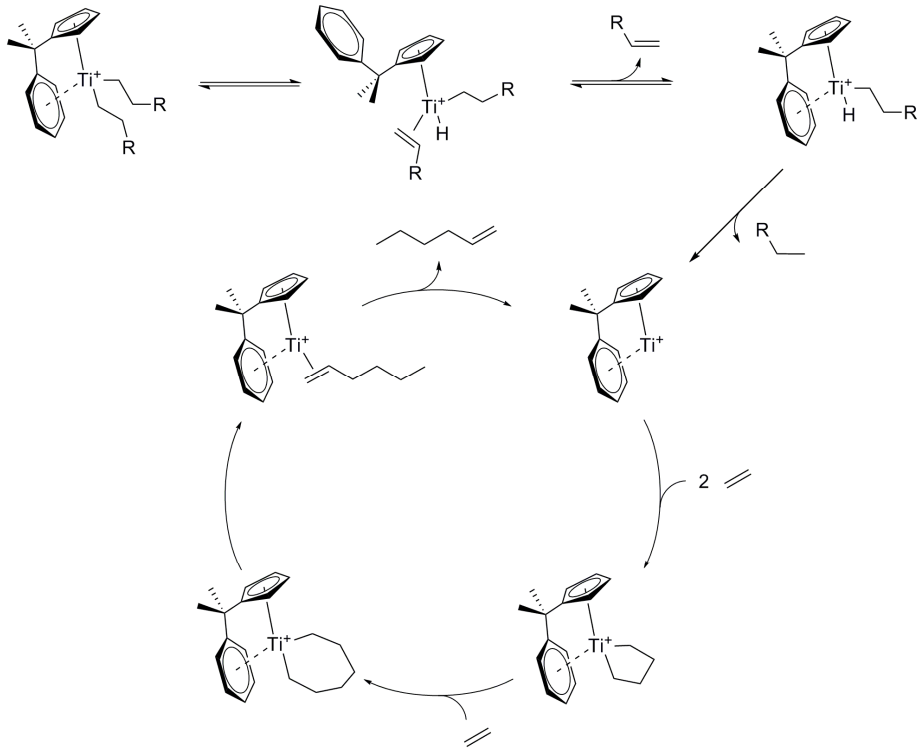

Scheme 2. Metallacyclic mechanism for the selective trimerization of ethylene on titanium.

The selectivity towards trimerization rather than dimerization is ascribed to the high activation barrier of both the 3,5 hydrogen shift or the stepwise process via an intermediate Ti(H)(alkenyl) species, when compared to the insertion of a third ethylene molecule into the titanacycle.[33] A more recent study by de Bruin *et al.* deals with the correlation of the dissociation energy of the pendant hemilabile group with the observed selectivity in the oligomerization reaction.[36] Selective formation of 1-hexene is thus predicted to occur when the dissociation energy is greater than 15 kcal/mol. Only recently, Otten *et al.* presented a combined experimental/theoretical study on the exact nature of the Ti^+-arene bonding depending on the number of coordinated ethylene molecules in the catalytic cycle. It was found that an η^6 coordination of the arene plus two ethylene units would be too sterically demanding and thus η^1 coordination of the arene moiety is adopted.[38]

Inspired by this trimerization system, we decided to study the activity of analogous phosphatitanocene complexes with hemilabile pendant donor groups in the catalyzed ethylene oligomerization/polymerization reaction (Figure 2).

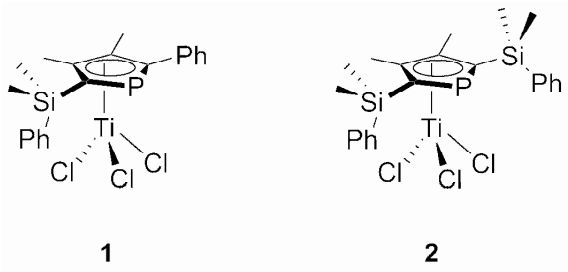

Figure 2. Phosphatitanocenes with one (**1**) and two (**2**) pendant phenyl groups.

Phospholyl ligands, because of their steric and electronic similarity to cyclopentadienyl ligands, as well as the well established routes to access them,[39, 40] have been extensively studied as alternatives to metallocenes. Due to the relevance of group IV metallocenes in olefin oligomerization and polymerization, phosphatitanocenes[9] such as complex **E** and phosphazirconocenes[41-43] have received particular attention as appropriate targets for potential catalyst precursors.[44, 45]

2. Synthesis of Phospholyl Ligands with Pendant Hemilabile Groups

Two completely different strategies were employed to yield the phospholide ligands **6** (one pendant $SiMe_2Ph$ group) and **12** (two pendant $SiMe_2Ph$ groups), respectively. Starting from the 3,4-dimethyl-2-phenyl-phospholyl anion **3**, the synthesis of the phospholyl ligand of **1** proceeds via reaction of **3** with $Me_2PhSiCl$ to form the intermediate silyl-phosphole **4**, which upon treatment with $KN(SiMe_3)_2$ at -78°C undergoes a base-induced deprotonation and 1,5 silyl shift,[46] to yield the desired phospholyl anion **5**, whose complete formation was controlled by $^{31}P\{^1H\}$ NMR (115.1 ppm) (Scheme 3).

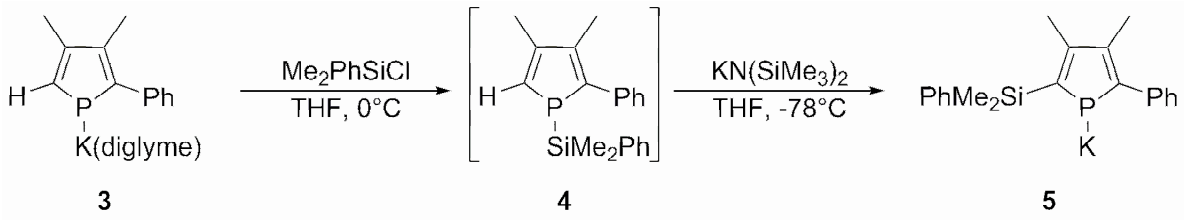

Scheme 3.

$KN(SiMe_3)_2$ was found to be superior to KO*t*Bu, and strict control of the reaction temperature proved to be essential to avoid the formation of phoshole dimers.

Direct coordination of alkali metal phospholes to $[TiCl_4]$ in THF does not yield the desired η^5-phosphatitanocenes, but instead oxidative coupling towards the corresponding bisphospholes is observed, as reported by Nief and Mathey.[47] They reported the passage via an intermediate trimethylstannyl-phosphole to avoid the coupling reaction. In an analogous fashion, **5** was reacted with Me_3SnCl as outline in scheme 4, however, the stannyl intermediate **6** was not isolated ($^{31}P\{^1H\}$ NMR = -29.1 ppm) and directly used for coordination to $[TiCl_4]$, as described in the next section.

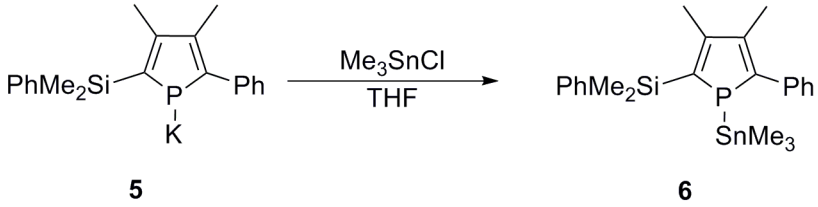

Scheme 4. Synthesis of the trimethylstannyl-phosphole **6**.

The symmetric phospholyl ligand on complex **2** was synthesized via a classical route relying on the formation of the phosphole heterocycle through formal zirconium to phosphorus bond metathesis (Scheme 4).[48, 49] 1-(dimethylphenylsilyl)-1-propyne[50] is reacted with zirconocene dichloride in the presence of finely divided magnesium metal,[51] activated with mercury chloride, yielding the zirconacyclopentadiene **7**[50] as a orange solid in 89% yield.

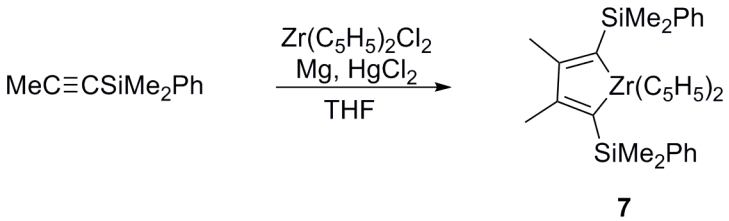

Scheme 5. Synthesis of the zirconacyclopentadiene **7**.

Reaction of **7** with PCl_3 in order to directly obtain the chlorophosphole **8** proved unsuccessful, as no reaction was observed at ambient temperature, and mainly decomposition products were formed upon

prolonged reaction at 70°C, as evidenced by $^{31}P\{^{1}H\}$ spectroscopy (Scheme 5). Treatment of **8** with iodine yields diene **9** as a colorless crystalline solid, which, when reacted with *n*-BuLi at -78°C, followed by $PhPCl_2$, yields the desired 1-phenyl-phosphole **10** in 72% yield. The reductive cleavage of the P-Ph bond is achieved using Li metal in THF, followed by the addition of *t*-BuCl to selectively quench the formed PhLi. The 1-lithio-phosphole **11** was not isolated ($^{31}P\{^{1}H\}$ = 147.6 ppm), but reacted directly with Me_3SnCl to yield **12**, the suitable precursor for the coordination to Ti(IV).

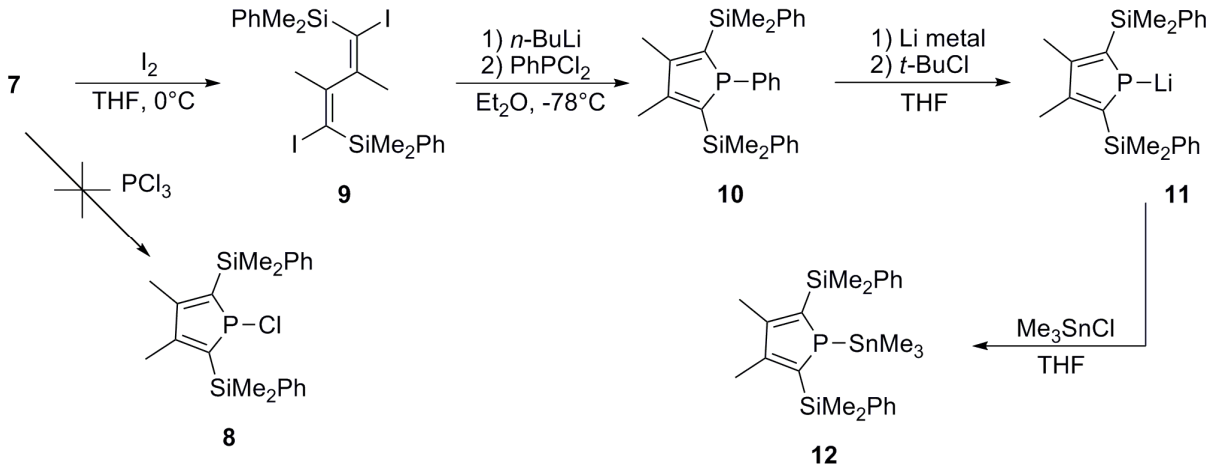

Scheme 6. Synthesis of the stannylphosphole **12**.

3. Coordination to $TiCl_4$

Addition of either **6** or **12** to toluene/hexane solutions of [$TiCl_4$] yielded the (η^5-phospholyl) titanium trichloride complexes **1** and **2**, respectively, as a deep red solid (**1**) or as a red solid (**2**). In the case of **2**, single crystals suitable for x-ray crystal structure analysis could be obtained by slow evaporation of a saturated hexane solution of **2** (Figure 3).

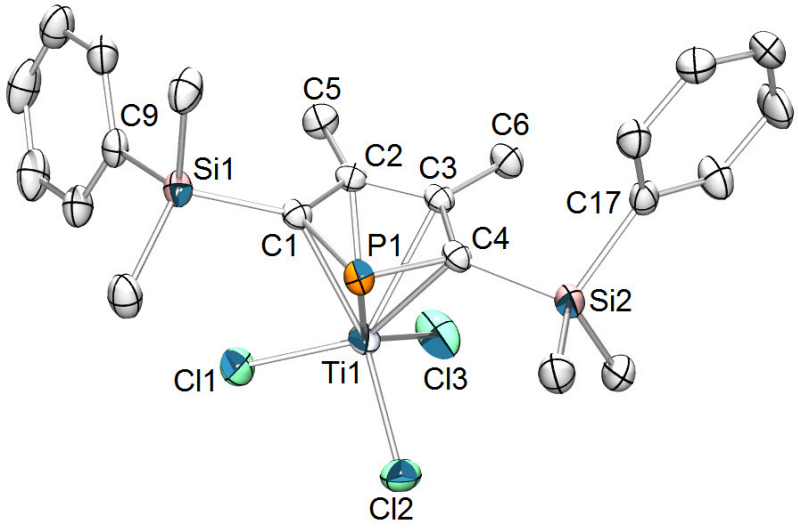

Figure 3. Ortep representation of the x-ray crystal structure of **2**. Hydrogen atoms have been omitted for clarity. Thermal ellipsoids are represented at the 50% level. Important bond lengths (Å) and angles (°):Ti1-P1 = 2.5607(5), Ti1-C1 = 2.429(2), Ti1-C2 = 2.418(2), Ti1-C3 = 2.418(2), Ti1-C4 = 2.383(2), Ti-Cl1 = 2.2299(6), Ti1-Cl2 = 2.2539(7), Ti-Cl3 = 2.2339(7), C1-Si1 = 1.896(2), C4-Si2 = 1.892(2), Ti1-Ctr = 2.051, Cl1-Ti1-Cl2 = 102.18(2), Cl1-Ti1-Cl3 = 100.69(3), P1-C1-Si1 = 117.1(1), P1-C4-Si2 = 122.7(1), C1-P1-C4 = 91.4(1), P1-C1-C2 = 111.2(1), C1-C2-C3 = 112.7(2).

One notable feature of the present structure is the out-of-plane deviation of 0.281 Å of one of the $SiMe_2Ph$ groups from the PC_4 heterocyclic ring system (Ctr-C1-Si1 = 168.64°), whereas the second silyl substituent shows no notable deviation from this plane (0.006 Å). Upon comparison with the analogous cyclopentadienyl complex $[(\eta^5\text{-}C_5H_4SiMe_2Ph)TiCl_3]$,[52] one notices the significant difference of the angles formed between the cyclopentadienyl-Si or phospholyl-Si bond, respectively, and the phenyl-Si bonds. Whereas in $[(\eta^5\text{-}C_5H_4CMe_2Ph)TiCl_3]$, this angle was found to be 105.1(3)°, the values found in **2** amount to 115.57(8)° (C1-Si1-C9) and 108.86(8)°, respectively. The observed metric dimensions lie within the range of previously reported monophospholyl titanium trichloride compounds.[53, 54]

Coordination to $[TiCl(O\textit{i}\text{-}Pr)_3]$ to both **6** and **12** was equally attempted, however, no reaction was observed even at temperatures of up to 110°C; this result is ascribed to the lower Lewis acidity of $[TiCl(O\textit{i}\text{-}Pr)_3]$ and thus lower reactivity compared to $[TiCl_4]$.

4. Evaluation of Complexes 1 and 2 in the Polymerization of Ethylene

Tests for ethylene polymerization were carried out on complexes **1** and **2** using toluene as solvent, and ethylene pressures from 4 to 30 bar, at a temperature of 45°C. The results of these experiments are summarized in table 1. Catalyst activation was carried out using either MAO, Et_3Al, or Et_2AlCl. Trimethylaluminium proved to be ineffective as activator for **2**. The combination of Et_3Al and the

perfluoroaluminate activator $[(Ph_3C)Al(OC(CF_3)_3)_4]$, which has proven to be highly efficient in chromium-based oligomerization systems,[55] was equally tested. In preliminary tests, carried out at the NMR tube scale, addition of $[(Ph_3C)Al(OC(CF_3)_3)_4]$ to a toluene solution of **2** resulted in an immediate color change to yellow and the formation of unidentifiable decomposition products, as evidenced by ^1H and ^{31}P NMR spectroscopy. This agrees with similar findings by Saßmannshausen *et al.*,[52] who described the decomposition of $[(\eta^5\text{-}C_5H_4EMe_2Ph)TiCl_3]$ (with E = Si) upon reaction with equimolar quantities of either $B(C_6F_5)_3$ or $[(Ph_3C)B(C_6F_5)_4]$ even at -60°C, whereas the E = C derivative cleanly formed cationic complexes, with the pendant phenyl group coordinating to the metal center. Consequently, no catalytic activity was observed with the co-catalyst combination $Me_3Al/[(Ph_3C)Al(OC(CF_3)_3)_4]$ in a 1:1 ratio (entry 15). Both **1** and **2** were most efficiently activated using MAO; activities of up to 17.2 and 19.8 Kg (PE) × $mmol^{-1}$ × h^{-1}, respectively, were observed. Analysis of the liquid phase of the catalytic runs by GC revealed only traces of butenes; the essential part of the products formed consisted of a highly insoluble polymeric material. Ethylene pressure increase from 4 to 30 bar resulted in a significant activity increase with both precursors **1** and **2** (entries 1-3, 6-8), with **2** exhibiting a slightly higher activity over the whole pressure range tested. This points towards a possible positive influence of two (**2**) versus one (**1**) pendant phenyl groups on the stability of the catalytic species. The activities observed with either Et_3Al or Et_2AlCl as activator were found to be rather low, compared to those obtained with MAO. Again, in the liquid phase, only trace amounts of butenes could be detected.

Table 1. Polymerization results.

Entry	Precatalyst	Activator	Al:Ti ratio	$P(C_2H_4)$/bar	Activity/ Kg(PE)/(mmol h)	Tm (polymer)/°C
1	**1**	MAO	600	4	9.2	137.3
2	**1**	MAO	600	20	13.9	143.6
3	**1**	MAO	600	30	17.2	145.9
4	**1**	Et_3Al	20	30	< 0.5	141.3
5	**1**	Et_2AlCl	20	30	< 0.5	140.9
6	**2**	MAO	600	4	10.3	137.7
7	**2**	MAO	600	20	15.4	143.8
8	**2**	MAO	600	30	18.7	145.7
9	**2**	MAO	1000	30	19.8	145.9
10	**2**	Et_3Al	20	30	< 0.5	142.3
11	**2**	Et_2AlCl	20	30	< 0.5	141.4
12	**2**	Me_3Al	20	30	-	-
13	**2**	Et_3Al	3	30	< 0.5	141.7
14	**2**	Et_2AlCl	5	30	< 0.5	140.9
15	**2**	TPTA[a]/Me_3Al	1/1	30	-	-

Conditions: 50 mL of a 10 µmol L^{-1} solution of [Ti] in toluene, 45°C [a] TPTA = $[(Ph_3C)Al(OC(CF_3)_3)_4]$

The insolubility precluded effective analysis of the formed polymers by high temperature ^{13}C NMR, as only swelling of the polymer was observed upon attempted dissolution in 1,3,5-trichlorobenzene at 135°C. DSC analysis revealed a single melting point in the range from 137.3-145.9°C, which is indicative of a high-molecular highly linear polyethylene. Both with **1** and **2**, the pressure increase concomitantly induced an increased melting point.

5. Conclusion

In conclusion, we have reported the synthesis and characterization of two new phosphatitanocenes with either one or two pendant $SiMe_2Ph$ groups on the phospholyl heterocycle. Activated with either MAO, Et_3Al or Et_2AlCl, the compounds proved to be active almost exclusively in the polymerization of ethylene, yielding a polyethylene with high melting points. The presence of two pendant groups seems to have a positive influence on catalyst activity.

5. Bibliography

[1] Y. Chauvin, H. Olivier, in *Applied Homogeneous Catalysis with Organometallic Compounds, Vol. 1* (Eds.: B. Cornils, W. A. Hermann), VCH, New York, **1996**, pp. 258.
[2] D. Commereuc, Y. Chauvin, J. Gaillard, J. Leonard, J. Andrews, *Hydroc. Process.* **1984**, *63*, 118.
[3] N. Ishihara, T. Seimiya, M. Kuramoto, M. Uoi, *Macromolecules* **1986**, *19*, 2464.
[4] N. Ishihara, M. Kuramoto, M. Uoi, *Macromolecules* **1988**, *21*, 3356.
[5] N. Tomotsu, N. Ishihara, T. H. Newman, M. T. Malanga, *J. Mol. Catal. A: Chem.* **1998**, *128*, 167.
[6] J. C. Stevens, F. J. Timmers, D. R. Wilson, G. F. Schmidt, P. N. Nickias, R. K. Rosen, G. W. Knight, L. S. E., EP 186075965 (to Dow Chemical Company), **1991**.
[7] J. Klosin, W. J. Kruper, P. N. Nickias, G. R. Roof, P. De Waele, K. A. Abboud, *Organometallics* **2001**, *20*, 2663.
[8] S. Feng, J. Klosin, W. J. Kruper, M. H. McAdon, D. R. Neithamer, P. N. Nickias, J. T. Patton, D. R. Wilson, K. A. Abboud, C. L. Stern, *Organometallics* **1999**, *18*, 1159.
[9] S. J. Brown, X. L. Gao, D. G. Harrison, L. Koch, R. E. V. Spence, G. P. A. Yap, *Organometallics* **1998**, *17*, 5445.
[10] V. Kotov, V., E. Avtomonov, V. , J. Sundermeyer, K. Harms, D. Lemenovskii, A., *Eur. J. Inorg. Chem.* **2002**, *2002*, 678.
[11] Y.-X. Chen, P.-F. Fu, C. L. Stern, T. J. Marks, *Organometallics* **1997**, *16*, 5958.
[12] E. E. C. G. Gielens, J. Y. Tiesnitsch, B. Hessen, J. H. Teuben, *Organometallics* **1998**, *17*, 1652.
[13] P. Cossee, *J. Catal.* **1964**, *3*, 80.
[14] E. J. Arlman, P. Cossee, *J. Catal.* **1964**, *3*, 99.
[15] J. C. W. Chien, Z. Salajka, S. Dong, *Macromolecules* **1992**, *25*, 3199.
[16] T. E. Ready, R. Gurge, J. C. W. Chien, M. D. Rausch, *Organometallics* **1998**, *17*, 5236.
[17] A. Grassi, A. Zambelli, F. Laschi, *Organometallics* **1996**, *15*, 480.
[18] Y. You, G. S. Girolami, *Organometallics* **2008**, *27*, 3172.
[19] C. Pellecchia, A. Grassi, *Top. Catal.* **1999**, *7*, 125.
[20] C. Pellecchia, D. Pappalardo, G.-J. Gruter, *Macromolecules* **1999**, *32*, 4491.
[21] C. Pellecchia, M. Mazzeo, G.-J. Gruter, *Macromol. Rapid Commun.* **1999**, *20*, 337.
[22] C. Pellecchia, D. Pappalardo, L. Oliva, M. Mazzeo, G.-J. Gruter, *Macromolecules* **2000**, *33*, 2807.
[23] R. M. Manyik, W. E. Walker, T. P. Wilson, *J. Catal.* **1977**, *47*, 197.
[24] J. R. Briggs, *J. Chem. Soc Chem. Commun.* **1989**, 674.
[25] P. J. W. Deckers, B. Hessen, EP1377535B1, (to Stichting Dutch Polymer Institut), **2008**.
[26] P. J. W. Deckers, B. Hessen, J. H. Teuben, *Angew. Chem. Intl. Ed.* **2001**, *40*, 2516.
[27] B. Hessen, *J. Mol. Catal. A: Chem.* **2004**, *213*, 129.
[28] W. Chen, H. Ji-Ling, *Chin. J. Chem.* **2006**, *24*, 1397.
[29] J. Huang, T. Wu, Y. Qian, *Chem. Commun.* **2003**, 2816.
[30] T. Wu, Y. Qian, J. Huang, *J. Mol. Catal. A: Chem.* **2004**, *214*, 227.
[31] P. J. W. Deckers, B. Hessen, J. H. Teuben, *Organometallics* **2002**, *21*, 5122.
[32] A. N. J. Blok, P. H. M. Budzelaar, A. W. Gal, *Organometallics* **2003**, *22*, 2564.

[33] S. Tobisch, T. Ziegler, *Organometallics* **2003**, *22*, 5392.
[34] T. J. M. de Bruin, L. Magna, P. Raybaud, H. Toulhoat, *Organometallics* **2003**, *22*, 3404.
[35] S. Tobisch, T. Ziegler, *Organometallics* **2004**, *23*, 4077.
[36] T. de Bruin, P. Raybaud, H. Toulhoat, *Organometallics* **2008**, *27*, 4864.
[37] Z.-X. Yu, K. N. Houk, *Angew. Chem. Intl. Ed.* **2003**, *42*, 808.
[38] E. Otten, A. A. Batinas, A. Meetsma, B. Hessen, *J. Am. Chem. Soc.* **2009**, *131*, 5298.
[39] P. J. Fagan, W. A. Nugent, *J. Am Chem. Soc.* **1988**, *110*, 2310.
[40] F. Mathey, *Chem. Rev.* **1988**, *88*, 429.
[41] E. J. M. de Boer, I. J. Gilmore, F. M. Korndorffer, A. D. Horton, A. van der Linden, B. W. Royan, B. J. Ruisch, L. Schoon, R. W. Shaw, *J. Mol. Catal. A: Chem.* **1998**, *128*, 155.
[42] C. Janiak, K. C. H. Lange, P. Marquardt, *J. Mol. Catal. A: Chem.* **2002**, *180*, 43.
[43] J. Panhans, F. W. Heinemann, U. Zenneck, *J. Organomet. Chem.* **2009**, *694*, 1223.
[44] L. Weber, *Angew. Chem. Intl. Ed.* **2002**, *41*, 563.
[45] P. Le Floch, *Coord. Chem. Rev.* **2006**, *250*, 627.
[46] T. K. Hollis, Y. J. Ahn, F. S. Tham, *Chem. Commun.* **2002**, 2996.
[47] F. Nief, F. Mathey, *J. Chem. Soc. Chem. Commun.* **1988**, 770.
[48] A. J. Ashe, J. W. Kampf, S. M. Al-Taweel, *J. Am. Chem. Soc.* **1992**, *114*, 372.
[49] S. M. Al-Taweel, *Phos. Sulf. Sil. Rel. Elem.* **1997**, *130*, 203.
[50] S. S. H. Mao, F.-Q. Liu, T. D. Tilley, *J. Am. Chem. Soc.* **1998**, *120*, 1193.
[51] W. A. Nugent, D. L. Thorn, R. L. Harlow, *J. Am. Chem. Soc.* **1987**, *109*, 2788.
[52] J. Saßmannshausen, A. K. Powell, C. E. Anson, S. Wocadlo, M. Bochmann, *J. Organomet. Chem.* **1999**, *592*, 84.
[53] F. Nief, L. Ricard, F. Mathey, *Organometallics* **1989**, *8*, 1473.
[54] Y. J. Ahn, R. J. Rubio, T. K. Hollis, F. S. Tham, B. Donnadieu, *Organometallics* **2006**, *25*, 1079.
[55] D. S. McGuinness, A. J. Rucklidge, R. P. Tooze, A. M. Z. Slawin, *Organometallics* **2007**, *26*, 2561.

Conclusion and Perspectives

Conclusions and Perspectives

The first part of the present work dealt with the both experimental and theoretical investigations aimed at a better understanding of the metallacyclic mechanism which is operative in the tri- and tetramerization reaction of ethylene with chromium catalysts. The assumption of a Cr(I)/Cr(III) redox couple could be affirmed notably by an ESR experiment, and theoretical calculations undertaken with the "Sasol" bis(phosphine)amine (PNP) ligand yielded reasonable results with this given redox couple. Importantly, the thermochemistry of the 1-octene elimination step in the catalytic cycle could be shown to proceed via a sigmatropic (3,9)-hydrogen shift without intermediate formation of a chromium-hydride species; on the other hand, for the formation of 1-hexene, both a (3,7)-hydrogen shift and chromium-hydride formation were found feasible. The latter pathway was identified as a putative source for the cyclic C_6 byproducts found as major byproducts in the product mixture of the oligomerization reaction.

The knowledge gained from this theoretic investigation then served as a starting point for a detailed investigation of the influence of the steric bulk of the substituents on the phosphino moieties of bis(phosphinomethyl)amine (PCNCP) ligands. After coordination to Cr(III) and upon activation with MAO, the resulting complexes were found to yield catalysts with very high selectivities towards ethylene trimerization. Bulky and highly basic bis(cyclohexyl)phosphine moieties proved beneficial for 1-hexene selectivity, and their replacement by the considerably less bulky bis(*n*-butyl)phosphine groups resulted in the apparition of 1-octene in the catalytic product mixture. This observation could thoroughly be explained to reside in the difference in activation energy required for the insertion of a fourth ethylene molecule into a chromacycloheptane intermediate. Overall, the obtained results affirmed the importance of steric bulk in the oligomerization reaction on chromium.

A second part consisted in the elaboration of some ligands, which, either form a sterical or electronic viewpoint, mimic the PNP ligand. While the replacement of the central nitrogen atom by a rigid sp^2 atom resulted in unselective oligomerization on chromium, roughly comparable results in terms of selectivity and catalyst productivity could be achieved with an bis(phenylacetylenyl)-P-substituted PNP ligand. Other trials towards alternative ligands with sulfur donors invariably resulted in inactive catalytic systems.

Another scope of this work was the investigation of ligands incorporating the iminophosphorane moiety. Cr(III) complexes with anionic bis(iminophosphoranyl)methanide ligands were found to be active in ethylene oligomerization with an unprecedented type of product distribution, alongside with some polymerization activity.

Previous work had pointed out ways to exploit the *ortho*-directing properties of the iminophosphorane functionality to prepare new mixed iminophosphorane-phosphine ligands by reaction of an *ortho*-

lithiated iminophosphorane. Coordination of these phosphine-iminophosphorane ligands to Ni(II) yielded complexes which proved highly active in selective ethylene dimerization to 1-butene. In order to enlarge the range of mixed ligands containing iminophosphorane moieties, the *ortho*-lithiated iminophosphorane was used as starting material to develop new mixed neutral and anionic (N,O)- and (N,S)- bidentate ligands, whose coordination behavior towards various transition metals was evaluated and a number of coordination complexes with Ni, Pd, and Rh could be prepared.

The oligomerization behavior of the Ni complexes after activation with MAO was evaluated and high activities accompanied with competitive selectivities towards 1-butene were observed.

Yet another and last part of this work concerned the preparation and catalytic evaluation in the oligomerization/polymerization reaction of two phosphatitanocene trichloride complexes bearing a pendant ancillary aryl group on the phospholyl heterocycle. Analogous cyclopentadienyl-Ti complexes with a pendant aryl group yielded the first and unique titanium-based catalytic system for selective ethylene trimerization to 1-hexene. Contrary to what was found with the cyclopentadienyl-Ti complexes, our phosphatitanoces were exclusively active in ethylene polymerization, yielding productivities of up to 19.8 Kg (PE) $\times$ mmol^{-1} $\times$ h^{-1}.

From the results obtained, two major strategies may be pursued as a source of future developments:

First, from the insight gained through the theoretical calculations (chapter 1), one may deduce the structural parameters for a ligand fitted to be a substitute to the predominant “Sasol” PNP ligand. It seems to emerge that the ligand’s bite angle (in the case of a bidentate ligand) and the degree of steric bulk in immediate vicinity to the catalytic chromium center are the two decisive factors determining the selectivity of the chromium catalyst. While steric bulk is relatively simple to modify on a given ligand, the bite angle of the PNP ligand is already at the lower limit of what may be achieved with a bis(phosphine) ligand. Therefore, a monodentate donor ligand with carefully adapted steric bulk in its periphery might be the ligand of choice. However, one has to consider the “entropic disadvantage” of a monodentate ligand with respect to a bidentate species, since ligand dissociation in the case of a monodentate species results in desactivation, whereas a bidentate ligand may dissociate partially and recoordinate subsequently, a process which seems to be part of the metallacyclic mechanism of ethylene oligomerization anyway. Hemilabile ancillary ligand moieties in the vicinity of the main monodentate donor to prevent this complete dissociation might be the solution of choice. The concept of a sufficiently strongly bound monodentate ligand might even enable the formation of metallacycles greater than the chromacyclononane, and thus enable the selective formation of 1-decene.

A second possible gateway opened during this thesis concerns the further exploitation both in coordination chemistry and, subsequently, in catalysis, the numerous ligand structures available through the extension of the *ortho*-lithiation-functionalization route of the iminophosphorane

Ph_3P=NR. Aside from ethylene oligomerization reactions, the potential of the new ligands has not yet been explored, even though their coordination chemistry seem rich and promising, as illustrated by a number of examples given in this thesis.

Possible catalytic applications might include various C-C coupling reactions as well as aromatic and, more challenging, aliphatic C-H activation, a field, where work is left to be done.

Experimental Part

Experimental Part

General Remarks

Unless stated otherwise, all preparative reactions have been carried out under a protective nitrogen atmosphere using standard glove box and Schlenk techniques. All used solvents were freshly distilled under nitrogen atmosphere prior to their use. THF, hexanes, petrol ether 40/60 and diethyl ether were distilled over Na/benzophenone. Dichloromethane was distilled over P_2O_5. Toluene was prepared by preliminary distillation on the rotatory evaporator, then distilled under nitrogen atmosphere over Na.

Characterization Techniques

NMR spectroscopy was carried out on a Bruke 300SY working at 300 MHz for ^{1}H nucleus, at 75.5 MHz on ^{13}C, and at 121.5 MHz on ^{31}P. The chemical shifts were reported in positive values towards low field, in parts per million (ppm), and with respect to internal references TMS (tetramethylsilane) for ^{1}H and ^{13}C spectroscopy, and 85% aqueous H_3PO_4 for ^{31}P spectroscopy. The spectra were all recorded at 20°C. The coupling constants are reported in Hertz (Hz). X-ray crystal data were recorded on a Nonius Kappa-CCD diffractometer, using Mo-Kα radiation (λ = 0.71070 Å) and a graphite monochromator. Data acquisition was carried out at 150 ± 1 K, using an Oxford Cryostream 600 gas jet cryostat. The structures were solved with direct methods using SIR-97 and least-square refinement was carried out with SHELXL-97.[1] Crystal structure drawings were made using ORTEP-III. Gas chromatography was carried out on a PERICHROM 2100 gas chromatograph equipped with a HP PONA column (50 m × 0.2 mm × 0.5 µm)) and a FID detector, using helium as vector gas. Elemental analysis were carried out at the "Service d'analyse CNRS" at Gif-sur-Yvette, France.

Theoretical calculations were carried out using the Gaussian 03 suite; the optimized structures were visualized using GaussView.

Used Compounds and Precursors

Unless stated otherwise, all mentioned starting materials were obtained from standard commercial sources (Sigma-Aldrich, Acros Organics, Fluka, Strem) and used without further purification. MAO was obtained as a 10 wt% solution in toluene from Sigma-Aldrich.
The following compounds were prepared and purified following standard literature procedures: *n*-Bu_2PH,[2] 1-chloro-2,5-bis(trimethylsilyl)-3,4-dimethyl-phosphole,[3, 4] 1-bromo-2,5-diphenyl-phosphole,[5] $[CrCl_3(THF)_3]$,[6] $[CrBr_3(THF)_3]$,[6] $[NiBr_2(DME)]$,[7] $[Rh(cod)Cl]_2$.[8]

General Oligomerization Procedure

Unless stated otherwise, all catalytic reactions were carried out in a magnetically stirred stainless steel autoclave (300 mL), equipped with a pressure gauge and needle valves for injections, and heated in an oil bath. The interior of the autoclave was protected from corrosion by a Teflon/protective coating. A typical reaction was performed by introducing in the reactor under nitrogen atmosphere a suspension of the complex (32 μmol) in toluene (80 mL). After injection of the MAO solution (10 wt% in toluene, Aldrich), the reactor was immediately brought to the desired working pressure, and continuously fed by ethylene using a reserve bottle. The reaction was stopped by closing the ethylene supply and cooling down the system to -70°C. After release of residual pressure, the reaction was quenched by adding acidified methanol (5 mL). *n*-heptane used as internal standard was also introduced and the mixture was analyzed by quantitative GC.

Syntheses and Preparations

Chapter 1

Synthesis of 1

In an analogous fashion as described before,[9] $[CrBr_3(THF)_3]$ (254 mg, 0.50 mmol) and $(Ph_2P)N(Ph)$ (231 mg, 0.50 mmol) were suspended in toluene (25 mL). The reaction mixture was heated over 16 h at 80°C, resulting in the precipitation of a light grey solid, which was recovered by filtration. The residue was washed twice with hexanes (5 mL), then dried in vacuo. Yield 309 mg (0.21 mmol, 82%) of a light grey powder. Elemental analysis calcd (%) for $C_{60}H_{50}Br_6Cr_2N_2P_4$: C 47.84, H 3.35, N 1.86; found: C 47.71, H 3.06, N 2.09.

Synthesis of 2

Me_3Al (1.0 mL of a 0.50 M solution in toluene, 0.50 mmol) was added dropwise to a suspension of **1** (151 mg, 0.1 mmol) in toluene (5 mL) at -78°C. The reaction mixture immediately took a deep green color. After 15 min., the reaction mixture was brought to r.t., then filtered. The solvent volume was reduced in vacuo to approx. 1.5 mL, then 5 mL of hexanes was added to precipitate a deep green solid, which was recovered by filtration. After drying in vacuo, 105 mg (0.073 mmol, 73%) of highly moisture sensitive **2** were obtained, the sensitivity precluding further analysis of the product. Single crystals suitable for x-ray crystal structure analysis were obtained by slow diffusion of cyclohexane on a saturated toluene solution of **2**.

General Procedure for the Synthesis of 3a-g

Solid paraformaldehyde (74 mg, 2.47 mmol) was added to an equimolar quantity of secondary phosphine R_2PH, and the resulting mixture was heated to 110°C during 1 h. Subsequently, toluene (5 mL) was added to the mixture, followed by the corresponding primary amine $R'NH_2$ (1.24 mmol). This reaction mixture was heated to 60°C during 2 h. The solvent was removed in vacuo, typically resulting in a colorless viscous oil, which was triturated with a mixture of methanol and petroleum ether, upon which white powdery solids were obtained.

3a: Yield: 463 mg (1.02 mmol, 82%). $^{31}P\{^1H\}$ NMR ([D$_6$]benzene, 20°C): δ = -26.5 ppm (s; *P*); ^1H NMR ([D$_6$]benzene, 20°C): δ = 0.80 (d, ^3J (H,H) = 6.6 Hz, 6H; NCH(C*H*$_3$)$_2$), 3.55 (d, ^2J (H,P) = 3.8 Hz, 4H; NC*H*$_2$P), 3.78 (sept, ^3J (H,H) = 6.6 Hz, 1H; NC*H*(CH$_3$)$_2$), 7.08 (m, 12H; *m*,*p*-C*H* (PPh$_2$)), 7.54 ppm (dd, ^3J (P,H) = 6.0 Hz, ^3J (H,H) = 6.0 Hz, 8H; *o*-C*H* (PPh$_2$)); ^{13}C NMR ([D$_6$]benzene, 20°C): δ = 16.2 (s; NCH(*C*H$_3$)$_2$), 50.1 (t, ^3J (C,P) = 9 Hz; N*C*H(CH$_3$)$_2$), 53.2 (d, ^1J (C,P) = 5.7 Hz; N*C*H$_2$P), 128.7 (s; *p*-*C*H (PPh$_2$)), 128.9 (d, ^3J (C,P) = 11.1 Hz; *m*-*C*H (PPh$_2$)), 132.8 (d, ^2J (C,P) = 7.2 Hz; *o*-*C*H(PPh$_2$)), 137.7 ppm (d, ^1J (C,P) = 87.5 Hz; *ipso*-*C*(PPh$_2$)); MS (CI): m/z (%): 457 $[M+H]^+$.

3b: Yield: 519 mg (1.10 mmol, 89%). The spectral parameters coincided with the published values.[10]

3c: Yield: 498 mg (1.02 mmol, 82%). The spectral parameters coincided with the published values.[11]

3d: Yield: 381 mg (0.794 mmol, 64%). $^{31}P\{^1H\}$ NMR ([D$_6$]benzene, 20°C): δ = -14.9 (s; *P*); ^1H NMR ([D$_6$]benzene, 20°C): δ = 0.99 (d, ^3J (H,H) = 6.7 Hz, 6H; NCH(C*H*$_3$)$_2$), 1.05-1.67 (m, 44H; C*H*$_2$ (Cy)), 3.89 (s, 4H; NC*H*$_2$P), 4.09 (m, 1H; NC*H*(CH$_3$)$_2$); ^{13}C NMR ([D$_6$]benzene, 20°C): δ = 16.8 (s; NCH(*C*H$_3$)$_2$), 27.0, 27.7, 30.3, 33.2 (*Cy*), 47.6 (pseudo t; P*C*H$_2$N), 49.5 (t, ^3J (C,P) = 10.5 Hz; N*C*H(CH$_3$)$_2$); MS (CI): m/z (%): 480 $[M+H]^+$.

3e: Yield: 429 mg (0.868 mmol, 70%). $^{31}P\{^1H\}$ NMR ([D$_6$]benzene, 20°C): δ = -14.7 (s; *P*); ^1H NMR ([D$_6$]benzene, 20°C): δ = 0.82 (s, 9H; NC(C*H*$_3$)$_3$), 1.09-1.70 (m, 44H; CH$_2$ (Cy)), 3.88 (s, 4H; NC*H*$_2$P); ^{13}C NMR ([D$_6$]benzene, 20°C): δ = 14.2 (s; NC(*C*H$_3$)$_3$), 27.0, 27.6, 30.2, 33.2 (*Cy*), 47.2 (dd, ^1J (P,C) = 15.8 Hz, ^3J (P,C) = 11.7 Hz; N*C*H$_2$P), 47.5 (t, ^3J (P,C) = 10.1 Hz; N*C*(CH$_3$)$_3$); MS (CI): m/z (%): 494 $[M+H]^+$.

3f: Yield: 433 mg (0.843 mmol, 68%). $^{31}P\{^1H\}$ NMR ([D$_6$]benzene, 20°C): δ = -15.0 (s; *P*); ^1H NMR ([D$_6$]benzene, 20°C): δ = 1.14-1.83 (m, 44H; C*H*$_2$ (Cy)), 3.93 (s, 4H; NC*H*$_2$P), 6.77 (t, ^3J (H,H) = 7.2 Hz, 1H; *p*-C*H* (NPh)), 7.05 (d, ^3J (H,H) = 8.1 Hz, 2H; *o*-C*H* (NPh)), 7.24 (pseudo t; *m*-C*H* (NPh)); ^{13}C NMR ([D$_6$]benzene, 20°C): δ = 26.9, 27.7, 30.3, 33.3 (*Cy*), 47.9 (dd, ^1J (P,C) = 16.1 Hz, ^3J (P,C) =

11.8 Hz; P*C*H$_2$N), 118.2 (s; *o-C*H (NPh)), 118.8 (s; *p-C*H (NPh), 129.2 (s, *m-C*H (NPh)); MS (CI): m/z (%): 514 $[M+H]^+$.

3g: Yield: 247 mg (0.657 mmol, 53%). $^{31}P\{^1H\}$ ([D$_6$]benzene, 20°C): δ = -48.4 (s; *P*). ^1H ([D$_6$]benzene, 20°C): δ = 0.90 (t, ^3J (H,H) = 6.9 Hz, 12H; P(CH$_2$)$_3$C*H*$_3$), 1.01 (d, ^3J (H,H) = 6.4 Hz, 6H; NCH(C*H*$_3$)$_2$), 1.24-1.69 (m, 24H; P(C*H*$_2$)$_3$CH$_3$), 3.72 (s, 4H; PC*H*$_2$N), 4.18 (m, 1H; NC*H*(CH$_3$)$_2$); ^{13}C ([D$_6$]benzene, 20°C): δ = 15.4 (s; NCH(*C*H$_3$)$_2$), 17.8 (d, ^3J (P,C) = 8.1 Hz; PCH$_2$CH$_2$*C*H$_2$), 25.9 (d, ^2J (P,C) = 3.8 Hz; PCH$_2$*C*H$_2$), 33.4 (d, $^3J_{PC}$ = 17.0 Hz; P*C*H$_2$); MS (CI): m/z (%): 410 $[M^+H]^+$.

General Procedure for the Synthesis of 4a-g

To a stirred suspension of [CrCl$_3$(THF)$_3$] (225 mg, 0.601 mmol) in THF (5 mL), an equimolar quantity of ligand **3** was added, resulting in an immediate color change of the reaction mixture to dark blue. After stirring for 2h, the solvent was removed in vacuo and the resulting blue powder was washed with petroleum ether (2 × 5 mL), followed by further drying in vacuo.

4a: Yield: 391 mg (0.570 mmol, 95%) of a dark blue powder. Elemental analysis calcd (%) for C$_{33}$H$_{39}$Cl$_3$CrNOP$_2$: C 57.78, H 5.73, N 2.04; found: C 57.98, H 5.21, N 1.95.

4b: Yield: 408 mg (0.583 mmol, 97%) of a dark blue powder. Elemental analysis calcd (%) for C$_{34}$H$_{41}$Cl$_3$CrNOP$_2$: C 58.34, H 5.90, N 2.00; found: C 57.91, H 5.49, N 2.03.

4c: Yield: 402 mg (0.559 mmol, 93%) of a dark blue powder. Elemental analysis calcd (%) for C$_{36}$H$_{37}$Cl$_3$CrNOP$_2$: C 60.05, H 5.18, N 1.95; found: C 59.89, H 5.02, N 2.05.

4d: Yield: 423 mg (0.594 mmol, 99%) of a blue powder. Elemental analysis calcd (%) for C$_{33}$H$_{63}$Cl$_3$CrNOP$_2$: C 55.81, H 8.94, N 1.97; found: C 55.73, H 8.90, N 1.89. Single crystals suitable for x-ray crystal structure analysis could be obtained by slow evaporation of a THF solution of **4d**.

4e: Yield: 396 mg (0.547 mmol, 91%) of a blue powder. Elemental analysis calcd (%) for C$_{34}$H$_{65}$Cl$_3$CrNOP$_2$: C 56.39, H 9.05, N 1.93; found: C 56.09, H 8.93, N 1.87.

4f: Yield: 438 mg (0.589 mmol, 98%) of a blue powder. Elemental analysis calcd (%) for C$_{36}$H$_{61}$Cl$_3$CrNOP$_2$: C 58.10, H 8.26, N 1.88; found: C 57.98, H 8.12, N 1.75.

4g: Yield: 339 mg (0.559 mmol, 93%) of a blue-grey powder. Elemental analysis calcd (%) for C$_{25}$H$_{55}$Cl$_3$CrNOP$_2$: C 49.55, H 9.15, N 2.31; found: C 49.28, H 9.07, N 2.22.

Chapter 2

General Procedure for the Synthesis of 1a-c

To a solution of the corresponding 1-bromophosphole (for the synthesis of **1a**,**b**) or 1-chlorophosphole (for **1c**) (0.64 mmol), respectively in CH_2Cl_2 (5 mL), a solution of the corresponding primary amine R^1NH_2 (0.32 mmol) and Et_3N (380 mg, 3.8 mmol, 503 µL) in 5 mL of CH_2Cl_2 was added at -78°C. The cold bath was removed, upon which the reaction mixture turned yellow. After 2h, the formed salts were removed by filtration, the filtrate solvent removed in vacuo and the crude powdry product was quickly washed with cold methanol (3 mL), then dried in vacuo.

1a: Yield: 240 mg (0.45 mmol) 71%) of a bright yellow powder. $^{31}P\{^1H\}$ ([D_6]benzene, 20°C): δ = -73.9 (s; *P*). ^1H ([D_6]benzene, 20°C): δ = 0.33 (d, ^3J (H,H) = 6.7 Hz, 6H; NCH(CH_3)$_2$), 2.94 (m, 1H; NC*H*(CH_3)$_2$), 6.51 (d, ^3J(P,H) = 6.2 Hz, 4H; PCC*H*), 7.07 (m, 12H; *m*,*p*-C*H*), 7.57 (m, 8H; *o*-C*H*); ^{13}C ([D_6]benzene, 20°C): δ = 22.9 (s; CH(*C*H_3)$_2$), 127.1 (s, *p*-*C*H), 128.1 (d, ^3J (P,C) = 4.4 Hz; *o*-*C*H), 129.0 (s, *m*-CH), 130.3 (d, ^3J(P,C) = 8.4 Hz; PC*C*H), 138.1 (d, ^1J(P,C) = 8.4 Hz; P*C*C), 149.6 (s, P*C*H(CH_3)$_2$).

1b: Yield: 241 mg (0.43 mmol, 67% of a bright yellow powder. $^{31}P\{^1H\}$ ([D_6]benzene, 20°C): δ = -67.0 (s; *P*). ^1H ([D_6]benzene, 20°C): δ = 6.22 (m, 2H; N-aryl-o-C*H*), 6.38 (d, ^3J(P,H) = 6.3 Hz, 4H; PCC*H*), 6.52 (m, 3H; N-aryl-*m*,*p*-C*H*), 6.93-7.11 (m, 12H; PC-*m*,*p*-C*H*), 7.46-7.61 (m, 8H; PC-*o*-C*H*); ^{13}C ([D_6]benzene, 20°C): δ = 124.3 (s, N-aryl-*o*-*C*H), 125.2 (s, N-aryl-*p*-*C*H), 127.2 (s, N-aryl-*m*-*C*H), 127.8 (s, PC-*o*-CH), 128.3 (s, PC-*p*-*C*H), 128.9 (s, PC-*m*-*C*H), 131.3 (d, ^2J(P,C) = 8.1 Hz, PC*C*H) 137.1 (d, ^2J(P,C) = 9.3 Hz, PC*C*) 146.3 (d, ^2J(P,C) = 9.2 Hz, N*C*), 149.6 (s, P*C*).

1c: Yield 73% .$^{31}P\{^1H\}$ ([D_6]benzene, 20°C): δ = -52.3 (s; *P*). ^1H ([D_6]benzene, 20°C): δ = 0.81 (s, 36H; Si(CH_3)$_3$), 2.21 (s, 12H; CCH_3), 6.63, 6.71, 7.2 (m, 5H; C*H* (Ph)). ^{13}C ([D_6]benzene, 20°C): δ = 3.1 (s, Si(*C*H)$_3$), 19.4 (d, ^3J(P,C) = 25.7 Hz, C*C*H$_3$), 118.5 (d, *J*(P,C) = 5.3 Hz, *C*H(Ph)), 125.6 (d, ^1J(P,C) = 35.4 Hz, P*C*), 127.1 (s, *C*H (Ph)), 129.8 (s, *C*H (Ph)), 147.6 (d, ^2J(P,C) = 5.2 Hz, PC*C*) *ipso*-*C* (Ph) not observed.

Synthesis of 4

n-BuLi (5 mmol, 3.1 mL of a 1.6 M solution in hexanes) was added dropwise to a solution of phenylacetylene (511 mg, 5 mmol, 0.55 mL) in THF (10 mL) at -78°C. After 15 min. the solution was allowed to warm up to r.t., upon which the reaction mixture took a pale yellow color. The reaction mixture was added was added dropwise to a solution of *i*-Pr_2NPCl_2 (505 mg, 2.5 mmol) in THF (20 mL) at -78°C. The reaction mixture was stirred at that temperature for 1 h, then allowed to warm up to r.t. A single peak at δ = -16.1 ppm in the $^{31}P\{^1H\}$ NMR confirmed the complete formation of **3**.[12]

Subsequently, HCl gas was bubbled for 10 sec. through the reaction mixture, which was cooled with an ice bath during this operation. The solvent was then removed in vacuo, then CH_2Cl_2 (20 mL) was added, and the precipitating salts filtered off. After removal of solvent in vacuo, raw **4** was purified by vacuum distillation (bp = 165°C, approx. 1×10^{-2} mbar) and obtained as a yellowish oil. Yield 450 mg (1.68 mmol, 67%).

$^{31}P\{^1H\}$ ([D]chloroform, 20°C): δ = -19.4 (s; *P*). ^1H ([D]chloroform, 20°C): δ = 7.39-7.44 (m, 10H; Ph), ^{13}C ([D]chloroform, 20°C): δ = 79.3 (d, ^1J(P,C) = 17.2 Hz, P*C*CPh), 108.9 (d, ^2J(P,C) = 1.3 Hz, PC*C*Ph), 122.7 (d, ^3J(P,C) = 5.2 Hz, *ipso-C*), 128.4 (s, *m-C*H (Ph)), 128.6 (s, *p-C*H (Ph)), 132.3 (s, *o-C*H (Ph)).

Synthesis of 2

Compound **2** was prepared in an analogous fashion as reported before for other bis(phosphino)amines[13] from 450 mg (1.68 mmol) of **4**, *i*-$PrNH_2$ (50 mg, 0.84 mmol, 72 µL) and Et_3N (340 mg, 1.68 mmol, 234 µL).

Yield: 273 mg (0.52 mmol, 62%) of a pale yellow powder.

$^{31}P\{^1H\}$ ([D]chloroform, 20°C): δ = -16.3 (s; *P*). ^1H ([D]chloroform, 20°C): δ = 1.05 (d, 6H, ^3J(H,H) = 2.4 Hz, CH_3) 2.97 (m, 1H, CH(CH_3)$_2$) 7.43-7.49 (m, 20H, Ph), ^{13}C ([D]chloroform, 20°C): δ = 69.5 (d, ^1J(P,C) = 23.2 Hz, P*C*CPh), 101.8 (d, ^2J(P,C) = 2.5 Hz, PC*C*Ph), 124.7 (d, ^3J(P,C) = 8.4 Hz, *ipso-C*), 126.3 (s, *m-C*H (Ph)), 127.3 (s, *p-C*H (Ph)), 137.9 (s, *o-C*H (Ph)).

Synthesis of 5 and 6

The compounds were prepared as described by Cantat.[14]

General Procedure for the Synthesis of 7a,b

Compounds **7a**,**b** were prepared as described in the literature.[15]

Synthesis of 8

Compounds **8** was prepared as described in the literature.[16]

Synthesis of 9

A solution of **8**$(THF)_2$ (121 mg, 0.5 mmol) in THF (5 mL) was added dropwise to a stirred solution of [$CrCl_3(THF)_3$] (187 mg, 0.5 mmol) in THF (5 mL). An immediate precipitation of a brown powder was observed. The brown solid was isolated by filtration and subsequent washing with THF (5 mL). 190 mg of a brown powder insoluble in all common organic solvents were recovered. No further analysis was undertaken on this product.

Synthesis of 10

A stirred mixture of $[MnBr(CO)_5]$ (200 mg, 0.73 mmol) and $(Ph_2P)_2N(Ph)$ (337 mg, 0.73 mmol) in toluene (10 mL) was heated to reflux for 4 h, after which the solvent was removed in vacuo. The resulting crude product was purified by column chromatography (silica gel, petrol ether/CH_2Cl_2 100/0 to 50/50 v/v) to yield **10** as a yellow crystalline powder. Yield 257 mg (0.52 mmol, 71%). Single crystals suitable for x-ray crystal structure analysis could be grown by slow evaporation of a concentrated CH_2Cl_2 solution of **10**.

$^{31}P\{^1H\}$ ([D_6]benzene, 20°C): δ = 99.5 (s; *P*). ^1H ([D_6]benzene, 20°C): δ = 6.46-6.58 (m, 2H; *o*-C*H* (NPh)), 6.82-6.97 (m, 3H, *m*,*p*-C*H* (NPh)), 7.28-7.55 (m, 20H, *o*,*m*,*p*-C*H* (PPh_2)). ^{13}C ([D_6]benzene, 20°C): δ = 125.3 (s, *p*-C*H* (NPh)), 125.8 (s, *o*-C*H* (NPh)), 128.6 (d, ^2J(P,C) = 5.3 Hz, *o*-C*H* (PPh_2)), 128.8 (s, *m*-C*H* (NPh)), 130.8 (s, *p*-C*H* (PPh_2)), 131.8 (d, ^3J(P,C) = 6.8 Hz, *m*-C*H* (PPh_2)), 136.5 (d, ^1J(P,C) = 18.4 Hz, P*C*), 141.9 (d, ^2J(P,*C*) = 7.2 Hz, N*C*), 221.8 (d, ^2J(P,C) = 12.8 Hz, *C*O), 228.2 (d, ^2J(P,C) = 9.2 Hz, *C*O).

Synthesis of 11

To a solution of **10** (150 mg, 0.23 mmol) in CH_2Cl_2 (10 mL) at -78°C, bromine (55.1 mg, 0.345 mmol, 18 µL) were added dropwise. After 5 min., the reaction mixture was allowed to warm up to r.t. and stirred over 16 h. The solvent was then removed in vacuo, and the yellow powdery residue obtained was triturated with hexanes (2 × 5 mL). A highly air- and moisture sensitive yellow powder was obtained. Yield: 177 mg (0.21 mmol, 92%) Elemental analysis calcd. (%) for $C_{30}H_{25}Br_4MnNP_2$ C 43.10, H 3.01, N 1.68; found: C 43.24, H 2.89, N 1.73.

Chapter 3

General Procedure for the Preparation of Bis(iminophosphonium) bromides 1a-d

In analogy to the procedure previously described,[17] a solution of bis(diphenyphosphinomethane) (150 mg, 0.39 mmol) in dichloromethane (10 mL) was cooled to -78°C and bromine (125 mg, 0.8 mmol, 40 µL) was added dropwise through a syringe. The cold bath was removed and the reaction mixture was allowed to warm to ambient temperature. A yellow/white precipitate was observed. At -78°C, the corresponding primary amine (1.56 mmol) was added dropwise and the reaction mixture was allowed to warm to ambient temperature, upon which a white precipitate of ammonium bromide formed. The salt was filtered off, and the filtrate dried in vacuo. The solid residue was washed with THF (2 × 25 mL) to yield a white powder after drying in vacuo.

1a: Yield: 245 mg (0.37 mmol, 95%). The spectral parameters coincided with the published values.[17]

1b: Yield: 166 mg (0.24 mmol, 62%). Elemental analysis calcd. (%) for $C_{33}H_{42}Br_2N_2P_2$: C 57.57, H 6.15, N 4.07; found C 57.75, H 6.08, N 3.99. $^{31}P\{^1H\}$ ([D]chloroform, 20°C): δ = 29.5 (s, *P*). ^1H ([D]chloroform, 20°C): δ = 0.96 (s, 18H, C(C*H*$_3$)$_3$), 6.60 (t, ^2J(P,H) = 16.5 Hz, 2H, N-*H*), 6.96 (s, 2H, PC*H*$_2$P), 7.60 (m, 8H, *o*-C*H* (PPh$_2$)), 7.73 (t, ^3J(H,H) = 7.0 Hz, 4H, *p*-C*H* (PPh$_2$)), 8.07 (dd, $^4J_{HP}$ = 11.5 Hz, ^3J(H,H) = 8.0 Hz, 8H, *m*-C*H* (PPh$_2$)). ^{13}C ([D]chloroform, 20°C): δ = 25.6 (t, ^1J(P,C) = 64.5 Hz, P*C*H$_2$P), 31.1 (s, C(*C*H$_3$)$_3$), 56.4 (s, *C*(CH$_3$)$_3$), 121.6 (d, ^1J(P,C) = 102.0 Hz, *ipso-C* (PPh$_2$)), 129.2 (d, ^2J(P,C) = 6.7, *o-C*H (PPh$_2$)), 134.4 (d, ^3J(P,C) = 6.5 Hz, *m-C*H (PPh$_2$)), 134.8 (s, *p-C*H (PPh$_2$)).

1c: Yield 256 mg (0.35 mmol, 90%). The spectral parameters coincided with the published values.[17]

1d: Yield: 159 mg (0.28 mmol, 72%). Elemental analysis calcd. (%) for $C_{39}H_{38}Br_2N_2O_2P_2$: C 59.41, H 4.86 N 3.55; found C 59.36, H 4.92 N 3.37. $\delta_{P\{1H\}}$ (121.5 MHz, $CDCl_3$) 36.9 (s, *P*); δ_H (300 MHz, $CDCl_3$) 3.11 (6H, s, OC*H*$_3$), 5.78 (2H, t, $^2J_{HP}$ 14.5, PC*H*$_2$P), 6.31 (2H, d, $^3J_{HH}$ 7.0, N-CC*H*), 6.86 (4H, m, N-CCHC*H*C*H*), 7.36-7.48 (12H, m, *o*, *p*-C*H* (PPh$_2$)), 7.57 (2H, d, $^3J_{HH}$ 7.0, C(OCH$_3$)C*H*), 8.29 (8H, dd, $^3J_{HH}$ 9.0, $^3J_{HH}$ 7.5, *m*-C*H* (PPh$_2$)), 9.55 (2H, d, $^2J_{PH}$ 9.4, N*H*); δ_C (75.5 MHz, $CDCl_3$) 30.5 (t, $^1J_{CP}$ 60.9, P*C*H$_2$P), 54.4 (s, O*C*H$_3$), 111.0 (s, N-*C*CH), 121.8 (s, N-CCH*C*H), 122.4 (s, *ipso-C* (PPh$_2$)), 124.5 (s, N-CC(OCH$_3$)*C*H), 125.6 (s, C(OCH$_3$)CH*C*H), 125.8 (s, N-*C*), 129.5 (d, $^2J_{CP}$ 8.0, *o-C*H (PPh$_2$)), 132.2 (d, $^3J_{CP}$ 7.0, *m-C*H (PPh$_2$)), 148.5 (s, *C*(OCH$_3$).

General Procedure for the Preparation of the Bis(iminophosphoranyl)methanides 2a-d

KHMDS (38 mg, 0.19 mmol) was added to a suspension of 0.063 mmol of the corresponding bis(iminophosphonium) bromide **1** in THF (5 mL). The reaction mixture immediately became clear taking a pale yellow color. Precipitating potassium bromide was removed by centrifugation and the supernatant solution dried in vacuo to yield a pale yellow powder.

2a: Yield 33 mg (0.062 mmol, 98%). The spectral parameters coincided with the published values.[17]

2b: Yield: 34 mg (0.061 mmol, 98%). $\delta_{P\{1H\}}$ (121.5 MHz, [D$_8$]-THF) 3.9 (s, P); δ_H (300 MHz, [D$_8$]-THF) 0.89 (18H, s, C(C*H*$_3$)$_3$), 1.05 (1H, t, $^2J_{HP}$ 3.0, PC*H*P), 7.12 (16H, m, *o*-C*H*, *m*-C*H* (PPh$_2$)), 7.79 (8H, m, *p*-C*H* (PPh$_2$)); δ_C (75.5 MHz, [D$_8$]-THF) 35.8 (dd, $^3J_{CP}$ 5.5, C(*C*H$_3$)$_3$), 52.1 (s, *C*(CH$_3$)$_3$), 127.5 (dd, $^2J_{CP}$ 5.5, *o-C*H (PPh$_2$)), 128.5 (s, *p-C*H (PPh$_2$)), 133.2 (dd, $^3J_{CP}$ 4.5, *m*-C*H* (PPh$_2$)), 146.2 (d, $^1J_{CP}$ 87.5, *ipso-C* (PPh$_2$)).

2c: Yield: 38 mg (0.062 mmol, 99%). The spectral parameters coincided with the published values.[17]

2d: Yield: 41 mg (0.062 mmol, 99%); $\delta_{P\{1H\}}$ (121.5 MHz, [D$_8$]-THF) 11.5 (s, P); δ_H (300 MHz, [D$_8$]-THF) 2.07 (1H, s, PC*H*P), 3.48 (6H, s, OC*H*$_3$), 6.12-6.45 (8H, m, C(OCH$_3$)C*HCHCHCH*), 6.94 (12H,

m, *o*, *p*-C*H* (PPh_2)), 7.78 (8H, m, *m*-C*H* (PPh_2)); δ_C (75.5 MHz, [D_8]-THF) 11.6 (t, $^1J_{CP}$ 120.0, P*C*HP), 55.9 (s, O*C*H_3), 112.5 (s, C(OCH_3)CH*C*H), 114.3 (s, N-CCH*C*H), 121.9 (s, C(OCH_3)*C*H), 122.6 (dd, $^3J_{CP}$ 7.0, N-C*C*H), 128.1 (dd, $^2J_{CP}$ 5.5, *o*-*C*H (PPh_2)), 129.3 (s, *p*-*C*H (PPh_2)), 132.2 (dd, $^3J_{CP}$ 4.0, *m*-*C*H (PPh_2)), 140.5 (d, $^1J_{CP}$ 101.0, *ipso*-*C* (PPh_2)), 145.6 (s, N-*C*), 153.6 (dd, $^3J_{CP}$ 11.0, N-C*C*(OCH_3)).

General Procedure for the Preparation of the Complexes 3a-d

In THF (5 mL), [$CrCl_3(THF)_3$] (24 mg ,0.063 mmol) was added to a solution of the corresponding bis(iminophosphoranyl)-methanide **2** (0.063 mmol) resulting in an immediate color change of the reaction mixture. After 1 h of stirring, the reaction mixture was centrifuged and the supernatant solution was dried in vacuo. The solid residue was finally washed with petrol ether (2 × 5 mL).

3a: Yield: 38 mg (0.029 mmol, 92%) of a dark blue powder. X-ray quality crystals were obtained by overnight standing of a concentrated dichloromethane solution of **3a**. Elemental analysis calcd. (%) for $C_{62}H_{70}Cl_4Cr_2N_4P_4$: C 60.01, H 5.69, N 4.51; found C 60.14, H 5.42, N 4.27.

3b: Yield: 36 mg (0.026 mmol, 84%) of a blue powder. X-ray quality crystals were obtained by overnight standing of a concentrated THF solution of **3b**. Elemental analysis calcd. (%) for $C_{66}H_{78}Cl_4Cr_2N_4P_4$: C 61.12, H, 6.06, N 4.32; found C 60.97, H 6.22, N 4.19.

3c: Yield: 38.5 mg (0.028 mmol, 88%) of a blue powder. X-ray quality crystals wee obtained by overnight standing of a concentrated THF solution of **3c**. Elemental analysis calcd. (%) for $C_{74}H_{62}Cl_4Cr_2N_4P_4$: C 64.55, H 4.54, N 4.07; found C 65.02, H 4.37, N 3.91.

3d: Yield: 43 mg (0.055 mmol, 87 %) of a brown powder. X-ray quality crystals were obtained by overnight standing of a concentrated THF solution of **3d**. Elemental analysis calcd. (%) for $C_{39}H_{35}Cl_2CrN_2O_2P_2$: C 62.58, H 4.71, N 3.74; found C 62.41, H 4.88, N 3.59.

Synthesis of 4

[$NiBr_2$(DME)] (19 mg, 0.061 mmol) was added to a solution of **2b** (34 mg, 0.061 mmol) in THF, resulting in an immediate color change of the reaction mixture to green. After 1 h, the potassium salts were removed by filtration. The solvent of the filtrate was removed in vacuo to yield **4** (34 mg, 0.051 mmol, 84%) as a highly air-sensitive deep red powder. Single crystals suitable for x-ray crystal structure analysis were obtained by cooling to -20°C a saturated solution of **4** in toluene.

Chapter 4

Synthesis of 4

Compound **4** was prepared as reported.[18]

General Procedure for the Synthesis of 7a-c

To a solution of **4** (262 mg, 0.78 mmol) in CH_2Cl_2 (20 mL), bromine (125 mg, 0.78 mmol, 40 µL) was added at -78°C. The cold bath was removed and stirring continued for 1 h. Then the corresponding amine (1.56 mmol) was added dropwise at -78°C. Subsequently, the reaction mixture was allowed to warm up again to r.t.. After 2 h, the precipitated ammonium salts were filtered off, then the CH_2Cl_2 solvent was removed to leave a white solid of crude **6**. MeOH (10 mL) was added, then HCl gas was bubbled through the MeOH solution for a couple of seconds. Water (20 mL) was added and **7** was extracted twice with CH_2Cl_2 (20 mL). The combined organic phases were dried over MgSO4, the solvent removed in vacuo to yield **7** as white powders.

7a:

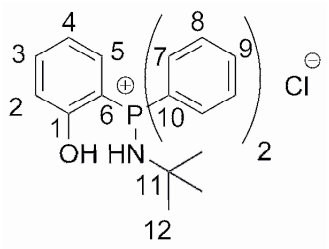

Yield: 166 mg (0.43 mmol, 55%). $^{31}P\{^1H\}$ ([D]chloroform, 20°C): δ = 35.2 (s, *P*). ^1H ([D]chloroform, 20°C): δ = 1.14 (s, 9H, C(12)H_3), 4.94 (sl, 1H, N*H*), 6.81-6.75 (m, 1H, C(2 or 4)*H*), 7.45-7.35 (m, 2H, C(3,5)*H*), 7.62-7.53 (m, 5H, C(8,2 or 4)*H*), 7.80-7.66 (m, 6H, C(7,9)*H*). ^{13}C ([D]chloroform, 20°C): δ = 33.1 (d, ^3J(P,C) = 4.4 Hz, *C*(12)), 56.8 (d, ^2J(P,C) = 4.8 Hz, *C*(11)), 108.1 (d, ^1J(P,C) = 107.3, *C*(6)), 121.2 (d, ^3J(P,C) = 13.9 Hz, *C*(2 or 4)), 123.7 (d, ^1J(P,C) = 101.8 Hz, *C*(10)), 129.8 (d, ^3J(P,C) = 12.4 Hz, *C*(2 or 4)), 130.8 (d, ^3J(P,C) = 13.3 Hz, *C*(8)), 133.1 (d, ^2J(P,C) = 10.5 Hz, *C*(5)), 135.0 (d, ^2J(P,C) = 11.4 Hz, *C*(7)), 135.8 (d, ^4J(P,C) = 3.0 Hz, *C*(9)), 137.7 (d, ^4J(P,C) = 1.7, *C*(3)), 162.6 (d, ^2J(P,C) = 1.8 Hz, *C*(1)). MS (CI): m/z (%): 350 $[M]^+$

7b:

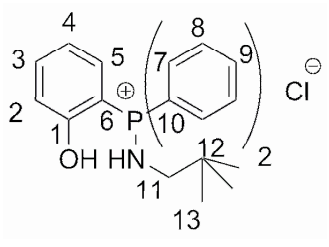

Yield: 124 mg (0.31 mmol, 40%). $^{31}P\{^{1}H\}$ ([D]chloroform, 20°C): δ = 36.4 (s, *P*). ^{1}H ([D]chloroform, 20°C): δ = 0.97 (d, 6H, ^{3}J(H,H) = 1.9, C(13)H_3), 2.11 (dd, 2H, ^{3}J(H,H) = 2.1 Hz, ^{3}J(H,H) = 1.9 Hz, C(11)H_2), 2.41 (s, 1H, O*H*), 4.90 (br s, 1H, N*H*) 6.92 (d, 1H, ^{3}J(H,H) = 4.1 Hz, C(2)*H*), 7.55-7.43 (m, 5H, C(4,8)*H*), 7.71-7.61 (m, 2H, C(3,5)*H*), 7.91-7.78 (m, 4H, C(7,9)*H*). ^{13}C ([D]chloroform, 20°C): δ = 25.7 (s, C(13)), 45.3 (d, ^{3}J(P,C) = 12.4 Hz, *C*(12)), 75.8 (d, ^{2}J(P,C) = 2.3 Hz, *C*(11)), 108.1 (d, ^{1}J(P,C) = 105.7 Hz, *C*(6)), 124.3 (d, ^{3}J(P,C) = 12.5 Hz, *C*(2)), 126.2 (d, ^{1}J(P,C) = 109.1 Hz, *C*(10)), 129.1 (d, ^{3}J(P,C) = 14.1 Hz, *C*(4)), 129.7 (d, ^{3}J(P,C) = 14.3 Hz, *C*(8)), 132.5 (d, ^{2}J(P,C) = 2.1 Hz, *C*(7)), 135.5 (d, ^{2}J(P,C) =1.7 Hz, *C*(5)), 136.3 (s, *C*(3)), 136.0(s, *C*(9)), 159.8 (d, ^{2}J(P,C) = 1.2 Hz, *C*(1)). MS (CI): m/z (%): 364 $[M]^+$

7c:

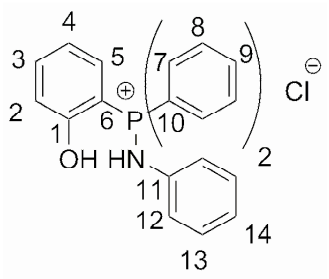

Yield: 165 mg (0.41 mmol, 52%). $^{31}P\{^{1}H\}$ ([D]chloroform, 20°C): δ = 39.9 (s, *P*). ^{1}H ([D]chloroform, 20°C): δ = 1.93 (s, 1H, O*H*), 5.21 (s, 1H, N*H*), 7.03 (d, 1H, 3J(H,H) = 4.4 Hz, C(2)*H*), 7.49-7.36 (m, 6H, C(4,8,13)*H*), 7.79-7.65 (m, 3H, C(3,5,14)*H*), 7.93-7.81 (m, 3H, C(7,9,12)*H*). ^{13}C ([D]chloroform, 20°C): δ = 107.8 (d,^{1}J(P,C) = 108.4 Hz, *C*(6)), 111.5 (s, *C*(14)), 117.3 (s, *C*(13)) 121.2 (d, ^{3}J(P,C) = 11.2 Hz, *C*(2)), 121.5 (d, ^{1}J(P,C) = 101.8, *C*(10)), 126.2 (d, ^{3}J(P,C) = 14.7 Hz, *C*(12)), 127.3 (d, ^{3}J(P,C) = 17.3 Hz, *C*(4)), 128.1 (d, ^{3}J(P,C) = 16.9 Hz, *C*(8)), 131.2 (d, ^{2}J(P,C) = 1.9 Hz, *C*(7)), 132.6 (d, ^{2}J(P,C) = 2.1 Hz, *C*(11)), 134.7 (d, ^{2}J(P,C) = 1.4 Hz, *C*(5)), 137.9 (s, *C*(3)), 135.1(s, *C*(9)), 167.2 (d,^{2}J(P,C) = 1.4 Hz, *C*(1)). MS (CI): m/z (%): 370 $[M]^+$

Synthesis of 13

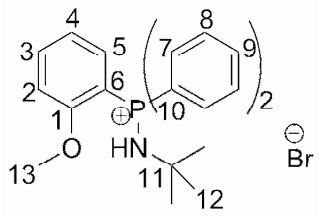

Bromine (125 mg, 0.78 mmol, 40 µL) was added dropwise to a solution of *o*-methoxyphenyl-diphenylphosphine (**11**) (228 mg, 0.78 mmol) in CH_2Cl_2 (20 mL) at -78°C. The reaction mixture is then warmed up to r.t., resulting in the formation of a white cloudy precipitate. Subsequently, *t*-BuNH_2 (114 mg, 1.56 mmol, 164 µL) was added to the reaction mixture at -78°, then the cold bath is removed and the reaction mixture stirred for 1 h. Water (30 mL) is added to the reaction mixture and the

organic phase extracted with CH_2Cl_2 (2 × 25 mL), dried over $MgSO_4$, and the solvent removed at reduced pressure. The pale white residue was then washed with a small quantity of THF, and after drying in vacuo, **13** was obtained as a white solid. Yield 222 mg (0.50 mmol, 64%).

$^{31}P\{^1H\}$ ([D]chloroform, 20°C): δ = 35.0 (s; *P*). ^1H ([D]chloroform, 20°C): δ = 1.57 (s, 9H; C(12)H_3), 3.89 (s, 3H; C(13)H_3), 7.00 and 7.20 (m, 1H; C(2,4)*H*), 7.45-7.58 (m, 4H; C(7)*H*), 7.59-7.73 (m, 3H; C(3,9)*H*), 7.76-7.93 (m, 5H; C(5,8)*H*). ^{13}C ([D]chloroform, 20°C): δ = 30.3 (s, C12), 54.7 (s, C11), 109.4 (d, ^1J(P,C) = 104.0 Hz, *C*(6)), 120.3 (d, ^3J(P,C) = 12.9 Hz, *C*(2 or 4)), 110.9 (d, ^3J(P,C) = 7.1 Hz, *C*(2 or 4)) 121.8 (d, ^1J(P,C) = 105.4 Hz, *C*(10)), 127.5 (d, ^3J(P,C) = 13.5 Hz, *C*(8)), 131.7 (d, ^2J(P,C) = 11.5 Hz, *C*(7)), 132.3 (s, *C*(9)), 133.9 (d, ^2J(P,C) = 8.4 Hz, *C*(5)), 135.5 (s, C(3)), 159.7 (d, ^2J(P,C) = 3.7 Hz, C(1)). MS (CI): m/z (%): 364 $[M]^+$

General Procedure for the Synthesis of 17a-e.

Following a procedure described before,[19] bromine (80 µL, 1.56 mmol) was added dropwise to a solution of bis(diphenylphosphino)methane (0.600 g, 1.56 mmol) in CH_2Cl_2 (40 mL) at -78°C. The reaction mixture was stirred for 20 minutes. $^{31}P\{1H\}$ (CH_2Cl_2) δ = 23.2 (d, ^2J(P,P) = 83 Hz), 58.6 (d, ^2J(P,P) = 83 Hz). The 2,2-dimethylpropylamine (0.365 mL, 3.12 mmol) was added to the reaction mixture at –78°C. The cold bath was removed and the reaction mixture was stirred for 1 h at room temperature. The solution was washed twice with water (20 mL), the organic layer was dried over $MgSO_4$ and the solvent was removed under vacuum to deliver a white solid, which was washed with a small quantity of diethyl ether.

1a Yield 0.584 g (1.15 mmol, 74%). $^{31}P\{^1H\}$ ([D]chloroform, 20°C): δ = -30.7 (d, ^2J(P,P) = 78.5 Hz, Ph_2PCH_2), 42.9 (d, ^2J(P,P) = 78.5 Hz, $Ph_2PN(CH_2)$). ^1H ([D]chloroform, 20°C): δ = 0.76 (9H, s, CH_3), 2.48 (2H, dd, ^3J(H,H) = 7.0 Hz, ^3J(P,H) = 8.0 Hz, $CH_2C(CH_3)_3$), 4.30 (2H, d, ^2J(P,H) = 17.0 Hz, PCH_2P), 7.00(1H, d, ^{3}J(H,H) = 7.0 Hz, N*H*),7.21 (4H, m, *p-H* (PPh_2)), 7.35 (4H, td, ^3J(H,H) = 7.5 Hz, ^4J(H,P) = 3.0 Hz, *m-H* (PPh_2)), 7.49 (4H, td, ^3J(H,H) = 7.5 Hz, ^{4}J(H,P) = 3.0 Hz, *m-H* (PPh_2)), 7.60 (4H, t, ^3J(H,H) = 7.5 Hz, *p-H* (PPh_2)), 7.78 (4H, dd, ^3J(H,H) = 7.5 Hz, ^3J(H,P) = 12.5 Hz, *o-H* (PPh_2)). ^{13}C ([D]chloroform, 20°C): δ = 22.7 (^1J(P,C) not measurable, PCH_2P), 27.3 (s, CH_3), 32.4 (d, ^3J(P,C) = 8.0 Hz, $CH_2C(CH_3)_3$), 53.7 (d, ^2J(P,C) = 4.5 Hz, $CH_2C(CH_3)_3$), 119.5 (d, ^1J(P,C) = 98 Hz, *ipso-C* (PPh2)), 128.8 (d, ^3J(P,C) = 8.0 Hz, *m-C*H (Ph_2P)), 129.4 (d, ^3J(P,C) = 13.0 Hz, *m-C*H (Ph_2P)) ,129.6 (s, *p-C*H (Ph_2P)), 133.0 (d, ^2J(P,C) = 21 Hz, *o-C*H (Ph_2P)), 133.7 (dd, ^2J(P,C) = 10.5 Hz, ^4J(P,C) = 3.0 Hz, *o-C*H (Ph_2P)), 134.4 (d, ^4J(P,C) = 3.0 Hz, *p-C*H (Ph_2P)), 135.2 (^3J(P,C) not measurable, *ipso-C* (PPh_2)). Elemental analysis calcd. (%) for $C_{29}H_{32}BrNP_2$: C 64.93, H 6.01, N 2.61; found: C 65.06, H 6.22, N 2.47.

17b-e: The syntheses were carried out in an analogous fashion. Spectral parameters coincided with the reported values.[19]

Synthesis of 18

18 was synthesized similarly to **17a-e** using 1,2-bis(diphenylphosphino)ethane (1g, 2.50 mmol) instead of bis(diphenylphosphino)methane.

Yield: 0.84 g (1.63 mmol , 65%). $^{31}P\{^{1}H\}$ ([D]chloroform, 20°C): δ = -12.0 (d, $^{3}J(P,P)$ = 46.0 Hz , Ph_2PCH_2), 38.9 (d, $^{3}J(P,P)$ = 46.0 Hz , $Ph_2PN(CH_2)$). ^{1}H ([D]chloroform, 20°C): δ = 6.86 (1H, t, $^{3}J(H,H)$ = 6.5 Hz, *H*NPh), 7.08 (2H, d, $^{3}J(H,H)$= 6.5 Hz, *H*NPh), 7.30-7.42 (8H, m, *H*-(Ph_2P)), 7.47 (3H, m, N*H* and *H*-NPh), 7.60 (4H, dd, $^{3}J(H,H)$ = 7.5 Hz, $J(P,H)$ = 3.0 Hz, *H*-(Ph_2P)), 7.70 (2H, t, $^{2}J(H,H)$ = 7.5.0 Hz, *H*-(Ph_2P)), 7.79 (4H, dd, $^{3}J(H,H)$ = 7.5 Hz, $^{3}J(H,H)$ = 13.5 Hz, *H*-(Ph_2P)). ^{13}C ([D]chloroform, 20°C): δ = 19,7 (*J* not measurable, *C*H_2P), 23.6 (*J* not measurable, *C*H_2P), 119.0 (d, $^{1}J(P,C)$ = 40.0 Hz, *ipso-C* (Ph_2P)), 127.8 (d, $J(P,C)$ = 8.0 Hz, *C*H-(Ph_2P)), 128.0 (s, *C*H-(NPh)), 128.6 (s, *C*H-(NPh)), 129.1 (d, $J(P,C)$ = 13.0 Hz, *C*H-(Ph_2P)), 129.5 (d, $^{1}J(P,C)$ = 51.0 Hz, *ipso-C* (Ph_2P)), 129.9 (d, $J(P,C)$ = 5.0 Hz, *C*H-(Ph_2P)), 131.2 (s, *C*H-(NPh)), 132.0 (d, $J(P,C)$ = 5.0 Hz, *C*H-(Ph_2P)), 132.2 (d, $J(P,C)$ = 3.0 Hz, *C*H-(Ph_2P), 134.0 (dd, $J(P,C)$ = 13.5 Hz, $J(P,C)$ = 3.0 Hz , *C*H-(Ph_2P)), 140.0 (*J* not measurable, *ipso-C* (NPh)). Elemental analysis calcd. (%) for $C_{32}H_{30}BrNP_2$: C 67.38, H 5.30, N 2.46; found : C 67.39, H 5.13, N , 2.41.

General Procedure for the Synthesis of 19a-c

Bromine (1.96 mL, 38.13 mmol) was added to a solution of triphenylphosphine (10g, 38.13 mmol) in CH_2Cl_2 (200 mL) at –78°C. While warming to room temperature the solution turned yellow, stirring was pursued 1 h. Then, the reaction mixture was cooled to -78°C and Et_3N (5.31 mL, 38.13 mmol) followed by the amine (38.13 mmol) were added. After stirring 2 h at room temperature, the solution was washed twice with water (100 mL), the organic layer was dried over $MgSO_4$ and the solution was concentrated under vacuum. After reducing the solvent volume to 50 mL, THF (50 mL) was added, the product precipitated. After removing the CH_2Cl_2, the phosphine-aminophosphonium salts **19a-c** were isolated by filtration as a white solid.

19a: Yield 92% (35.10 mmol, 7.5 g). $^{31}P\{^{1}H\}$ ([D]chloroform, 20°C): δ = 39.2 (s, *P*). ^{1}H ([D]chloroform, 20°C): δ = 0.74 (9H, s, C*H*$_3$), 2.82 (2H, dd, $^{3}J(H,H)$ = 8.0 Hz ,$^{3}J(H,P)$ = 10.0 Hz, NC*H*$_2$), 7.62 (6H, td, $^{3}J(H,H)$ = 7.5 Hz, $^{4}J(H,P)$ = 4.5 Hz, *m*-C*H* (Ph_3P)), 7.71 (3H, t, $^{3}J(H,H)$ = 7.5, *p*-C*H* (Ph_3P)), 7.86 (6H, dd, $^{3}J(H,H)$ = 7.5 Hz, 3$J(H,P)$ = 8.5 Hz, *o*-C*H* (Ph_3P)), NH not observed. ^{13}C ([D]chloroform, 20°C): δ = 27.3 (s, *C*H$_3$), 32.7 (d, $^{3}J(C,P)$ = 6.5 Hz, *C*(CH$_3$)$_3$), 56.6 (d, $^{2}J(C,P)$ = 1.0 Hz, *C*H$_2$), 121.5 (d, $^{1}J(C,P)$ = 102.5 Hz, *ipso-C* (Ph_3P)), 129.9 (d, $^{2}J(C,P)$ = 13.1 Hz, *o*-*C*H (Ph_3P)), 134.1 (d, $^{3}J(C,P)$ = 10.8 Hz, *m*-*C*H (Ph_3P)), 134.7 (t, $^{4}J(C,P)$ = 2.8 Hz, *p*-*C*H (Ph_3P)).

19b: Yield 80% (30.50 mmol, 6.1 g). $^{31}P\{^{1}H\}$ ([D]chloroform, 20°C): δ = 36.6 (s, *P*). ^{1}H ([D]chloroform, 20°C): δ = 1.35 (6H, d, $^{3}J(H,H)$ = 6.0 Hz, C*H*$_3$), 3.16 (1H, hept d, $^{3}J(H,H)$ = 6.0 Hz, $^{3}J(H,P)$ = 3.0 Hz, C*H*), 7.20 (1H, bd, $^{2}J(H,P)$ = 10.0 Hz, N*H*), 7.60 (6H, td, $^{3}J(H,H)$ = 7.5 Hz, $^{4}J(H,P)$

= 3.0 Hz, *m*-C*H* (Ph_3P)), 7.72 (3H, vt, ^3J(H,H) = 7.5 Hz, *p*-C*H* (Ph_3P)), 7.83 (6H, dd, ^3J(H,H) = 7.5 Hz, ^3J(H,P) = 6.0 Hz, *o*-C*H* (Ph_3P)). ^{13}C ([D]chloroform, 20°C): δ = 24.8 (t, ^3J(C,P) = 13.0 Hz, *C*H_3), 47.0 (d, ^2J(C,P) = 2.0 Hz, *C*H), 121.8 (d, ^1J(C,P) = 102.0 Hz, *ipso-C* (Ph_3P)), 129.7 (d, ^3J(C,P) = 13.0 Hz, *m*-*C*H (Ph_3P)), 133.6 (t, ^2J(C,P) = 11.0 Hz, *o*-*C*H (Ph_3P)), 134.6 (t, ^4J(C,P) = 3.0 Hz, *p*-*C*H (Ph_3P)).

19c: Yield 76% (29.0 mmol, 6.0 g). ^{31}P{^{1}H} ([D]chloroform, 20°C): δ = 34.2 (s, *P*). ^{1}H ([D]chloroform, 20°C): δ = 1.27 (9H, s, C(C*H*$_3$)$_3$), 7.14 (1H, d, ^2J(H,P) = 6.5 Hz, N*H*), 7.58 (6H, td, ^3J(H,H) = 7.5 Hz, ^4J(H,P) = 3.5 Hz, *m*-C*H* (Ph_3P)), 7.67 (3H, td, ^3J(H,H) = 7.6 Hz, ^5J(H,P) = 2.0 Hz, *p*-C*H* (Ph_3P)), 7.90 (6H, dd, ^3J(H,H) = 7.0 Hz, ^3J(H,P) = 1.5 Hz, *o*-C*H* (Ph_3P)). ^{13}C ([D]chloroform, 20°C): δ = 32.2 (d, ^3J(C,P) = 4.5 Hz, C(*C*H$_3$)$_3$), 56.6 (d, ^2J(C,P) = 4.5 Hz, *C*(CH$_3$)$_3$), 123.1 (d, ^1J(C,P) = 102.0 Hz, *ipso-C* (Ph_3P)), 129.6 (d, ^2J(C,P) = 13.0 Hz, *o*-*C*H (Ph_3P)), 133.9 (d, ^3J(C,P) = 11.0 Hz, *m*-*C*H (Ph_3P)), 134.5 (t, ^4J(C,P) = 3.0 Hz, *p*-*C*H (Ph_3P)).

General Procedure for the Synthesis of Compounds 20a-d

n-BuLi (5.84 mmol, 3.90 mL of a 1.6 M solution in hexanes) was added to a suspension of compound **19** (2.92 mmol) in Et_2O (100 mL) cooled at -78°C. The cold bath was then removed and stirring was pursued 30 min. at room temperature leading to a clear yellow solution. Then, the reaction mixture was cooled to -78°C, the corresponding chlorophosphine (2.92 mmol) was added and a white precipitate appeared. After stirring 2 h at room temperature, Et_2O was removed under vaccum, CH_2Cl_2 (50 ml) was added, the solution was washed with a aqueous solution of tetrafluoroboric acid (1 M, 30mL) and twice with a saturated aqueous solution of $NaBF_4$ (20 mL). The organic layer was dried over $MgSO_4$ and the solution was concentrated under vacuum, the obtained white solid was washed with Et_2O (20 mL).

20a: Yield: 1.41 g (2.28mmol, 78%). ^{31}P{^{1}H} ([D]chloroform, 20°C): δ = -15.8 (d, ^2J(P,P) = 24.5 Hz), 41.3 (d, ^2J(P,P) = 24.5 Hz). ^{1}H ([D]chloroform, 20°C): δ = 0.76 (9H, s, C*H*$_3$), 2.78 (2H, dd, ^3J(H,H) = 7.0 Hz, ^3J(P,H) = 7.5 Hz, C*H*$_2$C(CH$_3$)$_3$), 4.90 (1H, vt, ^3J(H,H) = 7.0 Hz, N*H*), 6.80 (4H, dd, *3J*(H,H) = 7.5 Hz, ^3J(H,P) = 8 Hz, *o*-C*H* (PPh_2)), 7.20 (4H, vt, ^3J(H,H) = 7.5 Hz, *m*-C*H* (PPh_2)), 7.30 (2H, t, *3J*(H,H) = 7.5 Hz, *p*-CH (PPh_2)), 7.49 (6H,m, PPh_2 and C*H*-(ArPP)), 7.62 (2H, vt, ^3J(H,H) = 8.0 Hz, *p*-C*H* (PPh_2)), 7.76 (4H, dd, ^3J(H,H) = 7.5 Hz, ^3J(H,P) = 7.5 Hz, *o*-C*H* (PPh_2)), 7.82 (1H, m, C*H*-(ArPP)), 8.16 (1H, dd, ^3J(H,H) = 7.5 Hz, *J*(H,P) = 8.0 Hz, C*H*-(ArPP)). ^{13}C ([D]chloroform, 20°C): δ = 26.9 (s, *C*H$_3$), 32.4 (s, *C*(CH$_3$)$_3$), 54.7 (s, *C*H$_2$C(CH$_3$)$_3$), 121.0 (d, ^2J(C,P) = 109.0 Hz, *ipso-C* (PPh_2)), 128.7 (d, ^3J(P,C) = 7.0 Hz, *m*-*C*H (Ph_2P)), 129.2 (d, ^2J(C,P) = 13.0 Hz, *C*H-(ArPP)), 129.4 (s, *p*-*C*H (Ph_2P)) ,129.7 (d, ^2J(C,P) = 13.5 Hz, *o*-*C*H (Ph_2P)), 131.6 (dd, ^2J(C,P) = 12.5 Hz, ^3J(C,P) = 10.5, *C*H-(ArPP)), 132.9 (d, ^3J(C,P) = 7.5 Hz, *m*-*C*H (Ph_2P)), 133.8 (dd, ^2J(C,P) = 10.5 Hz, ^3J(C,P) = 3.0 Hz, *o*-*C*H (Ph_2P)), 134.9 (d, ^4J(C,P) = 2.5 Hz, *p*-*C*H (Ph_2P)), 135.2 (*J*(C,P) not measurable, *ipso-C* (PPh_2)),

136.7 (dd, ^{3}J(C,P) = 9.5 Hz, ^{2}J(C,P) = 10.0 Hz, *C*H-(ArPP)). Elemental analysis calcd. (%) for $C_{35}H_{36}BF_4NP_2$: C 67.87, H 5,86, N 2.26; found: C 68.12, H 5.77, N 1.97.

20b: Yield: 1.24 g (2.10 mmol, 72%). $^{31}P\{^{1}H\}$ ([D]chloroform, 20°C): δ = -15.2 (d, ^{3}J(P,P) = 25.5 Hz, 36.7 (d, ^{3}J(P,P) = 25.5 Hz). ^{1}H ([D]chloroform, 20°C): δ = 1.34 (6H, d, ^{3}J(H,H) = 6.50 Hz, CH_3), 3.07 (1H, bs, C*H*), 6.76 (4H, vt, ^{3}J(H,H) = 7.5 Hz, *m*-C*H* (Ph_2P)), 7.16 (4H, vt, ^{3}J(H,H) = 7.5 Hz, *m*-C*H* (Ph_2P)), 7.28 (2H, *m*, *p*-C*H* (Ph_2P)), 7.40 (4H, dd, ^{3}J(H,H) = 7.5 Hz, ^{3}J(H,P) = 11.0 Hz, *o*-C*H* (Ph_2P)), 7.52 (2H, vt, ^{3}J(H,H) = 7.5 Hz, *p*-C*H* (Ph_2P)), 7.68 (1H, vt, ^{3}J(H,H) = 8.0 Hz, C*H*-(ArPP)), 7.83 (1H, m, C*H*-(ArPP)), 7.97 (dd, 4H, ^{3}J(H,H) = 7.5 Hz, ^{3}J(H,P) = 13.0 Hz, *o*-C*H* (Ph_2P)), 8.40 (1H, mt, ^{3}J(H,H) = 8.0 Hz, C*H*-(ArPP)), 8.64 (1H, m, C*H*-(ArPP)), N*H* not observed. ^{13}C ([D]chloroform, 20°C): δ = 25.5 (s, *C*H_3), 47.5 (s, *C*H), 123.9 (d, ^{1}J(C,P) = 103.0 Hz, *C*$(CH_3)_3$), 128.9 (d, ^{3}J(C,P) = 6.5 Hz, *m*-*C*H (Ph_2P)), 129.4 (vs, *p*-*C*H (Ph_2P)), 129.6 (d, ^{3}J(C,P) = 5.5 Hz, *m*-*C*H (Ph_2P)), 130.1 (vt, *J*(CP) = 10.0 Hz, *C*H-(ArPP)), 131.5 (d, *J*(C,P) = 12.5 Hz, *C*H-(ArPP)), 133.3 (d, ^{2}J(C,P) = 18.5 Hz, *o*-*C*H (Ph_2P)), 134.0 (d, ^{2}J(C,P) = 15.5 Hz, *o*-*C*H-(Ph_2P)), 134.1 (vs, *ipso-C*), 134.6 (vs, *p*-*C*H (Ph_2P)), 135.2 (vs, *ipso-C*), 137.4 (d, *J*(C,P) = 12.0 Hz, *C*H-(ArPP)), 139.0 (d, *J*(C,P) = 13.5 Hz, *C*H-(ArPP)), 141.6 (vs, *ipso-C*). Elemental analysis calcd. (%) for $C_{33}H_{32}BF_4NP_2$: C 67.02, H 5.45, N 2.37; found: C 66.86, H 5.39, N 2.48.

20c: Yield: 1.49 g (2.45 mmol, 84%). $^{31}P\{^{1}H\}$ ([D]chloroform, 20°C): δ = -16.7 (d, ^{3}J(P,P) = 23.5 Hz), 34.9 (d, ^{3}J(P,P) = 23.5 Hz). ^{1}H ([D]chloroform, 20°C): δ = 1.14 (9H, s, C(C$H_3)_3$), 4.60 (1H, bd, ^{2}J(H,P) = 6.5 Hz, N*H*), 6.70 (4H, dd, ^{3}J(H,H) = 7.5 Hz, ^{4}J(H,P) = 8.0 Hz, *m*-C*H* (Ph_2P)), 7.13 (4H, td, ^{3}J(H,H) = 7.5 Hz, ^{5}J(H,P) = 1.5 Hz, *p*-C*H* (Ph_2P)), 7.35 (1H, bd, ^{3}J(H,H) = 7.5 Hz, C*H*-(ArPP)), 7.42 (4H, td, ^{3}J(H,H) = 7.5 Hz, ^{4}J(H,P) = 3.5 Hz, *m*-C*H* (Ph_2P)), 7.53 (4H, dd, ^{3}J(H,H) = 7.5 Hz, ^{3}J(H,P) = 15.0 Hz, *o*-C*H* (Ph_2P)), 7.66 (2H, t, ^{3}J(H,H) = 7.5 Hz, C*H*-(ArPP)), 7.79 (4H, dd, 3*J*HH= 7.5 Hz, ^{3}J(H,P) = 12.0 Hz, C*H*-(ArPP)). ^{13}C ([D]chloroform, 20°C): δ = 32.3 (d, ^{3}J(C,P) = 4.0 Hz, *C*H_3), 57.1 (d, ^{2}J(C,P) = 5.0 Hz, *C*$(CH_3)_3$), 123.2 (d, ^{1}J(C,P)= 104.0 Hz, ^{1}J(C,P) = 2.5 Hz, *ipso-C* (Ph_2P), 129.1 (d, 3*J*(C,P) = 7.0 Hz, *m*-*C*H-(Ph_2P)), 129.2 (s, *p*-*C*H (Ph_2P)) 130.0 (d, ^{2}J(C,P) = 13.5 Hz, *o*-*C*H-(Ph_2P)), 130.3 (dd, ^{3}J(C,P) = 5.5 Hz, ^{2}J(C,P) = 13.0 Hz, *C*H-(ArPP)), 131.4 (d, ^{3}J(C,P) = 13.0 Hz, *C*H-(ArPP)), 133.3 (d, ^{2}J(C,P) = 19.0 Hz, *o*-*C*H (Ph_2P)), 134.3 (d, ^{3}J(C,P) = 11.0 Hz, *m*-*C*H (Ph_2P)), 135.0 (d, ^{4}J(C,P) = 3.0 Hz, *p*-*C*H (Ph_2P)), 139.3 (bd, ^{2}J(C,P) = 12.0 Hz, *C*H-(ArPP)), 141.6 (dd, ^{3}J(C,P) = 14.0 , Hz, ^{1}J(C,P) = 20.0, *ipso-C* (Ph_2P)), *ipso-C* of ArPP not observed. Elemental analysis calcd. (%) for $C_{34}H_{34}BF_4NP_2$: C 67.45, H 5.66, N 2.31; found: C 67.61, H 5.45, N 2.23.

20d: Yield 1.18 g (1.72 mmol, 75%). $^{31}P\{^{1}H\}$ ([D]chloroform, 20°C): δ = -1.8 (d, ^{3}J(P,P) = 18.5 Hz), 39.3 (d, ^{3}J(P,P) = 18.5 Hz). ^{1}H ([D]chloroform, 20°C): δ = 0.63 (6H, dd, ^{3}J(H,H) = 7.0 Hz, ^{3}J(H,P) = 14.5 Hz, CH(C$H_3)_2$), 1.27 (9H, s, C$(CH_3)_3$), 1.72 (1H, hept, ^{2}J(H,H) = 7.0 Hz, C*H*$(CH_3)_2$), 5.94 (1H, bd, 2*J*(H,P) = 12.0 Hz, N*H*), 7.73-7.90 (m, 14H, C*H*-(ArPP) and *o*,*m*,*p*-C*H* (PPh_2)). ^{13}C

([D]chloroform, 20°C): δ = 18.5 (d, ^2J(C,P) = 16 Hz, CH(CH$_3$)$_3$), 19.4 (d, ^2J(C,P) = 12 Hz, CH(CH$_3$)$_2$), 24.8 (d, ^1J(C,P) = 11 Hz, CH(CH$_3$)$_2$), 31.4 (d, 3J(C,P) = 4 Hz, C(CH$_3$)$_3$), 56.2 (d, ^2J(C,P) = 5 Hz, C(CH$_3$)$_3$), 122.7 (d, ^1J(C,P) = 101 Hz, *ipso-C* (Ph$_2$P)), 127.9 (d, J(C,P) = 11 Hz, CH-(ArPP)), 128.6 (d, ^3J(C,P) =13.5 Hz, *m-C*H (Ph$_2$P)), 129.4 (d, J(C,P) = 14 Hz, CH-(ArPP)), 130.8 (d, J(C,P) = 10 Hz, CH-(ArPP)), 132.7 (d, ^4J(C,P) = 3 Hz, *p-C*H-(Ph$_2$P)), 133.5 (td, ^2J(C,P) = 13.5 Hz, ^5J(C,P) = 3 Hz, *o-C*H (Ph2P)), 134.2 (d, J(C,P) = 13 Hz, CH-(C$_6$H$_4$P$_2$)). *ipso-C*-(ArPP) not observed. Elemental analysis calcd. (%) for $C_{28}H_{38}BF_4NP_2$: C 62.58, H 7.13 N 2.61; found: C 62.39, H 7.22, N 2.41.

Synthesis of 21

KHMDS (38 mg, 0.19 mmol) was added to a solution of **17d** (111 mg, 0.19 mmol) in THF (7 mL). Subsequently, [CrBr$_3$(THF)$_3$] (97 mg, 0.19 mmol) were added, resulting in an immediate color change to dark violet of the reaction mixture. After filtration of the precipitated potassium salts, the solvent was removed in vacuo, and the violet residual powder was triturated with hexanes (5 mL). After drying in vacuo, **21** was obtained as a violet powder. Yield: 135 mg (0.17 mmol, 89%).

Elemental analysis calcd. (%) for $C_{32}H_{29}Br_3CrNOP_2$: C 48.21, H 3.67, N 1.76; found C 48.54, H 3.98, N 1.52. Single crystals suitable for x-ray crystal structure analysis could be obtained by slow diffusion of hexanes into a concentrated solution of **21** in THF.

Synthesis of 22

KHMDS (38 mg, 0.19 mmol) was added to a solution of **17e** (109 mg, 0.19 mmol) in THF (7 mL). Subsequently, [CrCl$_3$(THF)$_3$] (71 mg, 0.19 mmol) were added, resulting in an immediate color change to dark violet of the reaction mixture. After filtration of the precipitated potassium salts, the solvent was removed in vacuo, and the violet residual powder was triturated with hexanes (5 mL). After drying in vacuo, **22** was obtained as a violet powder. Yield: 117 mg (0.18 mmol, 95%).

Elemental analysis calcd. (%) for $C_{31}H_{28}Cl_3CrN_2P_2$: C 57.38, H 4.35, N 4.32; found C 57.99, H 4.89.98, N 4.11. Single crystals suitable for x-ray crystal structure analysis could be obtained by slow diffusion of hexanes into a concentrated solution of **22** in CH_2Cl_2.

General Procedure for the Synthesis of 23a-d, 24, 25a-d

n-BuLi (178.5 µL, 0.285 mmol) was added to a suspension of ligand **17**, **18**, or **20** (0.285 mmol) in THF (5 mL) cooled at -78 °C. The cold bath was removed and the solution allowed to warm to room temperature. Then, [NiBr$_2$(DME)] (88 mg, 0.285 mmol) was added and the solution turned immediately from colorless to blue. After stirring for 30 min. at room temperature, a blue (red in the case of **23d**,**e**) solid precipitated, which was isolated by filtration. This solid was dissolved in CH_2Cl_2 (5 mL) to remove the insoluble lithium salts. After removal of solvent under vacuum, the obtained blue solid was washed with Et_2O (10 mL).

23a: Yield 157 mg (0.23 mmol, 80%). HR-EI-MS: 684.9825 (M $C_{30}H_{33}NP_2NiBr_2$; calc. 684.9809), 606.0633 (M $C_{30}H_{33}NP_2NiBr$; calc. 606.0625). Elemental analysis calcd. (%) for $C_{30}H_{33}NP_2NiBr_2$: C 52.37, H 4.83, N, 2.04; found: C 52.42, H 4.93, N, 2.18.

23b: Analytical data coincided with the reported values.[20]

23c Yield 154 mg (0.22 mmol, 78%). HR-EI-MS: 690.9351 (M $C_{31}H_{27}NP_2NiBr_2$; calc. 690.9339). 612.0148 (M $C_{31}H_{27}NP_2NiBr$; calc. 612.0156). Elemental analysis calcd. (%) for $C_{31}H_{27}NP_2NiBr_2$: C, 53.65, H 3.92, N 2.02; found: C 53.72, H 3.81, N 2.37.

23d: Yield: 142 mg (0.19 mmol, 69%). HR-EI-MS: 707.9434 (M $C_{32}H_{29}NOP_2NiBr_2$; calc. 722.9429), 644.0251 (M $C_{32}H_{29}NOP_2NiBr$; calc. 629.0268). Elemental analysis calcd. (%) for $C_{32}H_{29}NOP_2NiBr_2$: C 53.08; H 4.04, N 1.93; found: C 52.89, H 3.86, N 2.02.

23e: Yield: 164 mg (0.23 mmol, 81%). HR-EI-MS: 707.9481 (M $C_{31}H_{28}N_2P_2NiBr_2$; calc. 707.9415), 629.0231 (M $C_{31}H_{28}N_2P_2NiBr$; calc. 629.0217). Elemental analysis calcd. (%) for $C_{31}H_{28}N_2P_2NiBr_2$: C 59.18, H 4.49, N 4.45; found: C 59.32, H 4.91, N 4.16.

24: Yield: 151 mg (0.20 mmol, 71%). HR-EI-MS: 704.9456 (M $C_{29}H_{32}NP_2NiBr_2$; calc. 704.9496), 626.0304 (M $C_{29}H_{32}NP_2NiBr$; calc. 626.0312). Elemental analysis calcd. (%) for $C_{29}H_{32}NP_2NiBr_2$: C 54.28, H 4.13, N 1.98; found: C 54.35, H 4.22, N 1.72.

25a: Yield: 175 mg (0.23 mmol, 82%) HR-EI-MS: 746.9969 (M $C_{35}H_{35}NP_2NiBr_2$; calc. 746.9965). 668.0761 (M $C_{35}H_{35}NP_2NiBr_2$; calc. 668.0782). Elemental analysis calcd. (%) for $C_{35}H_{35}NP_2NiBr_2$: C 56.04, H 4.70, N 1.87. Found: C 56.19, H 4.83, N 2.06.

25b: Yield 161 mg (0.22 mmol, 78%). HR-EI-MS: 718.9645 (M $C_{33}H_{31}NP_2NiBr_2$; calc. 718.9652), 639.0402 (M $C_{33}H_{31}NP_2NiBr$; calc. 639.0390). Elemental analysis calcd. (%) for $C_{33}H_{31}NP_2NiBr_2$: C 54.89, H 4.33, N 1.94; found: C 54.64, H 4.24, N 1.89.

25c: Yield 147 mg (0.20 mmol , 70%). HR-EI-MS: 732.9783 (M $C_{34}H_{33}NP_2NiBr_2$; calc. 732.9809), 654.0595 (M $C_{34}H_{33}NP_2NiBr$; calc. 654.0625). Elemental analysis calcd. (%) for $C_{34}H_{33}NP_2NiBr_2$: C 55.48, H 4.52, N 1.90; found: C 55.28, H 4.34, N, 1.81.

25d: Yield 143 mg (0.21 mmol, 75%). HR-EI-MS: 665.0091 (M $C_{28}H_{37}NP_2NiBr_2$; calc. 665.0122), 586.0948 (M $C_{28}H_{37}NP_2NiBr$; calc. 586.0938). Elemental analysis calcd. (%) for $C_{28}H_{37}NP_2NiBr_2$: C 50.34, H 5.58, N 2.10; found: C 50.43, H 5.47, N 2.20.

General Procedure for the Synthesis of 28a,b.

MeLi (2 mmol, 1.24 mL of a 1.6 M solution in Et_2O) was added dropwise to a suspension of the starting aminophosphonium salt **19** (1 mmol) in Et_2O (15mL) at -78°C. The cold bath was removed and stirring was continued at room temperature for 90 minutes to give an orange solution. The corresponding disulfide (1 mmol) was then added at -78°C and the mixture was stirred at room temperature during 12 h. Et_2O was removed in vacuum and CH_2Cl_2 (15mL) was added. The reaction mixture was washed twice with an aqueous solution of HBF_4 0.1 M (10 mL), once with a saturated solution of $NaBF_4$ in water (10 mL), then dried over $MgSO_4$. The volume of CH_2Cl_2 was reduced and the pale white raw product was recrystallized from a minimum amount of THF/Et_2O to yield **28** as white powders.

28a:

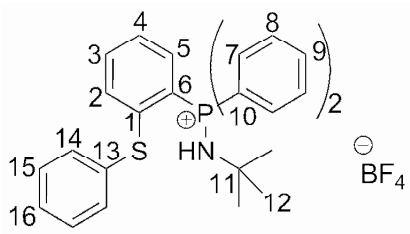

Yield: 434 mg (0.82 mmol, 82%). $^{31}P\{^1H\}$ ([D]chloroform, 20°C): δ = 32.3 (s, *P*). ^1H ([D]chloroform, 20°C): δ = 1.20 (s, 9H, C(12)H_3), 6.62-6.60 (m, 1H, C(14)*H*), 7.24-7.0 (m, 4H, C(2 or 4,15,16)*H*), 7.41-7.24 (m, 1H,C(2 or 4)*H*), 7.69-7.50 (m, 7H, C(8,3)*H*), 7.89-7.80 (m, 4H, C(7)*H*), 8.22-8.13 (m, 1H, C(5)*H*). ^{13}C ([D]chloroform, 20°C): δ = 30.2 (d, ^3J(P,C) = 3.9 Hz, *C*(12)), 55.1 (d, ^2J(P,C) = 4.3 Hz, *C*(11)), 128.6 (s, *C*(16)), 129.0 (d, ^3J(P,C) = 12.2 Hz, *C*(2 or 4)), 129.9 (s, *C*(15)), 130.1 (d, ^3J(P,C) = 13.5 Hz, *C*(8)) 131.1 (s, *C*(14)), 133.6 (s, *C*(13)), 134.1 (d, ^2J(P,C) = 11.2 Hz, *C*(7)), 135.0 (d, ^4J(P,C) = 2.8 Hz, *C*(9)), 135.6 (s, *C*(3)), 135.6 (d, ^3J(P,C) = 9.5 Hz, *C*(2 or 4)), 136.3 (d, ^2J(P,C) = 10.3 Hz, *C*(5)), 139.8 (d, ^2J(P,C) =10.1 Hz, *C*(1)). MS (CI): m/z (%): 442 $[M]^+$.

Single crystals suitable for x-ray crystal structure analysis could be obtained by slow evaporation of a concentrated solution of **28a** in CH_2Cl_2.

28b:

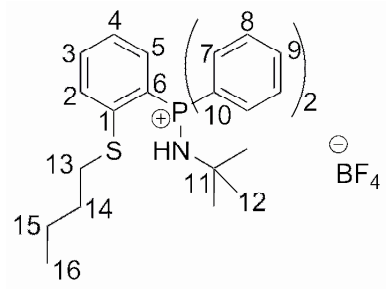

Yield: 351 mg (0.69 mmol, 69%). $^{31}P\{^1H\}$ ([D]chloroform, 20°C): δ = 35.2 (s, *P*). ^1H ([D]chloroform, 20°C): δ = 0.82 (t, 3H, C(16)H_3), 1.22 (s, 9H, C(12)H_3), 7.24-7.0 (m, 4H, C(2 or 4,15,16)*H*), 7.41-7.24 (m, 1H,C(2 or 4)*H*), 7.69-7.50 (m, 7H, C(8,3)*H*), 7.89-7.80 (m, 4H, C(7)*H*), 8.22-8.13 (m, 1H, C(5)*H*).

^{13}C ([D]chloroform, 20°C): δ = 30.2 (d, ^{3}J(P,C) = 3.9 Hz, *C*(12)), 55.1 (d, ^{2}J(P,C) = 4.3 Hz, *C*(11)), 128.6 (s, *C*(16)), 129.0 (d, ^{3}J(P,C) = 12.2 Hz, *C*(2 or 4)), 129.9 (s, *C*(15)), 130.1 (d, ^{3}J(P,C) = 13.5 Hz, *C*(8)) 131.1 (s, *C*(14)), 133.6 (s, *C*(13)), 134.1 (d, ^{2}J(P,C) = 11.2 Hz, *C*(7)), 135.0 (d, ^{4}J(P,C) = 2.8 Hz, *C*(9)), 135.6 (s, *C*(3)), 135.6 (d, ^{3}J(P,C) = 9.5 Hz, *C*(2 or 4)), 136.3 (d, ^{2}J(P,C) = 10.3 Hz, *C*(5)), 139.8 (d, ^{2}J(P,C) =10.1 Hz, *C*(1)). MS (CI): m/z (%): 422 $[M]^{+}$.

General Procedure for the Synthesis of 29a,b

MeLi (2 mmol, 1.24 mL of a 1.6 M solution in Et_2O) was added dropwise to a suspension of the starting aminophosphonium salt **19** (1 mmol) in THF (10mL) at -78°C. The cold bath was removed and stirring was continued at room temperature for 6 h hours to give an orange solution. S_8 (32 mg, 0.125 mmol) was then added. Stirring was continued for further 30 min. upon which an excess of HBF_4/ether was added. THF was removed in vacuum and CH_2Cl_2 (15mL) was added. The reaction mixture was washed twice with an aqueous solution of HBF_4 0.1M (5 mL), once with a saturated solution of $NaBF_4$ in water, then dried over $MgSO_4$. The volume of CH_2Cl_2 was reduced in vacuo, then a minimum amount of THF was added to precipitate **29** as white solids.

29a:

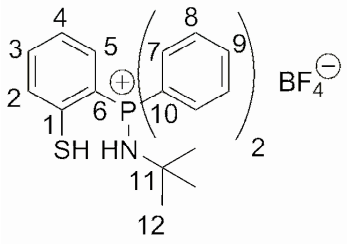

Yield 326 mg (0.72 mmol,72%). $^{31}P\{^{1}H\}$ ([D]chloroform, 20°C): δ = 29.5 (s, *P*). ^{1}H ([D]chloroform, 20°C): δ = 1.22 (s, 9H, C(12)H_3), 3.96 (large, 1H, S*H*) 4.76 (d, ^{2}J(P,H) = 7.7 Hz, 1H, N*H*), 7.46-7.38 (m, 1H, C(2 or 4)*H*), 7.56-7.51 (m, 2H, C(3,2 or 4)*H*) 7.63-7.56 (m, 4H, C(8)*H*) 7.72-7.65 (m, 2H, C(9)*H*),7.85-7.74 (m, 5H, C(5,7)*H*). ^{13}C ([D]chloroform, 20°C): δ = 32.0 (d, ^{3}J(P,C) = 4.0 Hz, *C*(12)) 57.2 (d, ^{2}J(P,C) = 4.5 Hz, *C*(11)), 121.8 (d, ^{1}J(P,C) = 105.1 Hz, *C*(6)), 122.2 (d, ^{1}J(P,C) = 103.8 Hz, *C*(10)), 127.4 (d, ^{3}J(P,C) = 12.7 Hz, *C*(2 or 4)) 130.4 (d, ^{3}J(P,C) = 13.4 Hz, *C*(8)), 133.9 (d, ^{2}J(P,C) = 11.3 Hz, *C*(7)), 135.3 (d, ^{4}J(P,C) = 2.9 Hz, *C*(9)), 135.5 (d, ^{3}J(P,C) = 10.0 Hz, C(2 or 4)) 135.5 (s, *C*(3)),136.6 (d, ^{2}J(P,C) = 11.3 Hz, *C*(5)), 138.8 (d, ^{2}J(P,C) = 8.4 Hz, *C*(1)). MS (CI): m/z (%): 366 $[M]^{+}$

Single crystals suitable for x-ray crystal structure analysis could be obtained by slow evaporation of a concentrated CH_2Cl_2 solution of **29a**.

29b:

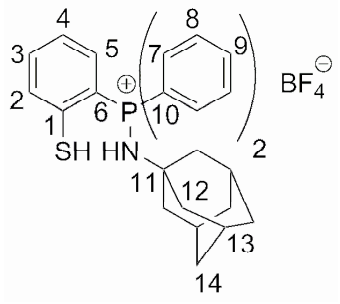

Yield: 399 mg (0.75 mmol, 75%). $^{31}P\{^{1}H\}$ ([D]chloroform, 20°C): δ = 34.0 (s, *P*). ^{1}H ([D]chloroform, 20°C): δ = 1.49-1.39 (m, 6H, C(14)H_2), 1.87 (s, 9H, C(12,13)*H*/H_2), 5.78 (d, ^{2}J(H,P) =7.1 Hz, 1H, N*H*), 7.33-7.28 (m, 1H, C(4)*H*), 7.51-7.48 (m, 1H, C(3)), 7.58-7.52 (m, 4H, C(8)*H*), 7.63-7.68 (m, 3H, C(5,9)*H*), 7.79-7.74 (m, 1H, C(2)*H*), 7.83 (dd, ^{3}J(H,H) = 7.4 Hz, ^{3}J(P,H) = 13.3 Hz, 4H, C(7)*H*). ^{13}C ([D]chloroform, 20°C): δ = 30.3 (s, C(13)), 35.9 (s, C(14)), 44.7 (d, ^{3}J(P,C) = 3.9 Hz, *C*(12)), 58.4 (d, ^{2}J(P,C) = 5.1 Hz, *C*(11)), 122.1 (d, ^{1}J(P,C) = 105.5 Hz, *C*(6)), 123.2 (d, ^{1}J(P,C) = 102.9 Hz, *C*(10)), 126.8 (d, ^{3}J(P,C) = 13.1 Hz, *C*(4)), 130.0 (d, ^{3}J(P,C) = 13.3, *C*(8)), 134.2 (d, ^{2}J(P,C) = 11.3 Hz, *C*(7)) 135.0 (d, ^{4}J(P,C) = 2.7 Hz, *C*(9)), 135.2 (d, ^{4}J(P,C) = 2.6 Hz, *C*(3)), 135.5 (d, ^{3}J(P,C) = 9.5 Hz, *C*(2)), 136.4 (d, ^{2}J(P,C) = 12.5 Hz, *C*(5)), 140.3 (d, ^{2}J(P,C) = 6.1 Hz, *C*(1)). MS (CI): m/z (%): 444 $[M]^+$

Synthesis of 31

MeLi (2 mmol, 1.24 mL of a 1.6 M solution in Et_2O) was added dropwise to a suspension of the aminophosphonium salt $[Ph_3PN(H)Ph]Br$[21] (434 mg, 1 mmol) in THF (10mL) at -78°C. The cold bath was removed and stirring was continued at r.t. during 4 h. S_8 (32 mg, 0.125 mmol) was then added in give. A precipitate appeared after 1 h. After 3 h of further stirring, the precipitate was recovered by filtration, then washed with a minimum amount of THF. An excess of HBF_4/ether was added. THF was removed in vacuum and CH_2Cl_2 (15mL) was added. The reaction mixture was washed twice with an aqueous solution of HBF_4 0.1M (5 mL), once with a saturated solution of $NaBF_4$ in water, then dried over $MgSO_4$. The volume of CH_2Cl_2 was reduced in vacuo, then a minimum amount of THF was added to precipitate **31** as a white solid. Yield: 226 mg (0.55 mmol, 55%).

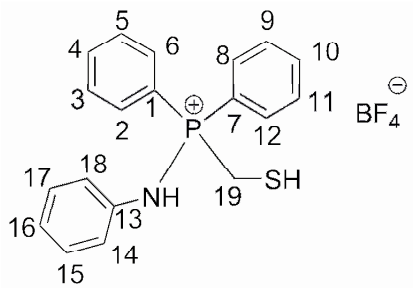

$^{31}P\{^{1}H\}$ ([D]chloroform, 20°C): δ = 35.9 (s, *P*). ^{1}H ([D]chloroform, 20°C): δ = 2.00 (td, 1H, ^{2}J(H,H) = 2.2 Hz, ^{3}J(P,H) = 9.0 Hz, S*H*) 3.85 (m, 2H, C(19)H_2) 6.80 (d, 2H, ^{3}J(H,H) = 8.1 Hz, C(18,14)*H*), 6.87 (t, 1H, ^{3}J(H,H) = 7.6 Hz, C(16)*H*) 7.00 (m, 2H, C(15,17)*H*), 7.34 (d, 1H, ^{2}J(H,P) = 9.4 Hz, N*H*) 7.56

(m, 4H, C(3,5,9,11)*H*), 7.69 (t, 2H, ^{3}J(H,H) = 6.9 Hz, C(4,10)*H*), 7.86 (m, 4H, C(2,6,8,12)*H*). ^{13}C ([D]chloroform, 20°C): δ = 18.7 (d, ^{1}J(P,C) = 66.8 Hz, *C*(19)), 116.8 (d, ^{1}J(P,C) = 99.4 Hz, *C*(1,7)), 119.0 (d, ^{3}J(P,C) = 6.5 Hz, *C*(14,18)), 123.1(s, *C*(16)), 128.6 (s, *C*(15,17)), 129.2 (d, ^{3}J(P,C) = 13.3 Hz, *C*(3,5,9,11), 132.5 (d, ^{2}J(P,C) =10.6 Hz, *C*(2,6,8,12)), 134.7 (d, ^{4}J(P,C) = 2.9Hz, *C*(4,10)), 136.3 (d, ^{2}J(P,C) = 2.7 Hz, *C*(13)). MS (CI): m/z (%): 411 $[M]^{+}$.

Chapter 5

Synthesis of 1.

To a stirred solution of **3**(diglyme) (400 mg, 1.08 mmol) in THF (10 mL), $Me_2PhSiCl$ (185 mg, 1.08 mmol, 182 µL) was added dropwise through a syringe at 0°C and stirring was continued for 15 min. Subsequently, a solution of KHMDS (215 mg, 1.08 mmol) in THF (5 mL) was added dropwise at 0°C, yielding an orange solution. The reaction mixture was then allowed to warm up to r.t., upon which Me_3SnCl (215 mg, 1.08 mmol) was added, resulting in an immediate color change to yellow. After stirring for 30 min. the solvent was removed by thorough evacuation under reduced pressure, leaving a viscous yellow oil as residue, which was resuspended in toluene (10 mL), followed by removal of the potassium salts by filtration. The yellow toluene solution was then added slowly to a solution of $TiCl_4$ (204 mg, 1.08 mmol, 0.13 mL) at 0°C, leading to an immediate color change to deep red. After 20 min, the reaction mixture was allowed to heat up to r.t., then the solvent was removed in vacuo. The solid residue was triturated with petroleum ether (3 × 5 mL), followed each time by filtration of the red solid residue, then thorough drying in vacuo, to obtain **2** (344 mg, 0.72 mmol,67% from **3**) as a deep red creamy solid.

$^{31}P\{^{1}H\}$ NMR ([D_6]benzene, 20°C): δ = 213.9 (s; *P*); ^{1}H NMR ([D_6]benzene, 20°C): δ = 0.51 (s, 6H; SiCH_3), 1.92 (s, 3H, CCH_3), 2.23 (s, 3H; CCH_3), 6.89-7.48 (m, 10H; SiC_6H_5 and CC_6H_5); ^{13}C NMR ([D_6]benzene, 20°C): δ = -0.5 (s; Si(*C*H_3)), 17.3 (d; ^{3}J (P,C) = 15.3 Hz; C*C*H_3), 26.2 (d; ^{3}J (P,C) = 10.5 Hz; C*C*H_3), 129.2, 130.4, 133.2, 134.7, 137.2, 137.4 (all s; *o*-, *m*-, *p*-*C*H SiPh and CPh), 143.2 (d; ^{3}J (P,C) = 6.7 Hz; *ipso*-*C*(Si)), 145.5 (d; ^{2}J (P,C) = 4.3 Hz; *ipso*-*C*(CPh)), 151.7 (d; ^{2}J (P,C) = 5.1 Hz; *C*CH_3), 157.3 (d; ^{2}J (P,C) = 7.2 Hz; *C*CH_3), 168.3 (d; ^{1}J (P,C) = 75.7 Hz; P*C*Si), 170.5 (d; ^{1}J (P,C) = 63.5 Hz; P*C*Ph); MS (CI): m/z (%): 474 $[M+H]^{+}$.

Synthesis of 7

Finely divided magnesium powder (3.1 g, 129 mmol) and $HgCl_2$ (3.5 g, 12.9 mmol) were cautiously suspended in THF (120 mL), while cooling the reaction mixture with an ice bath. While stirring, zirconocene dichloride (7.55 g, 25.8 mmol), and MeC≡C$SiMe_2$Ph (9 g, 51.6 mmol) were added. The mixture was stirred during 16 h, after which a deep yellow suspension had formed, of which the salts were filtered off. THF was removed in vacuo, and the solid residue taken up in a petroleum ether

40/65 – toluene solvent mixture (1.6:1) (240 mL). Filtration of residual salts, followed by solvent removal in vacuo yielded **8** as a bright yellow powder (13.1 g, 22.9 mmol, 89%). The sprectral parameters coincided with the published values.[22]

Synthesis of 9

Iodine (4.36 g, 17.19 mmol) was added in small portions over a period of 2 h to a stirred solution of **7** (4.90 g, 8.59 mmol) in 50 mL of THF at 0°C, the color of the reaction mixture changing from yellow to brown. While stirring for 1h, the mixture was allowed to warm up to r. t. THF was then removed in vacuo and the product recovered by addition of petroleum ether 40/65, followed by filtration. After drying of the filtrate in vacuo, the reddish raw product was purified by recrystallization from a saturated methanol solution at -8°C. Colorless crystals of **9** (3.45 g, 5.73 mmol, 67%) were obtained after drying in vacuo.

^{1}H NMR ([D$_6$]benzene, 20°C): δ = 0.45 and 0.51 (both s, 12H; SiC*H*$_3$), 1.63 (s, 6H; CC*H*$_3$), 7.06-7.16 (m, 6H; *o*-, *p*-C*H*), 7.54 (dd, ^{3}J (H,H) = 3.3 Hz, ^{3}J (H,H) = 3.8Hz, 4H; *m*-C*H*); ^{13}C NMR ([D$_6$]benzene, 20°C): δ = 0.7 and 1.32 (both s; Si(*C*H$_3$)), 20.2 (s; C*C*H$_3$), 100.5 (s; I*C*=C), 128.3 (s; *p*-*C*H), 129.6 (s; *o*-*C*H), 134.3 (s; *m*-*C*H), 138.3 (s; *ipso*-*C*H), 164.2 (s; IC=*C*); MS (CI): m/z (%): 602 [M+H]$^{+}$.

Synthesis of 10

A solution of *n*-BuLi in hexanes (11.36 mmol, 7.1 mL of a 1.6 M solution) was added to a stirred solution of 9 (3.4 g, 5.64 mmol) in diethyl ether at -78°C. The reaction mixture was warmed up to r. t. after 1h, then cooled again to -78°C. PhPCl$_2$ (1.01 g, 5.64 mmol, 0.76 mL) was added dropwise through a syringe, then the reaction mixture was allowed to heat up to r. t. and stirred for further 16 h. Water (80 mL) was added to the brownish suspension, and the product was extracted with diethyl ether (3 × 50 mL). The combined organic phases were dried over sodium sulfate, filtered, and the solvent removed in vacuo to yield **10** as pale yellow creamy solid (1.85 g, 4.06 mmol, 72%).

^{31}P{^{1}H} NMR ([D]chloroform, 20°C): δ = 35.7 (s; *P*); ^{1}H NMR ([D]chloroform, 20°C): δ = 0.41 (s, 12H; SiC*H*$_3$), 2.65 (d, ^{4}J (P,H) = 3.5 Hz, 6H; CC*H*$_3$), 6.80-6.95 (m, 6H; SiC$_6$*H*$_5$), 7.09-7.23 (m, 6H; PC$_6$*H*$_5$), 7.43 (m, 4H; SiC$_6$H$_5$); ^{13}C NMR ([D]chloroform, 20°C): δ = 3.75 (d, ^{3}J (P,C) = 11.7 Hz; Si(*C*H$_3$)), 12.9 (d, ^{3}J (P,C) = 3.1 Hz; C*C*H$_3$), 125.7 (d, ^{3}J (P,C) = 7.2 Hz; *m*-*C*H(P)), 126.3 (s; *p*-*C*H(P)), 128.9 (s; *m*-*C*H(Si)), 129.6 (s; *o*-*C*H(Si)), 131.5 (s; *p*-*C*H(Si)), 133.1 (d, ^{2}J (P,C) = 17.3 Hz; *o*-*C*H(P)), 135.4 (s; *C*CH$_3$), 141.9 (d, ^{1}J (P,C) = 12.3 Hz; P*C*Si); MS (CI): m/z (%): 457 [M+H]$^{+}$.

Synthesis of 2

To a stirred solution of **10** (1.65 g, 3.61 mmol) in THF (40 mL), freshly beaten lithium strips (70 mg, 10 mmol) were added. After 2 h, the complete formation of the lithiated species **11** was confirmed by the appearance of a single peak at 147.6 ppm in the ^{31}P{^{1}H} NMR. *t*BuCl (786 mg, 8.5 mmol, 0.9 mL)

was then added to the reaction mixture, followed by heating at 59°C for 45 min. Subsequently, Me_3SnCl (719 mg, 3.61 mmol) was added, resulting in the formation of a new single peak at -12.7 ppm, corresponding to the 1-stannylphosphole **12**. The solvent was removed in vacuo, and the solid residue was extracted with toluene (3 × 20 mL), and the residual salts removed by filtration. The yellow toluene solution was then added slowly to a solution of $TiCl_4$ (717 mg, 3.61 mmol, 0.42 mL) at 0°C, leading to an immediate color change to deep red. After 20 min, the reaction mixture was allowed to heat up to r.t., then the solvent was removed in vacuo. The solid residue was triturated with petroleum ether (3 × 10 mL), followed each time by filtration of the red solid residue, then thorough drying in vacuo, to obtain **2** (1.25 g, 2.35 mmol,65%) as a deep red solid.

$^{31}P\{^1H\}$ NMR ([D$_6$]benzene, 20°C): δ = 255.9 (s; *P*); ^1H NMR ([D$_6$]benzene, 20°C): δ = 0.67 and 0.80 (both s, 12H; SiC*H*$_3$), 2.11 (s, 6H; CC*H*$_3$), 7.07-7.37 (m, 10H; C$_6$*H*$_5$); ^{13}C NMR ([D$_6$]benzene, 20°C): δ = -1.9 and -0.3 (both s; Si(*C*H$_3$)), 19.0 (s; C*C*H$_3$), 130.0 (s; *o*-*C*H), 131.5 (s; *p*-*C*H), 136.0 (s, *m*-*C*H), 141.9 (s; *ipso*-*C*(Si)), 160.8 (s; *C*CH$_3$), 166.2 (d; ^1J (P,C) = 80.7 Hz; P*C*Si); MS (CI): m/z (%): 535 $[M+H]^+$.

Bibliography

[1] G. M. Sheldrick, SHELXL-97, Göttingen, Germany, **1997**.

[2] C. A. Busacca, J. C. Lorenz, N. Grinberg, N. Haddad, M. Hrapchak, B. Latli, H. Lee, P. Sabila, A. Saha, M. Sarvestani, S. Shen, R. Varsolona, X. Wei, C. H. Senanayake, *Org. Lett.* **2005**, *7*, 4277.

[3] M. Visseaux, F. Nief, L. Ricard, *J. Organomet. Chem.* **2002**, *647*, 139.

[4] M. Melaimi, L. Ricard, F. Mathey, P. Le Floch, *Org. Lett.* **2002**, *4*, 1245.

[5] C. Charrier, H. Bonnard, F. Mathey, D. Neibecker, *J. Organomet. Chem.* **1982**, *231*, 361.

[6] P. Bondjouk, J.-H. So, *Inorg. Syntheses* **1992**, *29*, 108.

[7] R. B. King, *Organomet. Syntheses* **1965**, *1*, 71.

[8] G. Giordano, R. H. Crabtree, *Inorg. Syntheses* **1990**, *28*, 248.

[9] A. Bollmann, K. Blann, J. T. Dixon, F. M. Hess, E. Killian, H. Maumela, D. S. McGuinness, D. H. Morgan, A. Neveling, S. Otto, M. Overett, A. M. Z. Slawin, P. Wasserscheid, S. Kuhlmann, *J. Am. Chem. Soc.* **2004**, *126*, 14712.

[10] M. Keles, Z. Aydin, O. Serindag, *J. Organomet. Chem.* **2007**, *692*, 1951.

[11] A. L. Balch, M. M. Olmstead, S. P. Rowley, *Inorg. Chim. Acta* **1990**, *168*, 255.

[12] N. Pirio, S. Bredeau, L. Dupuis, P. Schütz, B. Donnadieu, A. Igau, J.-P. Majoral, J.-C. Guillemin, P. Meunier, *Tetrahedron* **2004**, *60*, 1317.

[13] N. A. Cooley, S. M. Green, D. F. Wass, K. Heslop, A. G. Orpen, P. G. Pringle, *Organometallics* **2001**, *20*, 4769.

[14] T. Cantat, *Ph. D. Thesis*, Ecole Polytechnique, Palaiseau, France, **2007**.

[15] T. C. Whitner, E. E. Reid, *J. Am. Chem. Soc.* **1921**, *43*, 638.

[16] H. D. Verkruijsse, L. Brandsma, *J. Organomet. Chem.* **1987**, *332*, 95.

[17] M. Demange, L. Boubekeur, A. Auffrant, N. Mezailles, L. Ricard, X. L. Goff, P. L. Floch, *New J. Chem.* **2006**, *30*, 1745.

[18] A. Bianchi, A. Bernardi, *J. Org. Chem.* **2006**, *71*, 4565.

[19] L. Boubekeur, *Ph. D. Thesis*, Ecole Polytechnique, Palaiseau, France, **2006**.

[20] L. Boubekeur, L. Ricard, N. Mezailles, P. Le Floch, *Organometallics* **2005**, *24*, 1065.

[21] L. Boubekeur, L. Ricard, N. Mezailles, M. Demange, A. Auffrant, P. Le Floch, *Organometallics* **2006**, *25*, 3091.

[22] S. S. H. Mao, F.-Q. Liu, T. D. Tilley, *J. Am. Chem. Soc.* **1998**, *120*, 1193.

Crystallographic Appendix

Chapter 1

Crystallographic Data for 2

Compound	**2**
Molecular formula	$C_{64}H_{62}Al_2Br_6Cr_2N_2P_4$
Molecular weight	1569.97
Crystal habit	light blue plate
Crystal dimensions(mm)	0.22x0.10x0.06
Crystal system	monoclinic
Space group	C2/c
a(Å)	62.415(5)
b(Å)	9.630(5)
c(Å)	26.835(5)
α(°)	90.00
β(°)	113.871(5)
γ(°)	90.00
V(Å^3)	14750(8)
Z	8
d(g-cm^{-3})	1.414
F(000)	5984
μ(cm^{-1})	3.691
Absorption corrections	multi-scan ; 0.4973 min, 0.8089 max
Diffractometer	KappaCCD
X-ray source	MoKα
λ(Å)	0.71069
Monochromator	graphite
T (K)	150.0(1)
Scan mode	phi and omega scans
Maximum θ	27.48
HKL ranges	-80 80 ; -12 11 ; -34 34
Reflections measured	28895
Unique data	16875
Rint	0.0312
Reflections used	11244
Criterion	I > 2σI)
Refinement type	Fsqd
Hydrogen atoms	mixed
Parameters refined	782
Reflections / parameter	14
wR2	0.1942
R1	0.0604
Weights a, b	0.1167 ; 0.0000
GoF	1.054
difference peak / hole (e Å^{-3})	1.735(0.135) / -2.725(0.135)

Crystallographic Data for 4d

Compound	**4d**
Molecular formula	$C_{33}H_{63}Cl_3CrNOP_2$
Molecular weight	710.13
Crystal habit	Blue Block
Crystal dimensions(mm)	0.16x0.10x0.08
Crystal system	monoclinic
Space group	$P2_12_12_1$
a(Å)	11.298(1)
b(Å)	17.980(1)
c(Å)	18.192(1)
α(°)	90.00
β(°)	90.00
γ(°)	90.00
V(Å^3)	3695.5(4)
Z	4
d(g-cm^{-3})	1.276
F(000)	1524
μ(cm^{-1})	0.639
Absorption corrections	multi-scan ; 0.9046 min, 0.9506 max
Diffractometer	KappaCCD
X-ray source	MoKα
λ(Å)	0.71069
Monochromator	graphite
T (K)	150.0(1)
Scan mode	phi and omega scans
Maximum θ	22.98
HKL ranges	-12 10 ; -19 18 ; -19 18
Reflections measured	28341
Unique data	5128
Rint	0.1425
Reflections used	3557
Criterion	I > 2σI)
Refinement type	Fsqd
Hydrogen atoms	constr
Parameters refined	372
Reflections / parameter	9
wR2	0.1006
R1	0.0513
Flack's parameter	-0.03(3)
Weights a, b	0.0400 ; 0.0000
GoF	0.963
difference peak / hole (e Å^{-3})	0.434(0.073) / -0.343(0.073)

Chapter 2

Crystallographic Data for 10

Compound	**10**
Molecular formula	$C_{33}H_{25}BrMnNO_3P_2$
Molecular weight	1360.66
Crystal habit	Orange Block
Crystal dimensions(mm)	0.20x0.20x0.12
Crystal system	triclinic
Space group	Pbar1
a(Å)	10.6730(10)
b(Å)	16.2310(10)
c(Å)	18.5150(10)
α(°)	70.8120(10)
β(°)	81.4660(10)
γ(°)	87.2750(10)
V(Å^3)	2995.7(4)
Z	2
d(g-cm^{-3})	1.508
F(000)	1376
μ(cm^{-1})	1.916
Absorption corrections	multi-scan ; 0.7005 min, 0.8026 max
Diffractometer	KappaCCD
X-ray source	MoKα
λ(Å)	0.71069
Monochromator	graphite
T (K)	150.0(1)
Scan mode	phi and omega scans
Maximum θ	27.48
HKL ranges	-13 12 ; -21 21 ; -24 21
Reflections measured	21337
Unique data	13668
Rint	0.0212
Reflections used	11237
Criterion	I > 2σI)
Refinement type	Fsqd
Hydrogen atoms	mixed
Parameters refined	758
Reflections / parameter	14
wR2	0.1017
R1	0.0379
Weights a, b	0.0403 ; 3.4809
GoF	1.020
difference peak / hole (e Å^{-3})	0.857(0.070) / -1.069(0.070)

Chapter 3

Crystallographic Data for 3a

Compound	**3a**
Molecular formula	$C_{62}H_{70}Cl_4Cr_2N_4P_4,6(CH_2Cl_2)$
Molecular weight	1750.46
Crystal habit	blue plate
Crystal dimensions(mm)	0.22x0.22x0.10
Crystal system	triclinic
Space group	Pbar1
a(Å)	12.7790(10)
b(Å)	12.9560(10)
c(Å)	13.7000(10)
α(°)	77.2520(10)
β(°)	69.7760(10)
γ(°)	69.6420(10)
V(Å^3)	1982.4(3)
Z	1
d(g-cm^{-3})	1.466
F(000)	898
μ(cm^{-1})	0.936
Absorption corrections	multi-scan ; 0.8205 min, 0.9122 max
Diffractometer	KappaCCD
X-ray source	MoKα
λ(Å)	0.71069
Monochromator	graphite
T (K)	150.0(1)
Scan mode	phi and omega scans
Maximum θ	30.03
HKL ranges	-17 17 ; -18 17 ; -16 19
Reflections measured	29661
Unique data	11583
Rint	0.0219
Reflections used	9507
Criterion	I > 2σI)
Refinement type	Fsqd
Hydrogen atoms	mixed
Parameters refined	429
Reflections / parameter	22
wR2	0.1001
R1	0.0354
Weights a, b	0.0491 ; 0.7747
GoF	1.051
difference peak / hole (e Å^{-3})	0.895(0.064) / -0.783(0.064)

Crystallographic Data for 3b

Compound	**3b**
Molecular formula	$C_{66}H_{78}Cl_4Cr_2N_4P_4,2(C_4H_8O)$
Molecular weight	720.61
Crystal habit	Dark Blue Block
Crystal dimensions(mm)	0.26x0.16x0.12
Crystal system	monoclinic
Space group	$P2_1/c$
a(Å)	11.078(5)
b(Å)	22.191(5)
c(Å)	14.487(5)
α(°)	90.000(5)
β(°)	97.136(5)
γ(°)	90.000(5)
V(Å^3)	3534(2)
Z	4
d(g-cm^{-3})	1.354
F(000)	1516
μ(cm^{-1})	0.598
Absorption corrections	multi-scan ; 0.8600 min, 0.9317 max
Diffractometer	KappaCCD
X-ray source	MoKα
λ(Å)	0.71069
Monochromator	graphite
T (K)	150.0(1)
Scan mode	phi and omega scans
Maximum θ	27.46
HKL ranges	-14 14 ; -26 28 ; -13 18
Reflections measured	25183
Unique data	8075
Rint	0.0331
Reflections used	6023
Criterion	I > 2σI)
Refinement type	Fsqd
Hydrogen atoms	mixed
Parameters refined	412
Reflections / parameter	14
wR2	0.1360
R1	0.0449
Weights a, b	0.0762 ; 1.3757
GoF	1.048
difference peak / hole (e Å^{-3})	0.955(0.074) / -0.618(0.074)

Crystallographic Data for 3c

Compound	**3c**
Molecular formula	$C_{74}H_{62}Cl_4Cr_2N_4P_4,3(CH_2Cl_2)$
Molecular weight	1631.73
Crystal habit	Blue Block
Crystal dimensions(mm)	0.20x0.10x0.10
Crystal system	monoclinic
Space group	$P2_1/c$
a(Å)	22.448(1)
b(Å)	19.697(1)
c(Å)	19.014(1)
α(°)	90.00
β(°)	112.1760(10)
γ(°)	90.00
V(Å^3)	7785.3(7)
Z	4
d(g-cm^{-3})	1.392
F(000)	3344
μ(cm^{-1})	0.749
Absorption corrections	multi-scan ; 0.8646 min, 0.9288 max
Diffractometer	KappaCCD
X-ray source	MoKα
λ(Å)	0.71069
Monochromator	graphite
T (K)	150.0(1)
Scan mode	phi and omega scans
Maximum θ	25.35
HKL ranges	-27 26 ; -22 23 ; -22 22
Reflections measured	42895
Unique data	14195
Rint	0.0579
Reflections used	9004
Criterion	I > 2σI)
Refinement type	Fsqd
Hydrogen atoms	constr
Parameters refined	847
Reflections / parameter	10
wR2	0.1796
R1	0.0603
Weights a, b	0.1039 ; 0.0000
GoF	1.022
difference peak / hole (e Å^{-3})	1.373(0.090) / -1.160(0.090)

Crystallographic Data for 3d

Compound	**3d**
Molecular formula	$C_{39}H_{36}Cl_2CrN_2O_2P_2,2(C_4H_8O)$
Molecular weight	893.75
Crystal habit	pink needle
Crystal dimensions(mm)	0.22x0.10x0.06
Crystal system	triclinic
Space group	Pbar1
a(Å)	9.4120(1)
b(Å)	13.128(1)
c(Å)	18.731(1)
α(°)	72.651(1)
β(°)	83.444(1)
γ(°)	80.124(1)
V(Å^3)	2171.5(3)
Z	2
d(g-cm^{-3})	1.367
F(000)	936
μ(cm^{-1})	0.506
Absorption corrections	multi-scan ; 0.8967 min, 0.9703 max
Diffractometer	KappaCCD
X-ray source	MoKα
λ(Å)	0.71069
Monochromator	graphite
T (K)	150.0(1)
Scan mode	phi and omega scans
Maximum θ	25.35
HKL ranges	-10 11 ; -15 15 ; -22 21
Reflections measured	16829
Unique data	7856
Rint	0.0422
Reflections used	5263
Criterion	I > 2σI)
Refinement type	Fsqd
Hydrogen atoms	mixed
Parameters refined	525
Reflections / parameter	10
wR2	0.2266
R1	0.0732
Weights a, b	0.1084 ; 6.4709
GoF	1.022
difference peak / hole (e Å^{-3})	1.037(0.100) / -0.730(0.100)

Crystallographic Data for 4

Compound	**4**
Molecular formula	$C_{33}H_{39}BrN_2NiP_2$
Molecular weight	1328.44
Crystal habit	Red Block
Crystal dimensions(mm)	0.34x0.14x0.10
Crystal system	triclinic
Space group	Pbar1
a(Å)	10.588(1)
b(Å)	15.682(1)
c(Å)	19.364(1)
α(°)	80.943(1)
β(°)	88.586(1)
γ(°)	83.471(1)
V(Å^3)	3154.5(4)
Z	2
d(g-cm^{-3})	1.399
F(000)	1376
μ(cm^{-1})	2.008
Absorption corrections	multi-scan ; 0.5485 min, 0.8245 max
Diffractometer	KappaCCD
X-ray source	MoKα
λ(Å)	0.71069
Monochromator	graphite
T (K)	150.0(1)
Scan mode	phi and omega scans
Maximum θ	28.70
HKL ranges	-13 14 ; -20 21 ; -26 25
Reflections measured	25701
Unique data	16255
Rint	0.0347
Reflections used	9385
Criterion	I > 2σI)
Refinement type	Fsqd
Hydrogen atoms	mixed
Parameters refined	715
Reflections / parameter	13
wR2	0.0944
R1	0.0428
Weights a, b	0.0346 ; 0.0000
GoF	0.919
difference peak / hole (e Å^{-3})	0.547(0.079) / -0.604(0.079)

Chapter 4

Crystallographic Data for 7a

Compound	**7a**
Molecular formula	$C_{22}H_{25}NOP,Cl$
Molecular weight	1543.40
Crystal habit	Colorless Block
Crystal dimensions(mm)	0.25x0.22x0.18
Crystal system	orthorhombic
Space group	$P2_12_12_1$
a(Å)	9.453(1)
b(Å)	14.521(1)
c(Å)	14.989(1)
α(°)	90.00
β(°)	90.00
γ(°)	90.00
V(Å^3)	2057.5(3)
Z	1
d(g-cm^{-3})	1.246
F(000)	816
μ(cm^{-1})	0.274
Absorption corrections	multi-scan ; 0.9347 min, 0.9524 max
Diffractometer	KappaCCD
X-ray source	MoKα
λ(Å)	0.71069
Monochromator	graphite
T (K)	150.0(1)
Scan mode	phi and omega scans
Maximum θ	27.09
HKL ranges	-12 8 ; -18 18 ; -18 19
Reflections measured	14231
Unique data	4504
Rint	0.0407
Reflections used	4228
Criterion	I > 2σI)
Refinement type	Fsqd
Hydrogen atoms	mixed
Parameters refined	242
Reflections / parameter	17
wR2	0.2536
R1	0.0897
Flack's parameter	-1.51(15)
Weights a, b	0.1697 ; 2.3840
GoF	1.118
difference peak / hole (e Å^{-3})	2.384(0.198) / -0.606(0.198)

Crystallographic Data for 9

Compound	pa116
Molecular formula	$C_{40}H_{38}ClNOP_2Pd$
Molecular weight	752.50
Crystal habit	orange block
Crystal dimensions(mm)	0.20x0.14x0.06
Crystal system	triclinic
Space group	P -1
a(Å)	10.274(1)
b(Å)	11.515(1)
c(Å)	16.850(1)
α(°)	97.475(1)
β(°)	100.265(1)
γ(°)	116.410(1)
V(Å^3)	1706.5(2)
Z	2
d(g-cm^{-3})	1.464
F(000)	772
μ(cm^{-1})	0.749
Absorption corrections	multi-scan ; 0.8646 min, 0.9564 max
Diffractometer	KappaCCD
X-ray source	MoKα
λ(Å)	0.71069
Monochromator	graphite
T (K)	150.0(1)
Scan mode	phi and omega scans
Maximum θ	29.99
HKL ranges	-14 14 ; -16 16 ; -23 23
Reflections measured	27191
Unique data	9896
Rint	0.0322
Reflections used	7904
Criterion	I > 2σI)
Refinement type	Fsqd
Hydrogen atoms	constr
Parameters refined	418
Reflections / parameter	18
wR2	0.0829
R1	0.0337
Weights a, b	0.0288 ; 0.7793
GoF	1.054
difference peak / hole (e Å^{-3})	0.786(0.079) / -0.741(0.079)

Crystallographic Data for 10b

Compound	**10b**
Molecular formula	$C_{30}H_{39}BrClLiNNiO_3P$
Molecular weight	673.60
Crystal habit	Blue Block
Crystal dimensions(mm)	0.20x0.18x0.14
Crystal system	monoclinic
Space group	$P2_1/n$
a(Å)	9.094(1)
b(Å)	16.079(1)
c(Å)	21.897(1)
α(°)	90.00
β(°)	91.467(1)
γ(°)	90.00
V(Å^3)	3200.8(4)
Z	4
d(g-cm^{-3})	1.398
F(000)	1392
μ(cm^{-1})	2.018
Absorption corrections	multi-scan ; 0.6884 min, 0.7654 max
Diffractometer	KappaCCD
X-ray source	MoKα
λ(Å)	0.71069
Monochromator	graphite
T (K)	150.0(1)
Scan mode	phi and omega scans
Maximum θ	27.47
HKL ranges	-8 11 ; -19 20 ; -28 28
Reflections measured	22529
Unique data	7317
Rint	0.0522
Reflections used	4857
Criterion	I > 2σI)
Refinement type	Fsqd
Hydrogen atoms	constr
Parameters refined	401
Reflections / parameter	12
wR2	0.1178
R1	0.0416
Weights a, b	0.0608 ; 0.2478
GoF	1.011
difference peak / hole (e Å^{-3})	0.605(0.071) / -0.449(0.071)

Crystallographic Data for 21

Compound	21
Molecular formula	$3(C_{32}H_{29}Br_3CrNOP_2),2(CH_2Cl_2)$
Molecular weight	2561.55
Crystal habit	Green Block
Crystal dimensions(mm)	0.20x0.12x0.10
Crystal system	triclinic
Space group	P -1
a(≈)	12.2870(10)
b(≈)	15.2620(10)
c(≈)	27.5710(10)
α(∞)	91.3430(10)
β(∞)	100.4540(10)
γ(∞)	97.8200(10)
V(≈^{3})	5031.0(6)
Z	2
d(g-cm^{-3})	1.691
F(000)	2538
μ(cm^{-1})	4.144
Absorption corrections	multi-scan ; 0.4911 min, 0.6820 max
Diffractometer	KappaCCD
X-ray source	MoKα
λ(≈)	0.71069
Monochromator	graphite
T (K)	150.0(1)
Scan mode	phi and omega scans
Maximum θ	26.37
HKL ranges	-15 15 ; -19 18 ; -34 33
Reflections measured	49318
Unique data	20248
Rint	0.0298
Reflections used	14941
Criterion	$I > 2\sigma(I)$
Refinement type	Fsqd
Hydrogen atoms	mixed
Parameters refined	1139
Reflections / parameter	13
wR2	0.1959
R1	0.0595
Weights a, b	0.1108 ; 16.409
GoF	1.057
difference peak / hole (e Å $^{-3}$)	1.673(0.160) / -1.773(0.160)

Crystallographic Data for 22

Compound	**22**
Molecular formula	$C_{31}H_{28}Cl_3CrN_2P_2,1.5(C_4H_8O)$
Molecular weight	757.00
Crystal habit	blue plate
Crystal dimensions(mm)	0.22x0.20x0.12
Crystal system	monoclinic
Space group	C2/c
a(Å)	26.3540(10)
b(Å)	15.4400(10)
c(Å)	18.5110(10)
α(°)	90.00
β(°)	101.2420(10)
γ(°)	90.00
V(Å^3)	7387.7(7)
Z	8
d(g-cm^{-3})	1.361
F(000)	3144
μ(cm^{-1})	0.647
Absorption corrections	multi-scan ; 0.8708 min, 0.9264 max
Diffractometer	KappaCCD
X-ray source	MoKα
λ(Å)	0.71073
Monochromator	graphite
T (K)	150.0(1)
Scan mode	phi and omega scans
Maximum θ	27.48
HKL ranges	-34 34 ; -20 18 ; -24 24
Reflections measured	15419
Unique data	8438
Rint	0.0240
Reflections used	6330
Criterion	I > 2σI)
Refinement type	Fsqd
Hydrogen atoms	mixed
Parameters refined	433
Reflections / parameter	14
wR2	0.1351
R1	0.0454
Weights a, b	0.0689 ; 8.5694
GoF	1.042
difference peak / hole (e Å^{-3})	.717(.067) / -.506(.067)

Crystallographic Data for 23d

Compound	**23d**
Molecular formula	$C_{32}H_{29}Br_2NNiOP_2,2CH_2Cl_2$
Molecular weight	893.88
Crystal habit	red plate
Crystal dimensions(mm)	0.18x0.08x0.04
Crystal system	monoclinic
Space group	$P2_1/c$
a(≈)	11.049(1)
b(≈)	20.203(1)
c(≈)	16.132(1)
α(∞)	90.00
β(∞)	101.119(1)
γ(∞)	90.00
V(≈^{3})	3533.4(4)
Z	4
d(g-cm^{-3})	1.680
F(000)	1792
μ(cm^{-1})	3.234
Absorption corrections	multi-scan ; 0.5937 min, 0.8815 max
Diffractometer	KappaCCD
X-ray source	MoKα
λ(≈)	0.71069
Monochromator	graphite
T (K)	150.0(1)
Scan mode	phi and omega scans
Maximum θ	24.11
HKL ranges	-12 12 ; -23 21 ; -16 18
Reflections measured	18106
Unique data	5599
Rint	0.0493
Reflections used	3372
Criterion	I > 2σ(I)
Refinement type	Fsqd
Hydrogen atoms	constr
Parameters refined	370
Reflections / parameter	9
wR2	0.1456
R1	0.0508
Weights a, b	0.0791 ; 0.0000
GoF	0.989
difference peak / hole (e ≈$^{-3}$)	0.550(0.085) / -0.577(0.085)

Crystallographic Data for 25b

Compound	**25b**
Molecular formula	$C_{33}H_{31}Br_2NNiP_2$
Molecular weight	722.06
Crystal habit	Blue Needle
Crystal dimensions(mm)	0.20x0.04x0.04
Crystal system	monoclinic
Space group	$P2_1/c$
a(≈)	9.087(1)
b(≈)	16.597(1)
c(≈)	21.913(1)
α(∞)	90.00
β(∞)	110.180(1)
γ(∞)	90.00
V(≈^{3})	3102.0(4)
Z	4
d(g-cm^{-3})	1.546
F(000)	1456
μ(cm^{-1})	3.328
Absorption corrections	multi-scan ; 0.5558 min, 0.8784 max
Diffractometer	KappaCCD
X-ray source	MoKα
λ(≈)	0.71069
Monochromator	graphite
T (K)	150.0(1)
Scan mode	phi and omega scans
Maximum θ	26.37
HKL ranges	-11 11 ; -19 20 ; -27 27
Reflections measured	10809
Unique data	6329
Rint	0.0279
Reflections used	4492
Criterion	I > 2σ(I)
Refinement type	Fsqd
Hydrogen atoms	mixed
Parameters refined	354
Reflections / parameter	12
wR2	0.0652
R1	0.0315
Weights a, b	0.0219 ; 0.0000
GoF	0.988
difference peak / hole (e ≈$^{-3}$)	0.346(0.073) / -0.409(0.073)

Crystallographic Data for 28a

Compound	**28a**
Molecular formula	$C_{28}H_{29}NPS,BF_4$
Molecular weight	529.36
Crystal habit	Colorless Block
Crystal dimensions(mm)	0.44x0.26x0.15
Crystal system	triclinic
Space group	P -1
a(Å)	10.267(1)
b(Å)	10.307(1)
c(Å)	14.111(1)
α(°)	101.133(1)
β(°)	104.791(1)
γ(°)	110.442(1)
V(Å^3)	1285.5(2)
Z	2
d(g-cm^{-3})	1.368
F(000)	552
μ(cm^{-1})	0.236
Absorption corrections	multi-scan ; 0.9034 min, 0.9655 max
Diffractometer	KappaCCD
X-ray source	MoKα
λ(Å)	0.71069
Monochromator	graphite
T (K)	150.0(1)
Scan mode	phi and omega scans
Maximum θ	30.02
HKL ranges	-14 13 ; -14 14 ; -19 19
Reflections measured	17218
Unique data	7499
Rint	0.0185
Reflections used	6226
Criterion	I > 2σI)
Refinement type	Fsqd
Hydrogen atoms	mixed
Parameters refined	331
Reflections / parameter	18
wR2	0.1236
R1	0.0398
Weights a, b	0.0652 ; 0.3682
GoF	1.087
difference peak / hole (e Å^{-3})	0.919(0.101) / -0.778(0.101)

Crystallographic Data for 29a

Compound	**29a**
Molecular formula	$C_{22}H_{25}NPS,BF_4$
Molecular weight	453.27
Crystal habit	Colorless Block
Crystal dimensions(mm)	0.30x0.12x0.08
Crystal system	orthorhombic
Space group	Pbca
a(Å)	15.666(1)
b(Å)	16.486(1)
c(Å)	17.614(1)
α(°)	90.00
β(°)	90.00
γ(°)	90.00
V(Å^3)	4549.2(5)
Z	8
d(g-cm^{-3})	1.324
F(000)	1888
μ(cm^{-1})	0.254
Absorption corrections	multi-scan ; 0.9278 min, 0.9800 max
Diffractometer	KappaCCD
X-ray source	MoKα
λ(Å)	0.71069
Monochromator	graphite
T (K)	150.0(1)
Scan mode	phi and omega scans
Maximum θ	27.45
HKL ranges	-20 16 ; -17 20 ; -15 22
Reflections measured	21003
Unique data	5177
Rint	0.0258
Reflections used	3908
Criterion	I > 2σI)
Refinement type	Fsqd
Hydrogen atoms	mixed
Parameters refined	280
Reflections / parameter	13
wR2	0.1107
R1	0.0382
Weights a, b	0.0541 ; 1.0556
GoF	1.066
difference peak / hole (e Å^{-3})	0.348(0.045) / -0.514(0.045)

Crystallographic Data for 32b

Compound	**32b**
Molecular formula	$2(C_{40}H_{38}BrNP_2PdS),CH_2Cl_2$
Molecular weight	855.49
Crystal habit	orange plate
Crystal dimensions(mm)	0.22x0.20x0.12
Crystal system	triclinic
Space group	P -1
a(Å)	9.798(1)
b(Å)	9.884(1)
c(Å)	20.216(1)
α(°)	87.730(1)
β(°)	83.800(1)
γ(°)	72.090(1)
V(Å^3)	1852.0(3)
Z	2
d(g-cm^{-3})	1.534
F(000)	866
μ(cm^{-1})	1.825
Absorption corrections	multi-scan ; 0.6896 min, 0.8107 max
Diffractometer	KappaCCD
X-ray source	MoKα
λ(Å)	0.71073
Monochromator	graphite
T (K)	150.0(1)
Scan mode	phi and omega scans
Maximum θ	30.02
HKL ranges	-13 13 ; -12 13 ; -28 27
Reflections measured	23799
Unique data	10763
Rint	0.0199
Reflections used	9318
Criterion	I > 2σI)
Refinement type	Fsqd
Hydrogen atoms	mixed
Parameters refined	445
Reflections / parameter	20
wR2	0.1442
R1	0.0456
Weights a, b	0.0790 ; 4.4523
GoF	1.033
difference peak / hole (e Å^{-3})	1.076(0.131) / -2.924(0.131)

Crystallographic Data for 33

Compound	**33**
Molecular formula	$C_{30}H_{35}NPRhS$
Molecular weight	575.53
Crystal habit	Orange Block
Crystal dimensions(mm)	0.22x0.22x0.20
Crystal system	monoclinic
Space group	$P2_1/c$
a(Å)	10.868(1)
b(Å)	14.189(1)
c(Å)	17.654(1)
α(°)	90.00
β(°)	108.048(4)
γ(°)	90.00
V(Å^3)	2588.4(3)
Z	4
d(g-cm^{-3})	1.477
F(000)	1192
μ(cm^{-1})	0.822
Absorption corrections	multi-scan ; 0.8399 min, 0.8529 max
Diffractometer	KappaCCD
X-ray source	MoKα
λ(Å)	0.71069
Monochromator	graphite
T (K)	150.0(1)
Scan mode	phi and omega scans
Maximum θ	30.00
HKL ranges	-15 15 ; -13 19 ; -24 18
Reflections measured	18918
Unique data	7475
Rint	0.0180
Reflections used	6121
Criterion	I > 2σI)
Refinement type	Fsqd
Hydrogen atoms	constr
Parameters refined	310
Reflections / parameter	19
wR2	0.0802
R1	0.0300
Weights a, b	0.0348 ; 1.2520
GoF	1.046
difference peak / hole (e Å^{-3})	0.713(0.072) / -0.896(0.072)

Crystallographic Data for 33

Compound	**34**
Molecular formula	$C_{48}H_{54}N_2O_4P_2,C_4H_8O,_2(Cl)$
Molecular weight	927.88
Crystal habit	Colorless Block
Crystal dimensions(mm)	0.40x0.30x0.20
Crystal system	monoclinic
Space group	$P2_1/c$
a(Å)	11.119(1)
b(Å)	20.883(1)
c(Å)	22.039(1)
α(°)	90.00
β(°)	107.817(3)
γ(°)	90.00
V(Å^3)	4872.0(5)
Z	4
d(g-cm^{-3})	1.265
F(000)	1968
μ(cm^{-1})	0.247
Absorption corrections	multi-scan ; 0.9075 min, 0.9522 max
Diffractometer	KappaCCD
X-ray source	MoKα
λ(Å)	0.71069
Monochromator	graphite
T (K)	150.0(1)
Scan mode	phi and omega scans
Maximum θ	27.48
HKL ranges	-14 11 ; -25 27 ; -28 28
Reflections measured	36196
Unique data	11152
Rint	0.0370
Reflections used	7695
Criterion	I > 2σI)
Refinement type	Fsqd
Hydrogen atoms	mixed
Parameters refined	576
Reflections / parameter	13
wR2	0.1515
R1	0.0518
Weights a, b	0.0740 ; 1.9674
GoF	1.050
difference peak / hole (e Å^{-3})	0.859(0.061) / -0.805(0.061)

Chapter 5

Crystallographic Data for 2

Compound	**2**
Molecular formula	$C_{22}H_{28}Cl_3PSi_2Ti$
Molecular weight	533.84
Crystal habit	Red Plate
Crystal dimensions(mm)	0.28x0.10x0.06
Crystal system	monoclinic
Space group	$P2_1/c$
a(Å)	25.723(1)
b(Å)	8.003(1)
c(Å)	12.470(1)
α(°)	90.00
β(°)	92.316(1)
γ(°)	90.00
V(Å^3)	2565.0(4)
Z	4
d(g-cm^{-3})	1.382
F(000)	1104
μ(cm^{-1})	0.810
Absorption corrections	multi-scan ; 0.8050 min, 0.9530 max
Diffractometer	KappaCCD
X-ray source	MoKα
λ(Å)	0.71069
Monochromator	graphite
T (K)	150.0(1)
Scan mode	phi and omega scans
Maximum θ	28.70
HKL ranges	-24 34 ; -9 10 ; -16 16
Reflections measured	18521
Unique data	6554
Rint	0.0384
Reflections used	4399
Criterion	I > 2σI)
Refinement type	Fsqd
Hydrogen atoms	constr
Parameters refined	268
Reflections / parameter	16
wR2	0.0840
R1	0.0364
Weights a, b	0.0322 ; 0.0000
GoF	0.995
difference peak / hole (e Å^{-3})	0.382(0.065) / -0.362(0.065)